CRANFIELD UNIVERSITY

D. ZAMMIT-MANGION

Design and development of an algorithm for a take-off performance monitor

COLLEGE OF AERONAUTICS

PhD THESIS

CRANFIELD UNIVERSITY

COLLEGE OF AERONAUTICS

FLIGHT TEST AND DYNAMICS GROUP

PhD THESIS

Academic Year 2000-1

D. ZAMMIT-MANGION

Design and development of an algorithm for a take-off performance monitor

Supervisor: M. E. Eshelby

February 2001

ABSTRACT

A take-off performance monitor is an instrument that is intended to monitor the progress of the take-off manoeuvre in real-time in order to ensure that the aircraft will meet the various distance constraints of the airfield. Several designs have to date been proposed but none have been successful commercially. This work has involved the development of a novel design concept based on the consideration of the time history of the run to obtain an accurate prediction of the distance required to V_1. Scheduled post-V_1 distances are then allowed for in the estimate of the actual distances required to complete the manoeuvre. A performance standard complementing SAE aerospace standard AS-8044 has also been established to ensure system reliability during operation. The algorithms developed were validated using the College of Aeronautics' Jetstream-100 flying laboratory and take-off data of B747 and B737 aircraft. A fixed-base simulator was also used to evaluate the algorithm in adverse operating conditions. The algorithm was demonstrated to meet the named performance standards and is shown to have the potential of being utilised in a successful commercial performance monitor. A novel display design concept is also proposed, providing a basis on which an attractive display can be further developed.

ACKNOWLEDGEMENTS

I would like to thank Dr. M. E. Eshelby for the dedicated supervision of this project. His support, guidance and advice have all been instrumental to the success of the programme. I would also like to thank Mr. M. Nebylowitsch, Manager, Flight Data Recording at British Airways for his continuous support and for providing the opportunity to validate the design with take-off recordings of jet transports. My thanks also go to the staff of the NFLC for their support relating to the Jetstream aircraft. Finally, I wish to thank those who have also supported this work and provided help in many ways.

CONTENTS

LIST OF FIGURES

LIST OF TABLES

ABBREVIATIONS

AEO	All engines operative
AFB	Air Force Base
AFM	Aeroplane flight manual
ARP	Aeronautical recommended practice
ASDA	Accelerate-stop distance available
ASDR	Accelerate-stop distance required
ASI	Airspeed indicator
BEA	British European Airways
CoA	College of Aeronautics, Cranfield University
CRT	Cathode ray tube
EPR	Engine pressure ratio
EPROM	Erasable-programmable read only memory
FAA	Federal Aviation Administration
FADEC	Full authority digital engine control
FAR	Federal Aviation Regulations
FOQA	Flight Operations Quality Assurance
IAS	Indicated airspeed
IC	Integrated ciruit
ICAO	International Civil Aviation Organization
IRS	Inertial Reference System
ISA	International Standard Atmosphere
JAA	Joint Aviation Authorities Committee
JAR	Joint Aviation Requirements
LED	Light emitting diode
MCP	Maximum continuous power
MTOW	Maximum take-off weight
NACA	National Advisory Committee for Aeronautics
NASA	National Aeronautics and Space Administration
NFLC	National Flying Laboratory Centre (College of Aeronautics, Cranfield University)
NLR	Nationaal Lucht-en Ruimtevaartlaboratorium
OEI	One engine inoperative
PF	Pilot flying

PNF	Pilot not flying
RAE	Royal Aircraft Establishment
RAM	Random access memory
ROM	Read only memory
rpm	Revolutions per minute
RTOW	Regulated take-off weight
SAE	Society of Automotive Engineers
SAT	Static air temperature
TAS	True airspeed
TAT	Total air temperature
TODA	Take-off distance available
TODR	Take-off distance required
TOPM	Take-off performance monitor
TORA	Take-off run available
TORR	Take-off run required
US	United States
USAF	United States Air Force

NOTATION

a	longitudinal (along runway) acceleration
$\bar{a}$	average longitudinal acceleration
a, b, c	variables of A, B, C
A, A', B, C	coefficients of the fitted 2nd order polynomial
C_D	coefficient of drag
C_L	coefficient of lift
D	drag
D_{comp}	3rd order compensation coefficient
D_{crit}	critical distance (scheduled distance to V_1)
D_{LO}	distance to lift-off
D_R	distance to V_R
D_{SCREEN}	distance to screen height
D_{STOP}	distance to come to a halt following a rejected run
D_1	distance to V_1
f, g	functions
k	weighting coefficient
k_1, k_2	constants
K, M, N	coefficients of the acceleration profile
L	lift
m	mass
M	mach number
n	parametric engine speed
N	engine speed
P, Q, R	constants
P_S	static ambient pressure
P_T	total pressure
R	gas constant
s	distance
S	wing reference area
t	time
t_1	time to V_1
T	thrust

v_w	wind speed (headwind component)
V	true airspeed
V_{act}	instantaneous velocity
V_{EF}	engine failure speed
V_g	ground speed
V_{LO}	lift-off speed
V_{MCG}	minimum control speed, ground
V_R	rotation speed
V_{SCREEN}	airspeed at screen height
V_1	decision speed
V_2	take-off safety speed
w	parametric static power
W	weight; power
$\bar{x}$	average

$\alpha_0, \alpha_1, \alpha_2$	coefficients of the thrust characteristic
δ	relative pressure
Δt	time elapse
Δw	parametric static power correction
ε	velocity error
γ	matrix variable; ratio of specific heats
$\gamma_1, \gamma_2, \gamma_3$	components of matrix γ
μ	coefficient of rolling friction
θ	runway slope; relative temperature
ρ	air density
σ	standard deviation; relative density

Chapter 1: INTRODUCTION

In order to take-off, a conventional fixed-wing aircraft must accelerate and achieve an airspeed allowing it to become airborne before the end of the runway and climb away over any obstacles. Further to this basic requirement, a number of safety restrictions are often also imposed to cater for other contingencies relevant to the operational environment of the aircraft in question. Transport aircraft heavier than 5700kg constitute the backbone of commercial aviation and they are classified as 'large' by the regulatory bodies[1]. Aircraft in this category are exposed to the most restricting of airworthiness requirements, defined in Part 25 of the regulations. Dealing with the certification of new aircraft types, Part 25 requires aircraft manufacturers to demonstrate that they meet specific performance criteria and the performance data must be made available to operators through the aeroplane flight manual (AFM). Operators are then obliged[2] to operate the aircraft within the prescribed limits of performance and in accordance with the procedures approved during certification. In this way, the Joint Aviation Authorities Committee (JAA) ensures that aircraft operations meet the safety requirements laid down by the organisation.

A fundamental concept in the Part 25 regulations is that the aircraft must be capable of continuing safe flight even if an engine failure is experienced during any phase of the journey, including take-off. Consequently, the very bases of the take-off manoeuvre and take-off performance of Part 25 certified aircraft are developed around this contingency. Since airfields are finite in length, a take-off effectively has to be aborted if an engine failure is experienced at low speeds early on in the run, since the reduced thrust may not be sufficient to allow the aircraft to become airborne within the remaining length of the runway. If, instead, the failure is experienced towards the end of the run, the take-off is continued because there might not be sufficient runway left to bring the aircraft safely to a halt. All large aircraft, including those with only two engines, are naturally designed with excess thrust installed in order to ensure that, even if one engine has failed, they continue to

---

[1] The two major regulatory bodies are the European Joint Aviation Authorities Committee (JAA) and the American Federal Aviation Administration (FAA). These bodies regulate general and commercial aviation through the Joint Aviation Requirements (JARs) and the Federal Aviation Regulations (FARs) respectively. The two documents are fundamentally similar, particularly in those sections concerning the certification of large aircraft, and only the JARs will be referred to in this text.

[2] Operators are regulated by the JAA through JAR-OPS 1, which classifies performance into Classes A, B and C. Further discussion in this text addresses multi-engined turbine powered large aircraft which constitute Class A.

accelerate and are capable of becoming airborne and climb away safely, clearing any obstacles. The take-off run can therefore be seen to consist of two stages, namely an initial stage during which the run must be aborted if an anomaly is detected, and a final stage in which the run must always be continued (unless the aircraft is clearly not airworthy). The critical point dividing the two stages of the run is identified as the decision speed V_1 by the regulations (Figure 1.1).

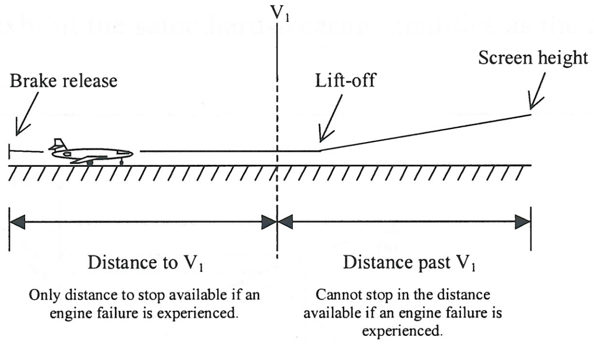

Figure 1.1: The decision speed V_1 as a point of no return during take-off.

The take-off manoeuvre is considered complete when the aircraft achieves the screen height[3] above the runway at a minimum airspeed of V_2 [4] or else when the aircraft has come to rest following a rejected run. The regulations appropriately define the distance required for the aircraft to reach the screen height from brake-release as the take-off distance required (TODR) and the distance required to bring the aircraft to a halt after aborting the run at the latest possible moment (V_1) as the accelerate-stop distance required (ASDR). The regulations also define another distance, the take-off run required (TORR), which is that required for the aircraft to lift off the runway. For a take-off to be successful[5] the runway must naturally accommodate all three distances required. In order to facilitate the operator ensuring this is actually the case, the equivalent distances available (defined as TODA, TORA and ASDA) of the relevant runway are declared and published.

---

[3] The screen height is currently 35ft for take-offs from dry runways and 15ft in wet conditions.

[4] V_2 is defined as the take-off safety speed that must be achieved before the screen height and guarantees the minimum climb gradient specified by the regulations is met.

[5] A take-off attempt is in this text defined as successful if the manoeuvre is completed without an accident and unsuccessful otherwise.

TODA, TORA and ASDA are not necessarily equal in length. TODA is longer than TORA whenever a length termed the clearway is available, even if it is unable to support the aircraft on the ground. The clearway must not have any obstacles projecting above a plane of 1.25% gradient from the end of TORA to ensure no interference with the take-off path of the aircraft, and can be either terrain or water. Its length is restricted to a maximum of 50% of TORA. ASDA is longer than TORA whenever a stopway is available. When present at the far end of the runway, this area must be capable of supporting the aircraft without causing any structural damage but need not exhibit the same hard-wearing qualities as the area in TORA.

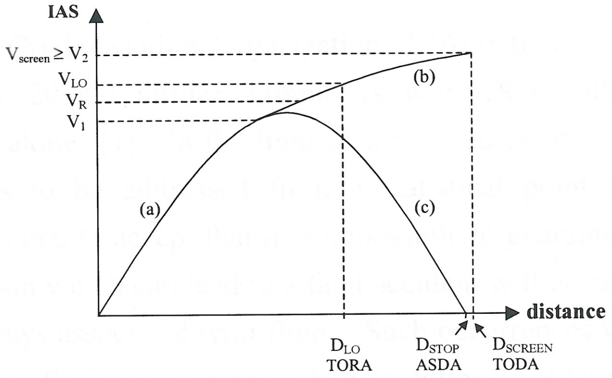

Figure 1.2: The take-off performance schedule.

(a) Acceleration to V_1, all engines operative (AEO). Sufficient runway is available to bring the aircraft safely to a halt if the run is aborted. In the event of an engine failure the run must be aborted as insufficient runway is available to allow the aircraft to lift off or reach screen height within the remaining runway distances (TORA/TODA).

(b) Acceleration past V_1 to V_R, V_{LO} and V_2. The aircraft becomes airborne before TORA and achieves screen height before the end of the runway (TODA). The aircraft is too fast and too far down the runway to be brought to rest in the remaining distance if an engine fails. Aircraft scheduled performance, however, allows the aircraft to achieve screen height even if an engine failure is experienced at any time.

(c) Run aborted at V_1. This is the latest point along the run at which the take-off may be aborted. The aircraft is brought to rest in ASDA using the retarding mechanisms allowed for by regulation. V_1 consequently defines a 'point of no return'.

The length of TODR, TORR and ASDR depend not only on the aircraft type, but also on a number of prevailing environmental and operational conditions such as ambient temperature, pressure and humidity, thrust setting, runway slope, wind conditions and aircraft dispatch weight. It follows, therefore, that the aircraft operators need to calculate the expected (scheduled) distances required for each take-off prior to dispatch to ensure that the distances available accommodate those required.

The two most significant variables within the operator's control which affect the scheduled distances are dispatch weight and scheduled thrust setting. On short runways, the dispatch weight may have to be limited to ensure that all required distances fit those available. In such circumstances the take-off is said to be field-limited. If, instead, the runway distances are not restricting, the scheduled thrust may be reduced, allowing the required distances to be increased to a point where the take-off is once again field limited. Such a practice is common as it contributes to prolonged engine life and favours noise abatement policies.

1996 International Civil Aviation Organization (ICAO) figures reveal that 16,000 aircraft[6] flew over 20,000 million kilometers with 18.5 million departures on scheduled services alone[7] [1]. In the light of these figures, it is not surprising that aviation safety has to be addressed from a statistical point of view. Such a perspective requires one to accept that it is impossible to guarantee 100% safe flight where no malfunction which can lead to a fatal accident will occur, and that a risk of fatal disaster is always associated with flight. Such occurrences will happen as long as aircraft continue to fly. It is necessary, then, to define what level of risk is deemed acceptable, or, in other perhaps more crude terms, what accident rate is considered satisfactory. The authorities decide on this figure by considering what level of risk the general public is willing to associate with flying. Unfortunately, every safety precaution comes at a financial cost, and whilst the normal passenger is most likely to expect the highest level of safety, he is just as unlikely to be prepared to pay higher fares to cover these costs [2]. This is not a unique situation, since after all, the balance between risk and cost is considered in many decisions taken in life.

In order to facilitate the quantification of the risk of accident associated with a failure or, indeed, any action or decision, the JAA defines occurrences according to their frequency (or probability of occurrence) and incidents according to the severity of their effects. What is considered as an acceptable accident rate is then defined by allotting probability limits to incidents. Current safety targets aimed for by the JAA are presented in Figure 1.3. Although this table is extracted from ACJ25.1309 [3] which deals with aircraft systems and is presented in the context of system failures, it

---

[6] MTOW 9000kg or more, not including China and the Russian Federation.

[7] Figures include only ICAO contracting states.

expresses the JAA's target failure rates and can be used directly to assess the risk associated with take-off[8].

Frequency of occurrence	Probability	Effect classification
Frequent Likely to occur often in the life of an aircraft	↓	**Minor** 'Normal' (< 10^{-2}) or Nuisance (<10^{-3}) effect on aircraft and occupants
	10^{-3}	
Reasonably probable Unlikely to occur often but may occur several times during the life of each aircraft	↕	**Minor** Results in operating limitations, emergency procedures adopted.
	10^{-5}	
Remote Unlikely to occur to each aircraft during the life of a number of aircraft of the type	↕	**Major** Significant reduction in safety margins. Difficult for crew to cope with adverse conditions. Passenger injuries.
	10^{-7}	
Extremely remote Possible but unlikely to occur in the total life of a number of aircraft of the same type.	↕	**Hazardous** Large reduction in safety margins. Crew extended because of workload or environmental conditions. Serious or fatal injury to a small number of occupants.
	10^{-9}	
Extremely improbable	↑	**Catastrophic** Multiple deaths, usually with the loss of the aircraft.

Figure 1.3: JAA relationship between probability and severity of failure condition.

Reconstructed from AMJ25.1309. Probabilities given per hour.

In the take-off environment a run aborted at slow speed might be classified as a minor incident whilst a high speed rejection close to V_1 would constitute at least a major incident, depending on the circumstances. In major incidents the crew could reasonably be expected to continue flight (and make a safe landing), notwithstanding the difficulties of doing so [2]. In comparison, a low speed runway excursion or failure to achieve the screen height within TODA, possibly hitting obstacles as the aircraft climbs away safely would constitute a hazardous condition. In such circumstances, the risk of catastrophe is potentially high (higher than 1 in 100, by definition and possibly as high as 1 in 2). Such occurrences are classified as an

---

[8] JAR-25 treats systems as a whole [2] and this allows the system failure rates in Figure 1.3 to be used to describe or address occurrences of incidents during various phases of flight, including take-off.

accident[9] whenever significant damage, injury or death results. High speed excursion or failure to become airborne resulting in a crash would be classified as a catastrophic accident.

In order to reduce the probability of an aircraft not achieving the screen height within TODA with all engines operative (AEO) to a level of 10^{-7}, a leeway is introduced in TODR. It can be fairly expected that different take-off runs carried out in the same operating and environmental conditions exhibit a normal distribution of the distances required to lift-off and achieve the screen height. Statistically, a variation of 5 standard deviations about the mean of a normal distribution caters for all but about 10^{-7} of the population. Variations of take-off distance and take-off run are expected to result in a standard deviation of 3% in the relevant distance [4]. Consequently, by allowing for 15% above the average TODR and TORR, it can be confidently assumed that these distances will prove adequate for all but 1 in about 10^{7} 'normal' take-off runs.

For the one engine inoperative (OEI) case the average TODR is not factored. As a result, if an engine failure is experienced at V_1, the aircraft will only have a 50% chance of achieving the screen height within TODA (in the case of the continued run), or coming to rest within ASDA (in the case the run is aborted). Nevertheless, the probability of such an outcome is calculated to be of the order of 10^{-7}, similar to that for a failed AEO take-off. The probability of an engine failure is expected to be less than 10^{-3} per hour of operation [5]. Assuming that a 4 second window around V_1 ($V_1 \pm 2s$) constitutes the greatest risk of an incident resulting in an unsuccessful run, the probability of an engine failure during this exposure period is expected to be about 10^{-6}. Taking into account the 50% probability of success associated with an engine failure at V_1 and the probability that such a situation develops in a field-limited run results in a risk factor of a similar order as for the AEO continued run case.

It may be noted that two values of TODR have been addressed, namely the factored value for the AEO case and the unfactored value for the OEI case. Naturally, the regulations stipulate that the scheduled value is the greater of the two. It is

---

[9] The definition of the term *accident* is in this text defined as [6]: An occurrence associated with the operation of an aircraft which takes place between the time any person boards the aircraft with the intention of flight and the time when all such persons have disembarked, and in which any person suffers death or serious injury, or in which the aircraft receives substantial damage. This definition originates from ARP-4107. The term *incident* is likewise defined as an occurrence other than an aircraft accident, associated with the operation of an aircraft, which adversely affects or could affect the safety of operations.

appropriate to point out at this stage that whichever is the greater largely depends on the aircraft engine configuration. Since all Class A aircraft are required to cope with a single engine failure, two engined aircraft must be capable of continuing the run, lift off and achieve positive climb in the dispatch conditions with one engine operating, whilst four engined aircraft are required to do so with three engines operating. It becomes immediately clear, then, that since the two engined aircraft has far more excess thrust available than its four engined counterpart in the AEO case, the former's factored AEO TODR could be less than the OEI calculated distance [7]. This may not be the case for a four engined aircraft.

The TORR is similarly defined by JAR-25 as the larger of the factored value for the AEO case and the unfactored value for the OEI condition. A further leeway, however, is introduced to increase the probability of a successful lift-off, by defining the distance as that from the start of take-off to the mid-point between the estimated lift-off point and the point at which the screen height is achieved. Leeway is introduced in the calculation of ASDA by allowing for ample time for pilots to react to an engine failure at a critical time close to V_1 and apply full braking. Whilst the regulations in general are designed to cater for the average pilot not possessing 'exceptional piloting skills or alertness', variation in piloting technique and even some extent of abuse are also catered for in the continued run case[10].

This discussion is primarily intended to address the significance of the authorities' concern with safety and the general mechanisms used to achieve the desired result. Consequently, various other important safety margins also in force have not been pointed out. These include allowing for only 50% of any estimated headwind component and 150% for any tailwinds in order to generate a conservative distance calculation, and imposing limitations on the allowable range of salient airspeeds such as V_1, V_R and V_2. Several other refinements have also been introduced through the years, such a clearer definition of V_1 and allowing for aircraft positioning on the runway prior to the start of the run.

When attempting the take-off, the crew is required to follow the procedure in the flight manual, which will invariably comply with Part 25 regulations. Once the

---

[10] JAR-25 requires manufacturers to allow for 'reasonably expected variations in service from the established take-off procedures for the operation of the aeroplane (such as over-rotation and out-of-trim conditions)', and this 'may not result in unsafe flight characteristics or marked increases in the scheduled take-off distance'. (JAR25.107(e)(4)). The term 'marked increase' is interpreted as 'any amount in excess of 1% of the scheduled take-off distance' (ACJ no. 2 to JAR25.107(e)(4)).

failure is detected by the crew. If an engine failure is experienced crew is well trained to continue with the take-off on the remaining are also trained to handle other serious incidents such as pilot / thus addressing issues which, although not directly involved with ce are equally as serious with respect to the outcome of the take-gins are further improved.

it attention the authorities devote towards aircraft performance and rements, other factors also implicitly take account of the safety ng take-off. Contingencies such as hydraulic failure, control loss, ı may cause further damage), brake failure and bird strike are all conducting a hazard analysis of the relevant system and the ented in Figure 1.3 are satisfied by design. Unsuccessful take-offs, › be a direct result of human factors or error[12]. Such causes are ıemes such as the development of sound operational procedures, ınel selection, rigorous training and human (and in particular crew) nent and enhancing cockpit ergonomics. Although these are ncepts and their effectiveness is perhaps difficult to quantify in they have definitely contributed significantly towards the overall in commercial aviation.

nsiderations towards safety have been successful in reducing the ent rate in commercial aviation to the region of 1 in 10^6 flights by], with those related with take-off constituting approximately 12%

---

craft require a two man crew, one of whom, the pilot flying (PF), will have control of the her, the pilot not flying (PNF), assists the PF by monitoring the progress of the run.

at any incident or accident can be invariably traced back to human error. In this context, nt resulting from human error is considered to be one in which an error of action, dure directly results or contributes to an unsuccessful take-off.

thrust is set to the desired value, the aircraft is allowed to accelerate down the runway. The pilot not flying (PNF)[11] monitors the engine instruments and the airspeed indicator (ASI), calling out a selection of pre-decided salient speeds, including V_1, V_R and V_2, as the aircraft transits them. At V_R the pilot flying (PF) rotates the aircraft at the desired rotation rate to the target attitude and as the aircraft unsticks, it climbs out at a pre-determined airspeed. This is usually achieved by flying on instruments such as the ASI and the Flight Director to control attitude and airspeed. Whilst it is mandatory to abort the run if an engine failure is experienced before V_1, it is also common practice to abort the run at an early stage if any significant system failure is detected by the crew. If an engine failure is experienced at or past V_1, the crew is well trained to continue with the take-off on the remaining engines. Crews are also trained to handle other serious incidents such as pilot incapacitation. By thus addressing issues which, although not directly involved with aircraft performance are equally as serious with respect to the outcome of the take-off run, safety margins are further improved.

Besides the explicit attention the authorities devote towards aircraft performance and field length requirements, other factors also implicitly take account of the safety requirements during take-off. Contingencies such as hydraulic failure, control loss, tyre bursts (which may cause further damage), brake failure and bird strike are all considered when conducting a hazard analysis of the relevant system and the requirements presented in Figure 1.3 are satisfied by design. Unsuccessful take-offs, however, can also be a direct result of human factors or error[12]. Such causes are challenged by schemes such as the development of sound operational procedures, appropriate personnel selection, rigorous training and human (and in particular crew) resource management and enhancing cockpit ergonomics. Although these are relatively new concepts and their effectiveness is perhaps difficult to quantify in traditional terms, they have definitely contributed significantly towards the overall increase in safety in commercial aviation.

The numerous considerations towards safety have been successful in reducing the overall fatal accident rate in commercial aviation to the region of 1 in 10^6 flights by the mid 1990s [1], with those related with take-off constituting approximately 12%

---

[11] Part 25 certified aircraft require a two man crew, one of whom, the pilot flying (PF), will have control of the aircraft whilst the other, the pilot not flying (PNF), assists the PF by monitoring the progress of the run.

[12] It is often argued that any incident or accident can be invariably traced back to human error. In this context, however, an incident resulting from human error is considered to be one in which an error of action, judgement or procedure directly results or contributes to an unsuccessful take-off.

of this figure [8, 9]. This translates to a fatal accident currently occurring on average approximately once every two weeks. In anticipation of the significant increase in air transport expected within the next fifteen years, the FAA is currently committed towards reducing the 'U.S. aviation fatal accident rate per aircraft departure, as measured by a year moving average, by 80 percent from the year average for 1994-1996' [10]. If such an improvement in safety is to be mirrored in the take-off phase of flight, the adequacy of current procedures needs to be questioned. The most crucial aspect of the take-off run is the crew's continuous decision up to V_1 to continue with or else abort the run. In order to effectively carry out this task, good situational awareness is required. The crew must effectively be able to also determine the risk factor associated with either decision at all times and if an incident occurs, quick, correct identification of the problem and its effect on either option must be determined. This task is rendered particularly difficult by the fact that during take-off the aircraft is accelerating in the very close proximity of obstacles, allowing only at most a few seconds for the crew to correctly identify and react positively to any anomaly.

Unfortunately, current flight decks are not sufficiently equipped to provide good situational awareness to the crew. Several monitoring systems in the cockpit do allow crews to check the condition of various systems, including engines, tyres, brakes and numerous others which may or may not be vital to safety during take-off. What is crucially unavailable, however, is a system or method whereby the crew can objectively assess the aircraft's performance through the progress of the take-off run. Despite all the pre-dispatch attention towards scheduled distances, when it comes to the actual take-off manoeuvre, crews are not adequately equipped to determine the aircraft's position on the runway. As a result, they cannot really relate the progress of the run with the achieved airspeed and it is not possible for them to objectively judge whether the aircraft's performance is within the scheduled threshold - that is, whether the aircraft will lift-off and achieve screen height within the scheduled values of TORR and TODR respectively, or, in the case of a rejected run, it is capable of coming to a stop within the calculated ASDR.

It is true that the leeways introduced are designed to ensure statistically, with the desired probability, that the aircraft will actually perform within the limits expected, but the whole procedure, in effect, is an open-loop operation. Once the dispatch conditions are calculated, the aircraft is left to perform within particular performance limits and no real attempt is made to assist the crew in confirming that this is actually the case. In fact, crews only have their intuition and experience to go by in measuring the aircraft's progress and considering the fact that they operate different aircraft in continuously changing operating conditions, detecting subtle under-performance would at best be described as difficult. In any case, such judgement is invariably subjective, which surely is not satisfactory in critical conditions. This is a serious shortcoming, particularly in the light of the crew's role becoming an increasingly managerial and supervisory one.

Although marginal safety improvements can be achieved by further enhancing system reliability and refining pre-dispatch and take-off procedures, there is doubtless sufficient scope in providing a system on the flight deck that enables the crew to objectively monitor the progress of the run. In this way, the performance issue can become, like so many other situations in aviation, a closed-loop one, where actions or decisions taken in advance are at appropriate times checked out to ensure that their effects are those originally desired. A system providing such feedback on performance can be defined as a take-off performance monitor, the primary role of which would be to provide objective and timely indication of whether the take-off attempt is progressing in a satisfactory manner or otherwise.

Although at face value a take-off performance monitor might be considered useful only in field-restricted cases, further consideration suggests otherwise. Not only can such a system be designed to identify shortcomings in performance that, whilst allowing the safe continuation of the run, may result in more serious problems in flight, but it also provides means to monitor the trend in take-off performance of specific aircraft. Such a facility will fit well with and enhance the scope of Flight Operations Quality Assurance (FOQA) programmes[13] used to improve safety during flight.

It may also be possible to exploit commercial advantages from the installation of a take-off performance monitor. By effectively reducing the risk of accident during take-off, some leeway in the scheduled TODR, TORR and ASDR may be relaxed whilst maintaining the desired level of risk associated with the manoeuvre. From an operational point of view, this would directly translate to higher regulated take-off

---

[13] The main goal of FOQA programmes is to identify data from 'uneventful' flights in order to pick out potential problems and correct them before they lead to accidents.

weights (RTOWs)[14] in field-limited cases. This is very attractive to airlines, as it would allow aircraft to carry a larger payload further from short runways.

The work involved with this programme has been mainly focused on the development of an algorithm which can reliably provide situational awareness to the crew in terms of whether the aircraft is performing as expected or otherwise. In order to achieve this, a concept for effective monitoring had first to be developed. This paved the path for the algorithm design which, once finalised, was validated with flight testing on the National Flying Laboratory Centre's (NFLC) Jetstream-100 G-NFLC and with records of actual take-offs of large jet transports in commercial operations. A basic display was also developed to assist visual interpretation of the results. Although not a task defined within this project, its design has been carefully considered so that it could form a sound basis on which an acceptable display could be proposed following further study. The merits of the models available for performance estimation and a discussion of monitoring designs to date are also presented in this document so that the reasons behind the philosophy and several design decisions could be well appreciated.

---

[14] The RTOW is the maximum take-off weight in field-limited take-offs allowed by regulation that will still allow the runway to accommodate TODR, TORR and ASDR.

Chapter 2:

PREDICTING TAKE-OFF PERFORMANCE

THE EQUATIONS OF MOTION

2.1 Introduction

The take-off run constitutes a complex manoeuvre and, as a result, several models have been developed for performance prediction, each providing a trade-off between accuracy and complexity of formulation. The aircraft is usually approximated to a point mass, thus facilitating the application of Newton's Laws to describe the motion of the vehicle. The most detailed of these models results in no particular reduction of accuracy when compared to a full six-degree-of-freedom model, whilst enjoying a significant reduction in complexity of algorithm. The equations discussed herein provide adequate accuracy for the purpose of real-time performance monitoring and are also used in the calculation of scheduled performance.

In order to optimise on accuracy with point mass formulation it is necessary to split the manoeuvre into a number of phases according to the attitude or motion of the aircraft during that period. Four phases are clearly identified. The ground roll phase describes the motion of the aircraft from brake release to rotation, a period during which the aircraft attitude and therefore the coefficients of lift and drag, are largely constant. The rotation phase commences with the initiation of the pilot's action to rotate the aircraft and ends when the aircraft has just become airborne, giving way to the transition phase. During this phase the aircraft's pitch is increasing, resulting in a curved airborne trajectory. It terminates when the aircraft attains a steady climb gradient and once this is achieved the aircraft is considered to be in the fourth phase, termed the climb-out phase (Figure 2.1).

In the case of the rejected take-off, the run can be split into three phases. The acceleration phase describes the aircraft's motion prior to an anomaly or the initiation of any aborting action by the crew, whilst the transition phase covers that period during which the aircraft's configuration is dynamic as thrust is reduced and braking mechanisms applied. Once full braking is established, the deceleration phase commences, describing the motion of the aircraft until it is brought to a halt.

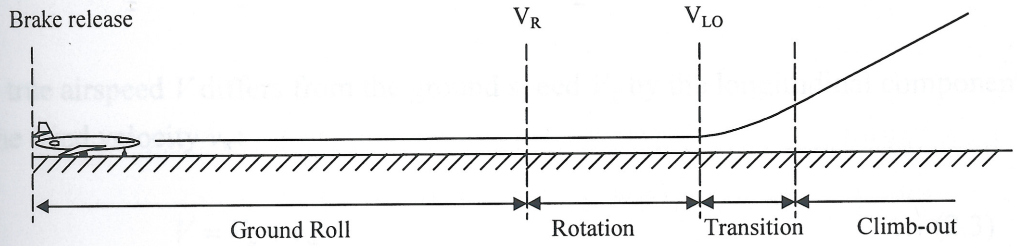

Figure 2.1: The four phases of take-off.

2.2 The ground roll phase

The external forces acting on the aircraft are shown in Figure 2.2.

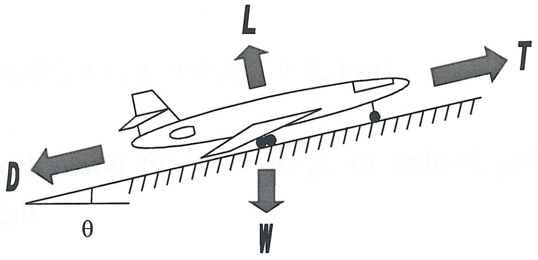

Figure 2.2: The forces acting on the point mass model of the aircraft during take-off.

Resolving along the runway:

$$T - D - W \sin\theta = ma \qquad \ldots (2.1)$$

The total drag D comprises the aerodynamic drag and rolling friction:

$$D = \frac{1}{2}\rho V^2 S C_D + \mu\left(W\cos\theta - \frac{1}{2}\rho V^2 S C_L\right) \qquad \ldots (2.2)$$

The true airspeed V differs from the ground speed V_g by the longitudinal component of the wind velocity v_w:

$$V = V_g + v_w \qquad \ldots (2.3)$$

The acceleration a is therefore expressed, in terms of ground speed, as:

$$a(V_g) = \frac{T - \left[\frac{1}{2}\rho S\left(C_D - \mu C_L\right)\right](V_g + v_w)^2 - W\left[\sin\theta + \mu\cos\theta\right]}{m} \qquad \ldots (2.4)$$

where T is also a function of (V_g+v_w).

The thrust function T is quite adequately modelled as a second order polynomial of true air speed:

$$T = \alpha_0(V_g + v_w)^2 + \alpha_1(V_g + v_w) + \alpha_2 \qquad \ldots (2.5)$$

This results in the acceleration function $a(V_g)$, or indeed, $a(V_g+v_w)$, also being a second order polynomial:

$$a(V_g) = \frac{K(V_g)^2 + M(V_g) + N}{m} \qquad \ldots (2.6)$$

where: $K = \alpha_0 - \frac{1}{2}\rho S(C_D - \mu C_L)$ … (2.7)

$M = 2\alpha_0 v_w + \alpha_1 - v_w\rho S(C_D - \mu C_L)$ … (2.8)

$N = \alpha_0 v_w^2 + \alpha_1 v_w + \alpha_2 - \frac{1}{2}v_w^2\,\rho S(C_D - \mu C_L) - W(\sin\theta + \mu\cos\theta)$ … (2.9)

The distance D_R from brake release to rotation is given by the solution of the differential equation:

$$a = V_g \frac{\partial V_g}{\partial s} \qquad \text{... (2.10)}$$

Therefore,

$$D_R = \int_0^{V_R - v_W} \frac{mV_g}{K(V_g)^2 + M(V_g) + N} dV_g \qquad \text{... (2.11)}$$

For the purpose of calculation a number of parameters have to be assumed constant, either because the actual variations have an insignificant effect or else because the variation simply cannot be reliably predicted with current state-of-the-art technology. Weight change due to fuel burn and variations in the coefficients of lift and drag resulting from the slight variations in flap settings and aircraft pitch fall under the former category. The estimation of rolling friction[15], ambient temperature and pressure (density[16]) and wind vector fall under the latter, since these are actually complex functions of either time or position. Runway slope is often approximated to an average value, even though in extreme cases this approximation can significantly affect the prediction accuracy [7].

An alternative to Equation 2.11 for determining the ground roll distance is to identify an average equivalent acceleration for the period of the phase[17] and then use the equations of constant acceleration to determine the distance to V_R:

$$D_R = \frac{(V_R - v_w)^2}{2\bar{a}} \qquad \text{... (2.12)}$$

Boeing claim that this simpler formulation has an accuracy of within 1% [11]. Equation 2.12 can be readily modified to determine the distance-to-go to V_R in real time at any point during the run.

---

[15] Rolling resistance of an aircraft on a dry, hard runway can account for up to 10% of the aircraft's available thrust, and is of the same order as the aerodynamic drag. The value of the coefficient of friction, however, is known to vary along the run and is a function of wheel speed, tyre loading and inflation pressure [12]. When operating from contaminated runways, predicting rolling friction is particularly difficult due to the complex phenomena involved [13].

[16] The ambient density also significantly affects the coefficients of the thrust function, the accurate determination of which is clearly of paramount importance for distance prediction purposes.

[17] The average acceleration would be numerically equal to the acceleration at $0.7V_R$.

2.3 The rotation phase

The rotation phase is a highly dynamic manoeuvre, during which the acceleration, lift and drag of the aircraft all vary significantly. The duration and distance covered are largely dependent on how close to the target rotation speed the rotation is initiated and on the technique adopted in the actual rotation of the aircraft. A study carried out by the Royal Aircraft Establishment (RAE) at Bedford involving 422 take-offs by 23 pilots in a De Havilland Comet 3B reveals that a scatter of about 10kts exits in the actual rotation and lift-off speeds [14]. Rotation rates measured were mostly between 2° and 5° per second. Although these results[18] are over 35 years old and were obtained from a first generation jet transport aircraft, there is no reason to suggest that similar variations should not be expected in operations today, as the instrumentation and techniques currently in operation are largely the same as those used during the original tests. Besides the fact that the ASI is not designed for dynamic measurements and the low speeds associated with take-off, the procedure initiating rotation is inherently susceptible to variations in the actual rotation speed. As the PNF monitors the ASI, the rotation point has to be signalled to the PF and this introduces an added difficulty in selecting the correct moment for the initiation of rotation. The rotation profile commanded by the PF also significantly affects the distance covered and this varies not only between crews but also with aircraft weight and balance. This all contributes to a large uncertainty in the rotation distance covered.

In these circumstances and considering the complexity of the dynamic situation, only what effectively is an allowance for the distance covered during the rotation phase can be determined. One method is to calculate the product of the average velocity $(V_{LO}+V_R)/2$ with an allowance for the rotation time determined by flight testing [11]. Alternatively, the rotation time can be obtained by dividing the target rotation angle with the desired average rotation rate, usually in the order of 3°/s, or even by simply allowing 3s [15]. Such allowances highlight the approximate nature in predicting performance during rotation.

---

[18] The results of a joint NASA/FAA study [16] conducted a few years later at NASA Ames Research Centre agree with the RAE data.

2.4 The transition and climb-out phases

The transition phase exhibits similar difficulties when attempting to predict the distance requirements. Once again, variations in lift-off speed and piloting technique are the factors mainly affecting this distance. The transition trajectory is usually approximated to a circular arc and is discussed in detail in a number of textbooks [15, 17]. As the trajectory of the aircraft becomes a steady climb the transition phase gives way to the climb-out phase. The aircraft may or may not achieve the screen height during the transition phase and this increases the complexity and uncertainty of the calculations involved. An alternative and probably equally valid technique is to calculate an airborne-distance-to-screen-height by multiplying the average velocity $(V_{LO}+V_2)/2$ with an allowance for the time required determined once again by flight testing [11]. Nevertheless, the uncertainty involved during this phase must not be underestimated, with the RAE study revealing a variation of up to ±30% in the airborne distance to 35ft in their results.

2.5 The OEI case

The distances required to the screen height following an engine failure can be calculated in a manner similar to that described above for the AEO case and allowing for failed engine spool-down and for the reduced thrust and increased drag in the post-engine-failure phases. The ground roll phase is usually also split into a normal (AEO) run up to V_{EF} and a reduced thrust segment up to V_R.

2.6 The rejected take-off case

The distance of interest in the rejected take-off case is that required to bring the aircraft to a halt. Two approaches are available for the calculation of this distance in real-time calculations. One relates to the distance requirement if the run were to be rejected immediately, whilst the other considers the worst case, allowing for a rejection at the latest possible moment (V_1). The two techniques are largely similar, differing only in the point at which the transition phase is assumed to start.

The transition phase can only be calculated by allowing for the regulated reaction time of the crew to reduce thrust and deploy maximum braking, since the actual crew response cannot be predicted. Likewise, the braking distance required to bring the aircraft to a halt can only be calculated assuming reference braking performance, since the braking capacity is very dependent on a host of parameters such as runway, brake and tyre condition, the actual values of which cannot as yet be determined with any significant accuracy or confidence.

Chapter 3:

TAKE-OFF PERFORMANCE MONITORING

A REVIEW OF CONCEPTS TO DATE

3.1 Introduction

Before the introduction of jet aircraft into civil air transport operations there was serious concern within the aviation community regarding the take-off performance of this new class of aeroplane, as these aircraft were to be heavier and have significantly different performance characteristics when compared with their piston-engined counterparts. This led to the general belief that the safety margins associated with take-off would be seriously reduced and that action had to be taken to reduce the risk of accident. Such was the concern that two new instruments were conceived: the take-off monitor and the take-off director [18, 19]. Whilst the latter would direct the pilot in rotating the aircraft to reduce the variation in performance due to piloting technique, the former would assist the crew in determining whether all was well during the first part of the run before rotation. It was thus hoped that together these systems would reduce the possibility of over-running the end of the runway or failing to take-off within the runway constraints.

Notwithstanding the various efforts to develop such instruments, jet transport aircraft were brought into service without either instrument [20]. In the absence of the performance monitor manual line-checks were introduced in an attempt to obtain an indication of the progress of the run. The speed-time check, where the time to a pre-determined airspeed (usually 100kts) is measured, was widely used by early operators of the B707 and DC-8 [21]. The technique, however, eventually fell into disuse, mainly because of its lack of accuracy and reliability [21, 22, 23]. This must have been not only due to the inaccuracies involved with the time measurement, but also because of the lag effects of the ASI and the technique's failure to indicate situations of acceleration degradation at higher speeds. There is at least one documented incident where a B707 inadvertently overloaded by 22,000lbs just managed to take-off despite the fact that the time-to-100kt check was within 1s of that scheduled for the planned take-off weight [24]. In fact, trials carried out by

British European Airways (BEA) [21, 25] indicated that speed-time measurements, after correction to standard conditions, exhibited a large scatter in the results, with a standard deviation of 6.1% (1.4s) in the time-to-100kt. The military adopted the distance-to-speed check, but the BEA trials indicated that their speed-distance checks at 700 yards resulted in a standard deviation of just under 5kt, or 5.1%. In contrast, the time-to-700-yards exhibited a standard deviation of 0.55s, or 2.5%. Nevertheless, these techniques are considered to have the significant disadvantage of distracting the crew from their normal duties at a critical phase of flight and this is not desirable [22]. These line checks were, in fact, not totally satisfactory, but were used because operators had no better tool with which they could measure performance.

Throughout the years numerous performance monitor designs have been proposed but all seem to have been considered unacceptable for one reason or another. As a result, no system has seen any operational service to date [9]. This lack of success has effectively been due to the difficulty experienced in creating a system capable of repeatedly providing information that is useful and reliable under all operational circumstances. Such a shortcoming generated serious opposition to the cause of take-off performance monitors in various sectors of the aviation community, resulting in a split in the view of the system's merits [26, 27, 22]. The situation today is that the issue of take-off performance monitoring does not really feature in the list of those involved with aviation safety, with attention and effort being directed to several other problems of seemingly higher priority. Nevertheless some interest does exist, and there are a number of patents in force at the time of writing, including ones filed by NASA [28], Boeing [29] and Aerospatiale [30]. There was an intention by Boeing to introduce their system with the first deliveries of the B777 [31] although this did not materialise, whilst Airbus are reportedly testing their design for introduction with the A340-500/600 in 2002 [32].

The history of take-off performance monitoring designs now spans half a century, during which time a technological development of major significance has been witnessed. As in the case of all control and other monitoring systems, the availability of high performance digital computers has taken the scope and capability of take-off performance monitors to a different dimension. Not only do they facilitate the numerical solution of the equations of motion, thereby allowing the use of better models for more accurate predictions, but now the display features can be well exploited to optimise information transfer to the crew. It is justified, therefore, to classify designs into two groups, namely the early type and the modern type, distinguished by the use or absence of digital processors for computing mathematical functions. The following text presents a review of the approaches adopted and the technologies used in the various designs proposed to date, thus providing a basis for comparison with the merits of the design developed in this work.

3.2 Early monitoring techniques

The absence of powerful digital computers rendered difficult the accurate modelling of aircraft dynamics, let alone the breakdown into the different flight phases. Faced with this problem, a number of designs centered on acceleration monitoring, with the premise that if the acceleration were sufficient (greater than the scheduled value), then the take-off would be viable and progressing well. This approach was adopted in an instrument constructed and tested at the NACA Langley Flight Research Division in the early 1950s [33]. Tests carried out early in the development stage and verified through flight testing on a jet fighter showed that acceleration dropped linearly with dynamic pressure. This principle was then used to design an instrument which displayed a constant reading of acceleration on an analogue display by compensating for the drop in acceleration with a component derived from dynamic pressure measured through the pitot-static system. A constant reading could be easily monitored by the crew and is conducive to the rapid detection of anomalies and sub-normal performance. Operational conditions were taken into consideration as prior to take-off the crew would obtain the expected (scheduled) display reading against which they could compare the actual compensated acceleration. It was claimed that calculations indicated that for all conditions under which take-offs were likely to be made, the ratio of scheduled to displayed acceleration would be approximately proportional to the ratio of the respective take-off distances. Thus the system would effectively indicate to the crew the safety margin associated with the take-off, assuming, obviously, that conditions did not change for the remainder of the run.

As the system depended on acceleration measurements, it was quick to respond to changes in performance due to discrete anomalies such as an engine failure. The system exhibited a 1Hz oscillation of up to 3% of the mean reading but although undesirable, this was not considered a serious defect. Later tests, however, exhibited larger fluctuations of up to 25% of full scale, and these were found to be due to a design fault of the instrument, rendering it unreadable [34]. Further damping was consequently introduced to increase the time constant of the instrument to approximately 1.5s, allowing the needle to settle at its constant position within 6s of brake release whilst not seriously compromising its capability of indicating a loss of thrust. In this way the oscillations were reduced to ±5% whilst the needle average position remained within about 1% throughout the run up to 140 miles per hour, confirming theoretical calculations. This system was further developed by Sperry Gyroscope Company [35] under USAF sponsorship and was one of at least four[19] monitors evaluated at Wright-Patterson AFB, Ohio, between 1959 and 1962 [36, 37, 38][20].

A Minneapolis-Honeywell Regulator Company's design was also evaluated at Wright-Patterson AFB. Essentially an acceleration monitoring system [40], rather than compensating the measured acceleration with dynamic pressure, the scheduled (steady) acceleration was compensated for according to the distance gone down the runway. Acceleration was measured via an accelerometer, whilst the distance gone was obtained from an odometer driven by a wheel on the aircraft's landing gear. In contrast with the Sperry system, this instrument only displayed an abort warning light, and this was illuminated if the measured acceleration was below the compensated scheduled value. The system also computed, from the acceleration and braking profiles according to the variables input by the pilot, the point of no return on the runway and the abort signal was only enabled if this point was not passed. It is worth noting that this system depended largely on resistive components to model the required characteristics, and the point of no return was set by the pilot with the aid of a null-meter.

Doman Helicopters Incorporated also designed an acceleration measuring instrument, called the Darto (for Doman Acceleration Rate Takeoff [21, 41] – and according to the 1958 reference, also allowed for the expected drop in acceleration as the aircraft speed increased. The actual acceleration, however, was obtained by differentiating the ground speed measured from a wheel revolution sensor, rather than an accelerometer. The system displayed the acceleration margin on a centre-zero analogue meter with the two halves labelled go and no/go. The later reference

---

[19] Instruments designed by the John Oster Manufacturing Company, Kollsman Instrument Corporation and Minneapolis-Honeywell Regulator Company were also evaluated at Wright-Patterson AFB. The Oster system essentially used the same design principle as its Sperry counterpart [39].

[20] References 36, 37 and 38 describing the evaluations are not available outside the United States. These references are cited in reference 39.

claims the acceleration signal was then used to estimate the distance still required to achieve take-off speed and it was the leeway resulting from its comparison with the scheduled distance that was displayed.

Considering the fact that the characteristic drop of acceleration with forward airspeed was already appreciated in the 1950s, it is perhaps quite surprising that a number of later designs endeavored to assume that the acceleration remains constant during the run. In fact, in a 1964 patent granted to United Aircraft Corporation [42] the acceleration is claimed to be generally constant during the take-off run because 'both the engine thrust and drag build up with air speed'. The viability of the take-off run was given as a measure of the velocity margin between the scheduled airspeed and that predicted at the end of the expected time-to-lift-off, using an acceleration value calculated from the rate of change of indicated airspeed. This margin was presented in analogue format on a centre-zero meter with go and stop regions on either side of the centre. An even more basic design was also granted a patent 22 years later [43], in which the inventor proposed using a reservoir with a vertical limb displaced to one side, up which a coloured liquid rose during acceleration. The level of the meniscus was effectively intended to indicate the amount of acceleration, so that this could be compared to an adjacent card, adjusted to take into consideration the dispatch weight, indicating the take-off and abort zones. It is not surprising that these designs did not go past the patenting stage.

A serious drawback of acceleration monitoring is that in reality it fails to objectively relate to the distance remaining and therefore may not always correctly determine the viability of continuing or rejecting the run. Concern regarding this shortcoming was documented as early as 1959 [44], leading Sperry Rand Corporation to propose a system which predicted the distance required to achieve the take-off airspeed. The acceleration was assumed to be constant and its chosen value would either be that measured at that instant or the average between the measured value and that expected at the target airspeed, with the latter option providing a better estimate. The distance margin was displayed on a centre-zero meter with go/no-go halves and a distance-to-go tape presented the aircraft's current position and the latest point at which the run could be aborted. A fundamentally similar system, called the Ground Run Predictor, was developed at Smiths Aviation Division [45, 46]. The value of acceleration used in the calculation of the distance to go, however, was that measured at the moment, factored by a quantity defined as a function of airspeed. The system determined the margin in the distance to V_1 and displayed this value on a moving tape mechanical meter.

An alternative and perhaps equally attractive approach to performance monitoring was the attempt to mechanise any of the three line checks already discussed. This was the technique adopted by Kollsman Instrument Corporation, whose instrument effectively performed a speed-time check [21]. A small moving marker (bug) indicating the scheduled airspeed at that particular time moved along the perimeter of the ASI and its position relative to the ASI needle continuously indicated the progress of the run [35]. Notwithstanding the fact that the speed-time technique was found not to be of any practical use during the Wright-Patterson AFB tests [39], a system effectively based on the same technique was patented in 1981 [47]. The time-to-V_1 was split into 10 equal segments and at each of these ten instances the actual airspeed would be compared with the scheduled value calculated from the threshold acceleration. The scheduled and threshold quantities were determined using the equations of motion for constant acceleration, using the distance to the latest point at which the run could be aborted at V_1 and the selected value of V_1 to determine the threshold acceleration. Three lights named 'take-off prohibited', 'take-off permitted' and 'abort take-off' were driven by the relevant logic, with the abort signal illuminated if the actual velocity was lower than expected on at least at three of the ten instances of comparison. Another idea also based on the speed-time characteristic was patented in 1998 [48, 49]. This design proposed the introduction of an extra needle on an analogue ASI driven by the scheduled speed-time profile, against which the pilot could assess the actual performance. For the modern tape-type instruments, an arrow, the length of which indicated the margin was proposed. The two versions also proposed displaying the distance margin at each moment in real time in numerical format.

Avien Incorporated attempted to mechanise the speed-distance check in the 1950s by comparing the actual and scheduled ground speeds at three pre-selected distances, displaying the result as a flashing red or green light and the distance gone on a counter type display [40][21]. Another system, called the V-theta monitor, also measured the progress of the ground speed with distance, but this comparison was performed at only three discrete instances. The first two were intended to alert the crew of poor performance, whilst the third would give the signal to abandon take-off [21].

---

[21] In a later version, the 'effective thrust' was compared to its scheduled counterpart [21, 9].

Another design intended to provide a continuous speed-distance check was proposed in the 1950s [50]. A mechanical pointer, the position of which was driven by the measured aircraft speed and distance gone, tracked over a special plate, part of which was conductive. With the delineation between the conductive and non-conductive parts describing the scheduled velocity-distance characteristic, the pointer's position (whether above or below the scheduled performance, either in the conductive or non-conductive area) determined whether a red or green light was illuminated. Another pointer tracking the scheduled characteristic drove a second needle on the ASI representing the reference performance for the particular position of the aircraft at the time, thus allowing the crew to quantitatively appraise the progress of the run. The values of V_1, V_2 and the distance to V_1 were also displayed numerically. This display proposal replaced an earlier suggestion of displaying only a 'safe', 'more than safe' or an 'unsafe' indication.

In a later design [51] the speed-distance characteristic was modelled with specially manufactured potentiometers, the wipers of which were driven by a servo according to the distance covered. Different potentiometers were used to simulate different operating conditions and other variable resistors were employed to compensate for effects of operational variables such as weight, temperature, pressure and runway slope. The design suggested the display of scheduled performance in the form of a tri-coloured band running along the ASI. The three colours defined the speed ranges that corresponded to satisfactory, marginal and unsatisfactory performance. This display seems to have been developed in favour of two other displays previously proposed by the inventor, both of which essentially displayed the distance-to-to to decision point and the outcome (go/no-go indications) of speed-time checks at three particular instances along the run [27].

Perhaps the ultimate in the early monitor designs was developed at the Massachusetts Institute of Technology [52]. This design acknowledged the problem of accelerometer bias generated by the gravitational component due to aircraft pitch and resolved the problem by employing two accelerometers aligned perpendicular to each other in the vertical plane[22]. Using analogue computing techniques to provide the various mathematical functions required, the system used either the scheduled or measured thrust and measured acceleration to estimate the rolling friction. The AEO distance to V_1, the OEI distance between V_1 and V_2 and the braking distance (both

---

[22] The patent provides the mathematical description of how this is achieved.

from the present position and from V_1) were then predicted by solving the equations of motion. Allowances for the increase in drag and reduction in rolling friction as the run progressed were provided by applying appropriate analogue feedback in the relevant integrating blocks. The braking friction was assumed to be proportional to the estimated rolling friction in the acceleration phase up to a maximum allowed value. The margins estimated at V_1 were to be displayed in the form of a sector of an arc coloured green on a CRT, the angle of which represented the amount of margin available. The display would illuminate in red when no margin is available, and an extra red indicator indicating an emergency situation where the crew must abort the run immediately was also suggested.

Whilst all the systems discussed up to this point were designed to be installed on the flight deck, Northrop Corporation took a different tack in the 1950s and developed a ground based system in an attempt to overcome the technological hurdles associated with airborne equipment of the time [53]. The system, developed at the company's Northronics Division, used a Doppler Radar to determine the aircraft's position, from which the distance to go to lift-off was then calculated and compared with the runway distance remaining. Being completely ground based and physically independent of the aircraft in question, the system was intended to be operated by the ground controller who would input the details of the aircraft and would have a go/no-go display during the take-off run. Enjoying no restriction on weight, it could afford greater complexity than its airborne counterparts (although it would have been far more expensive to install [35]. The system triggered automatically with the aircraft's velocity and as it crossed a pre-determined point on the runway and predicted the aircraft's lift-off point by calculating the expected distance to lift-off assuming an equivalent constant acceleration measured as the average of the current value and that expected at lift-off. Two modes of operation were intended, allowing the comparison of the expected lift-off distance to either that normally expected or to the latest possible before the end of the runway. Another ground based system patented in 1978 [54] relied on measuring the time the aircraft takes to transit 'gates' positioned along the runway to determine the aircraft's velocity and acceleration. The system was intended to be predictive, modelling the velocity of the aircraft as a third order polynomial of distance. The coefficients of the polynomial were updated according to the ratio of the measured and scheduled acceleration, and in this way the distance to go could be compared to the remaining runway distance. The scheduled braking distance was also taken into account to determine the viability of aborting the run. It was proposed to provide two methods of indicating the viability of continuing and aborting the run, either via radio link to the cockpit or through suitable visual signals along the runway.

The variety of the display designs proposed underlines the lack of agreement on what and how information is best presented to the crew[23], the situation being significantly aggravated with the flexibility offered by modern flight displays. From the early designs, Servomechanisms Incorporated took a very bold step in the 1950s by appreciating the importance of the form of presentation and believing that the display requirements should effectively dictate the system design. They appreciated the pilot's role in the loop and the importance of effective display of the information presented. They proposed a strip display representing the runway on which the scheduled and predicted take-off points, together with the point at which the aircraft would be brought to rest under full deceleration[24], were superimposed. The distance required for take-off was obtained by matching the distance gone and current IAS to a particular take-off characteristic within a family of such, and then using the chosen curve to predict the take-off point. Servomechanisms elected to obtain distance measurement from a ground wheel sensor on the landing gear because of a lack of accuracy they experienced when using accelerometers. Boeing had conducted studies which showed that the equivalent circumference of the tyre varied linearly with distance down the runway, suggesting that the plot of distance vs. wheel revolutions would be parabolic, thus allowing the effect of the variation in tyre circumference to be taken into account [55].

3.3 Modern performance monitors

The introduction of digital processing facilities has completely revolutionised the realisation of take-off performance monitors. Although early microprocessor-based digital computers were significantly constrained by their limited processing power when compared to today's systems, the possibility of performing numerical calculations significantly increased the potential of achieving high accuracy in modelling, as the calculations did not any longer rely on the accurate manufacturing

---

[23] Several other display designs not described in this text have been proposed [56, 57, 58, 59].

[24] A display based on the same concept was patented by Bendix Corporation in 1964 [60], where the aircraft's current position, expected lift-off point and the position where it would be brought to rest if brakes applied immediately were displayed in relation to the runway on a strip display. With manual adjustment of the aircraft position pointer to allow for the aircraft's initial position, the display also indicated 'committed to take-off', 'stop' and 'climb' advice in the form of three lights. These annunciations would be generated according to the positions of the three bugs (or pointers) in relation to the runway.

of passive electrical and mechanical components. Furthermore, digital processing, made possible through high-technology integrated-circuit design, has also significantly facilitated forward prediction of performance.

One of the first designs to fully utilise the digital processor was that proposed by The Boeing Company, for which an application for patent was filed in 1982 [61]. A continuation-in-part of a previous application filed in 1979 and later abandoned, the proposed system made use of the Intel 8080 family of processor and peripheral ICs. Typical of the technology of the time, this was based on an 8-bit architecture, used a number of 256x4 bit RAMs and 8K EPROMs, and would have had a clock frequency of about 1MHz or less. Such an architecture would not have been capable of computing complex mathematical functions with a satisfactory update rate in real-time. Furthermore, the limited address space and memory (ROM) size available must have significantly restricted data storage and program length (and complexity). In these circumstances, accurate modelling of the aircraft would have been difficult and simple models would have had to be used instead. Boeing took an interesting approach in their design, focussing on determining the urgency of any action to be taken by the crew. Identifying the difference between two classes of advisory indications on the flight deck, namely the caution and warning signals (defined according to the urgency of the response required), they pointed out that such indications alone failed to adequately quantify the urgency associated with the warning. They considered this a serious drawback, arguing that during take-off the crew should be informed of the time leeway available to the latest moment maximum action (application of either full thrust or full braking) needs to be taken to ensure a successful manoeuvre. Boeing defined this time-to-maximum-action as the 'chronodrasic interval' and proposed displaying the intervals for both the go and stop options on an LED bar-graph to the crew. The calculation of these intervals was based on simple algorithms determining the latest position on the runway at which maximum action would still allow the take-off manoeuvre to be completed successfully. The time available to such an action was then determined by dividing the leeway in distance available (the distance between the calculated point and the aircraft's current position) by the current velocity. The spool up time was also taken into account by subtracting it from the leeway available. The technique made use of an equivalent average (constant) acceleration determined by dividing the difference between the rotation and current velocities by the difference between the scheduled time-to-rotation and current time gone. The chronodrasic interval for the stop condition was calculated in a similar fashion.

Boeing acknowledged that this technique did not allow the display of the intervals to be constant at any time and this is proved mathematically in their patent. They consequently proposed a modification to eliminate this problem. Rather than provide a system that answered the question 'For the current airspeed, how much longer can the aircraft go before the pilot must fully advance the throttles to achieve rotation speed by the end of the runway and, subsequently, achieve the minimum required climb gradient?', the question was modified to 'If full thrust is immediately applied, what time interval will exist between the time when rotation speed is reached and the time at which the point is reached where rotation must occur if a safe take-off is to take place?'. In this way, it was possible to achieve a chronodrasic interval that remained constant throughout the run. This modification, in practice, involved replacing the instantaneous speed with the rotation speed for the calculation of the distance covered during the chronodrasic interval.

In a later patent application filed in 1984 [62], Boeing admit that chronodrasic measurements did not prove to be entirely satisfactory and that such time domain displays were not as effective under emergency conditions as desired. In the new design they proposed a display similar to that suggested by Servomechanisms, having a strip representing the runway on which six moving symbols would be superimposed. A 'go bug' and a 'stop bug' indicated the latest position at which maximum thrust application would allow a safe take-off and the latest position at which maximum braking would allow a safe rejection respectively. A 'rotate bar' indicated the latest point at which the aircraft could be rotated to achieve the screen height by the end of the runway and therefore would be stationary for a particular run. An 'EO bug' represented the latest point at which application of maximum thrust would allow a safe take-off after the loss of power from one engine. Finally, a 'VMC bar' indicated the latest point at which the run could be aborted at V_{MCG}. The sixth symbol represented the aircraft's current position as it progressed down the runway. It is clear that whilst Boeing seem to have given up on the idea of time intervals in preference of displaying positional information, they retained the concept of indicating the latest points at which particular manoeuvres could be executed successfully. The options available to the crew and any action necessary were determined by the position of the aircraft symbol in relation to the other bugs, many of which would be moving as the run develops. Interpreting the display during the run would have been rather more complicated than the previous proposal. Whilst the VMC and Rotate bars were stationary during the run, the Go and EO symbols would be located at pre-determined positions at the start (the latter closer to the near end of the runway) and moved towards the further end of the runway as the run progressed, both stopping at the Rotate bar. As the Go symbol reached the Rotate bar, the aircraft would be capable of rotating, irrespective of its position. The same applied for the EO symbol for the engine failure case. In the meantime, the Stop symbol moved towards the nearer end of the runway, having started at the further end at the beginning of the run. Should it have become apparent that the aircraft would pass the VMC bar before the Stop bar reached it, the crew was intended to abort the run. Furthermore, the four combinations of relative positions of the Go (or EO) and Stop symbols with respect to the aircraft symbol (whether in front or behind the latter) defined the four combinations of the viability of continuing or aborting the run.

A new architecture differing significantly from the original design made use of multiple processors, each responsible for the evaluation of one or more functions driving the symbols on the display. Together with the increased processing power, this allowed Boeing to develop a much more detailed model to determine the relevant parameters. Engine thrust and aircraft acceleration were approximated to 2nd order polynomial functions of airspeed (the coefficients of the thrust function were assumed to be a function of known environmental and engine parameters). The main program determined the coefficients of the acceleration polynomial for the AEO and OEI cases, being interrupted for the calculation of the distances to go to rotation using the Gauss-Legendre formula to algebraically solve the integral equation. The distance required to stop, measured from the far end of the runway, was calculated in a similar way.

In 1983, NASA contracted the University of Kansas to develop a take-off performance monitoring system [63], a project which was then followed on by NASA at Langley into the mid-1990s [64, 65]. The algorithm developed at the University of Kansas estimated the distances required to rotation and to bring the aircraft to a halt on the runway and compared these values with their scheduled counterparts. Prior to dispatch, the acceleration vs. TAS profile would be calculated for the expected operational and environmental conditions using a detailed model of the aircraft dynamics. Two profiles were calculated for the two limits of rolling friction (0.005 and 0.04) and the data was then used to determine the coefficients of 3rd order polynomials which were stored in memory for use during the run. The designers were concerned about the accuracy in the prediction of the rolling friction and introduced a feature, which, 10 seconds into the run, adjusted the value according to the acceleration and airspeed at the time[25]. The new coefficient of friction was then used to obtain the coefficients of the 'actual' scheduled performance by interpolating between the characteristics at the two limits of the rolling friction. In this way it was hoped to accurately determine the acceleration-TAS scheduled characteristic, from which the distance-to-go to rotation could be calculated by numerical integration. The one-time update of the coefficient of friction was later found by NASA to be of little practical use during flight tests carried out between 1987 and 1989 using NASA's Boeing 737 research aircraft [64].

The required stopping distance was calculated by a similar numerical integration technique assuming particular values for the various parameters and allowing for delays in the deployment or application of braking mechanisms. The system also monitored the engine pressure ratio (EPR) and acceleration to check for any engine failure or poor performance. An abort signal was generated if the runway length available was less than that required for rotation, if two engine failures were experienced or if a single engine failure or poor performance was detected with sufficient runway still available to stop. The algorithm was tested on a simulator at NASA Langley and a patent applied for in 1987 [66].

Following the work by the University of Kansas, NASA then proceeded to develop a display system which has been refined over a number of years [67, 68, 28, 69, 70, 71, 65]. Starting with a display similar in design to the Boeing proposal, the system displayed the aircraft position on the runway, together with the predicted and scheduled rotation points and the latest point at which the aircraft could be safely rotated, termed the ground roll limit line. The system also displayed the point at which the aircraft would be brought to a halt if the run were aborted. Another symbol displayed during the deceleration phase indicated the position the aircraft would come to a standstill with the current braking rate. Besides such graphical information, the monitor also displayed a number of other parameters, including current airspeed, V_1, V_R and runway length. A situation advisory flag illuminated green, amber (flashing) or red indicating a normal situation, OEI past V_1 but sufficient runway available to stop and abort advice respectively. This display was evaluated on NASA's simulator modelling their Boeing B737 research aircraft [69, 72, 73]. A number of pilots from NASA, the Air Force, commercial airlines and

---

[25] This effectively relegated the value of μ to a fudge factor that compensated for any variation in other parameters. In fact, abnormal and even negative values of rolling friction could result from such a calculation.

manufacturers took part in this evaluation programme. The display was reportedly well received by the pilots and was awarded an average rating of 3 ('Satisfactory-Good') on the Cooper-Harper scale, although a number of modifications were recommended. Another evaluation of modified displays and a head-up version was carried out in 1992 and the pilots were once again positive about the designs [70, 74].

A performance monitoring algorithm fundamentally similar to, though more complex than the Kansas design was developed at Bristol University [75, 76]. This algorithm was then used by the National Aerospace Laboratory, The Netherlands (NLR) to support their research in display design [77, 78, 79]. Three displays were appraised. One involved the presentation of the aircraft position on the runway, scheduled airspeed and a prediction of the airspeed in 5 seconds' time integrated with a modern tape-type ASI. The other two displays were essentially simplified versions of the NASA representation.

Aerospatiale of France developed a monitoring algorithm that determined the distance margin available at any moment during the run [80]. The distance still required for the aircraft to achieve the velocity that should have been achieved at that moment in the run (which effectively translates to the current distance margin) was calculated, to which the distance gone was then added. This sum was compared to the scheduled distance associated with that moment and the ratio of these two quantities determined. An alarm would be activated if this ratio were higher than a threshold value. The threshold value was defined as a linear function of airspeed, set to 1.50 at the beginning of the run and 1.15 at V_1. In a later design [30], the algorithm was modified to also calculate the distance required to stop the aircraft if the run had to be aborted immediately. The stop and take-off indications were controlled by appropriate logic comparing the distance margin to the threshold value and the estimated stopping distance with the runway available.

Besides the University of Kansas and Bristol University, other academic institutions have also attempted to devise a system capable of monitoring the progress of the take-off run. At the Texas Woman's University, a system was designed and flight tested on a Falcon 10 [81, 82] during the mid-1980s. In an attempt to reduce the uncertainty of performance prediction, the system stored (on the crew's command) the raw velocity vs. distance data recorded during the take-off, thus creating a data-bank history of past runs. When the next take-off was to be executed, the system would select the characteristic of a past run that was conducted in conditions most closely matching those at the time, and this data was then used to construct the reference performance profile. Displayed as a velocity against distance plot, the reference performance was superimposed, in real-time, with the actual run profile as it developed, allowing the pilot to compare the two, thereby assessing the progress of the take-off[26]. In an attempt to indicate to the crew how close the operational conditions of the reference trace matched current conditions, an arbitrary confidence index was calculated. The architecture this system involved was based on the Intel 80286 microprocessor with a 19Mb hard drive.

The concept of storing the history of past runs for future reference, allowing predictions to be aircraft specific, was also adopted at the University of Tennessee [83]. Rather than store the raw acceleration and velocity data for each run, only five constants were stored in memory. By manipulating the acceleration equation, normalised to standard operating and environmental conditions, five constants, three representing the thrust characteristic, one representing the coefficients of lift and drag and one representing rolling friction, could be determined. Together with pilot inputs of the actual conditions during the take-off, these five stored constants then allowed the construction of the expected acceleration profile. The five constants were calculated by solving the equation of acceleration using five sets of acceleration-velocity data pairs. When constructing the characteristic of the expected performance before the next run, the average value of the constants of the last twenty valid runs would be used. During the actual run, the acceleration was monitored and displayed on an analogue type display with three bands, namely green, amber and red. The needle would be in the green band if the measured acceleration were in the range of 90% to 110% of the reference acceleration, in the amber section if between 80% and 90% and in the red if lower. The reference distance, calculated from the reference acceleration profile, and the actual predicted distance required to take-off were also displayed in numerical format. The latter was estimated by solving the acceleration equation using five sets of acceleration and velocity data pairs from the past history of the current run. Green, amber and red lamps were illuminated according to the ratio of the expected to reference distances to take-off.

In a later development [84], the five constants were reduced to three, representing the three coefficients of the 2nd order polynomial function of airspeed, and these are determined by the method of least-squares rather than as previously described.

---

[26] This display is similar to an earlier design suggested by General Precision Systems, which traced the aircraft performance on a chart using a plotter [21].

Furthermore, the predicted distance remaining was calculated by scaling the reference distance-to-go by the ratio of the actual to predicted (scheduled) acceleration at the instant of calculation. The hardware used in realising this system was an accelerometer connected to an IBM PS/2 laptop via an RS-232 link and was flight tested using three light aircraft.

3.4 Conclusion

Since the initial identification of the need to objectively quantify the progress of a take-off run, various performance monitor design approaches have been proposed, with each attempting to overcome the various technological difficulties faced at the time. Before electronic (digital and analogue) computers became widely available, the major hurdle tended to be the lack of availability of tools to adequately model aircraft performance. This significantly restricted the possibility of forward predicting performance in terms of distance requirements. As a result, many of the early proposals have instead attempted to monitor other attributes such as acceleration and various forms of achieved performance (non-predictive monitoring such as distance-time checks). Such techniques have generally proved not to be sufficiently indicative of whether the 'go' and 'abort' options are truly viable. The few designs that actually attempted to forward predict performance have been restricted by crucial assumptions that would have surely compromised prediction reliability. Once digital computers became available, the factor that most significantly affected prediction reliability proved to be the difficulty experienced in accurately measuring (or appropriately selecting) values of the parameters relevant to the equations of motion. This has doubtless contributed to the fact that no design has as yet been commercially successful.

Nevertheless, there is also little doubt that a reliable take-off performance monitor would be very welcome in the cockpit. The key issue and, understandably, of major concern in this context is system reliability and most of the conservative reservations voiced to date are perhaps well founded. In such circumstances it would be bold to appreciate the development of affairs to date, as these effectively provide a clear indication of the qualities presently expected of a performance monitor. The experience and knowledge obtained from this background should therefore be carefully incorporated in any new design concept to ensure that ultimately a successful system can emerge.

Chapter 4: MONITOR DESIGN CONCEPT AND PERFORMANCE TARGETS

4.1 Introduction

Following the appraisal of previous works and publications, a detailed study was carried out to identify the best methodology that would support reliable performance monitoring. Performance targets were also established. These were refined as the project progressed and finalised in a design concept and performance standard described in detail in College of Aeronautics Report CoA-0010 [85][27]. This chapter presents the salient issues of the named report.

Two factors were identified as crucial for the success of the proposal. These were the need to achieve high accuracy and reliability in view of the criticality of the application, and the absolute necessity to win over the approval and favour of the aviation community, specifically that of the manufacturers, operators (in particular the crew) and the regulatory bodies. Whilst the former comprises a technological barrier, the latter is a psychological one, and it is immediately clear, particularly from the record of past monitoring attempts, that failing to overcome either will surely result in the failure of any new proposal.

The aviation community has long been divided on the case of take-off performance monitors. Most, if not all, of the arguments against could be summed up into one concern, namely whether such an instrument would, in fact, improve the current safety record or, instead, turn out to be a nuisance or even a threat to the safe completion of the manoeuvre. This is a very valid and justified concern, particularly in the light of the high crew workload, the relatively low safety margins available during take-off and the very nature of the role of the performance monitor. The system must be capable of providing correct, clear and unambiguous information to the crew in an appropriate manner under all foreseeable operating conditions, so as to avoid unnecessary rejections and, more critically, accidents or loss resulting from distraction or incorrect indication or interpretation of the instrument. Besides, the crew must have full confidence in the system, so that they do not hesitate or dismiss

---

[27] A copy of this report is attached in the Annex.

the indication in critical moments. Unfortunately, such a level of quality has not been achieved in previous designs, and whilst this can be identified as the reason for the absence of take-off monitors on the flight deck, it has also nurtured strong scepticism which is detrimental to the proposal of a good design.

4.2 The performance monitoring concept

The strategy adopted to overcome the latter hurdle was to design a performance monitor capable of integrating seamlessly with current operations and the V-speed technique. With the aviation community deeply entrenched in its stand on relying on current procedures, the only realistic solution was to complement the V-speed technique with a system optimised to cover the shortcomings of current practices. As a result, the concept of V_1 describing the latest point at which the crew can be expected to reject a run has been retained. The design, therefore, is based on comparing, up to V_1, the expected TORR, TODR and ASDR with their scheduled counterparts. This inherently implies that the system would be predictive in nature and would thus resolve the issue of the lack of positional awareness in current procedures. The capacity to forward predict performance offers the significant advantage of providing early warning of an anomaly to the crew. The significance of this feature cannot be over-stressed, since as the aircraft approaches V_1 it is quickly approaching the point of no return and the excess leeways that are available to bring the aircraft to a halt at lower speeds (and, consequently, the safety margins), are quickly diminishing. Any hesitation or delay in reaction seriously jeopardises the safety margin associated with a rejection manoeuvre and it is clear that providing early warning greatly enhances the scope of the performance monitor.

When modelling the aircraft during take-off, if expected rather than actual parameters are used to solve the relevant equations of motion, the calculation is effectively relegated to a re-evaluation and updating of scheduled performance. With current technology, this is invariably the case for the post V_1 predictions[28], where several parameters cannot be predicted with useful accuracy or reliability. This has been highlighted earlier in this text (Chapter 2) and also testified by previous design approaches. This appreciation is a crucial concept because it effectively justifies the use of pre-dispatch allowances for all post-V_1 distances. As a

---

[28] The distance from V_1 to V_R is also effectively a scheduled distance due to the uncertainty associated with the prediction of the actual moment of rotation.

result, the real-time calculation of the expected TODR, TORR and ASDR is reduced to the prediction of the distance-to-V_1 (D_1) and the viability of the take-off run is effectively determined by comparing D_1 with its scheduled counterpart, defined as the *critical distance* (D_{crit}) in this work. In other words, the advice to continue or abort the run is based on the real-time prediction of whether or not V_1 will be achieved within D_{crit}.

Using the scheduled performance for the post-V_1 distances is a very valid concept. Besides the advantage of having a degree of leeway inherently built in, these distances are legally considered necessary and sufficient to ensure safety and their use should therefore not raise objections from operators or the regulatory bodies.

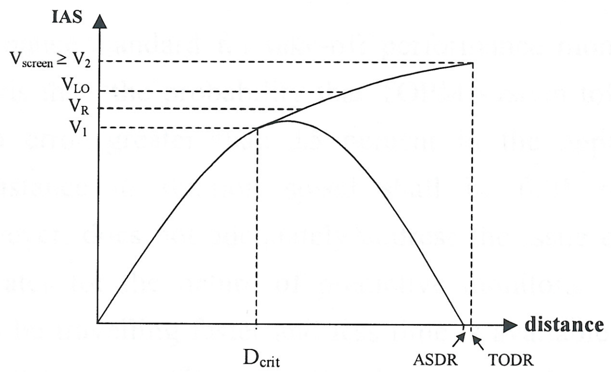

Figure 4.1: Defining the critical distance D_{crit} in scheduled performance.

Whilst the crew are well trained to react to a discrete anomaly during the run, they are most vulnerable to subtle, continuous under-performance. With no objective means to relate airspeed with their position on the runway, or indeed to determine how much runway is still required to complete the manoeuvre safely, they only have their intuition to assess the progress of the run. This has been highlighted in the introduction of this text and justifies the optimisation of the algorithm to detect subtle under-performance.

A closer look at the performance requirements confirms that, in actual fact, it is the critical distance and not V_1 that correctly defines the point of no return, for if the aircraft were to under-perform prior to that point, V_1 would be achieved further down the runway than allowed for by regulation. In field limited cases, this would significantly reduce the safety margins in both the continued and rejected run cases, particularly the latter. Defining D_{crit}, then, as the point of no return actually enhances the safety margins. If V_1 is achieved before D_{crit}, the flight crew will be committed to take-off with excess TODA and TORA still being available. Likewise, in the event of aborting at the critical distance, the velocity will by definition be lower than V_1 and the remaining distance (scheduled as the braking distance from V_1) will not be as critical in allowing the aircraft to be brought to a standstill. Collectively, these arguments provide a very good case for the proposed method of performance monitoring.

4.3 Performance standard

The minimum performance standard for take-off performance monitors, SAE AS-8044 [86], recommends that 'the probability that TOPM system tolerances will, of themselves, cause an error greater than ±5 percent in the apparent all-engine operating take-off distance to rotation speed shall be 0.01 or less'. This recommendation, however, does not adequately address the issue of accuracy, nor does it realistically cater for the nature of predictive monitors. As the aircraft approaches V_1, it will be travelling faster and less time is available for the crew to decide whether to abort the run. Consequently, the crew need greater reassurance that the advice or indication provided by the system is correct as the critical moment approaches. This translates to the prediction accuracy needing to be greater towards the end of the acceleration phase. Fortunately, this is possible, since as the run develops, the monitor is required to progressively look less far ahead and this, in turn, reduces the uncertainty associated with the estimate. Consequently, for the purpose of accuracy requirements, the run to V_1 should be split into three segments (Figure 4.2). The first segment refers to the first quarter of the run, the second covers quarter to half distance, whilst the third constitutes the remaining part of the run. In the first segment, the aircraft will be travelling at speeds below $V_1/2$ and will take approximately half the time-to-V_1 to cover this distance. Ample time to react and ample distance for braking are available and as a result the accuracy of the monitor in this segment is not considered critical, with a basic indication of progress deemed sufficient. In the second segment, the aircraft will achieve approximately $^2/_3V_1$ and by the end of it only a third of the time-to-V_1 will still be available for the initiation of an aborted run. Aircraft speeds are higher, but still well below V_1. As a result, if the crew elect to abort the take-off in this segment, less braking distance than that scheduled at V_1 will be necessary to bring the aircraft to rest. This leeway, together with the addition of more than half the distance to V_1 that will also available for braking, renders the event of aborting a run of relatively minor consequence. In the case of borderline performance, a slightly inaccurate prediction would not jeopardise safety, should the crew elect not to abort at this stage. During this segment of the run, therefore, it is considered sufficient to have a monitor prediction accuracy of 6% on 99% of the runs.

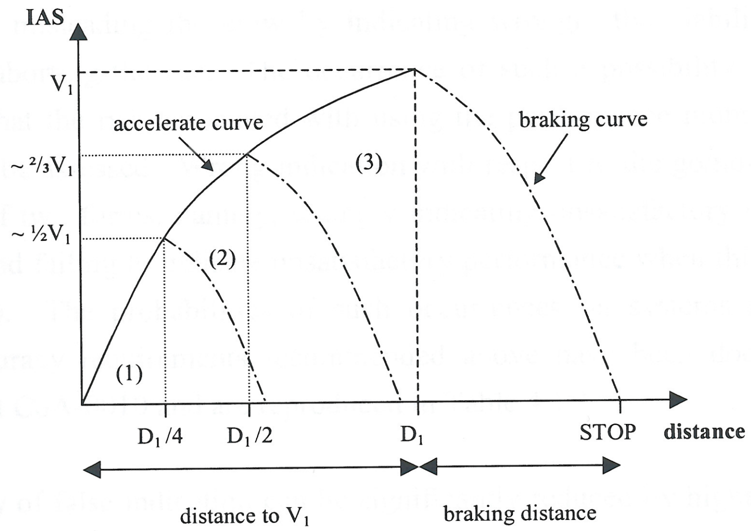

Figure 4.2: Segmentation of the run-to-V_1 for the purpose of hazard identification.

(1) Run to $\frac{1}{4}D_1$. Low IAS with ample distance to bring the aircraft to a halt safely. Aborting in this early stage of the run will not result in any significant increase in risk and is very unlikely to disrupt operations.

(2) Run from $\frac{1}{4}D_1$ to $\frac{1}{2}D_1$. During this stage the aircraft is accelerating to higher speeds but sufficient leeway is still available to render the option of aborting the run a relatively low-risk manoeuvre.

(3) Run from $\frac{1}{2}D_1$ to D_1. The aircraft is fast approaching V_1, rendering the decision to abort critical. Due to the high speed involved, the aircraft will cover this segment of the run in only 1/3 of the time from brake-release to V_1.

The third segment covers the remaining half of the critical distance. During this time, the aircraft will be approaching V_1 and as a result a relatively large distance is covered in just a third of the time-to-V_1. It is at this stage that decisions are most critical and the urgency associated with the decision aggravates the situation further. Besides the fact that the full scheduled braking distance will be required to bring the aircraft to rest in the event of a rejected run, any excess leeway previously available in the unused distance-to-V_1 is quickly being covered. As a result, the decision to abort a run is considered to be relatively hazardous and high precision in performance prediction is mandatory to ensure the crew is not led to hesitate or abort unnecessarily. Furthermore, as the aircraft will be approaching the point of no return, in the case of the continued take-off, the crew must be confident in the monitor's prediction that the take-off is indeed viable. It is for these reasons that in this phase of the run the accuracy should be within 3% on 99% of the runs.

An issue of primary concern in take-off performance monitor design is the possibility of the monitor misleading the crew by indicating wrongly the viability of either continuing or aborting the run. The occurrence of such a possibility needs to be quantified so that the risk associated with using the performance monitor in flight operations can be assessed. Wrong indication with respect to the go/no-go decision can take one of two forms, namely, wrongly indicating unsatisfactory performance (false alarm) and failing to indicate unsatisfactory performance when this is the case (missed alarm). The probabilities of such occurrences on systems meeting the prediction accuracy requirements recommended above have been documented in detail in Report CoA-0010 and are reproduced in Table 4.1[29].

The probability of false indication can be significantly reduced by higher prediction accuracies than those recommended above, but such standards would probably prove very difficult to comply with and are therefore considered as impractical. In these circumstances, a low false alarm rate may be traded for lower missed alarm rates. This would be achieved by reducing the critical distance, which in effect re-defines the threshold of performance to correspond to a performance level more stringent than scheduled performance. The false alarm and missed alarm rates resulting from a threshold set at 112% (rather than 115%) of gross scheduled performance are also presented in Table 4.1.

The false alarm rate can be interpreted as the probability of generating unnecessary rejections[30]. In the global perspective, the relevant figures for either performance

---

[29] The probabilities in Table 4.1 assume that the probability density functions of take-off performance and prediction error are both Gaussian in nature and independent of each other. The density function of take-off performance may not necessarily be Gaussian, particularly in regions pertinent to unsatisfactory performance that warrant the rejection of the run. Furthermore, the analysis considers only the 'alarm' function of the monitor, which translates to the indication or otherwise of the 'go' and 'abort' signals. As a result, no account is taken of the effect of quantifying marginal performance and displaying this to the crew. Such factors suggest that the probabilities presented in Table 4.1 might be conservative.

[30] Provided the crew abort the run when the monitor generates an alarm.

threshold in Table 4.1 appear to be acceptable. This is particularly so in the light that, in two studies carried out in the 1970s, the frequency of aborts were shown to be about 1 in every 3,000 take-off initiations [87]. A closer look, however, would reveal that statistically the majority of false alarms are expected to occur in cases of marginal performance and in these circumstances unnecessary rejections, particularly when late in the run, need to be avoided. However, good analogue display design supporting early indication of marginal performance, together with the introduction of appropriate operating procedures, should reduce the probability of the crew acting on a late false alarm. In this way, the effective risk associated of unnecessary high-speed rejection would be further reduced. The same techniques are applicable to missed alarms and can likewise reduce the risk of a continued run in the event of unsatisfactory performance.

Run Section	$D_{crit.}$ = 112% gross performance		$D_{crit.}$ = 115% gross performance	
	Correct alarm	False alarm	Correct alarm	False alarm
¼– ½ dist.	88%	2 in 1,000	57%	2 in 10,000
½ dist. to end	99%	2 in 10,000	63%	4 in 1 million

Table 4.1: Comparison of the probabilities of indication with performance thresholds at 112% and 115% gross performance.

Correct alarm is the probability that unsatisfactory performance is detected.
False alarm is the probability that satisfactory performance is wrongly indicated as unsatisfactory.

4.4 Algorithm design concept

Using instantaneous values to solve the equations of motion suffers from the significant drawback that any momentary disturbance or, indeed, error in measurement, will readily result in erroneous prediction. In an attempt to overcome this difficulty, a novel concept is being suggested. Greater accuracy should be achieved if the required information is instead extracted from either a section or the complete history of the actual run. In this way, the average values of the parameters during the measurement interval are obtained and these are less likely to be influenced by instantaneous effects or spurious errors. Furthermore, the past history is a shadow of what is to be expected further down the run, provided that the situation is invariant. This is precisely the case when monitoring the performance to V_1, provided no discrete incident such as an engine failure or any other anomaly is encountered. Conveniently, this approach is also well suited for the early detection of subtle under-performance. The least-squares curve-fitting technique is a very appropriate tool for this application and also offers the advantage that the algorithms are well established and relatively simple to implement.

Rather than reverse-model the past history of the current run to extract the various parameters which would then be used in the same equations, a study was carried out to investigate whether simply extrapolating the curve determined through the method of least-squares would be appropriate to forward predict aircraft performance. Provided a good fit is obtained, the fitted curve should implicitly contain all the information of the various parameters controlling the take-off run, rendering their explicit calculation unnecessary. If, then, the various parameters remain unchanged, the extrapolated curve would provide a good prediction of the performance of the aircraft. The findings of this study are presented in College of Aeronautics Report CoA-0013 [88][31]. The results indicated that this concept has the potential of being developed into a robust method for performance prediction and was therefore adopted as the basis of further work within this project.

Least-squares estimation also conveniently allows the statistical determination of the quality of fit. This figure can provide a realistic estimate of the confidence in the prediction of aircraft performance. Such knowledge could not only be presented to the crew if considered relevant in the display design, but could also facilitate the discarding of estimates that have been determined with low confidence. Such a facility should not only assist in the avoidance of displaying misleading information to the crew (a requirement in AS-8044) but could also facilitate certification of the instrument.

One issue worthy of discussion is whether a take-off performance monitor should incorporate extensive system monitoring and present such 'secondary' information to

---

[31] A copy of this report is attached in the Annex.

the crew. The main focus of this design is to provide a basic system that is reliable enough to be adopted on the flight deck and therefore intended to only determine whether performance criteria are expected to be met. Besides increasing the complexity and uncertainty in performance prediction, it is arguable whether displaying or indeed even using 'secondary' information is advantageous, particularly if this increases the mental processing required of the crew in interpreting the information displayed. As a result, the approach of extensive system monitoring has not been adopted. Anticipating that the least-squares technique might be slow to react to discrete anomalies, however, the monitoring of acceleration as a secondary parameter could provide a complementary means of ensuring that aircraft performance is adequate.

4.5 Summary

In conclusion, therefore, the fundamental concepts of this design can be summarised as follows:

- Seamless integration with current procedures and therefore also with the V-speed technique.
- System optimisation for the detection of subtle under-performance so that current procedures could be best complemented.
- Forward prediction of performance, to ensure that early warning of any poor performance is provided to the crew.
- The scheduled values for the post-V_1 distances would be allowed for, reducing the problem of monitoring to measuring the distance margin available at V_1.
- The prediction accuracy for the segment between $\frac{1}{4}D_1$ and $\frac{1}{2}D_1$ should be within 6% on 99% of the runs. That for the last half of the run to V_1 should be within 3% on 99% of the runs.
- Use of least-squares curve-fitting for performance measurement and extrapolation for the forward prediction of performance.
- Calculation of a confidence figure to indicate the accuracy of the performance estimate.

Chapter 5: ALGORITHM DEVELOPMENT FOR THE JETSTREAM-100

5.1 Introduction

The study detailed in Report CoA-0013 compares the performance of various least-squares fits on the recordings of four take-offs conducted by the NFLC's Jetstream-100 G-NFLC. Results indicated that most of the characteristics considered could be described well by second order polynomials when fitted over the complete run. Fitting over only part of the run (from the start to different points along the run simulating operation during take-off), however, did not offer satisfactory forecasts of performance through simple extrapolation. This was because although very good fits were obtained, the coefficients of the polynomials tended to change as the take-off progressed. The fits generated in the earlier part of the run were incapable of generating the necessary curvature, resulting in a prediction error that reduced to zero as V_1 was approached (Figure 5.1)[32].

In an attempt to reduce the prediction error, an unpublished study was carried out to investigate the merits of using a sliding window (such as only the last five seconds of the run history) in the least-squares fit. This technique resulted in a fit which was less 'stiff' (more responsive to change) than the polynomial fitted on the complete time history, thereby allowing the prediction error to fall earlier in the run, but it still did not provide a satisfactory solution. Various window sizes were analysed on different characteristics in an attempt to find a good compromise between stiffness generated by large windows and undesirable fluctuations in the estimate caused by small data populations and small window sizes. Although unsuccessful, this study was instrumental in confirming that the polynomials fitted were unable to sufficiently allow for the expected drop in performance (lower acceleration) associated with the latter parts of the run and alternative techniques had to be considered.

---

[32] Figure 5.1 presents the results of the velocity vs. time (V_g-t) fit which are typical of the results obtained on other successful fits in the study. The initial high amplitude oscillating error at the start of the run (Figures 5.1 (e) and (f)) is due to divergence of the fit from the actual characteristic caused by a combination of signal noise, small data population size and transients in the aircraft dynamic characteristic at the start of the run.

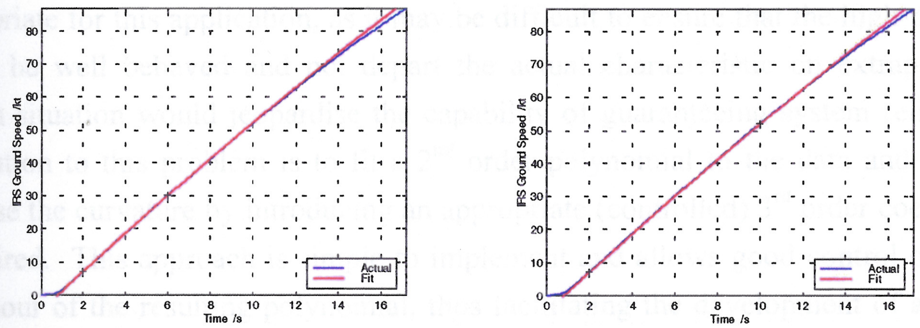

(a) fit 2s-6s

(b) fit 2s-8s

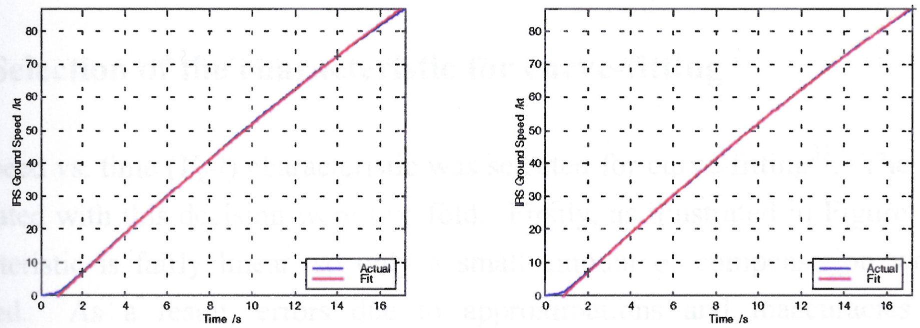

(c) fit 2s-10s

(d) fit 2s-end

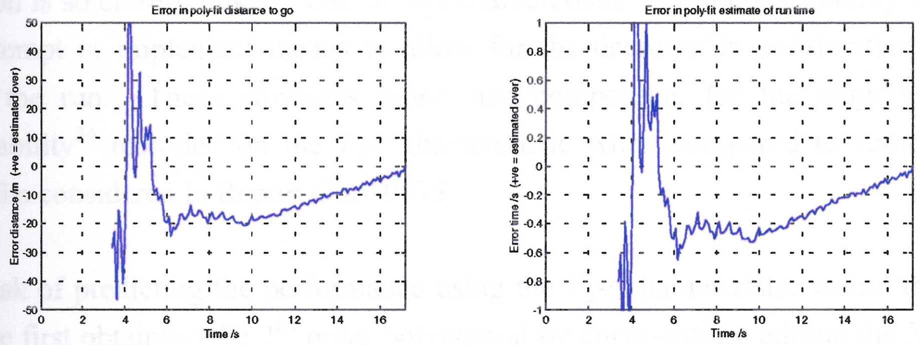

(e)

(f)

Figure 5.1: Prediction by simple extrapolation of the least-squares fit applied to the speed vs. time (V_g-t) characteristic.

Run 3 from Report CoA-0013. V_1 = 86.75kt, Distance to V_1 = 386m.

(a) – (d) Fit and extrapolation after 6s, 10s, 14s and at the end of the run respectively. Fit started after 2s.

(e) D_1 prediction error.

(f) Time-to-V_1 prediction error.

One way of increasing the curvature of the fitted polynomial is to introduce 3rd and higher order coefficients in the least-squares fit. This technique, however, is not appropriate for this application, as it may be difficult to ensure that the high-order fit would be well behaved and not depart the actual characteristic on extrapolation. Such a situation would jeopardise the capability of guaranteeing system reliability. A solution to this problem is to fit a 2nd order polynomial to the data and to then increase the curvature by introducing an appropriate (controlled) 3rd order coefficient as desired. This approach is simple to implement and allows good control over the behaviour of the resulting polynomial, thus facilitating the development of a robust design.

5.2 Selection of the characteristic for curve-fitting

The speed vs. time (V_g-t) characteristic was selected for curve-fitting[33]. The reasons associated with this decision were two-fold. Firstly, as illustrated in Figure 5.1, the characteristic is fairly linear, so only a small amount of compensation would be required. As a result, errors due to approximations and inaccuracies in the compensation employed would be secondary in nature. Secondly, the slope of the V_g-t characteristic relates directly to the acceleration profile with which the thrust function is so closely linked. Use of this characteristic would consequently simplify the attempt to implement means to allow for the decrease in acceleration further down the run. These attributes more than compensate for the slightly poorer repeatability[34] recorded on the V_g-t characteristic when compared to some of the other fits considered in Report CoA-0013.

The task of predicting the performance using the V_g-t characteristic would therefore involve first obtaining the 2nd order polynomial by curve-fitting, adding the 3rd order coefficient as desired (performance compensation) and then calculating the distance-to-go to V_1 by integrating the compensated function between the instantaneous velocity and V_1. The expected value of D_1 is obtained by adding the distance-to-go to the distance gone.

---

[33] The IRS ground speed, rather than other forms of aircraft speed (such as IAS) was selected as the dependent variable. This decision is justified in Report CoA-0013 and is based on the consideration that the IRS ground speed measurement is more reliable at slow speeds and the data is less susceptible to fluctuations caused by changes in operational conditions.

[34] Since an increase in curvature is being introduced to reduce the prediction error, repeatability of the error is more important than absolute error in this context.

5.3 Performance compensation

Modelling the V_g-t characteristic with a 2nd order polynomial inherently implies that the function is incapable of catering for acceleration-time functions other than linear. Considering that the V_g-t characteristic is fairly linear, it follows, then, that the function cannot be likewise expected to adequately model 2nd and higher order coefficients of the acceleration-velocity characteristic. Referring to Equations 2.6 and 2.7, this implies that components of the aerodynamic drag, rolling friction and the thrust characteristic that are proportional to the square of the velocity cannot be correctly accounted for. Fortunately, however, the non-linear increase in aerodynamic drag counters the non-linear fall-off in rolling friction, so that the non-linear component of the total drag function is small compared to the static AEO thrust of the aircraft. As a result, the non-linear component of the acceleration profile is mainly caused by the non-linearities in the thrust profile[35]. Compensation, therefore, would be required mainly to cater for the drop in thrust expected at higher speeds.

The thrust generated by the Turbomeca Astazou engine and Hamilton Standard propeller package installed on the Jetstream can be determined using manufacturer's performance charts (Appendix I). These charts are intended for use at normal airborne speeds and therefore had to be extrapolated to cover the slower speed regimes associated with the ground run. Although this results in some inaccuracy[36], no data specifically for take-off is available and therefore calculations of engine thrust had to be made using information extracted from these extrapolated graphs. Various thrust characteristics were constructed for different power settings and then successfully fitted to a second order polynomial (Figure 5.2). The thrust function can therefore be modelled by Equation 5.1:

$$T = \alpha_0 + \alpha_1 V + \alpha_2 V^2 \qquad \ldots (5.1)$$

For normal take-off conditions with take-off power selected and engine speed at 43,000 rpm (98.7% of nominal), the parametric power is within the region of 500kW

---

[35] This is particularly true for propeller driven aircraft, where the thrust drops significantly with airspeed.

[36] The issue is further complicated by the fact that during take-off the engine-propeller package operates in constant power mode, where the propeller pitch and fuel flow are increased until the target turbine temperature is reached, whilst in other flight regimes the package operates under variable pitch control [89].

to 650kW for temperature ranges between -40°C and +40°C [37]. The Jetstream-100 is designed to take-off specifically with take-off power, since the auto-feather mechanism (a feature facilitating the recovery during an engine failure) is enabled only at this power setting. This justifies the assumption that the operational envelope spans the range 500kW to 650kW. Over this range the 2nd order coefficient α_2 is numerically of the order of 1.65 $\times 10^{-5}$ of the static parametric power α_0 (Figure 5.2).

Since the thrust is much larger than the drag under normal AEO conditions, the latter can be ignored[38], so the acceleration can be approximated to:

$$a = dV_g/dt \approx (\alpha_0/m) + (\alpha_1/m)V + (\alpha_2/m)V^2 \qquad \ldots (5.2)$$

The average acceleration measured over 10 runs was calculated to be 5.43kt/s [90]. Consequently, Equation 5.2 can be re-written in terms of time by substituting V for $5.43t$ [39] and then integrated:

$$V_g = \int (\alpha_0 / m) + 5.43(\alpha_1 / m)t + 29.5(\alpha_2 / m)t^2 dt \qquad \ldots (5.3)$$

$$\Rightarrow \quad V_g = V_0 + (\alpha_0/m)t + 2.7(\alpha_1/m)t^2 + 9.8(\alpha_2/m)t^3 \qquad \ldots (5.4)$$

Equation 5.4 illustrates that the V_g-t characteristic can be consequently described by a 3rd order polynomial. Since the ratio α_2/α_0 is approximately 1.65×10^{-5} kt^{-2}, the controlled third order coefficient is numerically approximately 1.62×10^{-4} times the first order coefficient, providing a convenient means of introducing a controlled 3rd order coefficient for the purposes of performance prediction. This ratio can be conveniently rounded off to 1.6×10^{-4}.

The 2nd order polynomial fitted over the complete run fits the whole characteristic well and consequently the amount of compensation required reduces as the run progresses. A weighting of the controlled 3rd order coefficient which is gradually reduced to zero by the end of the run therefore had to be introduced. Empirical

---

[37] Refer to Appendix I. Although the engine speed is set by the pilot to 43,000rpm for take-off, a slight variation significantly affects the output power. Consequently, although calculations indicate that 600kW would be the maximum power obtained at nominal rpm, an upper limit of 650kW is considered practical. The lower limit of 500kW is achieved at +15°C for MCP as parametric power drops to about 460kN at 40°C with this setting.

[38] The effect of slopes of up to 1.5° can also be neglected as they contribute to less than 10% of the static acceleration.

[39] The wind velocity is assumed to be constant, so the rate of change of airspeed is equal to the aircraft acceleration.

testing suggested that satisfactory weighting would be proportional to the square root of the proportion of velocity that still has to be achieved to reach V_1. In other words, for a fitted curve $A+Bt+Ct^2$, the third order coefficient introduced would be:

$$D_{comp} = 0.00016B\sqrt{\frac{V_1 - V_{act}}{V_1}} \qquad \text{... (5.5)}$$

where: V_{act} is the instantaneous velocity measured at the moment of calculation.

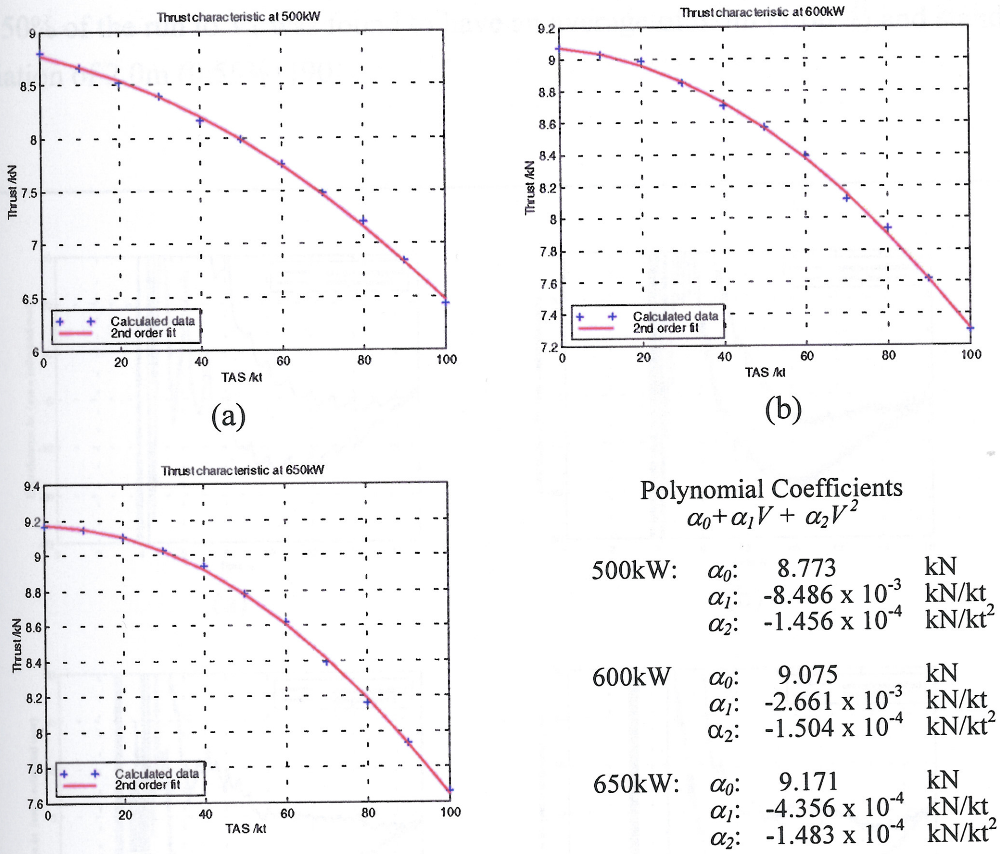

(a) (b)

(c)

Polynomial Coefficients
$\alpha_0+\alpha_1 V+\alpha_2 V^2$

500kW:	α_0:	8.773	kN
	α_1:	-8.486×10^{-3}	kN/kt
	α_2:	-1.456×10^{-4}	kN/kt^2
600kW	α_0:	9.075	kN
	α_1:	-2.661×10^{-3}	kN/kt
	α_2:	-1.504×10^{-4}	kN/kt^2
650kW:	α_0:	9.171	kN
	α_1:	-4.356×10^{-4}	kN/kt
	α_2:	-1.483×10^{-4}	kN/kt^2

Figure 5.2: Parametric thrust data and 2nd order polynomial fit for 500kW, 600kW and 650kW parametric power on the Turbomeca Astazou – Hamilton Standard package.

The model for the Jetstream during take-off is therefore expressed in Equation 5.6:

$$V = A' + Bt + Ct^2 + 0.00016B\left(\sqrt{\frac{V_1 - V_{act}}{V_1}}\right)t^3 \qquad \ldots (5.6)$$

where A' is adjusted appropriatedly so that the two equations (the compensated and uncompensated) generate the same value of velocity for the current value of time.

The compensation introduced in Equation 5.5 was implemented and the performance of the modified algorithm was compared to the results of Report CoA-0013 (Figure 5.3). Exhibiting a significant reduction in prediction error, this semi-empirical model was then further validated on ten runs, where the maximum prediction error in the last 50% of the run to V_1 was found to have an average of 6.5m (1.60%) and standard deviation of 2.0m (0.55%) [90].

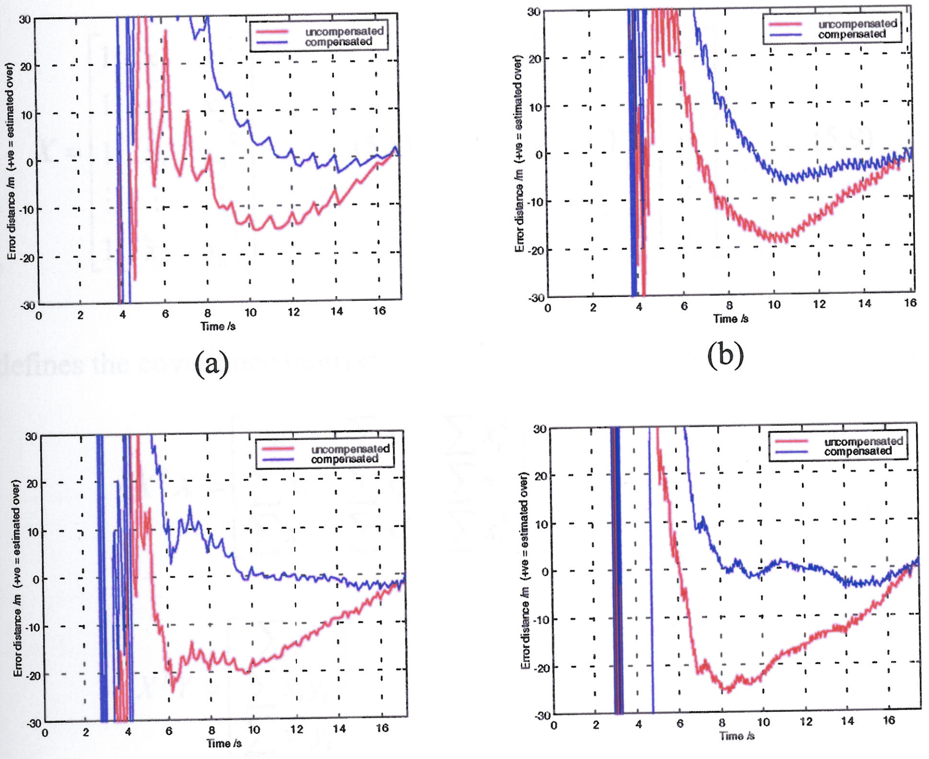

(a)

(b)

(c)

(d)

Figure 5.3: Comparison of prediction performance of uncompensated and compensated curve-fitting algorithms.

(a)-(d): Runs 1 to 4 of Report CoA-0013 respectively.

5.4 Implementation of the method of least-squares and estimation of the prediction uncertainty *

The coefficients of the polynomial resulting in the least-squares fit are obtained by solving the three normal equations presented in matrix form in Equation 5.7 [91]:

$$\begin{bmatrix} n & \sum x_i & \sum x_i^2 \\ \sum x_i & \sum x_i^2 & \sum x_i^3 \\ \sum x_i^2 & \sum x_i^3 & \sum x_i^4 \end{bmatrix} \begin{bmatrix} A \\ B \\ C \end{bmatrix} = \begin{bmatrix} \sum y_i \\ \sum x_i y_i \\ \sum x_i^2 y_i \end{bmatrix} \quad \ldots (5.7)$$

where: n = number of data points

$x_i = i^{\text{th}}$ data point of the independent variable (time)

$y_i = i^{\text{th}}$ data point of the dependent variable (velocity)

A, B and C define the coefficients of the polynomial $A+Bx+Cx^2$

Defining the matrices X and Y as:

$$X = \begin{bmatrix} 1 & x_1 & x_1^2 \\ 1 & x_2 & x_2^2 \\ 1 & x_3 & x_3^2 \\ \vdots & \vdots & \vdots \\ 1 & x_n & x_n^2 \end{bmatrix} \quad \ldots (5.8) \qquad Y = \begin{bmatrix} y_1 \\ y_2 \\ y_3 \\ \vdots \\ y_n \end{bmatrix} \quad \ldots (5.9)$$

$X^T X$ defines the covariance matrix:

$$X^T X = \begin{bmatrix} n & \sum x_i & \sum x_i^2 \\ \sum x_i & \sum x_i^2 & \sum x_i^3 \\ \sum x_i^2 & \sum x_i^3 & \sum x_i^4 \end{bmatrix} \quad \ldots (5.10)$$

and

$$X^T Y = \begin{bmatrix} \sum y_i \\ \sum x_i y_i \\ \sum x_i^2 y_i \end{bmatrix} \quad \ldots (5.11)$$

Using Equation 5.7, the values of the polynomial coefficients can be determined:

---

* The mathematical notation adopted in this and the following sections is derived from reference 91.

$$\begin{bmatrix} A \\ B \\ C \end{bmatrix} = (X^T X)^{-1}(X^T Y) \qquad \ldots (5.12)$$

The variables A, B and C in Equations 5.7 and 5.12 actually represent the expected values of the coefficients, defining the 2nd order polynomial function which is most likely to describe the data collected, from which the expected distance-to-go-to-V_1 can then be determined as outlined earlier in this chapter (Section 5.2). Statistically, however, a range exists in which each of the three variables are expected to lie for a particular level of confidence. This, in turn, results in a range of polynomials in which the actual characteristic would be expected to lie (Figure 5.4). An uncertainty in the distance-to-go is therefore associated with the prediction.

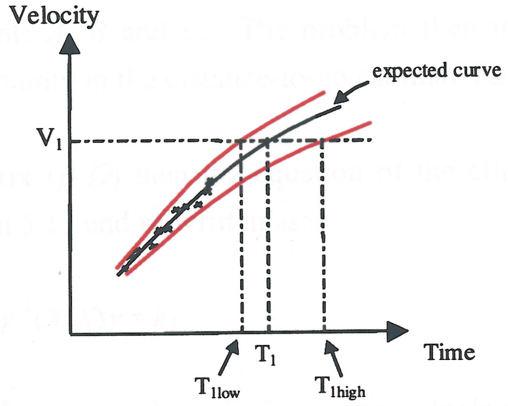

Figure 5.4: Sketch illustrating how the expected (black) and high and low limit (red) polynomials affect the time and distance to V_1.

For the identification of the range in question, the joint confidence interval of the three coefficients is of relevance, is given by Equation 5.13 [91]:

$$(\beta-\Omega)^T(X^T X)(\beta-\Omega) \leq ps^2 F(p, \nu, 1-\alpha) \qquad \ldots (5.13)$$

where: Ω is the 3x1 matrix of the expected polynomial coefficients A, B and C
β is the 3x1 matrix of the coefficient variables a, b and c, in this case all combinations within the selected confidence interval
p is the number of degrees of freedom (3)
$v = (n-p)$ with n being the number of data points
s is the standard deviation of the least-squares fit
$F(p, v, 1-\alpha)$ is the F-distribution value for p, v, $1-\alpha$
$(1-\alpha)$ is the confidence level of choice (0.99)[40]

$F(p, v, 1-\alpha)$ is therefore a constant of choice.

Equation 5.13 defines the volume of an ellipsoid in terms of a, b and c. All combinations of a, b and c on the surface form the limits of the possible polynomial, but only two unique polynomials from this set are associated with the maximum (positive and negative) deviation from the expected distance-to-V_1, obtained using the expected coefficients A, B and C. The problem then is to identify these two points so that the uncertainty in the distance-to-go estimate can be calculated.

Defining γ as the matrix $(\beta-\Omega)$ then the equation of the ellipsoidal surface can be obtained from Equation 5.13 and re-written as:

$$\gamma^T(X^TX)\gamma = k_1 \qquad \ldots (5.14)$$

where k_1 is a constant for a particular calculation, given by $[ps^2F(p, v, 1-\alpha)]$.

Consequently,

$$\begin{bmatrix} \gamma_1 & \gamma_2 & \gamma_3 \end{bmatrix} \begin{bmatrix} n & \sum x_i & \sum x_i^2 \\ \sum x_i & \sum x_i^2 & \sum x_i^3 \\ \sum x_i^2 & \sum x_i^3 & \sum x_i^4 \end{bmatrix} \begin{bmatrix} \gamma_1 \\ \gamma_2 \\ \gamma_3 \end{bmatrix} = k_1 \qquad \ldots (5.15)$$

Expanding the equation,

$$\gamma_1^2[n] + \gamma_1\gamma_2[\Sigma x_i] + \gamma_1\gamma_3[\Sigma x_i^2] + \gamma_1\gamma_2[\Sigma x_i] + \gamma_2^2[\Sigma x_i^2] + \gamma_2\gamma_3[\Sigma x_i^3] + \gamma_1\gamma_3[\Sigma x_i^2] + \gamma_2\gamma_3[\Sigma x_i^3] + \gamma_3^2[\Sigma x_i^4] = k_1 \qquad \ldots (5.16)$$

---

[40] In compliance with AS-8044.

where: Ω is the 3x1 matrix of the expected polynomial coefficients A, B and C
β is the 3x1 matrix of the coefficient variables a, b and c, in this case all combinations within the selected confidence interval
p is the number of degrees of freedom (3)
$\nu = (n-p)$ with n being the number of data points
s is the standard deviation of the least-squares fit
$F(p, \nu, 1-\alpha)$ is the F-distribution value for p, ν, $1-\alpha$
$(1-\alpha)$ is the confidence level of choice (0.99)[40]

$F(p, \nu, 1-\alpha)$ is therefore a constant of choice.

Equation 5.13 defines the volume of an ellipsoid in terms of a, b and c. All combinations of a, b and c on the surface form the limits of the possible polynomial, but only two unique polynomials from this set are associated with the maximum (positive and negative) deviation from the expected distance-to-V_1, obtained using the expected coefficients A, B and C. The problem then is to identify these two points so that the uncertainty in the distance-to-go estimate can be calculated.

Defining γ as the matrix $(\beta - \Omega)$ then the equation of the ellipsoidal surface can be obtained from Equation 5.13 and re-written as:

$$\gamma^T (X^T X) \gamma = k_1 \qquad \ldots (5.14)$$

where k_1 is a constant for a particular calculation, given by $[ps^2 F(p, \nu, 1-\alpha)]$.

Consequently,

$$\begin{bmatrix} \gamma_1 & \gamma_2 & \gamma_3 \end{bmatrix} \begin{bmatrix} n & \sum x_i & \sum x_i^2 \\ \sum x_i & \sum x_i^2 & \sum x_i^3 \\ \sum x_i^2 & \sum x_i^3 & \sum x_i^4 \end{bmatrix} \begin{bmatrix} \gamma_1 \\ \gamma_2 \\ \gamma_3 \end{bmatrix} = k_1 \qquad \ldots (5.15)$$

Expanding the equation,

$$\gamma_1^2[n] + \gamma_1\gamma_2[\Sigma x_i] + \gamma_1\gamma_3[\Sigma x_i^2] + \gamma_1\gamma_2[\Sigma x_i] + \gamma_2^2[\Sigma x_i^2] + \gamma_2\gamma_3[\Sigma x_i^3] + \gamma_1\gamma_3[\Sigma x_i^2] + \gamma_2\gamma_3[\Sigma x_i^3] + \gamma_3^2[\Sigma x_i^4] = k_1 \qquad \ldots (5.16)$$

---

[40] In compliance with AS-8044.

which reduces to:

$$\gamma_1^2[n] + 2\gamma_1\gamma_2[\Sigma x_i] + 2\gamma_1\gamma_3[\Sigma x_i^2] + \gamma_2^2[\Sigma x_i^2] + 2\gamma_2\gamma_3[\Sigma x_i^3] + \gamma_3^2[\Sigma x_i^4] = k_1 \quad \ldots (5.17)$$

The function of the surface is therefore given by:

$$f(\gamma_1, \gamma_2, \gamma_3) = \gamma_1^2[n] + 2\gamma_1\gamma_2[\Sigma x_i] + 2\gamma_1\gamma_3[\Sigma x_i^2] + \gamma_2^2[\Sigma x_i^2] + 2\gamma_2\gamma_3[\Sigma x_i^3] + \gamma_3^2[\Sigma x_i^4] - k_1 \quad \ldots (5.18)$$

Differentiating f with respect to γ_1, γ_2 and γ_3,

$$\frac{\partial f}{\partial \gamma_1} = 2\gamma_1 n + 2\gamma_2 \sum x_i + 2\gamma_3 \sum x_i^2 \quad \ldots (5.19a)$$

$$\frac{\partial f}{\partial \gamma_2} = 2\gamma_1 \sum x_i + 2\gamma_2 \sum x_i^2 + 2\gamma_3 \sum x_i^3 \quad \ldots (5.19b)$$

$$\frac{\partial f}{\partial \gamma_3} = 2\gamma_1 \sum x_i^2 + 2\gamma_2 \sum x_i^3 + 2\gamma_3 \sum x_i^4 \quad \ldots (5.19c)$$

The gradient function $grad(f)$ is therefore given by:

$$grad(f) = 2\begin{bmatrix} n & \sum x_i & \sum x_i^2 \\ \sum x_i & \sum x_i^2 & \sum x_i^3 \\ \sum x_i^2 & \sum x_i^3 & \sum x_i^4 \end{bmatrix}\begin{bmatrix} \gamma_1 \\ \gamma_2 \\ \gamma_3 \end{bmatrix} \quad \ldots (5.20)$$

or

$$grad(f) = 2(X^T X)\gamma = 2(X^T X)(\beta - \Omega) \quad \ldots (5.21)$$

where β contains the coefficients on the surface of the ellipsoid.

Theoretically, the polynomial that results in the maximum distance-to-go error is described by that function which results in the greatest variation in the expected time-to-go to V_1. Mathematically, therefore, it is a matter of determining the maximum variation of the independent variable for a target value of the dependent variable. In order to simplify the algebra involved, however, the polynomial that exhibits this maximum error is assumed, instead, to generate the maximum error in velocity at the expected time V_1 is reached. Although mathematically this is not necessarily correct, the error associated with this approximation is expected to be very small.

The velocity error ε at the target time t_1 is defined by Equation 5.22[41]:

$$\varepsilon = \mathrm{V}_1 - \{a + bt_1 + ct_1^2\} \qquad \dots (5.22)$$

Equation 5.22 can be expressed in terms of the function of a plane:

$$g(a,b,c) = a + bt_1 + ct_1^2 - \mathrm{V}_1 + \varepsilon \qquad \dots (5.23)$$

The location of the plane $g(a,b,c)$ is determined by the error ε. The plane will pass through the centre of the ellipsoid which defines the expected values A, B and C determined by the method of least-squares when ε is zero (Figure 5.5).

It follows that the coefficients generating the maximum velocity error, therefore, can be determined by increasing ε until the plane will just touch the extremities of the ellipsoid. In terms of vector algebra, these two points are identified by having their gradient vectors parallel to the plane in question[42]. The gradient function of the plane is defined by the partial differentiation with respect to a, b and c:

$$grad(g) = \begin{bmatrix} -1 \\ -t_1 \\ -t_1^{\,2} \end{bmatrix} \qquad \dots (5.24)$$

Since the two gradient functions $grad(f)$ and $grad(g)$ must be parallel,

$$\left[X^T X\right] y = \pm k_2 \begin{bmatrix} 1 \\ t_1 \\ t_1^{\,2} \end{bmatrix} \qquad \dots (5.25)$$

---

[41] The expected time at which V_1 is reached, termed t_1 in this text, is obtained by solving the compensated equation $\mathrm{V}_1 = A' + Bt_1 + Ct_1^2 + Dt_1^3$. An approximation is introduced in Equation 5.22, which assumes that the effect of the controlled 3rd order coefficient is negligible, thus significantly simplifying the algebra. This approximation implicitly translates to the assumption that the maximum velocity error between the compensated polynomials occurs at the same velocity as for the uncompensated functions. The error involved in this simplification is of the order of 0.5s but this is acceptable for the purpose of identifying the polynomial that generates the largest error in the distance-to-go to V_1.

[42] A shifting of the plane $g(a,b,c)$ due to a change in ε results only in an elongation of the gradient vector.

where k_2 is a positive constant equating the magnitude of the vectors and does not affect their direction.

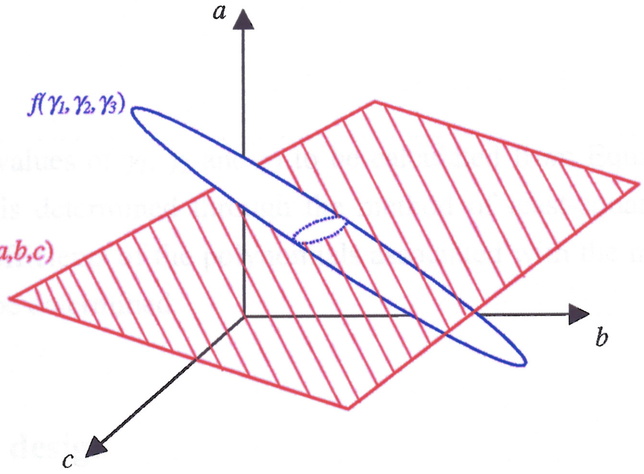

Figure 5.5: A typical ellipsoidal function f with a plane function g passing through it, as would be expected in the determination of the largest distance-to-go error.

Rearranging Equation 5.25,

$$\gamma = \pm k_2 \left[X^T X\right]^{-1} \begin{bmatrix} 1 \\ t_1 \\ t_1^{\,2} \end{bmatrix} \qquad \ldots (5.26)$$

Which can be expanded into three linear equations:

$$\gamma_1 = \pm k_2 P \qquad \ldots (5.27a)$$

$$\gamma_2 = \pm k_2 Q \qquad \ldots (5.27b)$$

$$\gamma_3 = \pm k_2 R \qquad \ldots (5.27c)$$

where P, Q and R represent the components of the matrix $[X^TX][1\ t_1\ t_1^2]^T$.

Substituting γ_1, γ_2 and γ_3 in Equation 5.17,

$$k_2 = \pm\sqrt{\frac{k_1}{P^2(n)+2PQ(\sum x_i)+2PR(\sum x_i^{\,2})+Q^2(\sum x_i^{\,2})+2QR(\sum x_i^{\,3})+R^2(\sum x_i^{\,4})}} \quad \ldots (5.28)$$

This allows the values of γ_1, γ_2 and γ_3 to be calculated from Equations 5.27. Since $\gamma=(\beta-\Omega)$ and Ω is determined through the method of least-squares, β, which now identifies the coefficients of the polynomials associated with the maximum distance-to-go error, can be determined.

5.5 Software design

Airborne software was designed and written in Pascal to facilitate interfacing with the data acquisition system on G-NFLC. Several features have been included to ensure the software is capable of handling exceptional conditions and will not generate erroneous data. Other features have been introduced to facilitate use during routine flight operations of the NFLC. These attributes are not discussed in this document, as they are not of direct relevance to the scope of this text. This section presents the fundamental concepts of the software design and implementation, focusing on particular attributes of interest.

5.5.1 THE MAIN PROGRAM

The main program is a simple routine that fetches the relevant parameters from the onboard data acquisition system and then executes the algorithms that predict D_1 and the uncertainty associated with this prediction as described in Section 5.4. The routine monitors the engine power output and IRS acceleration to detect the start of the take-off, following which the data is recorded and the prediction algorithms executed in real-time. It is appreciated that this technique of detecting the start of take-off will not be adequate for normal operations as implemented, but it proved totally satisfactory during the NFLC's flight operations, particularly since all the take-offs were to be carried out with full power applied prior to brake release.

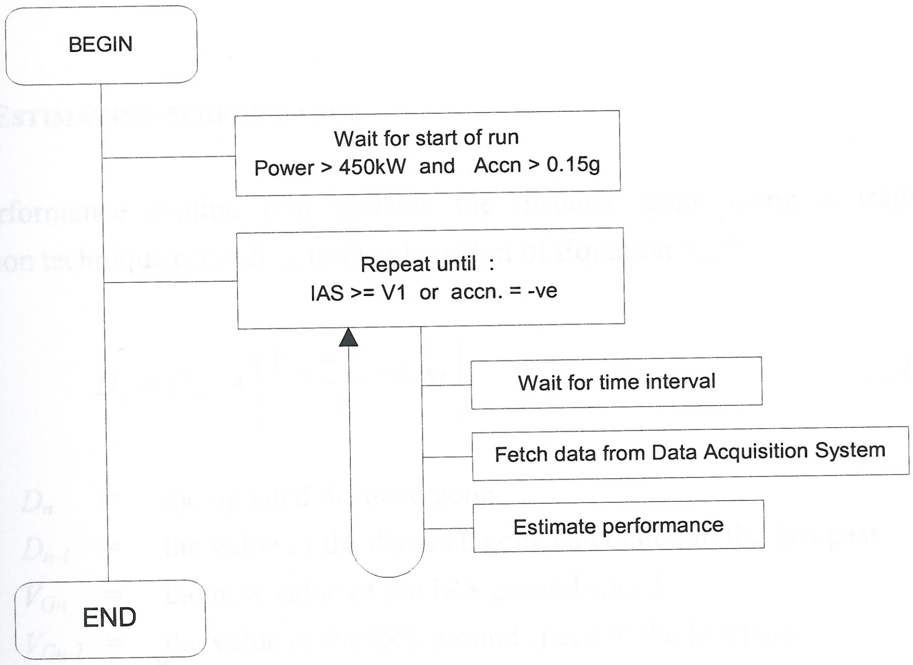

Figure 5.6: Jetstream-100 main routine flow chart.

The timing (50ms) controlling the frequency of the data acquisition rate is generated by polling the system time and simply waiting for 50ms to pass before initiating execution of the algorithm again. Apart from the fact that the routines executed in the loop are short enough to ensure that they are executed well within the 50ms bracket, the timing is not critical. This is because the least-squares curve-fitting technique does not require data to be acquired at regular intervals of the independent variable (time). A fundamental assumption of the technique, however, is that the independent variable data is assumed to be perfectly accurate so that any random errors in the dependent variable (velocity) can then be averaged out. The way it has been implemented, timing is only accurate to within a few milliseconds[43]. Conceptually, though, an error in time measurement can be translated to an error in velocity. Assuming a worst case acceleration of about 5kt/s, a 5ms delay could be expected to contribute to at most 0.025kt of uncertainty. Besides the fact that this is

---

[43] This includes the transportation delay introduced by the onboard data acquisition system.

significantly smaller than the resolution of the IRS ground speed signal[44], the error can be assumed to be random with zero mean and therefore will be averaged out during curve-fitting[45]. Whilst acknowledging that higher accuracy could be achieved with tighter control over timing through appropriate considerations in software and hardware implementation, the errors involved were acceptable for the scope of this work.

5.5.2 ESTIMATING PERFORMANCE

The performance routine first updates the distance gone using a trapizoidal integration technique according to the algorithm of Equation 5.29:

$$D_n = D_{n-1} + \left[\frac{V_{Gn} + V_{Gn-1}}{2}\Delta t\right] \qquad \ldots (5.29)$$

where: D_n = the updated distance gone
D_{n-1} = the value of the distance gone calculated in the last pass
V_{Gn} = the new value of the IRS ground speed
V_{Gn-1} = the value of the IRS ground speed at the last pass
Δt = the time elapse between the previous and current data acquisitions[46].

The routine then determines the expected distance-to-go to V_1 by integrating the expected polynomial obtained through the method of least-squares. This is added to the distance gone to generate the expected value of D_1. The uncertainty of the estimate is finally calculated in terms of the higher and lower expected limits of D_1 using the equations of Section 5.3.

The first two seconds of the run are not considered for the least-squares fitting technique because this period contains the transient characteristics associated with large rates of change of acceleration. Since the method of least-squares inherently assumes steady conditions with respect to the coefficients of the characteristic

---

[44] The Litton LTN-90 IRS fitted on G-NFLC has a resolution of 0.125kt [92].

[45] Nevertheless, such errors contribute to a larger standard deviation and uncertainty in the prediction.

[46] Δt is of the order of 50ms and is measured as the difference of the intervals between the moments of data acquisition and the start of the run and not as a delay between successive acquisitions. This approach restricts the error in the total distance gone to a bound of the order of 0.3m.

polynomial, such transients tend to de-stabilise the fit, particularly in the earlier stages when only a brief time history is yet available.

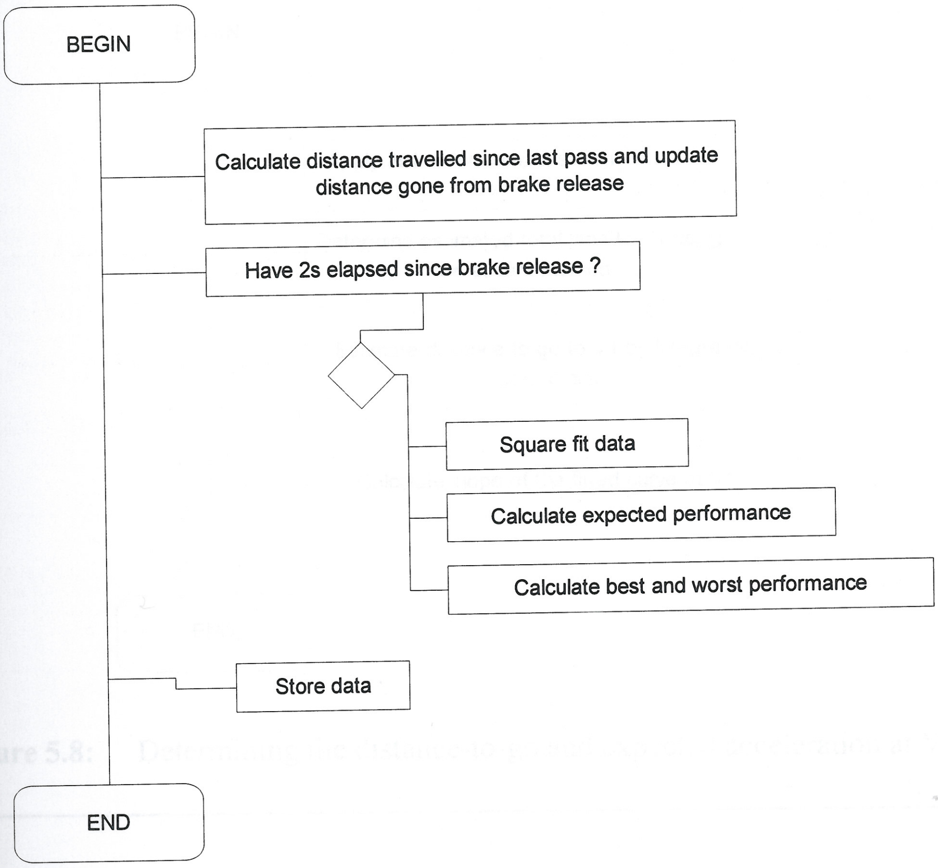

Figure 5.7: The performance estimating routine.

The expected, best and worst performance estimates are calculated using the same routines with the three sets of polynomial coefficients determined as described above. First, the controlled 3rd order compensation as described in Section 5.2 is introduced (Figure 5.8). The resulting polynomial is then used to determine t_1, the time at which V_1 would be achieved and this is used as the upper limit during integration of the function for the calculation of the distance-to-go. The slope at V_1 is determined to ensure that there is no indication that the acceleration at V_1 will drop below the desired level.

The output of the algorithm is stored in memory and then downloaded into secondary storage at the end of the run for post-flight performance analysis.

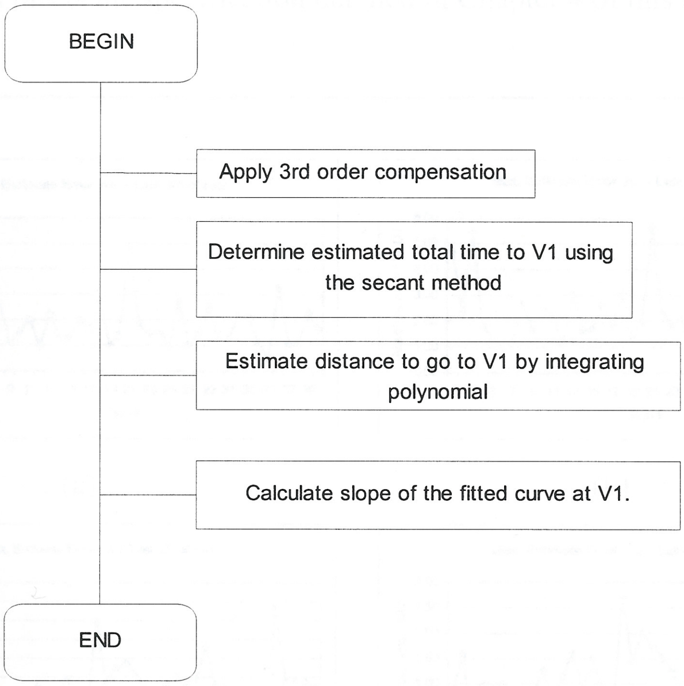

Figure 5.8: Determining the distance-to-go and expected acceleration at V_1.

5.6 Algorithm performance analysis and discussion

To validate the algorithm, 40 take-off runs were conducted in which take-off power was applied before brake-release. These take-offs were part of routine NFLC flight operations and covered a wide range of dispatch weight and balance configurations and meteorological conditions[47]. Algorithm performance was measured by determining, in post-flight analysis, the prediction error along the run. This prediction error was the difference, at every point, between the expected distance to V_1 and that eventually covered. In order to quantify the prediction qualities, the absolute maximum prediction error exhibited in the last ¾ of the run and that of the

---

[47] No take-offs are known to have been conducted in severe weather conditions or on heavily contaminated runways.

last ½ distance were determined. The results are presented in Appendix II and in graphical form in Figure 5.9. Since the absolute error can be considered random, the maximum error expected on 99% of the runs can then be determined. The relevant figures are also presented in Figure 5.9. These figures indicate that the performance of the algorithm meets the specification detailed in Chapter 4 of this text.

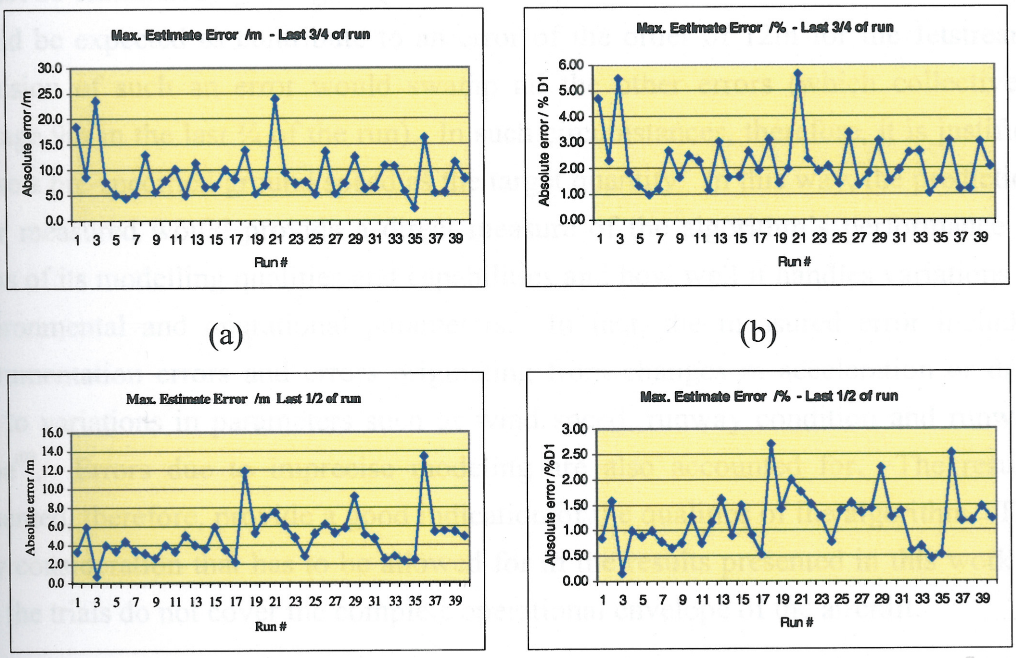

(a) (b)

(c) (d)

Figure 5.9: Algorithm performance measured on 40 take-offs.

¼ Distance error: average = 9.1m (2.26%)
std. dev. = 4.9m (1.11%)
99% conf. = 20.5m (4.83%)

½ Distance error: average = 4.8m (1.20%)
std. dev. = 2.5m (0.56%)
99% conf. = 10.6m (2.49%)

The source data is presented in Appendix II.

The algorithm uses ground speed for velocity, whilst the target velocity (V_1) is an indicated airspeed. As a result, the target velocity used by the algorithm as the upper limit of the integration in the calculation of the distance-to-go-to-V_1 should strictly take into account the discrepancy expected between the ground speed and V_1 at the moment the latter is indicated on the ASI. This discrepancy, however, has not been accounted for in the algorithm because such consideration would need to take into account the lag in the ASI[48] and would also require the algorithm to accurately predict the wind vector at V_1. This latter feature currently cannot be realistically implemented with an acceptable level of reliability. Consequently the uncertainty associated with the wind vector has to be accepted as a basic source of error which cannot be eliminated by design. Quantitatively, a variation of 1kt in headwind at V_1 would be expected to contribute to an error of the order of 12m for the Jetstream. Inclusion of such an error would swamp all the other errors (which collectively average 9m in the last ¾ of the run). In such circumstances, therefore, it is justified to use a pre-specified ground speed as the target quantity. In this way, the prediction error measured would provide a direct measure of the algorithm's performance in terms of its modelling qualities and capabilities and how well it handles variations in environmental and operational parameters. In fact, the measured error includes instrumentation errors and errors originating from changes in acceleration or drag due to variations in parameters such as wind speed, runway condition and runway slope[49]. Errors due to imprecise modeling are also accounted for. The results presented, therefore, provide a good indication of the qualities of the algorithm. The only consideration that has to be allowed for in the results presented in this work is that the trials do not cover the complete operational envelope of the aircraft.

One way the prediction error could be reduced is by controlling the system-generated errors. These are, in effect, those introduced by the IRS and the Jetstream's onboard data acquisition system. IRS ground speed errors involve offset (drift) and ratiometric errors, apart from quantisation errors. All three components do not affect the quality of fit, since the former two will result in an adjustment in the polynomial coefficients and the third will average out to zero[50]. Consequently, such errors do not affect the validation of the algorithm. The former two errors, however, do introduce an error in the total distance gone and this is of the order of 5% for the runs monitored. This error, however, does not significantly affect the results as presented.

---

[48] This lag is a function of the acceleration and can be of the order of a few knots for mechanical instruments.

[49] A fundamental assumption made in employing extrapolation in the least-squares fit is that identical conditions to those experienced in the fitted time history will be experienced in the period of extrapolation. This implies that 'unexpected' variations in parameters such as runway slope are not taken into account. This issue is further addressed in Chapter 7.

[50] Quantisation error will, however, increase the variance of the fitted data, resulting in a higher prediction uncertainty and a delay in the convergence of the algorithm.

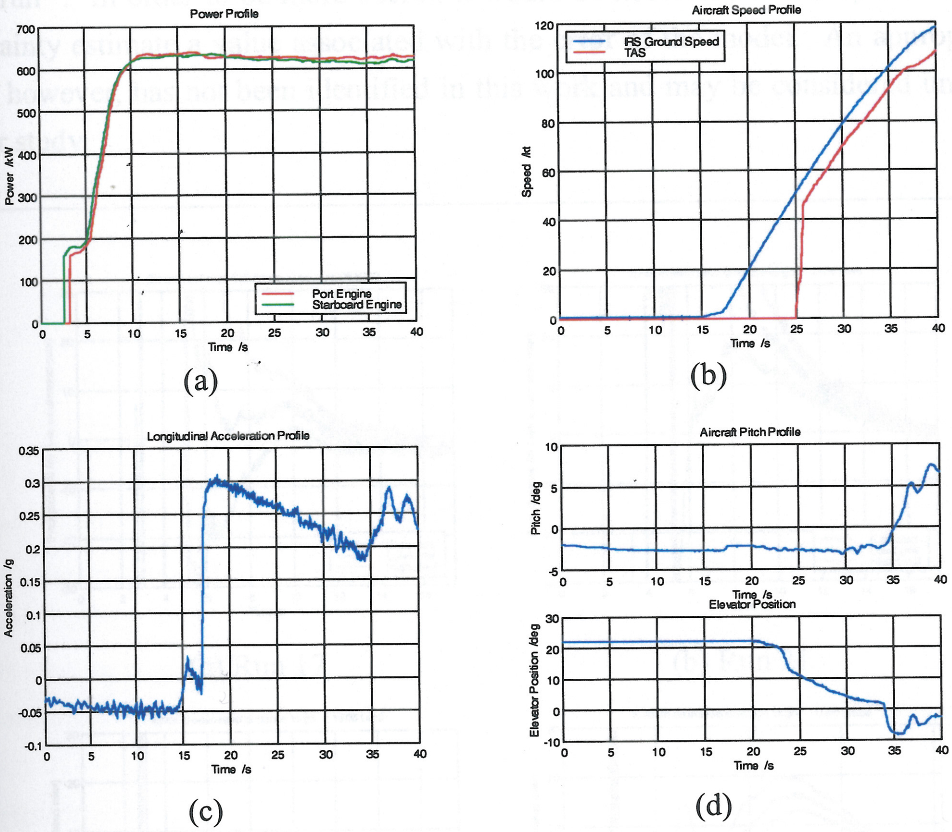

(a)

(b)

(c)

(d)

Figure 5.10: Various parameter profiles during a typical take-off.

The validity of the algorithm calculating the uncertainty of the prediction was also studied in post-flight analysis. The results indicated that since a very good fit is achieved throughout the run, the uncertainty associated with the lack-of-fit converges rapidly to very small quantities. Figure 5.11 illustrates this on four selected runs. Runs 17 and 33 exhibit low prediction errors throughout the last ¾ part of the run, whilst runs 21 and 36 exhibit high errors before and after the half way point respectively. Although runs 21 and 36 probably experienced some sort of anomaly during the run that could not be accounted for by the algorithm before they occurred, the four traces indicate that most of the prediction error is mainly due to modelling errors and not due to a lack of fit or signal noise. Use of the algorithm as implemented would probably be restricted to ensuring that a good fit is obtained in every run[51]. In order to be more useful, it would be necessary to incorporate in the uncertainty estimate a value associated with the error of the model. An appropriate value, however, has not been identified in this work and may be considered under a further study.

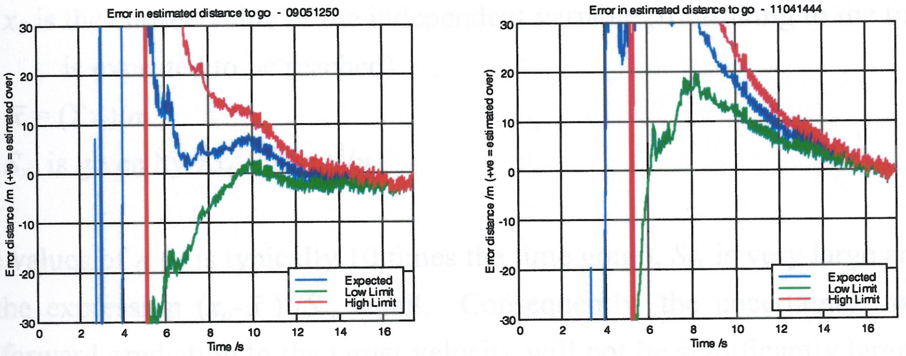

(a) Run 17 (b) Run 21

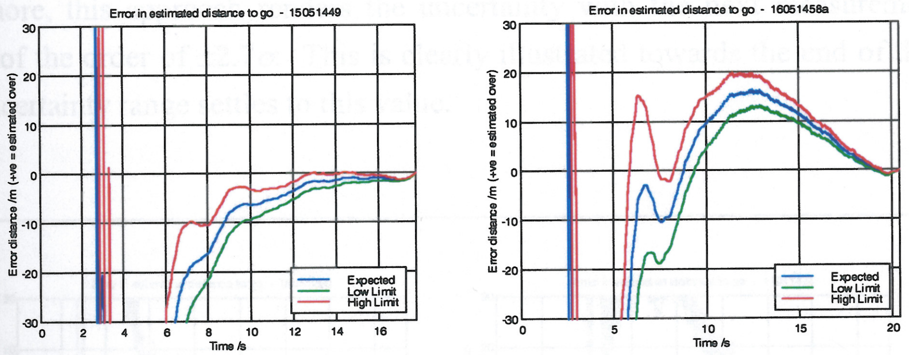

(c) Run 33 (d) Run 36

Figure 5.11: Performance of uncertainty calculations on four selected runs.

Text-book statistical tools for determining the uncertainty associated with the prediction of new 'observations' (values of the dependent variable – velocity) are also available [93]. Mathematically, this uncertainty can be presented as:

---

[51] This would nevertheless be a useful tool, ensuring the algorithm does not generate erroneous predictions in the exceptional cases where the 2nd order model does not fit an anomalous ground run. Indeed, this mechanism could also be used to highlight the anomaly.

$$\Delta y_0 = \pm t_{\alpha/2,n-3}\sqrt{\sigma^2\left[1+\frac{1}{n}+\frac{(x_0-\bar{x})^2}{S_{xx}}\right]} \qquad \ldots (5.30)$$

where: Δy_0 is the uncertainty associated with the 'observation' at a chosen x_0

$t_{\alpha/2,n-3}$ is about 2.7, the value of the t distribution for $\alpha/2=0.005$ and $n-3 > 40$

x_0 is the chosen value of the independent variable (translating to the time V_1 is expected to be reached)

$\bar{x} = (\Sigma x_i)/n$

S_{xx} is given by $\Sigma x_i^2 - (\Sigma x_i)^2/n$

For large values of n (n is typically 10 times the time gone), S_{xx} is very large and this renders the expression $(x_o - \bar{x})^2/S_{xx}$ small. Consequently, the uncertainty involved with the forward prediction to the target velocity will not be significantly larger than that to the next point 100ms away. This effect is exhibited in Figure 5.12. Furthermore, this approach renders the uncertainty with the next measurement of velocity of the order of ±2.7σ. This is clearly illustrated towards the end of the run as the uncertainty range settles to this value.

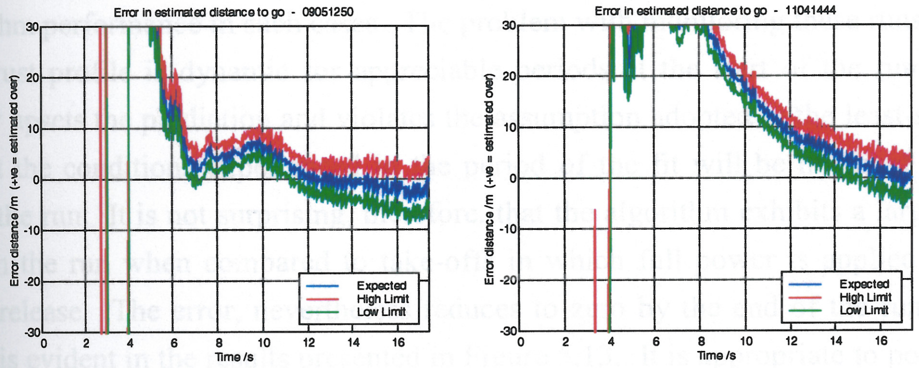

(a) Run 17

(b) Run 21

Figure 5.12: Performance of uncertainty calculations using a text-book standard statistical tool.

Such a high uncertainty at the end of the run is not realistic during take-off because the velocity signal is strictly monotonic in nature. In fact, the rate of change of velocity is much larger than the quantisation error and system noise is greatly reduced by the filtering carried out within the inertial system. As a result, the uncertainty should be expected to fall to zero at the end of the run. This is not allowed for by Equation 5.30 because of two fundamental assumptions implicitly adopted in the derivation of the equation. The first is that the regression line is assumed to correctly describe the function of the fitted data and the second is that that the deviation of each point from the regression line is assumed to be entirely random. This, clearly, is not actually the case. In fact, a significant amount of the deviation from the regression line is due to the imperfections in the model. As a result, the actual randomness of the data is much less than that calculated and a smaller uncertainty, therefore, should be associated with the prediction of the next point. Although the theory developed in Section 5.4 is also based on the same assumptions, the very nature of the approach supports the notion of a reduced uncertainty towards the end of the run. What is needed, then, is a quantification of the uncertainty due to the modelling error to complement the theory already developed. Such an addition would result in a more realistic estimate of the uncertainty associated with the prediction of the distance-to-go. It should be possible to empirically establish such an expression once a larger number of monitored runs are recorded and anlaysed.

Eight rolling start take-offs were also monitored to obtain a basic indication of algorithm performance in such cases. The problem with monitoring these runs is that the thrust profile is dynamic for appreciable periods at the start of the run. This clearly upsets the prediction and violates the assumption adopted in the least-squares fit that the conditions experienced in the period of the fit will be mirrored further down the run. It is not surprising, therefore, that the algorithm exhibits a large error later in the run when compared to take-offs in which full power is applied before brake-release. The error, nevertheless reduces to zero by the end of the run. This effect is evident in the results presented in Figure 5.13. It is appropriate to point out, however, that these figures are to be interpreted with caution, as the prediction accuracy is highly sensitive to the way the rolling start is conducted[52]. In fact, a large standard deviation can be noted in the results. It is interesting to note that the prediction error in the last half of the run appears to be comparable with that of non-rolling-start take-offs. If this actually is the case, then the algorithm will have been

---

[52] Besides the fact that the actual technique adopted during the rolling start affects the acceleration profile, it also influences the moment the take-off is assumed to be initiated. Take-off is assumed to be initiated in the algorithm implementation when power is greater than 450kW and acceleration is in excess of 0.15g.

demonstrated to be versatile enough to reduce the prediction error to acceptable levels sufficiently early, even with large disturbances at the start of the run. The results of Figure 5.13 and traces of Figure 5.15 suggest that that the algorithm predictions may, in fact, be useful during the last 5 or 6 seconds of the run. Such a claim, however, needs to be confirmed with further analysis involving more rolling-start take-offs.

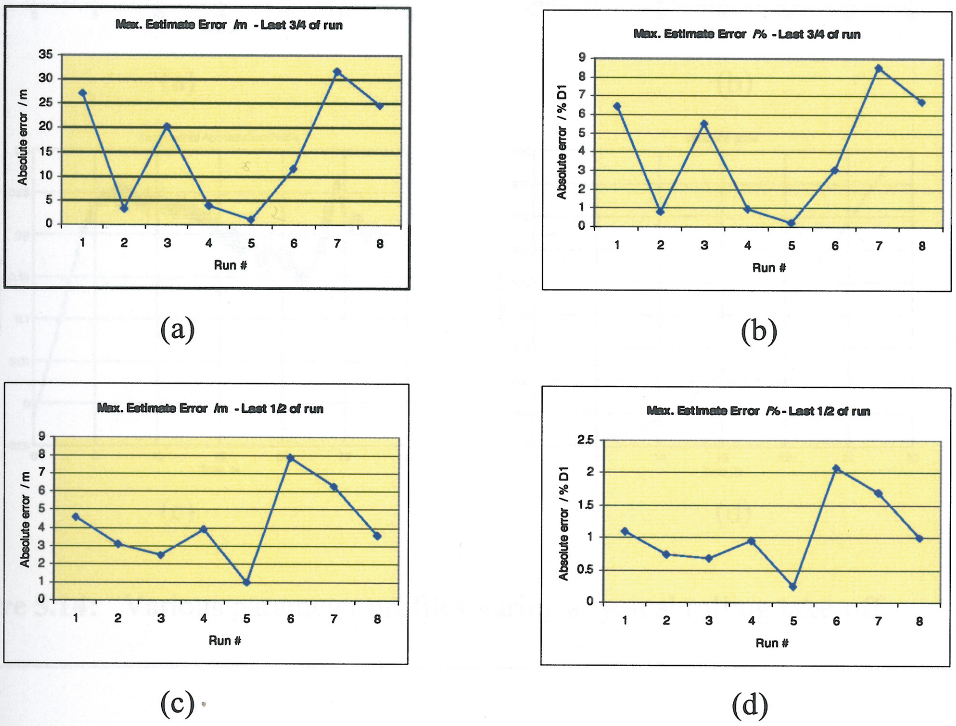

(a) (b) (c) (d)

Figure 5.13: Algorithm performance measured on 8 rolling take-offs.

¼ Distance error: average = 15.5m (4.03%)
std. dev. = 12.0m (3.17%)
99% conf. = 55.4m (14.6%)

½ Distance error: average = 4.1m (1.06%)
std. dev. = 2.2m (0.58%)
99% conf. = 11.3m (3.00%)

The source data is presented in Appendix II.

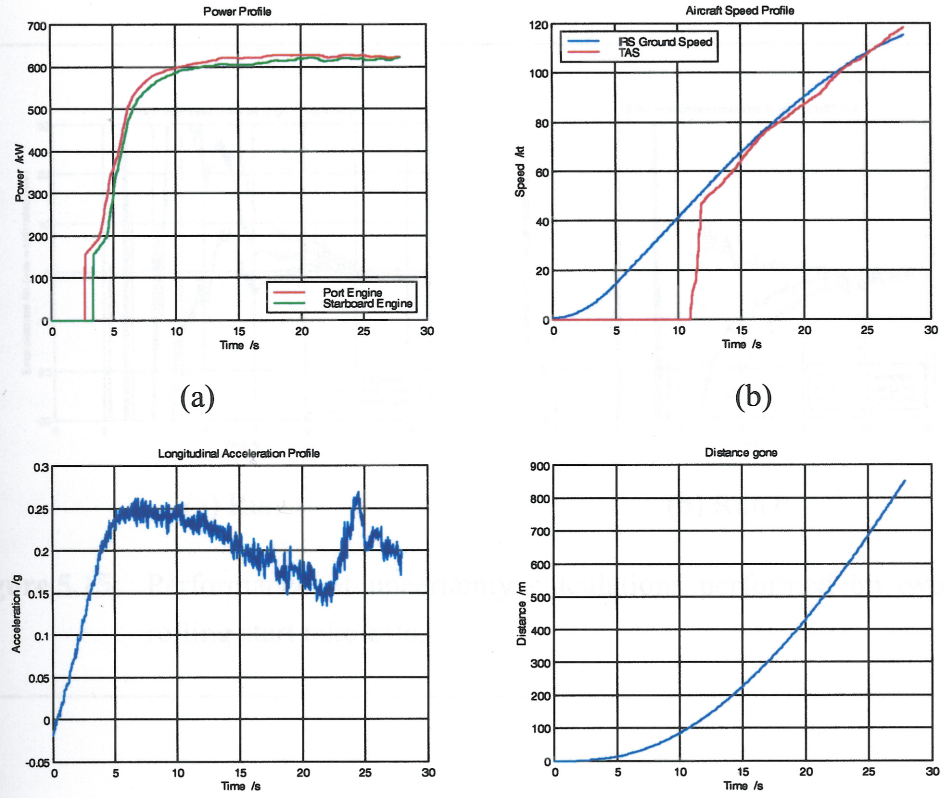

(a) (b)

(c) (d)

Figure 5.14: Various parameter profiles during a typical rolling take-off.

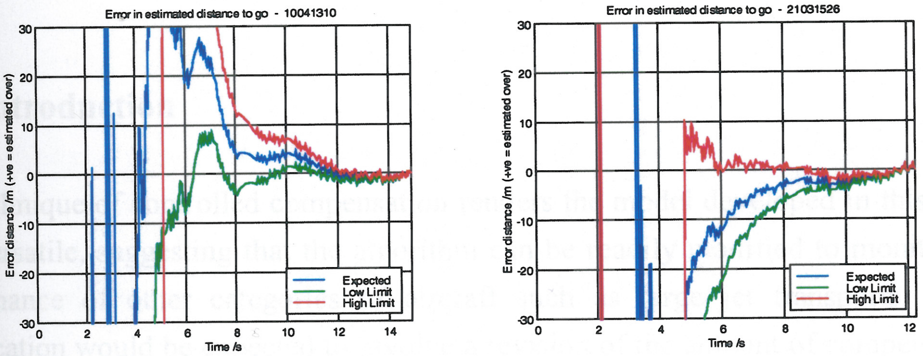

(a) Run 1

(b) Run 6

Figure 5.15: Performance of uncertainty calculations performed on two rolling start take-offs.

Chapter 6: ALGORITHM DEVELOPMENT FOR LARGE JET AIRCRAFT

6.1 Introduction

The technique of controlled compensation renders the model developed in this work very versatile, suggesting that the algorithm can be readily modified to monitor the performance of other categories of aircraft such as large jet transports. This modification would be expected to involve a revision of the amount of compensation applied, since the thrust characteristic of turbofan engines (as in the case of large jet transports) is significantly different from that of turbine-propeller driven aircraft.

6.2 Adapting the algorithm

As was the case for the turbine-propeller package on the Jetstream-100, the thrust function of turbofan and turbojet engines can be expressed as a second order function of airspeed for constant engine speed:

$$T = \alpha_0 + \alpha_1 V + \alpha_2 V^2 \qquad \ldots (6.1)$$

where α_0 is the static thrust, $\alpha_1 V$ defines the increase in momentum drag with forward speed and $\alpha_2 V^2$ models the effect of the increase in ram pressure at the entry of the fan or compressor. The second order effect, however, is expected to be small for speeds associated with the ground run during take-off, rendering the characteristic almost linear in the speed range of interest. In particular, for the Rolls-Royce RB-211-535E4 in the ISA, sea-level, take-off rating condition, the ratio α_2/α_0 is of the order of $4.34\text{x}10^{-6}$ $(\text{m/s})^{-2}$ [17]. This translates to $1.15\text{x}10^{-6}$ kt^{-2}, which is more than an order of magnitude smaller than the corresponding ratio of the thrust function of the Turbomeca Astazou-Hamilton Standard package on the Jetstream. Even when taking into account the fact that the target velocity of large transport aircraft is about 50% higher than that of the Jetstream[53], such a small second order

---

[53] The error in the distance-to-go estimate increases with higher target speeds (V_1) whenever a required compensation is not applied.

coefficient is not likely to justify the application of compensation with its associated complexity. This was actually found to be the case in preliminary testing using the College of Aeronautics' fixed base B747 simulator and also using traces recorded on actual runs during operations of B747-400 aircraft[54,55].

A basic monitor display was also designed to facilitate performance evaluation on the simulator[56]. This display proved instrumental in the analysis of anomalous runs having dynamic situations such as thrust resetting and momentary fluctuations in acceleration. Whilst predicting accurately on take-offs in which full thrust was allowed to develop before brake-release and the run progressed in steady conditions, the algorithm was found to be too stiff in dynamic situations, being reluctant to follow the change. Although it is appreciated that predicting the performance in such conditions has been considered beyond the scope of the design[57], the degree of stiffness recorded was considered excessive. Greater flexibility would not only allow the display to more appropriately represent the change in performance, but once steady conditions are re-established, the algorithm would be able to recover quicker to predict the correct distance-to-go. This is of particular relevance to large jet transport aircraft, since the ground run is significantly longer than that of the Jetstream, resulting in a greater exposure to disturbances that could affect the eventual distance travelled. Another consideration is that the majority of commercial take-offs have rolling starts and the prolonged dynamic conditions at the start tend to upset the predictions of a stiff algorithm. It was for these reasons that it was decided to modify the algorithm to be more sensitive to recent changes in performance.

This increase in sensitivity could be achieved by adopting the concept of weighted least-squares, where more recent data is given greater weighting than data from the earlier parts of the run when minimising the sum of the square of the error. Exponential weighting was selected because this technique offered the advantage of convenient control over the amount of flexibility introduced. The square of the weighted error, which is then minimised in the method of least-squares, is given by Equation 6.2:

---

[54] These and all other recordings of large jet transport operations used in this work were kindly provided by British Airways.

[55] For the simulator trials the Pascal program written for G-NFLC was re-written in Modula-2 and modified accordingly to facilitate integration with the simulator software. The real take-off recordings were analysed on Matlab.

[56] The display design is described in Chapter 7.

[57] The main role of the monitor has been defined to predict performance assuming steady conditions not only because of the likelihood that the predictive algorithm would fail under dynamic conditions but also because such conditions can be readily picked up by the crew through other cues.

$$\varepsilon_i^{\,2}.e^{2kx_i} = [a + bx_i + cx_i^{\,2} - y_i]^2.e^{2kx_i} \qquad \ldots (6.2)$$

where: x_i and y_i are the i^{th} measurement of time and velocity respectively

ε_i is the error in the data y_i (the fitted curve is assumed to define the error-free characteristic)

k is the coefficient which controls the weighting introduced

a, b and c are the three coefficients of the polynomial.

The normal equations are consequently modified from Equation 5.7 to accommodate the weighting:

$$\begin{bmatrix} e^{2kx_i} & \sum x_i e^{2kx_i} & \sum x_i^2 e^{2kx_i} \\ \sum x_i e^{2kx_i} & \sum x_i^2 e^{2kx_i} & \sum x_i^3 e^{2kx_i} \\ \sum x_i^2 e^{2kx_i} & \sum x_i^3 e^{2kx_i} & \sum x_i^4 e^{2kx_i} \end{bmatrix} \begin{bmatrix} A \\ B \\ C \end{bmatrix} = \begin{bmatrix} \sum y_i e^{2kx_i} \\ \sum x_i y_i e^{2kx_i} \\ \sum x_i^2 y_i e^{2kx_i} \end{bmatrix} \qquad \ldots (6.3)$$

The increased flexibility generated by the weighting given to recent history of the run could readily result in a significant departure of the extrapolated fit from the projected characteristic in adverse and highly dynamic situations. The severity of the effect would depend on the particular situation and the amount of weighting introduced by the algorithm and to a certain extent can be controlled by appropriate selection of the latter. Here, the major concern was the probability of misleading the crew with an erroneous estimate of performance. The nature of the algorithm tends to result in an exaggeration of the trend in performance in the dynamic condition. It is highly unlikely, however, that a significant drop in performance (which would result in an excessively large negative 2nd order coefficient) and an over-pessimistic prediction would mislead the crew because in such adverse conditions the crew would have already detected the drop in performance through other means. An over-pessimistic prediction would thus only confirm the crew's impression. If, however, for any reason the performance were to improve during the run, it would be very possible to mislead the crew into believing that sufficient progress is being made by displaying an over-optimistic prediction. This must clearly be avoided. The largest contribution to such an optimistic prediction is an erroneous 2nd order coefficient, suggesting that its value should be bound to a limit corresponding to the best performance practical. To this effect, the algorithm calculates the average value of the 2nd order coefficients calculated in previous fits earlier in the run and sets the upper bound of the coefficient of the new fit to 80% of this value[58]. Besides, new candidate values of the 2nd order coefficient are also screened to ensure they are within a realistic range. Whilst not affecting the fit during normal operations, this technique restricts the amount of any optimism in the prediction.

The data of all real jet transport runs considered in this work has been sourced from recordings generated by the flight data recording systems built specifically for British Airways' aircraft. The recorders repeatedly sample and record several parameters at various update rates throughout every flight so that, through post-flight analysis, the airline can monitor aircraft and crew performance. By identifying any exceedences, the airline then assesses the safety of its operations. IRS ground speed data is only sampled once a second by the system on the B747-400. This update rate is inadequate for the purposes of take-off performance monitoring and longitudinal acceleration data[59], sampled at 4Hz[60], was utilised instead. The acceleration data had to be adjusted to take into account the gravitational component due to aircraft pitch and then integrated to derive the ground speed prior to performing the least-squares fit.

6.3 Validation on wide-bodied jet transports

80 B747-400 runs conducted from various airfields were randomly sampled from normal operations[61] and used to validate the performance of the algorithm. Dispatch weights ranged between 463,000lbs and 874,000lbs. A typical take-off profile is presented in Figure 6.1. All take-offs monitored had rolling starts, where an intermediate thrust was commanded for a few seconds prior to advancing the levers to the thrust setting scheduled for the take-off. The duration of this dynamic condition varied significantly between the take-offs. It was decided, in these circumstances, to define the start of the run as the point at which the thrust levers

---

[58] As the 2nd order coefficient is negative, 80% of the average value will ensure a minimum amount of curvature. This value may be different for other powerplant types.

[59] Longitudinal acceleration data was obtained from a Sunstrand Data Control Inc. accelerometer, part no. 971-4193-001/2, acceleration range: -3g to +6g vertical, ±1g lateral and longitudinal. Output range 0.2V-5V. Static error band ±50mV, alignment within 0.5° of case reference surface.

[60] During preliminary studies carried out on the Jetstream it was realised that a 10Hz sampling rate was optimal. Lower sampling frequencies generated smaller data populations for the least-squares fit and this tended to compromise the prediction accuracy of the algorithm [88]. The 4Hz update rate, however, had to be accepted in these circumstances.

[61] Runs in which the final thrust setting was achieved very late in the run (even up to 10 seconds before rotation) were rejected, as these conditions are beyond the scope of the monitor's operational envelope and the poor accuracy achieved would significantly bias the statistical analysis.

were advanced following the intermediate setting. The monitoring phase, however, was not initiated until the engine speed (rpm) was within about 1% of the steady value, to ensure that the initial transients did not seriously affect the predictions. The target velocity was chosen to be the moment the PF commanded the initiation of rotation, detected by a change in elevator position.

The optimal amount of exponential weighting introduced in the least-squares fit had to be determined empirically. This was necessary because excessive weighting would render the system too sensitive to the last few data points, resulting in what effectively is an amplification of signal noise and even a significant departure from the actual characteristic in extreme cases. Various values of k in Equation 6.3 were applied to the algorithm and the resulting prediction error noted. Results are presented in Table 6.1, where the maximum error for the last ¾ and ½ sections of the run to V_R are calculated as a percentage of the total distance from the start of the run. The values in the table indicate that a weighting of $0.2t$ offers optimal flexibility without compromising accuracy and reliability. Moreover, the performance with this weighting meets the requirements set out in Chapter 4 and Report CoA-0010. It is relevant to note, however, that a sampling rate higher than 4Hz should allow a larger weighting to be employed as more data points will be available for the fit.

As was the case for the Jetstream runs, the performance observed on the 80 runs are representative of normal operations and are unlikely to have involved particularly adverse conditions (such as highly contaminated runways, deflated tyres and inappropriate flap settings) that would have significantly compromised the viability of the run. In order to attempt to assess the algorithm's capability of handling various degrees of subtle performance degradation, simulator take-offs with flap settings varying from 0° to 30° were considered. For typical take-off flap settings (up to 15°) the performance of the monitor did not vary significantly, with a good, stable prediction being achieved within ¼ distance gone. This is not surprising, since these settings are designed not to greatly increase the drag of the aircraft. Beyond 15° of flap, however, the algorithm tended to initially predict optimistically, with the error reducing quickly as the run developed. Once again, this result was expected, since the algorithm as implemented is incapable of compensating for the drop in performance due to the large increase in drag introduced with the selected flap settings. These results are presented in Figure 6.3.

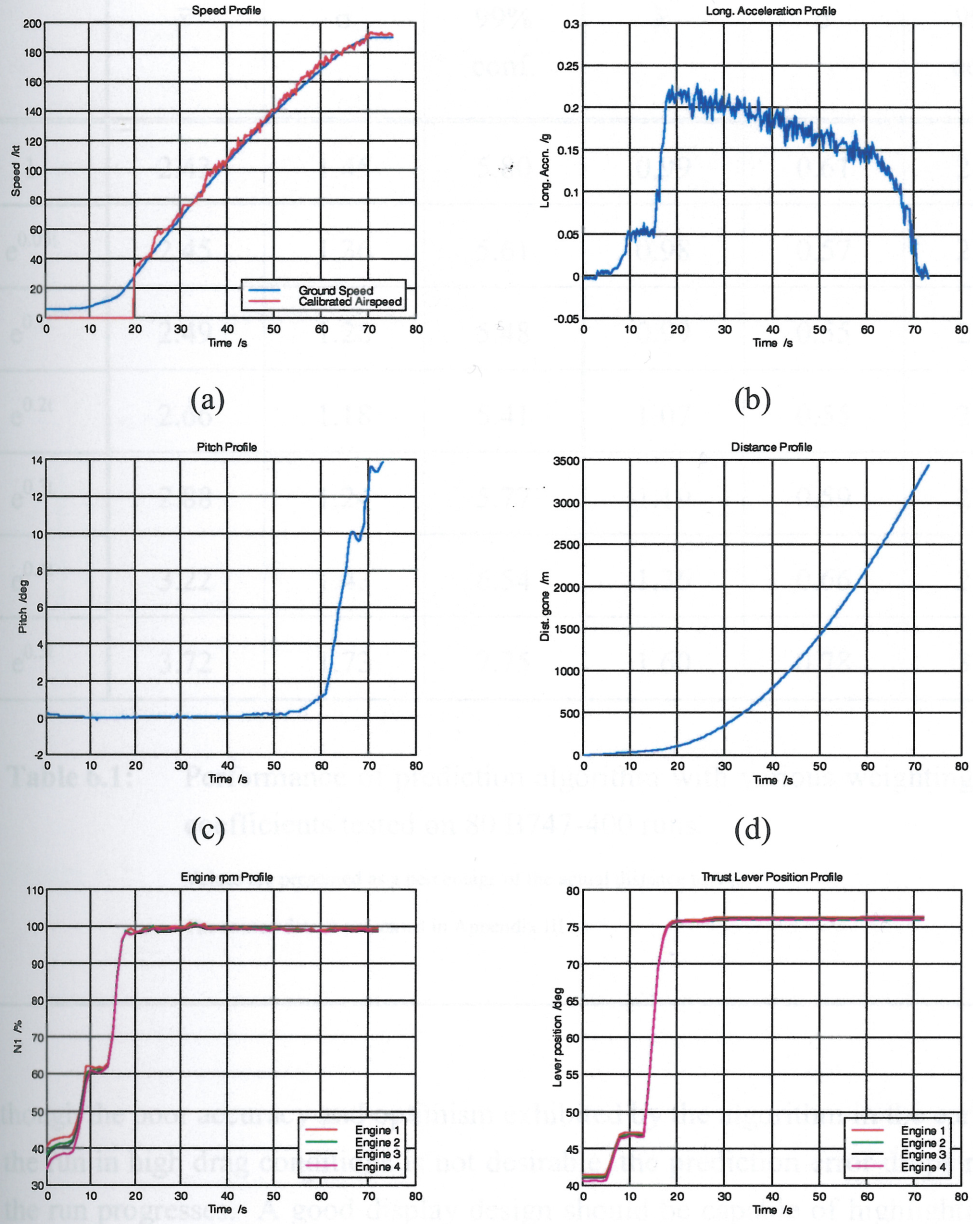

(a) (b) (c) (d) (e) (f)

Figure 6.1: Typical performance characteristics during take-off of a B747-400.

Run 62. Wt = 835520lbs.

Weight	Max. % error – last ¾ dist.-to-V_1			Max %. Error - last ½ dist.-to-V_1		
	$\bar{x}$	σ	99% conf.	$\bar{x}$	σ	99% conf.
1	2.43	1.45	5.80	0.99	0.61	2.41
$e^{0.05t}$	2.45	1.36	5.61	0.98	0.57	2.31
$e^{0.1t}$	2.49	1.28	5.48	0.99	0.55	2.27
$e^{0.2t}$	2.66	1.18	5.41	1.07	0.55	2.36
$e^{0.3t}$	2.88	1.24	5.77	1.19	0.59	2.57
$e^{0.4t}$	3.22	1.43	6.54	1.36	0.66	2.90
$e^{0.5t}$	3.72	1.73	7.75	1.60	0.78	3.41

Table 6.1: Performance of prediction algorithm with various weighting coefficients tested on 80 B747-400 runs.

Values are presented as a percentage of the actual distance to V_1.

The source data is presented in Appendix III.

Although the poor accuracy and optimism exhibited by the algorithm in the early part of the run in high drag conditions is not desirable, the prediction error drops rapidly as the run progresses. A good display design should be capable of highlighting the dynamic nature of the prediction. In fact, in these circumstances, the indication of the rapid drop in performance margin should provide adequate early warning of an anomalous situation to the crew. In this way, the drawbacks associated with the algorithm's lack of prediction accuracy would be compensated for. This, in fact, is achieved with the display designed in this work and discussed in further detail in Chapter 7.

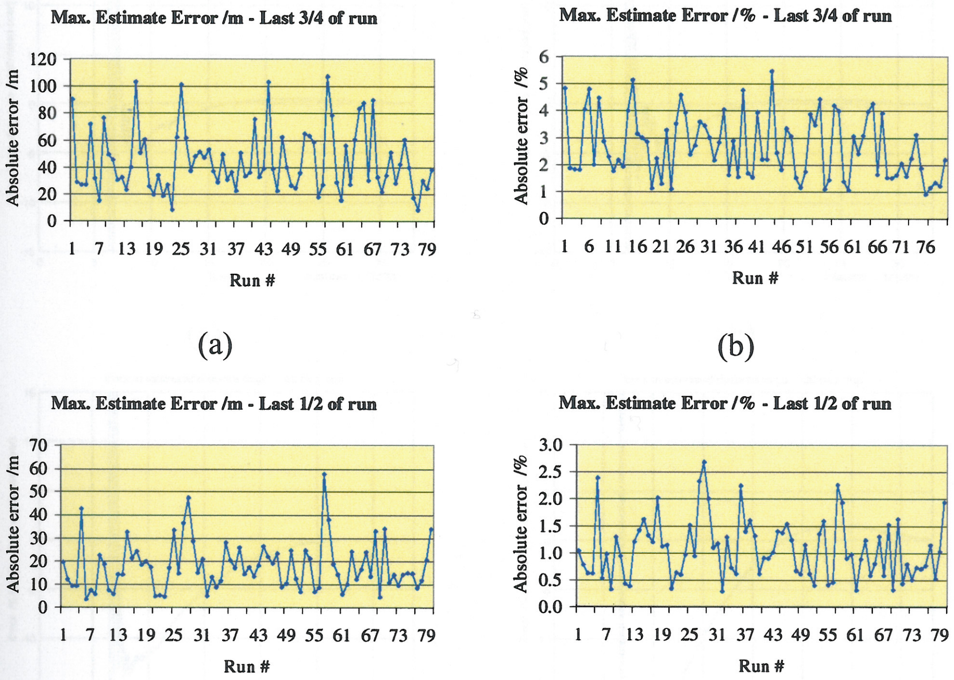

(a) (b)

(c) (d)

Figure 6.2: Algorithm performance measured on 80 B747-400 take-offs.

The source data is presented in Appendix III.

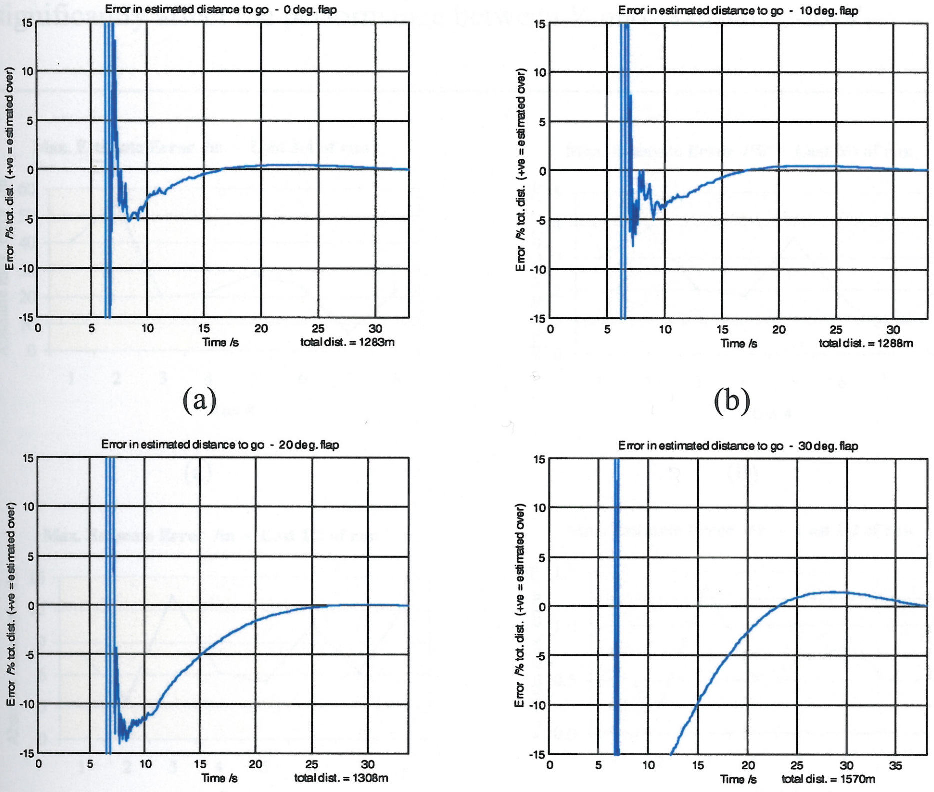

(a) (b)

(c) (d)

Figure 6.3: Algorithm performance in simulator runs with different flap settings.

(a) Flap at 0 degrees.
(b) Flap at 10 degrees.
(c) Flap at 20 degrees.
(d) Flap at 30 degrees.

6.4 Validation on single-aisle large jet transports

The algorithm was further tested on the Boeing 737-400 so that its validity could be extended to the 150-seat class of aircraft. Eight take-off recordings of British Airways B737 operations were used to verify the algorithm performance with a weighting of 0.2*t*. The results, presented in Figure 6.4, indicate that the requirements of Chapter 4 and Report CoA-0010 are once again satisfied. The algorithm, however, was found to be very sensitive to any changes in thrust, particularly at the start of the run. Any variations tended to delay the reduction in prediction error and could significantly affect the performance between ¼ and ½ distance-to-V_1.

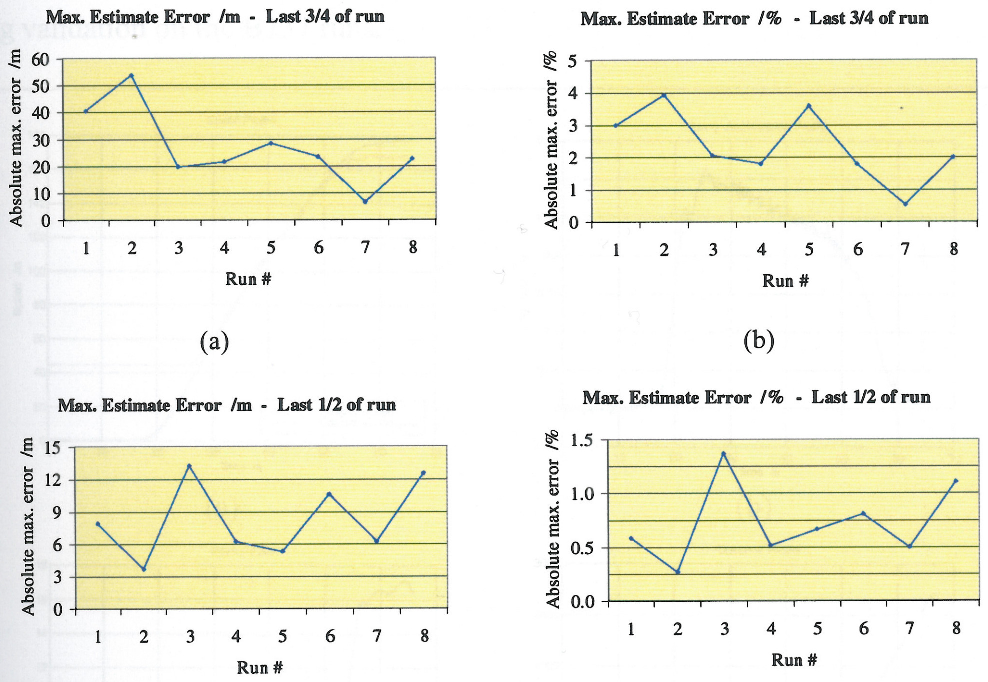

(a) (b)

(c) (d)

Figure 6.4: Algorithm performance measured on 8 B737-400 take-offs.

Last ¾ dist. error: $\bar{x}$ = 27.1m (2.33%)
σ = 14.3m (1.11%)
99% = 60.4m (4.92%)

Last ½ dist. error: $\bar{x}$ = 8.2m (0.73%)
σ = 3.5m (0.36%)
99% = 16.5m (1.56%)

The source data is presented in Appendix III.

This sensitivity is particular to the B737 runs mainly because the combination of a relatively short take-off run and the 4Hz sampling rate results in a small data population. In fact, at ¼ distance gone, the average data population size used for the least-squares fit is about 30 for the B737, compared with 50 for the B747 and 80 for the Jetstream[62]. Such a small population size not only restricts the amount of

---

[62] These values are obtained by considering the sample rate adopted on each aircraft and the average time to ¼ distance-to-V_1. Refer to Appendices II and III for the average times of the three aircraft.

weighting that can be applied, but also implicitly allows any variations in the earlier part of the run to have more effect on the least-squares fit. Consequently, the appropriate selection of the starting point of the monitor, ensuring that the thrust lever positions and engine speeds will have stabilised, was of paramount importance during validation on the B737 runs.

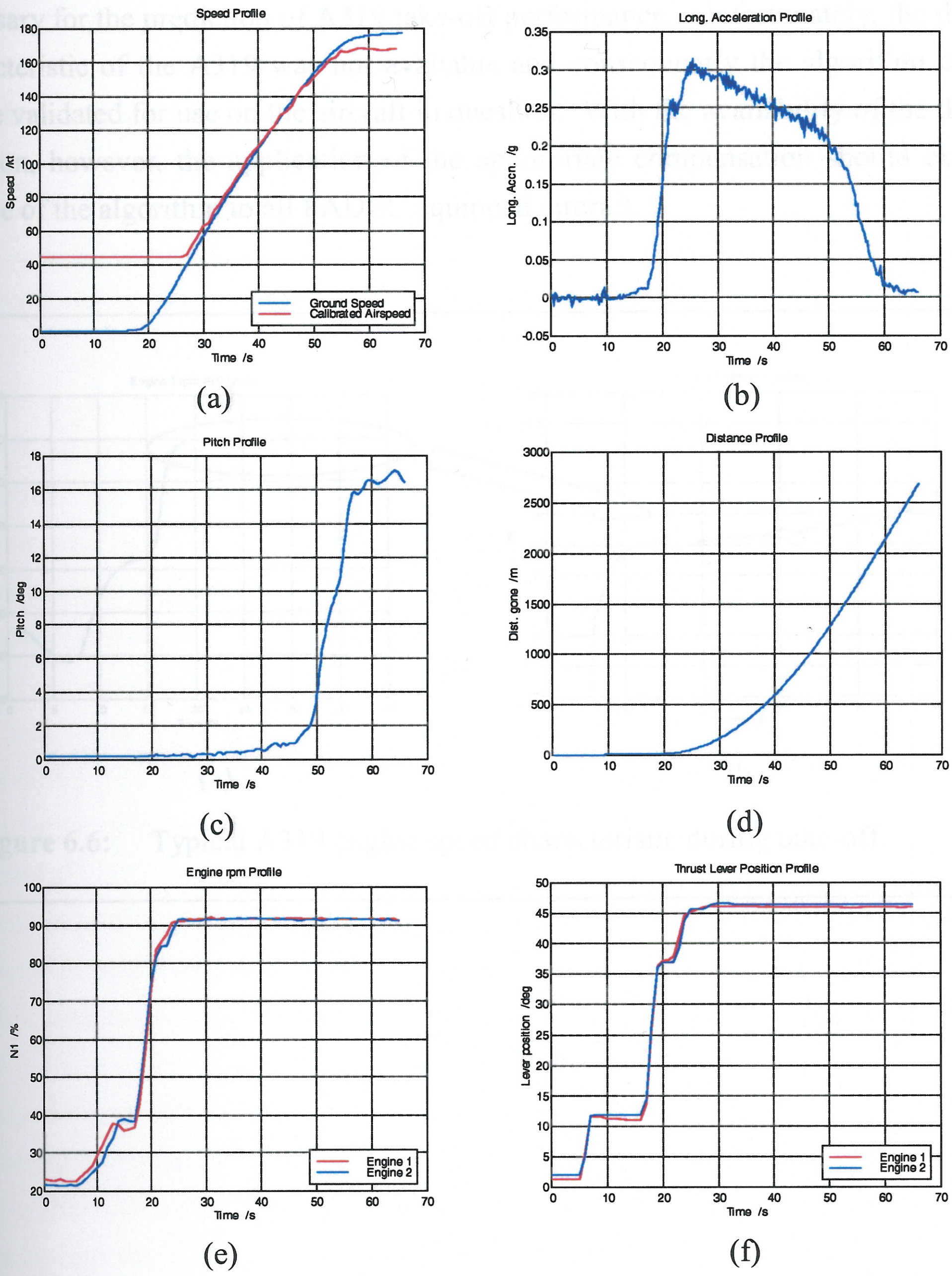

(a) (b)

(c) (d)

(e) (f)

Figure 6.5: Typical performance characteristics during take-off of a B737-400.

Run 7. Wt = 118400lbs.

Runs from A319s were also considered in the validation programme but unfortunately it was found that the engine speed tended to exhibit a non-linear increase during take-off (Figure 6.6). This was probably caused by the full authority digital engine control (FADEC) system installed on all Airbus A320 family aircraft. A variation in engine speed significantly affects the thrust characteristic and as a result, the latter could not be assumed to be linear, rendering compensation necessary for the prediction of A319 take-off performance. Unfortunately, the thrust characteristic of the A319 was not available and consequently the algorithm could not be validated for use on the aircraft in question. With the availability of the thrust function, however, the application of the appropriate compensation should extend the use of the algorithm to all FADEC equipped aircraft.

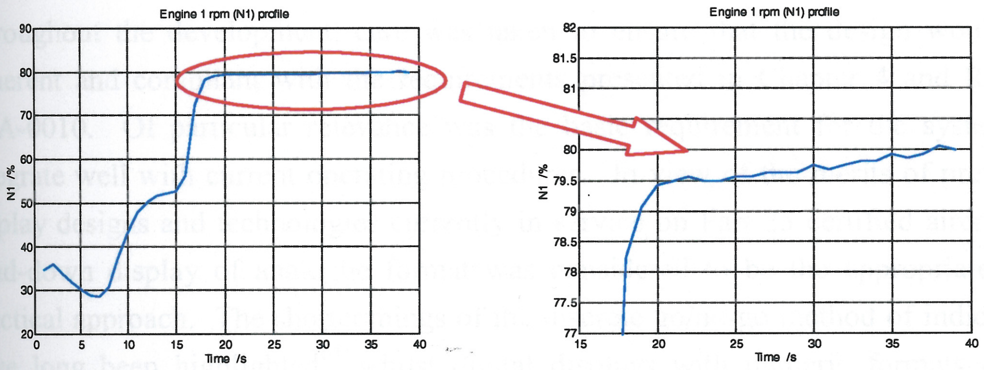

(a) (b)

Figure 6.6: Typical A319 engine speed characteristic during take-off.

Chapter 7: DISCUSSION AND CONCLUSION

7.1 Display design

A take-off performance monitor display was designed during the simulator evaluation of the algorithm in order to facilitate the visual interpretation of the prediction capabilities of the system. Although originally intended as an engineering tool, the design requirements were significantly extended to consider the crew's needs and their operational environment during take-off. This combination of requirements has been instrumental in rendering the resulting display a novel design with the potential of being further developed for use in commercial flight operations.

Throughout the development, care was taken to ensure that the design would be coherent and compliant with the requirements presented in Chapter 4 and Report CoA-0010. Of particular relevance was the basic requirement for the system to integrate well with current operating procedures. In view of the merits of previous display designs and technologies currently in service on Part 25 certified aircraft, a head-down display of analogue format was considered to be the appropriate and practical approach. The shortcomings of the discrete go/no-go method of indication have long been highlighted[63] whilst digital displays with numeric formats could prove difficult to interpret in adverse conditions. The analogue display, indicating the quantity of interest in graphical format, does not suffer from any of these drawbacks[64]. It is consequently well suited for the application, providing a convenient and effective means of information transfer to the crew. The proposed approach is also compatible with the monitoring role of the PNF and, following careful consideration, should avoid the addition of excessive workload to the crew.

Display designs of modern predictive monitors have tended to present the various parameters of interest individually. This inherently requires the crew member reading the display to monitor several sources of information simultaneously to obtain an impression of the progress of the run. Such an operation could prove to be a demanding task that requires considerable mental processing, particularly in

---

[63] The major shortcoming of the go/no-go type of display is its incapability of indicating a change in performance prior to the indication switching from one state to the other.

[64] The more notable research in display design, carried out by NASA [64, 69, 70, 71, 74] and the NLR [77, 78, 79], have, in effect, only considered displays that are largely graphical in format.

adverse, dynamic conditions when quick and correct interpretation would be of paramount importance. The number of individual items of information transferred to the crew in such circumstances needs to be kept to a minimum without compromising the latter's perspective in their ongoing judgement of the development of the run. The basic question the crew need answering during the run to V_1 is whether or not the aircraft will require take-off distances in excess of those available. With the concept of monitoring adopted in this work, such information can be easily presented as a single piece of information to the crew by displaying the distance margin available at V_1 on (or next to) the ASI[65]. In order to normalise (standardise) the information, the distance margin is presented as a percentage of the critical distance (scheduled distance to V_1) and displayed next to a calibrated scale on which both the gross and net performances are highlighted. In this way, the crew will be able to directly assess how the developing run compares with expected performance. In other words, they will be able to determine whether the current performance is better than average, below average, just within limits, and so forth. Such a comparison constitutes a novel and very powerful, yet simple, tool that can be readily exploited on the flight deck. This proposed arrangement is presented graphically in Figure 7.1.

A large (green) bar would be indicative of a large distance margin available at V_1, confirming that the run is progressing as desired. If an engine failure were to be experienced close to V_1 the decision taken in compliance with current procedures would have a greater probability of being successful. If, instead a small bar were to be displayed, only a small distance margin would be available. When the aircraft is performing worse than scheduled, a negative distance margin is available, indicated by a red negative bar on the display. This would imply that V_1 would be achieved further down the runway than scheduled, indicating that the viability of both the abort and continued-run case is being jeopardised. Consequently, the run needs to be aborted before V_1 (within the critical distance). The larger the negative margin, the earlier the run needs to be aborted. This representation also enjoys the advantage of allowing the crew to monitor any trend in the displayed bar, thus providing earlier warning of an anomaly.

---

[65] The proximity of the display to the ASI is intended to minimise the increase in work-load imposed on the PNF with the introduction of the performance monitor.

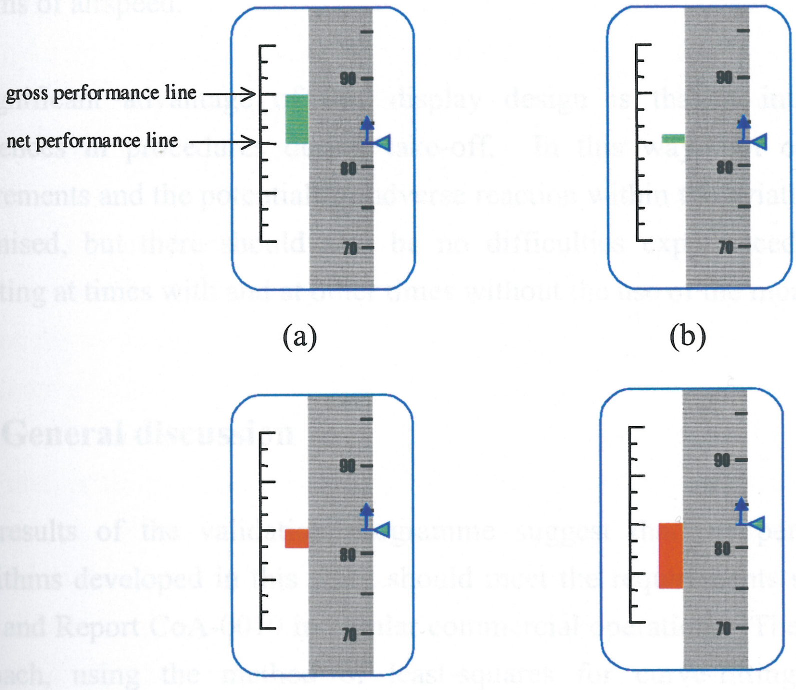

(a) (b)

(c) (d)

Figure 7.1: The display design.

(a) Aircraft performing well and average (gross) performance is predicted.
(b) Aircraft is predicted to perform well below gross performance but within regulation.
(c) Net performance will not be met and the run must be aborted before V_1.
(d) Performance is well below regulated and the run needs to be aborted well before V_1.

The bug indicating the latest moment the run can be aborted is not shown.

With such a display, it would be necessary to provide an indication of the latest moment the run should be aborted. Although Boeing might not have been satisfied with their method of determining the ‘chronodrasic interval’, their concept of providing the crew with a prior indication of the point of no return in the take-off is very valid. This point should be associated with the critical distance and must not be interpreted as a re-definition of the decision speed. Sub-standard performance does not imply a lower decision speed because the continued-run case may not be viable in such cases. In the realisation of such an indication, it may be advantageous to display the named salient point as a bug on the ASI. This would assume the value of V_1 for positive margins and lower airspeeds for negative margins. In effect, the bug would indicate the IAS expected at the critical distance. Such a presentation would facilitate interpretation because the crew are accustomed to refer to salient moments in terms of airspeed.

A significant advantage of this display design is that it introduces minimal differences in procedures during take-off. In this way, not only will training requirements and the potential for adverse reaction within the aviation community be minimised, but there should also be no difficulties experienced by crews when operating at times with and at other times without the use of the monitor[66].

7.2 General discussion

The results of the validation programme suggest that the performance of the algorithms developed in this work should meet the requirements stipulated by AS-8044 and Report CoA-0010 in regular commercial operations. The versatility of the approach, using the method of least-squares for curve-fitting and employing controlled compensation to model the desired performance characteristic, has been successfully demonstrated. The radically novel concept of utilising, in real-time, the past history of the particular run as a basis of the performance expected within the next few seconds has also been shown to be very valid. In this way, the explicit calculation of several parameters, the accuracy of which significantly affects the accuracy of the prediction, has been avoided. Instead, their collective effect is implicitly considered and averaged over the run history. This constitutes a significant advantage when compared to previous designs that have, in general, involved instantaneous measurement of the parameters of interest. Furthermore, most of the previous proposals have either involved gross assumptions (such as constant acceleration), used scheduled values of the relevant parameters, or essentially used variables as ‘fudge factors’ when solving the equations of motion. Such design concepts would doubtless have compromised the accuracy and reliability of the algorithms.

The only significant drawback of the method developed in this work is the incapability of the algorithm to provide a reliable estimate of performance at the start of the run, typically in the first quarter of the distance to V_1. Although, as explained

---

[66] This comment is valid not only if the crew elect not to make use of the monitor in a particular flight, but also in the situation where some aircraft may not be equipped with a monitor. Such a practical consideration is of particular relevance in the early years of operational service when the installation of the performance monitor may not be mandatory or widespread.

in Report CoA-0010, during this section of the run prediction accuracy is not considered crucial, such a deficiency warrants the implementation of other techniques so that performance can be quantified throughout the whole run to V_1. Non-predictive monitoring, which in effect measures instantaneous performance (or that achieved up to the moment of calculation), would be adequate in such circumstances, as the drawbacks associated with non-predictive techniques are not significant in the segment of the run in question. A convenient way of realising non-predictive monitoring would have been to compare the distance gone with that allowed for by scheduled performance for the instantaneous IAS. Such an approach would integrate well with the display technique developed. Initial trials on the College of Aeronautics' simulator, however, have suggested that this technique is unreliable, with the indication being often not at all representative of the eventual performance achieved[67]. This drawback is largely due to the fact that the distances involved in the early parts of the run are small and consequently any variation in the actual distance covered would greatly affect the outcome of the comparison. As a result, this approach was considered inadequate and acceleration monitoring would probably need to be considered instead. This technique is well developed and is unlikely to suffer from the reliability problems associated with the distance-gone comparisons. Acceleration monitoring would also be useful as a secondary monitoring technique, applied in parallel with predictive monitoring. This would facilitate the quick detection of a drop in performance, thus complementing well the curve-fitting technique, which is most suitable for steady conditions. Further development, however, would be required to confirm the adequacy of acceleration monitoring and to optimise its integration with the curve-fitting techniques.

Fluctuations of the wind vector adversely affect the prediction accuracy. Besides affecting the drag of the aircraft, by far the greatest effect of variations in the wind is the resulting fluctuation in the difference between V_1 and the current IAS. This quantity is what really affects the distance-to-go and therefore the distance to V_1. What is specifically of interest, therefore, is the headwind component that will be experienced in the vicinity of V_1. Current technologies do not support the reliable prediction of this quantity. As a result, this deficiency has to be accepted as a limitation in the prediction accuracy of any performance monitor. Previous designs have largely either used scheduled values of headwind or assumed that the headwind component in the vicinity of V_1 is that instantaneously experienced. The latter

---

[67] The difficulty experienced with the non-predictive distance-gone monitoring technique is in agreement with concerns expressed in earlier publications [24].

approach is effectively a re-evaluation of the scheduled wind vector and will probably result in a better prediction.

The algorithm is also sensitive to variations in thrust setting and requires steady conditions during the monitored part of the run to ensure prediction accuracy. During commercial operations and particularly in situations of extended rolling starts, care needs to be taken to ensure that monitoring is initiated only when engine thrust will have stabilised, otherwise the prediction error convergence towards zero could be significantly delayed. Furthermore, if the thrust level is re-set during the run, the algorithm will follow the trend in performance but cannot calculate the performance margin with accuracy during or immediately following the dynamic phase[68]. Such a limitation may also be expected of other designs. In any case, in most runs and surely in field-limited operations, such variations would not be expected. Furthermore, any large fluctuation in the predicted performance margin should quickly bring to the crew's attention the presence of an adverse condition, particularly as it would invariably be accompanied by a perceivable change in acceleration.

The algorithm implemented in this work does not take into account any expected variation in runway slope further down the runway. In most circumstances, the error due to this lack of consideration is small and insignificant. In fact, the prediction error measured in the algorithm validation programmes incorporates this error, proving that this is the case. In extreme circumstances, however, an appreciable error in the displayed margin (which reduces as the change in slope is encountered) may result. One way of compensating for this is through operating procedures, where the crew would be briefed to expect a particular margin in the initial part of the run until the change in slope is encountered, thus compensating for the difference in performance in the two sections of the run. If, however, this is considered unacceptable, the algorithm may be modified to automatically compensate for the change in slope. The runway may be divided into two or more sections, creating a piece-wise linear model of the runway profile with the equivalent slope of each section being stored in a database for use by the algorithm. A change in slope constitutes an offset in the acceleration profile, with each 1° contributing to a change in acceleration in the order of $0.17ms^{-2}$. There are various mathematical techniques with which the distance-to-V_1 can then be calculated. Perhaps the simplest approach

---

[68] This is also true for most other dynamic conditions or discrete incidents which may be experienced in exceptional conditions during the run.

would be to implement that depicted in Figure 7.2. This involves determining the point (D) at which the aircraft is expected to achieve V_1 by comparing the least-squares fit profile with the velocity profile generated by the variation in slope. The distance-to-go-to-V_1 is then the difference in the areas under the two profiles. Further study, however, is required to determine whether the advantage of displaying a compensated performance margin justifies the increase in algorithm complexity, or whether the previously suggested approach of incorporating the variation in operating procedures would be acceptable.

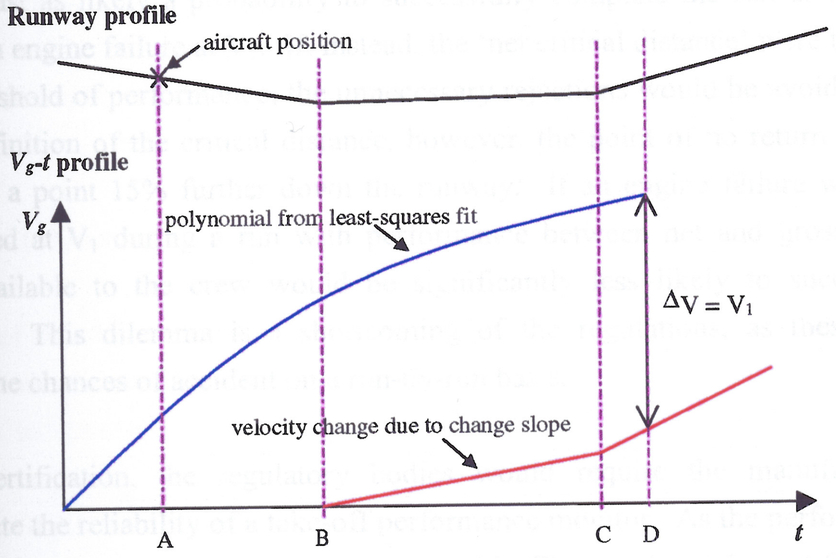

Figure 7.2: Proposed implementation of runway slope compensation.

(A)	Aircraft current position
(B),(C)	Runway slope break-points
(D)	Point at which V_1 is expected to be achieved

7.3 Current regulation and certification issues

Current performance requirements tend to indicate that the regulatory bodies have a global perspective of safety during take-off. In the AEO (continued run) case, the allowance of net performance ensures that all but 1 of 10^7 take-offs are successful[69]. Likewise, in the OEI case, if an engine failure is experienced at V_1, net performance ensures that the probability of successfully completing the run is at least 50%. The regulations, however, fail to define the scheduled distance to V_1, referred to as the critical distance in this work. A closer look suggests that this critical distance is, in effect, also factored by 15% in the calculation of net performance, whilst that for gross performance defines the average distance required to achieve V_1. A conflict of definition arises here, since the critical distance should be defined as only one distance. If the 'gross distance' were to be adopted, 50% of the runs would have to be unnecessarily rejected. Although rendering take-off operations impractical, the 'gross critical distance' would then ensure that the aircraft on any run will actually have at least as likely a probability to successfully complete the run as not in the event of an engine failure at V_1. If, instead, the 'net critical distance' were to be used as the threshold of performance, the unnecessary rejections would be avoided. With such a definition of the critical distance, however, the point of no return would be defined at a point 15% further down the runway. If an engine failure were to be experienced at V_1 during a run with performance between net and gross[70], either option available to the crew would be significantly less likely to succeed than otherwise. This dilemma is a shortcoming of the regulations, as these do not consider the chances of accident on a run-by-run basis.

During certification, the regulatory bodies would require the manufacturer to demonstrate the reliability of a take-off performance monitor. As the performance of the algorithm meets the requirements presented in Chapter 4 and Report CoA-0010, the system should meet the performance level presented in Table 4.1. These performance figures should satisfy the regulatory bodies. In practice, however, the system should prove safer than these figures suggest, since both failures (missed alarm and false alarm) are associated with a small performance margin and the crew would probably abort early in the run in such an event[71].

---

[69] The risk involved may be less than 10^{-7} because of the extra leeway allowed for in the definition of TORR and because the distances required are defined as the greater of the AEO and OEI calculations.

[70] In such circumstances the aircraft would, by definition, be at a point on the runway between the gross and net critical distances. Such a run would be perfectly viable in the AEO case.

[71] Furthermore, it is doubtful whether the actual probability density function of performance beyond 4σ is described adequately by the normal distribution model. Such concerns, however, need to be further investigated.

The algorithm can fail only when the fitted curve does not model the developing characteristic appropriately, thus producing an erroneous prediction[72]. Such a situation can develop in the presence of both an unsatisfactory and a good fit[73]. The former case would be detected by the algorithm, since a large standard deviation and uncertainty in the prediction would result. The latter, however, cannot be detected by statistical means because in such cases the error would only be due to the incorrect modelling of the characteristic and this is not catered for by the method of least squares[74]. Nevertheless, the curve fitting technique and the predictive nature of the algorithm ensure that an erroneous result cannot remain constant along the run. As a result, a highly dynamic output, whether the prediction were correct or otherwise, would unequivocally indicate an anomalous situation. Supported by appropriate crew training to indicate the limitations of the predictive capabilities of the system and to ensure correct interpretation of the display, the system developed should not at any time mislead the crew.

7.4 Conclusion

The issue of take-off performance monitoring has been considered by various sectors of the aviation community for several decades, with numerous proposals being developed to date but none being employed in commercial operations for any significant length of time. The need for such an instrument will probably become greater as flight becomes increasingly automated and efforts continue to render commercial aviation safer than present day standards.

The concepts adopted in this approach have targeted the need for a first generation performance monitor. Particular attention has been given to ensure acceptance by the aviation community so that the system's introduction into commercial operations can be facilitated. This has led to the fundamental approach that the monitor should not be authoritative, but instead respect the commanding role of the crew in current operational procedures. From the point of view of technology, the concept of monitoring the performance to V_1 and allowing for scheduled distances for the post-

---

[72] Failure caused by a failure of the supporting hardware (such as the data source, power supply or display) is not considered herein, as it is beyond the scope of this work.

[73] The latter was found to be the case in Report CoA-0013, where, despite a good fit, the algorithm failed to predict performance with the desired accuracy.

[74] Some anomalous fits, however, such as those with positive 2nd order coefficients, can be detected by appropriate validity checks. It is difficult, however, to ensure that such techniques are exhaustive.

V_1 distance is very valid and has rendered realistic the possibility of predicting performance reliably.

The monitoring technique has been shown in this work to be very robust and valid for both turbine-propeller and high-bypass ratio jet aircraft with take-off runs requiring at least 15s to rotation. Three aircraft types used in the validation programme involved a 12,000lb twin turboprop commuter, a twin engined 130,000lbs short range jet and a four engined 900,000lbs long range transport. A comprehensive range of transport aircraft has thus been covered in this programme, suggesting that the algorithms are also valid for other classes of transport aircraft currently in operation or being developed. The validation programme can be extended to further cover low-bypass ratio engined aircraft (such as the Boeing B727 and B737-200 and the formerly McDonell Douglas DC-9 families of aircraft powered by the Pratt and Whitney JT-8 engine) and jet commuter aircraft. Further development should also allow the application of the technique to aircraft equipped with FADEC systems (various Airbus types).

The display developed is also based on valid concepts, being simple and unambiguous to read, whilst providing the crew with sufficient information on the viability of the take-off run. It therefore has a good potential of being developed into an operational display. With the versatility of the complete system proposed herein, the proposed further work should be equally successful, suggesting that a system based on the concepts developed can be successfully developed into a reliable, operational system on the flight deck.

REFERENCES

[1] Anonymous. *The world of civil aviation - 1996-1999.* ICAO Circular 271-AT/112, 1998.

[2] Lloyd, E. and Tye, W. *Systematic Safety.* Civil Aviation Authority, 1998. ISBN: 0-86039-141-8.

[3] Joint Aviation Authorities. *Joint Aviation Requirements, JAR-25 – Large Aeroplanes.* Civil Aviation Authority, 1994.

[4] Stinton, D. *Flying qualities and flight testing of the aeroplane.* Blackwell Science, 1996. ISBN: 0-632-02121-7.

[5] Davies, R. V. *Aircraft performance requirements manual.* Airlife Publishing Ltd., 1991. ISBN: 1-85310-168-0.

[6] Tomsic, J. L. *SAE dictionary of aerospace engineering*, 2nd ed. Society of Automotive Engineers Inc., 1998. ISBN: 0-7680-0245-1.

[7] Grover, J. H. H. *Handbook of aircraft performance.* BSP Professional Books, 1989. ISBN: 0-632-02304-X.

[8] Person L. H. Jr. To go – or not to go. Situational awareness on takeoff. *Flight Safety Digest*, October 1989. pp. 35-42.

[9] Anonymous. Take-off monitors – A CAA view. In *Minutes of Meeting #1 of the take-of performance monitoring ad hoc committee of the Aircraft Division of the Aerospace Council.* Society of Automotive Engineers Inc., 1984.

[10] http://www.faa.gov/safetyinfo2.htm (accessed 16th June 2000).

[11] Anonymous. *Jet transport performance methods.* Boeing Flight Operations Engineering, 1989.

[12] Collingbourne, J. *A survey of available data on the value of rolling resistance on hard runways.* Royal Aircraft Establishment, Technical Memorandum Aero 1233, 1970.

[13] Hainline, B. C. *et al. Prediction of aircraft braking friction on wet runways. A look at past and current research activities.* SAE Technical Paper 831562, 1983.

[14] O'leary, C. O., Cannell, J. N. and Maltby, R. L. *Take-off tests on a transport aircraft including the use of a 'SCAT' take-off director.* Aeronautical Research Council R&M 3508, 1968.

[15] Ojha, S. K. *Flight performance of aircraft.* American Institute of Aeronautics and Astronautics Inc., 1995. ISBN: 1-56347-113-2.

[16] Snyder, T. C., Drinkwater, F. J. and Forrest, R. D. *Takeoff certification considerations for large subsonic and supersonic airplanes using the Ames flight simulator for advanced aircraft*. NASA TN-D-7106, 1973.

[17] Mair, W. A. and Birdsall, D. L. *Aircraft performance*. Cambridge University Press, 1996. ISBN: 0-521-56836-6.

[18] Illingworth, J. K. B. and Hopkin H. R. *A note on the design of take-off monitors*. Royal Aircraft Establishment Technical Memorandum IAP 697 (Aero 657), 1960.

[19] Bone, A. G. and Twiney, F. J. Consideration of a take-off monitor. Paper no. 2. In: *Royal Aircraft Establishment Report DD1*, 1963.

[20] Hall, L. J. W. The case for take-off monitors and directors. Paper no. 1. In: *Royal Aircraft Establishment Report DD1*, 1963.

[21] Page, R. B. *A survey of take-off monitors and take-off directors*. College of Aeronautics Technical Essay, 1965.

[22] Danaher, J. W. Pilot monitoring of airplane acceleration during takeoff. In: *2nd Aerospace behavioural engineering technology conference*. 1983. (Also SAE Technical Paper 831415).

[23] Wagenmakers, J. Aircraft performance in takeoff and landing: the good news and the bad news. In: *Proceedings of the 41st International flight safety seminar*, 1988. pp. 289-298.

[24] Field, H. J. The operator's point of view. Paper 11, *Royal Aircraft Establishment Report DD1*, 1963.

[25] Wagenmakers, J. Take-off performance monitoring. In: *Proceedings of the 43rd International air safety seminar*, 1990. pp. 106-116.

[26] Miles, E. C. Take-off and landing problems. In: *Journal of the Royal Aeronautical Society*, Vol. 67, no. 633, September 1963. pp. 539-543.

[27] Grover, J. H. H. Take-off instrument for assessing achieved performance during take-off and a take-off accident analysed in context. In: *Proceedings of the 8th International aerospace instrumentation symposium,* 1975.

[28] Middleton, D. B. *et al. Airplane takeoff and landing performance monitoring system*. US Patent 5,449,025. 1996.

[29] Cleary, P. J. *et al. Aircraft performance margin indicator*. US Patent 4,638,437. 1987.

[30] Coquin, L. *et al. System for deriving an anomaly signal during the take-off of an aircraft*. US Patent 5,668,541. 1997.

[31] Cadogan, A. Boeing aims TOPM work at 777. In: *Flight International*, 31st Jan. – 6th Feb. 1990. pp. 16.

[32] Jensen, D. Airbus' answer to safety with avionics. In: *Avionics Magazine*, June 1999. pp. 22-27.

[33] Morris, G. J. and Lina, L. J. *Description and preliminary flight investigation of an instrument for detecting subnormal acceleration during take-off.* NACA TN-3252, 1954.

[34] Kolnick, J. J. and Rind, E. *Investigation of the characteristics of an acceleration-type take-off indicator in a large airplane.* NASA Memo 4-21-59L, 1959.

[35] Klass, P. J. Monitor designed to aid jet takeoffs. *Aviation Week*, June 23, 1958. pp. 65-71.

[36] Swindle, E. M. *Flight test of Sperry Gyroscope Company takeoff monitor in a B-47 airplane.* Wright Patterson Air Force Base, Ohio, WADC Technical Note 59-360, 1959. Cited in: Zinn, S. V. Jr. *Develop acceleration and brake monitor system.* FAA Report no. FAA-RD-72-112, 1972.

[37] Swindle, E. M. *Flight tests of Minneapolis-Honeywell Regulator Company and Kollsman Instrument Corporation takeoff monitors in a B-47 airplane.* Wright Patterson Air Force base, Ohio, WADC Technical Note 60-193, 1960. Cited in: Zinn, S. V. Jr. *Develop acceleration and brake monitor system.* FAA Report no. FAA-RD-72-112, 1972.

[38] Lee, L. R. *Operational evaluations of Sperry, Kollsman and Oster take off monitors, and final conclusions based upon all recent take off monitor tests by Aeronautical Systems Division.* Wright Patterson Air Force Base, Ohio, Technical Documentary Report ASD-TDR-69-1971, 1963. Cited in: Zinn, S. V. Jr. *Develop acceleration and brake monitor system.* FAA Report no. FAA-RD-72-112, 1972.

[39] Zinn, S. V. Jr. *Develop acceleration and brake monitor system.* FAA Report no. FAA-RD-72-112, 1972.

[40] Berggren, L. E. *Aircraft instruments.* US Patent 3,048,329. 1962.

[41] Anonymous. Takeoff monitors compete for market. *Aviation Week*, July 28, 1958.

[42] Brahm, C. B. *Take-off computer.* US Patent 3,116,638. 1964.

[43] Cooper, M. F. *Aircraft takeoff and abort instrument.* US Patent 4,608,863. 1986.

[44] Gold, T. *System for monitoring the take-off performance of an aircraft.* US Patent 3,077,110. 1963.

[45] Fearnside, K. Instrument aids for take-off. *Journal of the Royal Aeronautical Society*, Vol. 67, September 1963. pp. 544-551.

[46] Rush, D. A. *Ground run prediction*. AGARD report 422, 1963.

[47] Aron, I. and Tomescu, I. *Take-off director system*. US Patent 4,251,868. 1981.

[48] Millard, W. C. and Millard, C. W. *Aircaft takeoff acceleration indicator system*. PCT International application no. PCT/CA97/00785. 1998.

[49] Millard, W. C. and Millard, C. W. *Aircraft takeoff acceleration indicator system*. US Patent 6,175,315. 2001.

[50] Hoekstra, H. D. *Take-off safety indicator*. US Patent 2,922,982. 1960.

[51] Grover, J. H. H. *Safe take-off indicators*. US Patent 4,130,015. 1978.

[52] Hall, R. L. and Siebens, R. H. *Aircraft take-off monitoring system*. US Patent 3,504,335. (1970).

[53] Lukesh, J. S. *et al. Take-off monitor system*. US Patent 3,120,658. 1964.

[54] Smith, G. R. *Aircraft ground monitoring system*. US Patent 4,122,522. 1978.

[55] Fusca, J. A. Takeoff monitor computes runway roll. *Aviation Week*, October 13, 1958. pp. 99-105.

[56] Arad, A. *Aircraft takeoff monitoring system*. US Patent 5,103,224. 1992.

[57] Leland, J. W. and Kirkpatrick, J. E. *Method and apparatus for onboard monitoring of aircraft takeoff*. US Patent 4,773,015. 1988.

[58] Manor, J. *Aircraft take off indicator systems*. US Patent 3,865,071. 1975.

[59] Roberts, G. E. *Take-off safety indicator for aircraft*. US Patent 4,284,029. 1981.

[60] Hosford, N. F. *Aircraft take-off monitoring*. US Patent 3,128,445. 1964.

[61] Cleary, P. J. and Hopperstad, C. A. *Method and apparatus for continuously determining a chronodrasic interval*. US Patent 4,454,582. 1984.

[62] Cleary, P. J., Kelman, L. S. and Horn, L. *Aircraft performance margin indicator*. US Patent 4,638,437. 1987.

[63] Srivatsan, R. and Dowding, D. R. *Development of a takeoff performance monitoring system*. NASA Contract Report NASA-CR-178255, 1987.

[64] Middleton, D. B., Srivatsan, R and Person, L. H. Jr. *Flight test of takeoff performance monitoring system*. NASA-TP-3403, 1994.

[65] Middleton, D. B., Person, H. L. Jr. and Srivatsan, R. Takeoff performance monitoring system display options. *Journal of Aircraft*, Vol. 31, No. 3, May-June 1994. pp. 666-671.

[66] Middleton, D. B., Srivatsan, R. and Person, L. H. Jr. *Airplane takeoff and landing performance monitoring system*. US Patent 4,843,554. 1989.

[67] Middleton, D. B., Srivatsan, R and Person, L. H. Jr. *Airplane takeoff and landing performance monitoring system*. US Patent 5,047,942. 1991.

[68] Middleton, D. B., Srivatsan, R. and Person, L. H. Jr. *Airplane takeoff and landing performance monitoring system.* US Patent 5,353,022. 1994.

[69] Middleton, D. B., Srivatsan, R. and Person, L. H. Jr. *Simulator evaluation of a display for a takeoff performance monitoring system.* NASA-TP-2908, 1989.

[70] Middleton, D. B., Srivatsan, R and Person, L. H. Jr. *Simulator evaluation of displays for a revised takeoff performance monitoring system.* NASA-TP-3270, 1992.

[71] Middleton, D. B., Srivatsan, R. and Person, L. H. Jr. Takeoff performance monitoring system display options. In: *Proceedings of the AIAA/AHS Flight Simulation Technologies Conference*, 1992. pp. 57-67.

[72] Middleton, D. B. and Srivatsan, R. Evaluation of a take-off performance monitoring system. In: *Proceedings of the AIAA Guidance, Navigation and Control Conference*, 1987. pp. 155-162.

[73] Middleton, D. B. and Srivatsan, R. Evaluation of a takeoff performance monitoring system display. *Journal of Guidance*, Vol. 12, No. 5, 1989. pp. 640-646.

[74] Middleton, D. B., Srivatsan, R. and Person, L. H. Jr. Simulator evaluation of takeoff performance monitoring system displays. In: *Proceedings of the AIAA Flight Simulation Technologies Conference*, 1988. pp. 206-214.

[75] Khatwa, R. The d*evelopment of a Take-off Performance Monitor (TOPM).* Ph.D. Thesis, University of Bristol, 1991.

[76] Khatwa, R. The development of an efficient take-off performanec (TOPM). In: *Proceedings of the 18th Congress of the International Council of the Aeronautical Sciences* (*ICAS*), 1992. Vol. 1, pp. 219 – 241.

[77] Verspay, J. J. L. H. and Khatwa, R. A comparative evaluation of three take-off performance monitor display types. In: *Proceedings of the AIAA Flight Simulation Technologies Conference*, 1993. pp. 147-155.

[78] Khatwa, R. and Verspay, J. J. L. H. Flight simulator evaluation of take-offs conducted with and without a take-off performance monitor (TOPM). In: *Proceedings of the 19th Congress of International Council of the Aeronautical Sciences* (*ICAS*), 1994. Vol. 2, pp. 1328 – 1339.

[79] Verspay, S. Take-off performance monitoring system algorithm and display development. In: *Proceedings of the AIAA Atmospheric Flight Mechanics Conference*, 1991. pp. 150-157.

[80] Bonafe, J. L. *System for generating on board an aircraft an alarm signal should any anomaly occur during take-off.* US Patent 5,124,700. 1992.

[81] Baldwin, S. F. *System design and avionics integration of a takeoff performance monitor*. M.Sc. Thesis, Texas Woman's University, 1986.

[82] Baldwin, S. F. *Method and apparatus for predicting and monitoring aircraft takeoff performance.* US Patent 4,837,695. 1989.

[83] Milligan, M. W. and Wilkerson, H. J. *Airplane take-off monitor with learning feature.* US Patent 4,980,833. 1990.

[84] Zhou, M. M. *A prototype airplane takeoff monitor with learning feature.* M.Sc. Thesis, The University of Tennessee, Knoxville, 1993.

[85] Zammit-Mangion, D. and Eshelby, M. *Design concept and performance standard for a take-off performance monitor design intended for use on part 25 certified aircraft.* College of Aeronautics Reports, no. CoA-0010, 2000.

[86] Anonymous. *Takeoff performance monitor (TOPM) system, airplane, minimum performance standard for.* Society of Automotive Engineers Inc., Aerospace Standard AS-8044, 1987.

[87] Gallimore, P. Go/No go – The takeoff decision. In: *Proceedings of the 40th International Air Safety Seminar,* 1987. pp. 443-446.

[88] Zammit-Mangion, D. *An investigation of the suitability of using curve-fitting techniques to predict take-off distance.* College of Aeronautics Reports, no. CoA-0013, 2000.

[89] Anonymous. *Handley Page servicing school notes – Jetstream airframe.* Product Support Group, Handley Page Aircraft Ltd., 1969.

[90] Zammit-Mangion, D. and Eshelby, M. Design and validation using flight data of a method for predicting the ground run required for take-off. In: *Proceedings of the 22nd Congress of the International Council of the Aeronautical Sciences* (*ICAS*), 2000.

[91] Draper, N. R. and Smith, H. *Applied regression analysis.* Wiley, 1998. ISBN: 0-471-17082-8.

[92] Anonymous. *Litton LTN-90 Inertial Reference System - Component Maintenance Manual.* Litton Aero Products. Part no. 464600.

[93] Hines, W. W. and Montgomery, D. C. *Probability and statistics in engineering and management science.* Wiley, 1980. ISBN: 0-471-04759-7.

APPENDICES

-

APPENDIX I

DERIVATION OF THE JETSTREAM-100 G-NFLC's SCHEDULED THRUST CHARACTERISTIC

-

APPENDIX II

PERFORMANCE RESULTS OF THE JETSTREAM-100 MONITORING ALGORITHM

-

APPENDIX III

PERFORMANCE RESULTS OF THE LARGE JET TRANSPORT MONITORING ALGORITHM

APPENDIX I

DERIVATION OF THE JETSTREAM-100 G-NFLC's SCHEDULED THRUST CHARACTERISTIC

AI.1 Introduction

The scheduled thrust characteristic is generated from the performance charts of the Turbomeca Astazou XIVC – Hamilton Standard Propeller Type 23-LF355 package provided by the manufacturers. G-NFLC had an engine upgrade[i], during which Astazou XVI-F1 powerplants were installed. These are essentially Type XVI engines modified to interface with the XIVC type controls. Unfortunately, no performance characteristics for such an installation are available and consequently the charts for the XIVC had to be used instead. Nevertheless, the performances of the two engines are quite similar. Moreover, as the calculations herein illustrate, the output power of the engine is mainly constant throughout any run. As a result, the thrust characteristic is dependent only on the parametric thrust curves, which are, in turn, dictated by the propeller type and engine control mechanism, both of which are the same as in the original installation. Consequently, the performance charts used can be expected to be valid.

AI.2 Calculations

The parametric static power w is determined by the parametric engine speed and power setting (Figure A1.1). The parametric engine speed is given by:

$$n = \frac{N}{43000rpm}\sqrt{\frac{288K}{TAT}} \qquad \text{... (AI.1)}$$

where N is the engine speed and TAT is the total air temperature in Kelvin. TAT is therefore given by:

$$TAT = SAT(1 + 0.2M^2) = SAT + 0.2\frac{V^2}{\gamma R} \qquad \text{... (AI.2)}$$

---

[i] This upgrade was required when Turbomeca stopped supporting the Astazou XIVC.

where M is the Mach number, SAT is the static air temperature in Kelvin, V is the true airspeed in m/s, γ is the ratio of specific heats of air and R the gas constant.

Assuming the engine speed is 43,000 r.p.m., which is the nominal speed during take-off, the parameter n can be determined for various operating temperatures (Table AI.1).

$n = N(228.16/TAT)^{0.5}$ with N=1

TAS /kt	*Δ TAT /K*	*n* @-40°C	*n* @-10°C	*n* @+15°C	*n* @+40°C
0	0	1.111706	1.046422	1	0.959254
10	0.013174	1.111674	1.046396	0.999977	0.959234
20	0.052696	1.111580	1.046317	0.999909	0.959173
30	0.118566	1.111423	1.046186	0.999794	0.959073
40	0.210783	1.111204	1.046003	0.999634	0.958932
50	0.329349	1.110921	1.045768	0.999429	0.958750
60	0.474263	1.110577	1.045480	0.999178	0.958529
70	0.645524	1.110170	1.045141	0.998882	0.958267
80	0.843134	1.109701	1.044750	0.998540	0.957965
90	1.067091	1.109170	1.044307	0.998154	0.957624
100	1.317397	1.108578	1.043813	0.997722	0.957243

Table AI.1: Values of *n* for various forwards speeds and ambient temperatures.

The parametric static power chart and the static power correction chart (Figure AI.1) can then be used to determine the total Parametric Static Power (w+Δw) (Table AI.2).

The actual power W is then given by:

$$W = (w+\Delta w)(P_T/101.32)(TAT/288)^{0.5}. \qquad \ldots \text{(AI.3)}$$

where P_T is the total pressure.

where M is the Mach number, SAT is the static air temperature in Kelvin, V is the true airspeed in m/s, γ is the ratio of specific heats of air and R the gas constant.

Assuming the engine speed is 43,000 r.p.m., which is the nominal speed during take-off, the parameter n can be determined for various operating temperatures (Table AI.1).

$n = N(228.16/TAT)^{0.5}$ with N=1

TAS /kt	Δ TAT /K	n @-40°C	n @-10°C	n @+15°C	n @+40°C
0	0	1.111706	1.046422	1	0.959254
10	0.013174	1.111674	1.046396	0.999977	0.959234
20	0.052696	1.111580	1.046317	0.999909	0.959173
30	0.118566	1.111423	1.046186	0.999794	0.959073
40	0.210783	1.111204	1.046003	0.999634	0.958932
50	0.329349	1.110921	1.045768	0.999429	0.958750
60	0.474263	1.110577	1.045480	0.999178	0.958529
70	0.645524	1.110170	1.045141	0.998882	0.958267
80	0.843134	1.109701	1.044750	0.998540	0.957965
90	1.067091	1.109170	1.044307	0.998154	0.957624
100	1.317397	1.108578	1.043813	0.997722	0.957243

Table AI.1: Values of n for various forwards speeds and ambient temperatures.

The parametric static power chart and the static power correction chart (Figure AI.1) can then be used to determine the total Parametric Static Power (w+Δw) (Table AI.2).

The actual power W is then given by:

$$W = (w+\Delta w)(P_T/101.32)(TAT/288)^{0.5}. \qquad \ldots \text{(AI.3)}$$

where P_T is the total pressure.

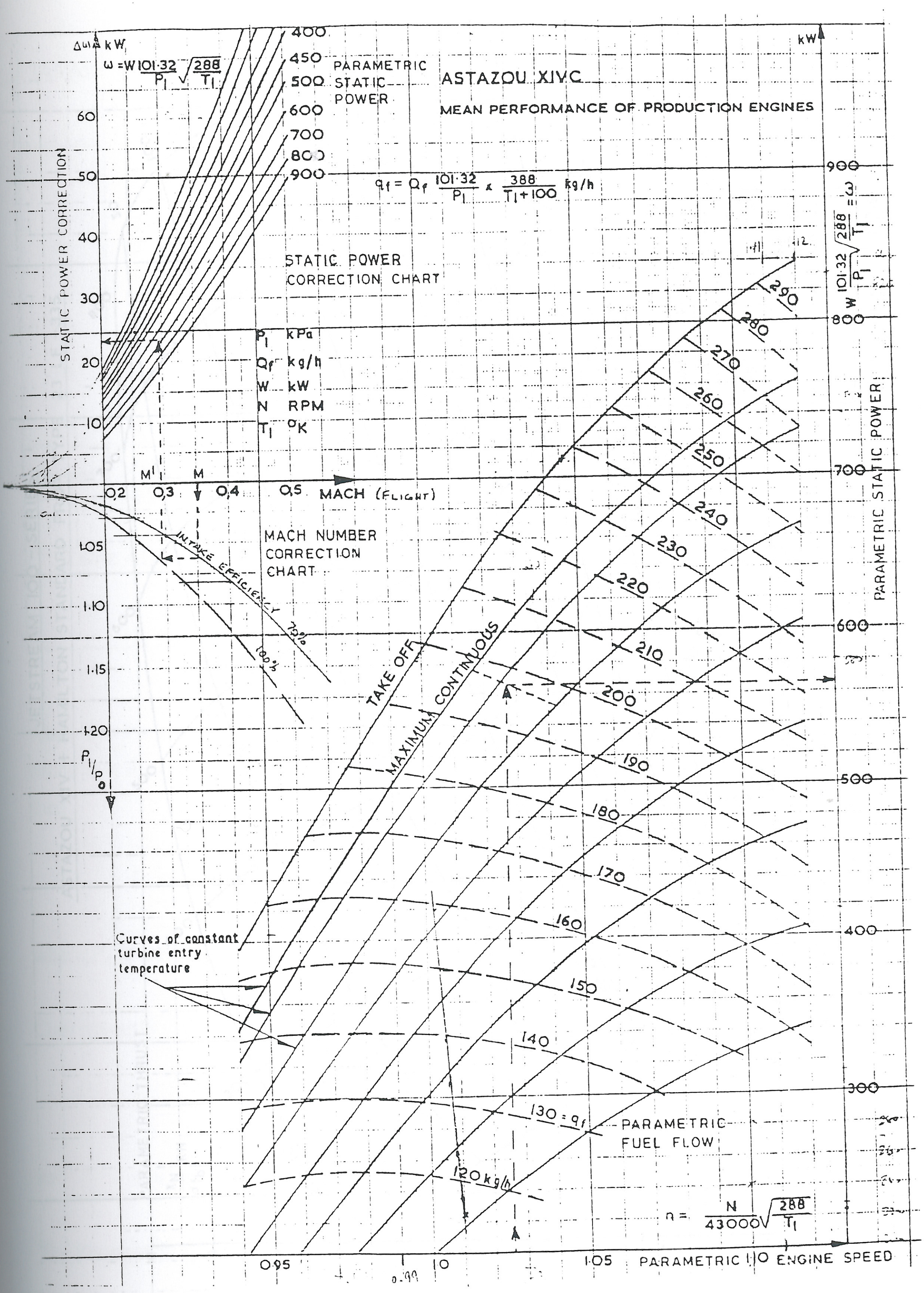

Figure AI.1: Mean performance of production Astazou XIVC engines.

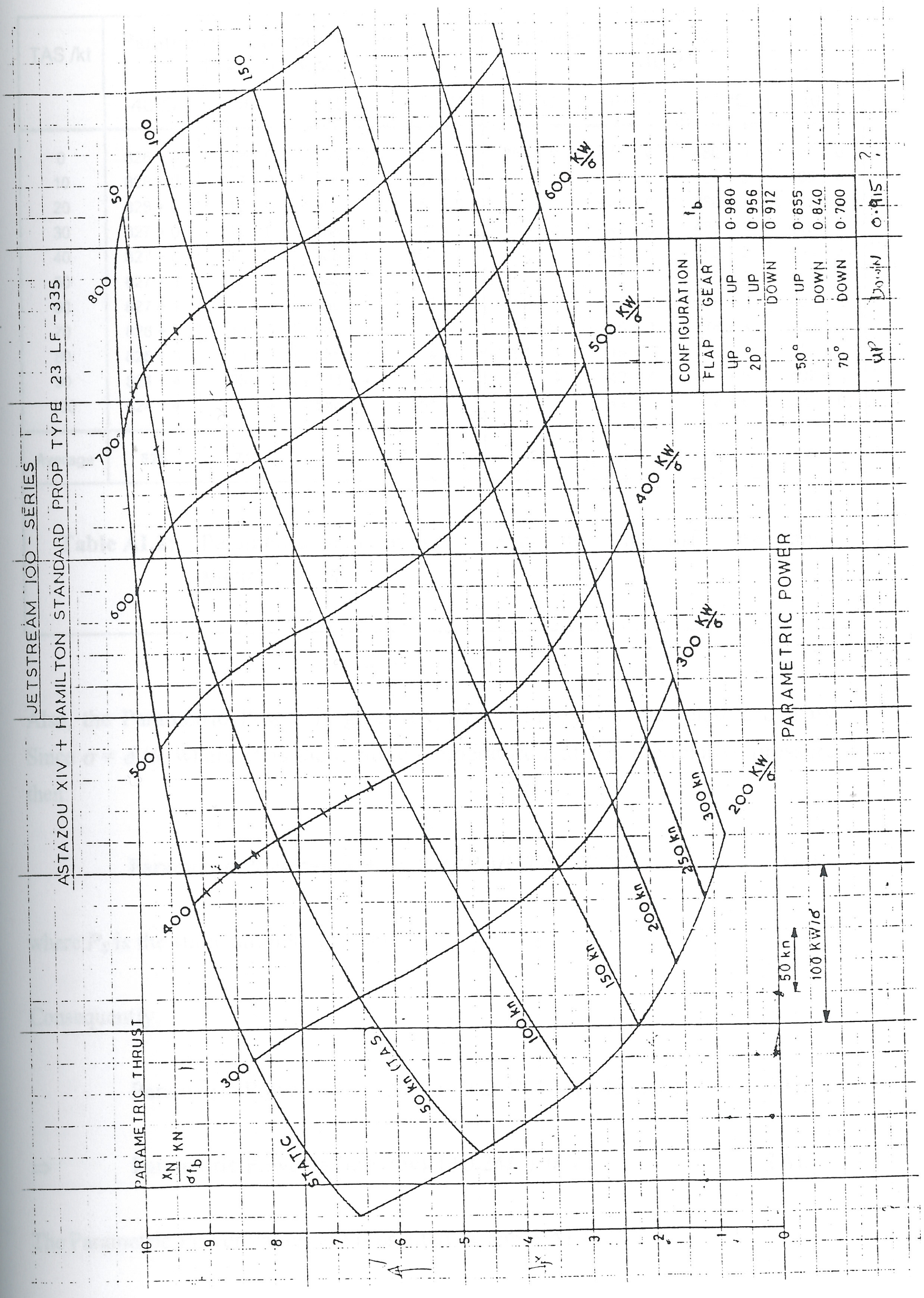

Figure AI.2: Astazou – Hamilton Standard thrust characteristic.

TAS /kt	Parametric static power $w+\Delta w$ Take-off power				Parametric static power $w+\Delta w$ MCP			
	-40°C	-10°C	+15°C	+40°C	-40°C	-10°C	+15°C	+40°C
0	828 + 0	712 + 0	588 + 0	457 + 0	753 + 0	647 + 0	480 + 0	405 + 0
10	828 + 0	712 + 0	588 + 0	457 + 0	753 + 0	647 + 0	480 + 0	405 + 0
20	828 + 0	712 + 0	588 + 0	457 + 0	753 + 0	647 + 0	480 + 1	405 + 0
30	827 + 0	712 + 0	588 + 0	457 + 1	752 + 0	647 + 0	480 + 1	405 + 1
40	827 + 0	712 + 1	588 + 1	457 + 2	752 + 0	647 + 1	480 + 2	405 + 2
50	827 + 1	712 + 1	586 + 1	457 + 2	752 + 1	647 + 1	478 + 2	405 + 2
60	827 + 1	712 + 1	586 + 1	457 + 2	752 + 1	647 + 2	478 + 2	405 + 2
70	826 + 2	710 + 2	586 + 2	454 + 3	751 + 2	645 + 3	478 + 3	402 + 3
80	826 + 3	710 + 2	586 + 3	454 + 4	751 + 3	645 + 3	476 + 4	402 + 4
90	824 + 4	706 + 3	583 + 4	454 + 5	751 + 4	642 + 4	476 + 5	402 + 5
100	824 + 4	706 + 4	583 + 5	451 + 6	751 + 4	642 + 5	476 + 6	399 + 6
Average	**828**	**712**	**588**	**458**	**753**	**647**	**481**	**406**

Table AI.2: Parametric static power ($w+\Delta w$) for Take-off power and MCP.

Also, the Parametric Power is given by W/σ, where σ is the relative density. Since $\sigma = \delta/\theta$, where θ is the relative temperature and δ is the relative pressure, then:

$$\text{Parametric Power} = (w + \Delta w)(P_T/P_S)\theta\,(TAT/288)^{0.5} \qquad \ldots\ (\text{AI.4})$$

where P_S is the static ambient pressure.

Consequently,

$$\text{Parametric Power} = (w + \Delta w)(1+0.2M^2)^{3.5}\theta\,(TAT/288)^{0.5} \qquad \ldots\ (\text{AI.5})$$

$$\Rightarrow \qquad \text{Parametric Power} = (w + \Delta w)(1+0.2M^2)^4\theta^{3/2} \qquad \ldots\ (\text{AI.6})$$

The Parametric Power values are presented in Table AI.4.

The Parametric Thrust is determined using the Parametric Power and the Astazou XIV – Hamilton Standard thrust characteristic (Figure AI.2, Table AI.5).

TAS /kt	$(1+0.2M^2)^4$			
	n @-40°C	*n* @-10°C	*n* @+15°C	*n* @+40°C
0	1	1	1	1
10	1.000226	1.000226	1.000226	1.000226
20	1.000905	1.000905	1.000905	1.000905
30	1.002037	1.002037	1.002037	1.002037
40	1.003624	1.003624	1.003624	1.003624
50	1.005666	1.005666	1.005666	1.005666
60	1.008167	1.008167	1.008167	1.008167
70	1.011128	1.011128	1.011128	1.011128
80	1.014553	1.014553	1.014553	1.014553
90	1.018445	1.018445	1.018445	1.018445
100	1.022809	1.022809	1.022809	1.022809
$\theta^{3/2}$	0.727688	0.87266	1	1.132994

Table AI.3: Computation of $(1+0.2M^2)^4$ and $\theta^{3/2}$ for various forwards speeds and ambient temperatures.

TAS /kt	Parametric Power Output /kW/σ Take-off power				Parametric Power Output /kW/σ MCP			
	-40°C	-10°C	+15°C	+40°C	-40°C	-10°C	+15°C	+40°C
0	603	621	588	518	548	565	480	459
10	603	621	588	518	548	565	480	459
20	603	622	589	518	548	565	481	459
30	603	623	589	520	548	566	482	461
40	604	624	591	522	549	568	484	463
50	606	626	590	523	551	569	483	464
60	607	627	592	524	552	571	484	465
70	609	628	595	524	554	572	486	464
80	612	630	598	526	557	574	487	467
90	614	630	598	530	560	574	490	470
100	616	634	601	530	562	577	493	470
Average	**607**	**626**	**593**	**523**	**553**	**570**	**485**	**464**

Table AI.4: Parametric power output for Take-off power and MCP.

TAS /kt	Parametric Thrust @ Parametric Power			
	400kW/σ	500kW/σ	600kW/σ	650kW/σ
0	9.15	9.65	9.95	10.05
10	8.95	9.50	9.90	10.03
20	8.75	9.35	9.85	9.98
30	8.45	9.20	9.70	9.90
40	8.20	8.95	9.55	9.80
50	7.80	8.75	9.40	9.63
60	7.45	8.50	9.20	9.45
70	7.10	8.20	8.90	9.20
80	6.70	7.90	8.70	8.95
90	6.35	7.50	8.35	8.70
100	5.95	7.05	8.00	8.40

Table AI.5: Parametric thrust for Take-off power and MCP.

APPENDIX II

PERFORMANCE RESULTS OF THE JETSTREAM-100 MONITORING ALGORITHM

Run #	File name	End IRS ground speed /kt	Run Time /s	Total Dist. /m	Prediction error				Time to stage		Time to go	
					/m last ¾ dist.	/% last ¾ dist.	/m last ½ dist.	/% last ½ dist.	¼ dist. /s	½ dist. /s	@¼ dist. /s	@½ dist. /s
1	980204	88.6	17.0	391.0	18.4	4.70	3.3	0.84	8.6	12.0	8.4	5.0
2	980210	88.6	16.2	371.5	8.6	2.32	5.9	1.58	8.1	11.4	8.1	4.8
3	980501a	93.3	17.4	429.9	23.5	5.46	0.7	0.15	8.7	12.2	8.7	5.2
4	980508b	90.6	17.0	407.6	7.6	1.85	4.0	0.98	8.5	11.9	8.5	5.1
5	981109	86.8	17.2	386.1	5.1	1.31	3.4	0.87	8.8	12.2	8.4	5.0
6	981112a	92.4	17.5	448.0	4.4	0.98	4.4	0.98	8.4	12.1	9.1	5.4
7	981112b	92.0	17.7	440.6	5.3	1.20	3.4	0.77	8.7	12.4	9.0	5.3
8	981124	94.8	19.0	483.0	12.9	2.67	3.1	0.65	9.4	13.3	9.6	5.7
9	981130rto1	84.5	15.8	346.1	5.7	1.65	2.6	0.75	8.0	11.2	7.8	4.6
10	981130rto2	80.8	14.8	317.6	7.9	2.49	4.0	1.27	7.3	10.3	7.5	4.5
11	990909	96.5	16.8	443.3	10.1	2.27	3.3	0.75	8.2	11.7	8.6	5.1
12	990909mcp1	93.6	17.1	437.6	5.0	1.15	5.0	1.15	8.4	11.9	8.7	5.2
13	990909mcp2	88.8	15.4	373.2	11.3	3.02	4.0	1.61	7.5	10.7	7.9	4.7
14	we140003	93.1	15.9	399.5	6.6	1.66	3.6	0.89	7.8	11.1	8.1	4.8
15	we135634	92.1	15.8	393.6	6.6	1.67	5.9	1.50	7.7	11.0	8.1	4.8
16	07041027	90.1	15.5	379.5	10.0	2.63	3.5	0.91	7.6	10.9	7.9	4.6
17	09051250	90.0	17.4	423.1	8.1	1.92	2.2	0.53	8.5	12.1	8.9	5.3
18	10051259	90.1	18.0	442.8	13.8	3.11	11.9	2.70	8.6	12.3	9.4	5.7
19	10051357	90.1	15.1	372.6	5.3	1.42	5.3	1.42	7.4	10.6	7.7	4.5
20	11021147	88.8	14.4	350.5	7.0	1.99	7.0	1.99	7.0	10.0	7.4	4.4
21	11041444	90.3	17.4	425.2	23.9	5.63	7.5	1.76	8.5	12.1	8.9	5.3
22	15051711	90.0	16.5	403.7	9.5	2.36	6.1	1.52	8.1	11.5	8.4	5.0
23	16041551	90.0	15.5	378.3	7.2	1.90	4.8	1.27	7.7	10.8	7.8	4.7
24	20030829	90.0	15.0	366.4	7.6	2.07	2.8	0.77	7.4	10.5	7.6	4.5
25	22031038	90.1	15.4	377.4	5.2	1.39	5.2	1.39	7.5	10.7	7.9	4.7

Table AII.1: Run details of the 40 standard take-offs conducted with Jetstream-100 G-NFLC.

Run #	File name	End IRS ground speed /kt	Run Time /s	Total Dist. /m	Prediction error				Time to stage		Time to go	
					/m last ¾ dist.	/% last ¾ dist.	/m last ½ dist.	/% last ½ dist.	¼ dist. /s	½ dist. /s	@¼ dist. /s	@½ dist. /s
26	22031434	90.0	16.5	402.6	13.5	3.36	6.2	1.54	8.1	11.5	8.4	5.0
27	22031619	90.0	16.1	389.1	5.3	1.35	5.3	1.35	8.0	11.3	8.1	4.8
28	25020847	90.0	16.5	404.7	7.3	1.80	5.8	1.43	8.1	11.5	8.4	5.0
29	25021230	90.1	16.7	409.4	12.5	3.06	9.2	2.24	8.2	11.6	8.5	5.1
30	25040634	90.3	16.7	406.3	6.2	1.53	5.1	1.26	8.3	11.7	8.4	5.0
31	11051344	79.0	15.6	336.2	6.4	1.92	4.7	1.38	7.6	10.9	8.0	4.7
32	15051243	84.4	17.9	414.0	10.8	2.60	2.5	0.60	8.8	12.4	9.1	5.5
33	15051449	83.4	17.7	402.8	10.7	2.64	2.8	0.68	8.7	12.4	9.0	5.3
34	16050917a	98.4	20.4	549.4	5.7	1.04	2.3	0.44	10.0	14.2	10.4	6.2
35	16051238a	88.4	18.9	458.8	2.4	1.52	2.4	0.52	9.2	13.1	9.7	5.8
36	16051458a	94.3	20.4	532.8	16.3	3.06	13.4	2.52	9.9	14.1	10.5	6.3
37	17050918a	90.1	18.7	459.0	5.4	1.18	5.4	1.18	9.2	13.0	9.5	5.7
38	18051240a	97.6	17.4	464.4	5.5	1.18	5.5	1.18	8.5	12.1	8.9	5.3
39	30030813	85.5	16.4	378.3	11.4	3.01	5.4	1.46	8.0	11.4	8.4	5.0
40	05080959	89.8	16.5	398.3	8.2	2.06	4.9	1.23	8.2	11.6	8.3	4.9
Minimum		**79.0**	**14.4**	**317.6**					**7.0**	**10.0**	**7.4**	**4.4**
Average		**89.9**	**16.8**	**410.2**	**9.13**	**2.26**	**4.84**	**1.20**	**8.3**	**11.7**	**8.6**	**5.1**
Maximum		**98.4**	**20.4**	**549.4**					**10.0**	**14.2**	**10.5**	**6.3**
Standard Deviation					**4.88**	**1.11**	**2.49**	**0.56**				
99% Confidence					**20.48**	**4.83**	**10.63**	**2.49**				

Table AII.1 (cont.): Run details of the 40 standard take-offs conducted with G-NFLC.

Run #	File name	End IRS ground speed /kt	Run Time /s	Total Dist. /m	Prediction error				Time to stage		Time to go	
					/m last ¾ dist.	/% last ¾ dist.	/m last ½ dist.	/% last ½ dist.	¼ dist. /s	½ dist. /s	@¼ dist. /s	@½ dist. /s
1	10041510	90.0	14.9	422.5	27.1	6.42	4.6	1.10	6.1	9.7	8.8	5.2
2	10041458	90.0	15.7	418.9	3.4	0.82	3.1	0.74	6.9	10.5	8.8	5.2
3	10041536	90.1	11.4	367.4	20.3	5.50	2.5	0.68	4.1	7.0	7.3	4.4
4	10041540	90.1	14.5	405.0	3.9	0.95	3.9	0.95	6.1	9.5	8.4	5.0
5	12041441	90.0	14.2	417.3	1.0	0.24	1.0	0.24	5.6	9.0	8.6	5.2
6	21031441	90.0	12.5	379.1	11.5	3.03	7.9	2.08	4.8	7.9	7.7	4.6
7	21031526	90.1	12.3	371.0	31.7	8.53	6.3	1.70	4.7	7.7	7.6	4.6
8	30031239	85.4	12.9	364.7	24.7	6.71	3.6	1.00	5.0	8.1	7.9	4.8
Minimum			**11.4**	**364.7**					**4.1**	**7.0**	**7.3**	**4.4**
Average			**13.5**	**393.2**	**15.5**	**4.03**	**4.1**	**1.06**	**5.4**	**8.7**	**8.1**	**4.9**
Maximum			**15.7**	**422.5**					**6.9**	**10.5**	**8.8**	**5.2**
Standard Deviation					**12.0**	**3.17**	**2.2**	**0.58**				
99% Confidence					**55.4**	**14.58**	**11.3**	**3.00**				

Table AII.1 (cont.): Run details of the 8 rolling start take-offs conducted with Jetstream-100 G-NFLC.

APPENDIX III

PERFORMANCE RESULTS OF THE LARGE JET TRANSPORT MONITORING ALGORITHM

B747-400

and

B737-400

Run #	Filename	Weight /lbs	Run time /s	Rotation ground speed /kt	Rotation distance /m	Monitored time /s	Speed @ start of monitor /kt	Monitored distance /m	Time to ¼ dist. /s	Speed @ ¼ dist. /kt	Time to ½ dist. /s	Speed @ ½ dist. /kt
1	cive1	771840	47	146	1870	43	12	1857	19.3	80	28.8	109
2	cive2	761600	40	144	1546	32	32	1477	12.8	80	20.5	108
3	civf1	685840	38	145	1489	33	21	1456	14.0	79	21.8	108
4	civf2	692480	39	145	1493	33	21	1456	14.0	79	21.8	108
5	civg1	771840	39	156	1786	35	31	1738	14.3	88	22.5	117
6	civg2	478400	20	114	660	15	39	590	5.5	69	9.3	88
7	civg3	494720	21	124	763	17	36	708	6.5	73	10.5	94
8	civg4	770560	41	156	1715	35	24	1671	14.8	85	23.0	116
9	civh1	732480	39	157	1729	34	28	1676	14.0	88	22.0	117
10	civh2	726400	41	167	1974	36	33	1914	14.8	94	23.3	126
11	civk1	850560	41	148	1721	30	50	1555	11.0	90	18.5	115
12	civk2	690880	35	149	1495	30	33	1433	12.0	84	19.3	112
13	civl1	688960	34	129	1196	31	14	1181	13.8	70	20.8	96
14	civl2	646400	20	133	995	20	59	995	6.8	87	11.8	106
15	civm1	855040	47	158	2008	41	21	1976	17.8	88	27.0	118
16	civm2	777920	40	142	1610	36	22	1576	15.3	79	23.5	106
17	civs1	866880	46	169	2023	41	14	2009	18.5	91	27.5	124
18	civs2	557120	29	127	909	22	23	864	9.3	70	14.3	94
19	civt1	717760	43	154	1757	35	27	1692	14.5	86	22.8	116
20	civt2	754560	37	142	1513	34	22	1486	14.3	78	22.3	106
21	civu1	764160	37	143	1447	33	19	1419	14.3	78	21.8	106
22	civu2	471360	24	124	821	19	31	770	7.5	71	12.0	94
23	civu3	462720	27	128	781	17	32	712	6.8	74	10.8	97
24	civu4	792960	42	158	1756	35	24	1708	14.8	87	23.0	119
25	civz1	788800	53	162	2203	43	22	2140	18.5	90	28.3	122

Table AIII.1: Run details of the 80 B747-400 take-offs.

Run #	Filename	Weight /lbs	Run time /s	Rotation ground speed /kt	Rotation distance /m	Monitored time /s	Speed @ start of monitor /kt	Monitored distance /m	Time to ¼ dist. /s	Speed @ ¼ dist. /kt	Time to ½ dist. /s	Speed @ ½ dist. /kt
26	civb1a	774720	41	134	1573	37	21	1542	15.8	75	24.3	101
27	civb1b	874240	40	144	1568	36	17	1547	15.8	78	24.0	107
28	civb2a	818240	42	144	1761	37	29	1708	15.0	82	23.8	108
29	civb2b	780800	38	133	1428	28	44	1293	10.3	80	17.3	102
30	civi1a	711680	36	132	1362	30	31	1300	11.8	76	19.0	100
31	civi1b	718720	44	149	1773	39	17	1749	17.0	82	26.0	112
32	civi2a	832960	37	156	1720	26	64	1484	9.0	99	15.5	122
33	civi2b	571840	28	124	1023	24	31	974	9.5	71	15.3	94
34	civi2c	587200	32	128	1228	28	31	1178	11.0	74	17.8	97
35	civp1a	803840	44	157	1907	40	18	1885	17.5	86	26.5	117
36	civp1b	775360	33	132	1258	27	35	1182	10.5	77	17.0	100
37	civp2a	858560	37	138	1462	33	25	1424	13.8	77	21.5	103
38	civp2b	633280	30	131	1062	27	15	1046	12.0	72	18.0	97
39	civw1a	796800	44	159	1967	40	21	1937	17.3	88	26.5	120
40	civw1b	854720	49	173	2352	36	54	2157	13.3	103	22.3	133
41	civw2a	869440	45	155	1921	34	44	1788	13.0	92	21.3	119
42	civw2b	693120	35	148	1501	31	29	1458	12.8	84	20.0	111
43	civw3a	798720	43	149	1784	39	18	1759	17.0	82	25.8	112
44	civw3b	831040	40	160	1889	34	40	1801	13.3	92	21.5	122
45	civw4a	735680	38	144	1597	35	24	1568	14.8	80	22.8	108
46	civw4b	662080	31	134	1235	27	32	1185	10.5	77	17.0	101
47	civw5a	783040	41	158	1866	37	27	1827	15.5	88	24.0	118
48	civw5b	798720	32	139	1309	27	37	1241	10.5	80	17.0	105
49	civw6a	802880	42	152	1729	32	41	1621	12.3	88	20.0	115
50	civw6b	752320	47	167	2135	41	23	2097	17.5	92	27.0	125

Table AIII.1 (cont.): Run details of the 80 B747-400 take-offs.

Run #	Filename	Weight /lbs	Run time /s	Rotation ground speed /kt	Rotation distance /m	Monitored time /s	Speed @ start of monitor /kt	Monitored distance /m	Time to ¼ dist. /s	Speed @ ¼ dist. /kt	Time to ½ dist. /s	Speed @ ½ dist. /kt
51	civx1a	812800	44	161	2058	39	31	2000	16.0	91	25.3	122
52	civx1b	682560	38	158	1672	32	32	1611	13.0	89	20.5	119
53	civx2a	816640	42	158	1818	39	15	1801	17.5	85	26.3	117
54	civx2b	616640	33	147	1321	25	38	1217	9.8	85	15.8	112
55	civf2b	739840	42	153	1651	35	21	1615	15.0	83	23.0	113
56	civj1a	856960	46	155	1886	35	38	1784	13.8	89	22.3	117
57	civj1b	849920	52	183	2552	38	53	2366	14.5	108	23.8	141
58	civj2b	824000	44	159	1963	39	26	1916	16.3	87	25.5	118
59	civj3a	809600	45	166	2091	31	61	1848	11.0	103	18.8	130
60	civj3b	736960	38	142	1458	32	24	1416	13.3	79	20.8	106
61	civj4a	835520	43	157	1834	26	69	1519	8.8	101	15.3	124
62	civj4b	605760	28	138	1132	24	34	1078	9.5	79	15.3	104
63	civj4d	850560	42	162	1961	29	63	1705	10.3	102	17.5	127
64	civl1a	840960	44	170	2101	30	65	1837	10.5	106	18.0	132
65	civl1b	841280	46	162	2056	38	33	1980	15.5	92	24.5	123
66	civl2a	828800	43	156	1843	36	30	1779	14.8	88	23.3	117
67	civl2b	818880	50	165	2295	44	25	2248	18.8	92	28.8	124
68	civo1a	798080	46	169	2157	40	28	2105	16.8	94	26.0	127
69	civo1b	739200	37	143	1436	29	35	1358	11.3	81	18.3	107
70	civo2a	815680	46	168	2087	31	60	1859	11.3	104	18.8	131
71	civo2b	828480	51	172	2485	38	55	2275	14.0	103	23.5	133
72	civt1a	833920	42	153	1800	35	33	1726	14.0	86	22.5	115
73	civt1b	766400	44	158	1895	40	16	1872	17.8	86	26.8	118
74	civt2a	857920	44	163	1945	39	21	1913	17.0	89	25.8	121
75	civt2b	816640	46	162	2131	40	32	2066	16.3	91	25.8	122

Table AIII.1 (cont.): Run details of the 80 B747-400 take-offs.

Run #	Filename	Weight /lbs	Run time /s	Rotation ground speed /kt	Rotation distance /m	Monitored time /s	Speed @ start of monitor /kt	Monitored distance /m	Time to ¼ dist. /s	Speed @ ¼ dist. /kt	Time to ½ dist. /s	Speed @ ½ dist. /kt
76	civu1a	800960	42	164	1917	36	30	1859	14.8	91	23.3	123
77	civu1b	493760	22	118	742	18	30	694	7.0	68	11.3	89
78	civz1a	847680	48	170	2252	36	50	2084	13.5	100	22.5	130
79	civz1b	784000	45	155	2007	41	24	1970	17.3	86	26.8	116
80	civz2a	823360	43	152	1751	29	54	1554	10.5	93	17.8	118
Minimum		**462720**	**20**	**114**	**660**	**15**	**12**	**590**	**6**	**68**	**9**	**88**
Average		**753325**	**40**	**150**	**1675**	**33**	**32**	**1598**	**13**	**86**	**21**	**113**
Maximum		**874240**	**53**	**183**	**2552**	**44**	**69**	**2366**	**19**	**108**	**29**	**141**

Table AIII.1 (cont.): Run details of the 80 B747-400 take-offs.

Run #	Monitored distance /m	Algorithm prediction error											
		Exponential weighting = 0.00				Exponential weighting = 0.05				Exponential weighting = 0.10			
		/m last ¾ dist.	/% last ¾ dist.	/m last ½ dist.	/% last ½ dist.	/m last ¾ dist.	/% last ¾ dist.	/m last ½ dist.	/% last ½ dist.	/m last ¾ dist.	/% last ¾ dist.	/m last ½ dist.	/% last ½ dist.
1	1857	40.7	2.17	19.5	1.04	51.5	2.76	19.1	1.02	64.0	3.42	18.7	1.00
2	1477	21.9	1.41	12.0	0.78	24.9	1.61	12.5	0.81	27.1	1.75	12.7	0.82
3	1456	22.3	1.50	10.5	0.71	17.7	1.19	11.1	0.75	20.5	1.38	11.1	0.74
4	1456	22.3	1.49	10.5	0.71	17.7	1.19	11.1	0.75	20.5	1.37	11.1	0.74
5	1738	40.3	2.26	37.8	2.12	47.4	2.65	39.2	2.20	55.1	3.08	40.5	2.27
6	590	34.2	5.18	1.8	0.27	33.5	5.08	2.3	0.35	32.9	4.99	2.7	0.41
7	708	14.1	1.84	7.6	0.99	14.4	1.88	7.5	0.98	14.6	1.92	7.5	0.98
8	1671	79.9	4.66	20.2	1.18	78.3	4.57	14.0	0.81	77.3	4.51	7.9	0.46
9	1676	62.6	3.62	7.4	0.43	59.2	3.43	11.0	0.64	56.0	3.24	15.1	0.87
10	1914	44.3	2.25	8.9	0.45	45.2	2.29	12.0	0.61	45.7	2.31	14.8	0.75
11	1555	30.9	1.79	13.6	0.79	30.2	1.75	12.1	0.70	29.9	1.74	10.4	0.61
12	1433	17.0	1.14	4.0	0.27	21.6	1.44	4.5	0.30	25.6	1.71	4.9	0.33
13	1181	19.4	1.62	16.3	1.36	20.1	1.68	16.1	1.35	21.0	1.76	15.8	1.32
14	995	27.5	2.76	13.8	1.38	30.6	3.07	13.8	1.39	33.7	3.39	13.9	1.40
15	1976	122.6	6.11	45.4	2.26	121.5	6.05	37.9	1.89	118.0	5.88	32.3	1.61
16	1576	33.0	2.05	25.7	1.60	36.1	2.24	25.7	1.59	38.7	2.40	24.8	1.54
17	2009	51.8	2.56	3.6	0.18	53.1	2.63	8.4	0.41	54.8	2.71	14.3	0.71
18	864	22.3	2.46	19.2	2.11	23.0	2.53	19.2	2.11	23.9	2.63	19.0	2.09
19	1692	14.1	0.80	13.0	0.74	14.3	0.82	14.0	0.80	15.0	0.85	15.0	0.85
20	1486	25.0	1.65	8.5	0.56	26.7	1.76	9.1	0.60	28.8	1.90	11.5	0.76
21	1419	18.8	1.30	4.7	0.33	18.0	1.24	4.2	0.29	17.7	1.23	4.4	0.30
22	770	23.4	2.86	2.9	0.35	24.5	2.98	3.4	0.41	25.4	3.10	4.0	0.49
23	712	4.9	0.63	4.4	0.57	5.5	0.71	4.6	0.59	6.5	0.84	4.6	0.60
24	1708	63.2	3.60	35.5	2.02	62.2	3.54	31.4	1.79	61.8	3.52	27.0	1.54
25	2140	37.8	1.71	23.9	1.08	57.9	2.63	26.9	1.22	75.5	3.43	29.7	1.35

Table AIII.2: Algorithm performance with different exponential weightings (0 to 0.10) on the 80 B747-400 take-offs.

Run #	Monitored distance /m	Algorithm prediction error											
		Exponential weighting = 0.00				Exponential weighting = 0.05				Exponential weighting = 0.10			
		/m last ¾ dist.	/% last ¾ dist.	/m last ½ dist.	/% last ½ dist.	/m last ¾ dist.	/% last ¾ dist.	/m last ½ dist.	/% last ½ dist.	/m last ¾ dist.	/% last ¾ dist.	/m last ½ dist.	/% last ½ dist.
26	1542	73.6	4.68	8.6	0.55	72.3	4.59	7.0	0.45	69.8	4.44	6.7	0.42
27	1547	29.8	1.90	29.8	1.90	32.0	2.04	32.0	2.04	34.0	2.17	34.0	2.17
28	1708	33.3	1.89	33.3	1.89	37.1	2.11	37.1	2.11	40.9	2.32	40.9	2.32
29	1293	29.5	2.06	27.4	1.92	35.2	2.46	27.9	1.96	41.0	2.87	28.3	1.98
30	1300	38.4	2.82	22.3	1.64	40.6	2.98	21.0	1.54	42.6	3.13	19.3	1.42
31	1749	40.5	2.29	16.6	0.94	42.5	2.39	16.5	0.93	44.9	2.53	17.1	0.97
32	1484	33.0	1.92	4.4	0.25	33.9	1.97	4.6	0.27	35.0	2.03	4.8	0.28
33	974	23.1	2.26	15.8	1.55	24.4	2.39	15.5	1.51	25.7	2.51	15.0	1.46
34	1178	23.7	1.93	7.5	0.61	30.2	2.46	6.4	0.52	36.7	2.99	4.9	0.40
35	1885	17.6	0.93	13.6	0.71	19.6	1.03	13.8	0.73	21.5	1.13	13.5	0.71
36	1182	49.2	3.91	18.9	1.51	46.2	3.67	21.3	1.70	43.1	3.42	23.9	1.90
37	1424	13.2	0.90	11.9	0.82	15.6	1.07	13.5	0.93	18.1	1.24	15.6	1.07
38	1046	58.9	5.54	29.5	2.78	56.3	5.31	26.5	2.49	53.9	5.08	23.4	2.20
39	1937	41.2	2.10	18.8	0.95	35.7	1.82	21.7	1.11	28.8	1.46	23.9	1.21
40	2157	24.8	1.05	7.5	0.32	26.1	1.11	8.3	0.35	27.7	1.18	10.3	0.44
41	1788	40.5	2.11	3.9	0.20	47.0	2.45	7.2	0.38	55.2	2.87	10.6	0.55
42	1458	20.2	1.35	8.0	0.53	23.2	1.55	7.8	0.52	26.3	1.76	7.5	0.50
43	1759	42.6	2.39	23.0	1.29	44.3	2.48	21.7	1.22	44.3	2.49	20.4	1.15
44	1801	97.9	5.18	13.2	0.70	100.4	5.31	17.2	0.91	102.0	5.40	20.2	1.07
45	1568	45.0	2.82	16.8	1.05	42.6	2.67	17.3	1.08	40.8	2.56	18.4	1.15
46	1185	28.4	2.30	15.6	1.26	21.0	1.70	16.4	1.32	17.2	1.39	17.2	1.39
47	1827	70.4	3.77	28.2	1.51	66.3	3.55	25.5	1.37	63.8	3.42	23.8	1.27
48	1241	53.0	4.05	12.7	0.97	49.8	3.80	11.4	0.87	46.5	3.55	10.3	0.79
49	1621	26.1	1.51	10.5	0.61	25.2	1.46	10.1	0.59	24.1	1.40	10.0	0.58
50	2097	15.6	0.73	13.8	0.65	16.4	0.77	15.4	0.72	18.0	0.84	17.6	0.82

Table AIII.2 (cont.): Algorithm performance with different exponential weightings (0 to 0.10) on the 80 B747-400 take-offs.

Run #	Monitored distance /m	Algorithm prediction error											
		Exponential weighting = 0.00				Exponential weighting = 0.05				Exponential weighting = 0.10			
		/m last ¾ dist.	/% last ¾ dist.	/m last ½ dist.	/% last ½ dist.	/m last ¾ dist.	/% last ¾ dist.	/m last ½ dist.	/% last ½ dist.	/m last ¾ dist.	/% last ¾ dist.	/m last ½ dist.	/% last ½ dist.
51	2000	16.9	0.82	8.8	0.43	20.9	1.02	9.4	0.46	25.5	1.24	10.4	0.51
52	1611	68.1	4.07	7.5	0.45	67.4	4.03	5.7	0.34	66.6	3.99	5.3	0.32
53	1801	78.6	4.32	37.2	2.04	74.9	4.12	33.0	1.81	71.2	3.91	29.4	1.62
54	1217	54.2	4.11	23.3	1.76	55.4	4.19	21.9	1.65	56.6	4.28	21.3	1.61
55	1615	13.0	0.79	6.5	0.39	13.2	0.80	5.36	0.3	14.0	0.85	4.1	0.25
56	1784	22.8	1.21	5.3	0.28	22.7	1.21	5.87	0.3	23.4	1.24	6.4	0.34
57	2366	116.0	4.54	48.3	1.89	114.7	4.50	42.88	1.7	112.9	4.42	38.4	1.50
58	1916	47.0	2.39	28.3	1.44	43.1	2.19	33.78	1.7	53.0	2.70	37.4	1.91
59	1848	17.9	0.86	15.3	0.73	20.6	0.98	16.73	0.8	23.3	1.11	17.8	0.85
60	1416	10.7	0.73	10.7	0.73	11.2	0.77	11.21	0.8	12.0	0.82	11.7	0.80
61	1519	44.3	2.41	6.3	0.34	46.4	2.53	5.32	0.3	48.8	2.66	4.9	0.27
62	1078	38.5	3.40	11.2	0.99	36.0	3.18	10.67	0.9	33.3	2.94	10.3	0.91
63	1705	64.4	3.29	10.9	0.56	64.1	3.27	14.82	0.8	63.3	3.23	18.4	0.94
64	1837	83.6	3.98	5.1	0.24	84.2	4.01	7.44	0.4	84.3	4.01	9.4	0.45
65	1980	85.5	4.16	44.1	2.14	85.7	4.17	37.92	1.8	86.0	4.18	31.3	1.52
66	1779	20.4	1.10	18.9	1.03	20.9	1.13	20.89	1.1	22.4	1.21	22.3	1.21
67	2248	182.9	7.97	39.1	1.70	163.1	7.11	25.20	1.1	141.0	6.14	14.3	0.62
68	2105	24.8	1.15	24.8	1.15	27.0	1.25	26.97	1.2	28.9	1.34	28.9	1.34
69	1358	17.6	1.23	6.4	0.45	18.4	1.28	5.37	0.4	19.4	1.35	4.2	0.29
70	1859	44.9	2.15	31.7	1.52	37.1	1.78	32.09	1.5	32.7	1.57	32.7	1.57
71	2275	28.2	1.13	7.2	0.29	35.1	1.41	7.96	0.3	41.2	1.66	8.8	0.35
72	1726	27.1	1.50	7.3	0.41	26.3	1.46	8.14	0.5	26.3	1.46	9.2	0.51
73	1872	63.9	3.37	11.8	0.62	59.0	3.11	8.46	0.4	53.8	2.84	7.8	0.41
74	1913	42.2	2.17	24.9	1.28	45.7	2.35	22.21	1.1	50.2	2.58	18.9	0.97
75	2066	21.7	1.02	12.4	0.58	21.9	1.03	12.91	0.6	27.7	1.30	13.4	0.63

Table AIII.2 (cont.): Algorithm performance with different exponential weightings (0 to 0.10) on the 80 B747-400 take-offs.

Run #	Monitored distance /m	Algorithm prediction error											
		Exponential weighting = 0.00				Exponential weighting = 0.05				Exponential weighting = 0.10			
		/m last ¾ dist.	/% last ¾ dist.	/m last ½ dist.	/% last ½ dist.	/m last ¾ dist.	/% last ¾ dist.	/m last ½ dist.	/% last ½ dist.	/m last ¾ dist.	/% last ¾ dist.	/m last ½ dist.	/% last ½ dist.
76	1859	7.1	0.37	7.1	0.37	9.8	0.51	8.89	0.5	13.7	0.71	10.7	0.56
77	694	12.5	1.69	7.5	1.02	10.6	1.44	7.76	1.0	8.8	1.19	8.0	1.08
78	2084	57.6	2.56	12.7	0.56	52.2	2.32	11.83	0.5	45.8	2.03	11.5	0.51
79	1970	53.9	2.69	14.4	0.72	41.0	2.04	14.41	0.7	30.7	1.53	15.7	0.78
80	1554	27.7	1.58	27.5	1.57	29.8	1.70	29.28	1.7	32.4	1.85	31.0	1.77
Average		**40.7**	**2.43**	**16.3**	**0.99**	**41.0**	**2.45**	**16.2**	**0.98**	**41.8**	**2.49**	**16.3**	**0.99**
Standard deviation		**29.0**	**1.45**	**11.0**	**0.61**	**27.2**	**1.36**	**10.0**	**0.57**	**25.7**	**1.28**	**9.6**	**0.55**
99 % confidence		**108.2**	**5.80**	**41.8**	**2.41**	**104.3**	**5.61**	**39.5**	**2.31**	**101.5**	**5.48**	**38.7**	**2.27**
Maximum		**182.9**	**7.97**	**48.3**	**2.78**	**163.1**	**7.11**	**42.9**	**2.49**	**141.0**	**6.14**	**40.9**	**2.32**

Table AIII.2 (cont.): Algorithm performance with different exponential weightings (0 to 0.10) on the 80 B747-400 take-offs.

Run #	Monitored distance /m	Algorithm prediction error											
		Exponential weighting = 0.20				Exponential weighting = 0.30				Exponential weighting = 0.40			
		/m last ¾ dist.	/% last ¾ dist.	/m last ½ dist.	/% last ½ dist.	/m last ¾ dist.	/% last ¾ dist.	/m last ½ dist.	/% last ½ dist.	/m last ¾ dist.	/% last ¾ dist.	/m last ½ dist.	/% last ½ dist.
1	1857	90.4	4.83	19.4	1.04	118.0	6.31	24.8	1.32	146.1	7.81	34.3	1.84
2	1477	29.0	1.87	12.1	0.78	27.5	1.78	9.7	0.63	30.0	1.94	8.3	0.53
3	1456	27.0	1.82	9.3	0.62	32.7	2.20	11.1	0.75	37.9	2.54	14.7	0.99
4	1456	27.0	1.81	9.3	0.62	32.7	2.19	11.1	0.75	37.9	2.54	14.7	0.99
5	1738	72.2	4.04	42.8	2.39	96.7	5.41	44.6	2.50	126.0	7.05	46.4	2.60
6	590	31.7	4.81	3.5	0.53	30.6	4.64	4.1	0.61	29.5	4.48	4.4	0.66
7	708	15.3	2.00	7.5	0.98	15.8	2.07	7.6	1.00	16.0	2.10	7.9	1.03
8	1671	76.8	4.48	5.6	0.33	77.6	4.53	12.7	0.74	78.5	4.57	18.4	1.07
9	1676	49.6	2.87	22.5	1.30	43.5	2.52	27.4	1.59	37.7	2.18	29.8	1.72
10	1914	45.5	2.31	18.7	0.95	43.7	2.21	20.0	1.01	40.1	2.03	19.4	0.98
11	1555	30.3	1.76	7.4	0.43	32.2	1.87	9.8	0.57	35.7	2.08	18.1	1.05
12	1433	32.5	2.17	5.8	0.39	38.1	2.55	6.2	0.41	43.8	2.93	6.2	0.41
13	1181	23.1	1.93	14.5	1.21	25.6	2.14	12.0	1.01	28.8	2.41	11.6	0.97
14	995	39.9	4.01	14.2	1.42	46.0	4.62	14.7	1.47	51.9	5.21	15.5	1.56
15	1976	103.3	5.15	32.6	1.63	77.7	3.87	37.3	1.86	60.3	3.00	45.5	2.27
16	1576	50.8	3.16	21.3	1.32	68.5	4.25	16.5	1.02	87.1	5.41	12.1	0.75
17	2009	60.6	3.00	24.3	1.20	70.1	3.46	27.7	1.37	82.2	4.06	24.1	1.19
18	864	26.0	2.86	18.3	2.02	28.1	3.09	17.2	1.89	30.4	3.35	15.4	1.69
19	1692	19.8	1.13	19.8	1.13	26.1	1.48	26.1	1.48	32.1	1.83	32.1	1.83
20	1486	33.9	2.24	17.4	1.15	40.2	2.66	23.1	1.53	47.4	3.13	28.4	1.88
21	1419	18.6	1.29	4.9	0.34	20.6	1.43	5.5	0.38	23.5	1.62	6.1	0.42
22	770	27.1	3.30	5.2	0.64	28.5	3.47	6.4	0.78	29.6	3.60	7.4	0.90
23	712	8.6	1.10	4.6	0.60	12.5	1.60	4.5	0.58	16.1	2.07	4.4	0.56
24	1708	62.2	3.54	17.1	0.97	64.1	3.65	9.4	0.53	67.4	3.84	13.8	0.79
25	2140	101.4	4.61	33.4	1.52	111.3	5.05	34.7	1.58	101.6	4.61	35.9	1.63

Table AIII.3: Algorithm performance with different exponential weightings (0.2 to 0.4) on the 80 B747-400 take-offs.

Run #	Monitored distance /m	Algorithm prediction error											
		Exponential weighting = 0.20				Exponential weighting = 0.30				Exponential weighting = 0.40			
		/m last ¾ dist.	/% last ¾ dist.	/m last ½ dist.	/% last ½ dist.	/m last ¾ dist.	/% last ¾ dist.	/m last ½ dist.	/% last ½ dist.	/m last ¾ dist.	/% last ¾ dist.	/m last ½ dist.	/% last ½ dist.
26	1542	61.8	3.93	14.8	0.94	50.2	3.19	20.5	1.30	36.5	2.32	22.9	1.46
27	1547	37.4	2.38	36.6	2.33	40.3	2.57	38.2	2.43	44.3	2.83	38.8	2.47
28	1708	47.9	2.72	47.4	2.69	53.3	3.03	51.9	2.95	63.0	3.58	54.3	3.08
29	1293	51.4	3.60	28.7	2.01	61.2	4.29	29.1	2.04	70.1	4.91	29.7	2.08
30	1300	47.2	3.46	15.0	1.10	52.1	3.83	12.9	0.95	57.2	4.20	14.2	1.04
31	1749	53.3	3.00	20.9	1.18	62.2	3.51	28.4	1.60	71.9	4.05	38.1	2.15
32	1484	37.2	2.17	5.0	0.29	39.8	2.31	5.1	0.30	42.5	2.47	5.7	0.33
33	974	28.9	2.83	13.2	1.30	33.1	3.24	10.6	1.03	38.9	3.80	6.9	0.67
34	1178	49.7	4.05	8.9	0.72	61.0	4.97	16.4	1.34	70.8	5.77	24.4	1.99
35	1885	30.9	1.62	11.7	0.61	42.9	2.25	14.3	0.75	58.0	3.04	18.1	0.95
36	1182	36.3	2.89	28.3	2.25	32.4	2.58	32.4	2.58	35.8	2.84	35.8	2.84
37	1424	22.6	1.55	20.4	1.40	27.1	1.86	26.3	1.80	30.7	2.10	27.1	1.86
38	1046	50.7	4.77	17.0	1.61	49.3	4.64	10.1	0.95	49.0	4.61	5.5	0.51
39	1937	33.4	1.70	26.0	1.32	42.1	2.14	26.7	1.36	46.5	2.36	28.4	1.45
40	2157	36.2	1.54	14.5	0.62	49.4	2.10	18.2	0.77	67.4	2.87	22.0	0.93
41	1788	75.9	3.95	17.4	0.90	103.3	5.38	25.3	1.32	135.2	7.04	30.6	1.59
42	1458	33.0	2.20	13.5	0.90	40.6	2.70	20.7	1.38	49.0	3.27	23.0	1.53
43	1759	39.3	2.20	18.1	1.01	28.8	1.61	25.0	1.40	40.2	2.25	40.2	2.25
44	1801	103.4	5.47	26.5	1.40	103.0	5.45	30.0	1.59	102.5	5.42	32.9	1.74
45	1568	39.1	2.45	22.0	1.38	39.6	2.48	26.8	1.68	42.1	2.64	31.9	1.99
46	1185	22.6	1.83	19.1	1.54	29.9	2.42	20.9	1.70	37.9	3.06	23.1	1.87
47	1827	62.7	3.36	23.3	1.25	65.0	3.48	26.4	1.41	70.0	3.75	32.3	1.73
48	1241	39.9	3.05	8.8	0.68	33.4	2.55	9.2	0.70	26.9	2.05	11.2	0.85
49	1621	26.4	1.53	10.5	0.61	33.4	1.93	12.1	0.70	43.1	2.49	15.4	0.89
50	2097	24.7	1.16	24.7	1.16	36.0	1.68	36.0	1.68	43.8	2.05	43.8	2.05

Table AIII.3 (cont.): Algorithm performance with different exponential weightings (0.2 to 0.3) on the 80 B747-400 take-offs.

Run #	Monitored distance /m	Algorithm prediction error											
		Exponential weighting = 0.20				Exponential weighting = 0.3				Exponential weighting = 0.40			
		/m last ¾ dist.	/% last ¾ dist.	/m last ½ dist.	/% last ½ dist.	/m last ¾ dist.	/% last ¾ dist.	/m last ½ dist.	/% last ½ dist.	/m last ¾ dist.	/% last ¾ dist.	/m last ½ dist.	/% last ½ dist.
51	2000	36.0	1.75	12.6	0.61	47.4	2.30	16.1	0.78	59.0	2.86	25.7	1.25
52	1611	65.1	3.90	6.7	0.40	64.4	3.85	10.1	0.60	64.0	3.83	14.6	0.88
53	1801	63.5	3.49	24.7	1.36	55.7	3.06	23.0	1.27	48.1	2.64	23.8	1.31
54	1217	58.8	4.45	21.1	1.60	60.9	4.61	22.0	1.66	62.7	4.74	23.8	1.80
55	1615	18.1	1.09	6.9	0.41	30.1	1.82	12.3	0.74	43.5	2.63	20.0	1.21
56	1784	27.2	1.44	8.6	0.46	34.4	1.82	11.0	0.58	45.6	2.42	13.7	0.73
57	2366	107.5	4.21	57.8	2.26	100.1	3.92	76.7	3.01	100.8	3.95	100.8	3.95
58	1916	78.7	4.01	38.0	1.94	106.7	5.43	28.8	1.47	144.3	7.35	17.6	0.90
59	1848	28.8	1.38	18.8	0.90	35.0	1.68	20.3	0.97	41.6	1.99	22.5	1.07
60	1416	15.6	1.07	14.3	0.98	19.1	1.31	17.9	1.23	25.9	1.78	22.3	1.53
61	1519	56.2	3.07	5.8	0.31	62.8	3.42	6.8	0.37	68.6	3.74	8.7	0.48
62	1078	27.3	2.41	10.1	0.89	20.6	1.82	10.4	0.92	13.0	1.15	11.0	0.97
63	1705	60.7	3.09	24.3	1.24	56.4	2.88	28.6	1.46	50.5	2.57	30.5	1.56
64	1837	83.8	3.99	12.3	0.58	82.3	3.92	15.0	0.72	80.3	3.82	17.6	0.84
65	1980	87.9	4.28	16.6	0.81	92.6	4.51	11.7	0.57	101.2	4.92	16.3	0.79
66	1779	30.2	1.64	24.1	1.31	37.6	2.04	24.8	1.35	46.8	2.54	25.3	1.37
67	2248	90.1	3.93	13.5	0.59	30.7	1.34	18.9	0.82	46.3	2.02	36.3	1.58
68	2105	33.0	1.53	33.0	1.53	36.9	1.71	36.9	1.71	42.1	1.95	42.1	1.95
69	1358	21.7	1.51	4.5	0.32	24.6	1.71	5.1	0.36	27.9	1.94	6.7	0.46
70	1859	34.1	1.63	34.1	1.63	35.4	1.70	35.4	1.70	36.4	1.75	36.4	1.75
71	2275	51.2	2.06	10.8	0.44	59.0	2.38	16.6	0.67	67.7	2.72	26.3	1.06
72	1726	28.3	1.57	14.2	0.79	33.3	1.85	18.6	1.03	42.4	2.36	19.7	1.09
73	1872	42.4	2.24	9.7	0.51	30.2	1.59	14.1	0.74	34.1	1.80	19.2	1.01
74	1913	60.7	3.12	14.3	0.74	72.1	3.71	13.2	0.68	80.7	4.15	16.3	0.84
75	2066	40.1	1.88	15.0	0.70	55.1	2.59	18.2	0.85	74.1	3.48	22.7	1.07

Table AIII.3 (cont.): Algorithm performance with different exponential weightings (0.2 to 0.4) on the 80 B747-400 take-offs.

Run #	Monitored distance /m	Algorithm prediction error Exponential weighting = 0.20 /m last ¾ dist.	/% last ¾ dist.	/m last ½ dist.	/% last ½ dist.	Exponential weighting = 0.30 /m last ¾ dist.	/% last ¾ dist.	/m last ½ dist.	/% last ½ dist.	Exponential weighting = 0.40 /m last ¾ dist.	/% last ¾ dist.	/m last ½ dist.	/% last ½ dist.
76	1859	17.4	0.91	14.8	0.77	19.1	0.99	19.1	0.99	22.8	1.19	22.8	1.19
77	694	8.6	1.15	8.6	1.15	9.1	1.23	9.1	1.23	9.7	1.31	9.7	1.31
78	2084	30.3	1.35	11.9	0.53	40.9	1.82	13.8	0.61	57.6	2.56	17.3	0.77
79	1970	24.4	1.21	20.7	1.03	34.3	1.71	26.5	1.32	53.8	2.68	31.8	1.58
80	1554	38.4	2.19	34.0	1.94	40.9	2.34	35.5	2.02	45.4	2.59	34.8	1.99
Average		**44.5**	**2.66**	**17.8**	**1.07**	**48.1**	**2.88**	**20.2**	**1.19**	**54.1**	**3.22**	**23.3**	**1.36**
Standard Deviation		**23.6**	**1.18**	**10.5**	**0.55**	**24.6**	**1.24**	**12.0**	**0.59**	**28.4**	**1.43**	**14.3**	**0.66**
99 % confidence		**99.4**	**5.41**	**42.3**	**2.36**	**105.2**	**5.77**	**48.1**	**2.57**	**120.1**	**6.54**	**56.7**	**2.90**
Maximum		**107.5**	**5.47**	**57.8**	**2.69**	**118.0**	**6.31**	**76.7**	**3.01**	**146.1**	**7.81**	**100.8**	**3.95**

Table AIII.3 (cont.): Algorithm performance with different exponential weightings (0.2 to 0.4) on the 80 B747-400 take-offs.

Run #	Monitored distance /m	Algorithm prediction error Exponential weighting = 0.50				Run #	Monitored distance /m	Algorithm prediction error Exponential weighting = 0.50			
		/m last ¾ dist.	/% last ¾ dist.	/m last ½ dist.	/% last ½ dist.			/m last ¾ dist.	/% last ¾ dist.	/m last ½ dist.	/% last ½ dist.
1	1857	182.3	9.75	44.3	2.37	26	1542	40.0	2.54	31.0	1.97
2	1477	27.2	1.76	9.3	0.60	27	1547	43.0	2.75	38.2	2.43
3	1456	41.7	2.80	19.7	1.33	28	1708	84.7	4.81	55.1	3.13
4	1456	41.7	2.79	19.7	1.32	29	1293	78.9	5.53	30.7	2.15
5	1738	155.7	8.71	46.7	2.61	30	1300	62.6	4.60	13.2	0.97
6	590	28.4	4.31	4.4	0.67	31	1749	99.1	5.59	41.6	2.35
7	708	16.0	2.09	8.3	1.09	32	1484	45.4	2.64	7.0	0.41
8	1671	72.8	4.24	18.9	1.10	33	974	46.0	4.50	7.3	0.71
9	1676	42.0	2.43	29.5	1.71	34	1178	80.4	6.55	32.3	2.63
10	1914	56.5	2.86	17.9	0.91	35	1885	70.8	3.71	25.8	1.35
11	1555	41.0	2.38	28.1	1.63	36	1182	39.8	3.16	38.8	3.08
12	1433	50.0	3.34	7.3	0.49	37	1424	42.7	2.92	27.3	1.87
13	1181	32.3	2.70	17.1	1.43	38	1046	49.5	4.66	8.7	0.82
14	995	57.4	5.77	16.8	1.68	39	1937	39.3	2.00	33.0	1.68
15	1976	75.1	3.74	54.4	2.71	40	2157	90.4	3.84	26.1	1.11
16	1576	106.5	6.61	12.1	0.75	41	1788	174.5	9.08	31.7	1.65
17	2009	96.1	4.75	24.1	1.19	42	1458	58.3	3.89	22.1	1.47
18	864	32.7	3.60	13.1	1.44	43	1759	56.6	3.17	56.6	3.17
19	1692	45.6	2.59	45.6	2.59	44	1801	105.9	5.60	37.6	1.99
20	1486	52.4	3.46	32.7	2.16	45	1568	46.3	2.90	42.2	2.64
21	1419	28.0	1.93	7.6	0.53	46	1185	44.6	3.61	25.1	2.03
22	770	30.3	3.70	8.2	1.00	47	1827	77.2	4.14	39.0	2.09
23	712	19.5	2.50	4.2	0.54	48	1241	20.2	1.54	12.7	0.97
24	1708	71.9	4.10	18.4	1.05	49	1621	45.2	2.61	20.8	1.20
25	2140	71.3	3.24	38.9	1.76	50	2097	54.5	2.55	43.1	2.02

Table AIII.4: Algorithm performance with exponential weighting of 0.50 on the 80 B747-400 take-offs.

Run #	Monitored distance /m	Algorithm prediction error Exponential weighting = 0.50 /m last ¾ dist.	/% last ¾ dist.	/m last ½ dist.	/% last ½ dist.	Run #	Monitored distance /m	Algorithm prediction error Exponential weighting = 0.50 /m last ¾ dist.	/% last ¾ dist.	/m last ½ dist.	/% last ½ dist.
51	2000	70.4	3.42	41.1	2.00	66	1779	66.1	3.59	26.8	1.45
52	1611	64.2	3.84	19.2	1.15	67	2248	98.4	4.29	58.6	2.55
53	1801	41.4	2.28	26.3	1.45	68	2105	47.5	2.20	47.5	2.20
54	1217	64.0	4.84	26.4	2.00	69	1358	31.4	2.18	8.4	0.58
55	1615	57.5	3.48	27.9	1.69	70	1859	37.7	1.81	37.7	1.81
56	1784	61.5	3.26	16.7	0.88	71	2275	79.4	3.19	47.0	1.89
57	2366	130.2	5.10	130.2	5.10	72	1726	58.2	3.23	19.7	1.10
58	1916	188.4	9.60	19.6	1.00	73	1872	55.3	2.92	23.9	1.26
59	1848	48.5	2.32	21.9	1.05	74	1913	79.2	4.07	24.9	1.28
60	1416	34.5	2.36	26.6	1.82	75	2066	97.4	4.57	28.0	1.31
61	1519	73.8	4.02	11.1	0.60	76	1859	28.7	1.50	26.0	1.36
62	1078	20.2	1.78	11.9	1.05	77	694	11.1	1.50	10.2	1.38
63	1705	46.6	2.37	30.3	1.54	78	2084	60.7	2.70	22.2	0.98
64	1837	77.8	3.70	20.4	0.97	79	1970	77.7	3.87	36.7	1.83
65	1980	113.9	5.54	30.5	1.48	80	1554	51.1	2.92	40.9	2.34
Average		**63.0**	**3.72**	**27.7**	**1.60**						
Standard Deviation		**35.4**	**1.73**	**17.7**	**0.78**						
99 % confidence		**145.5**	**7.75**	**68.9**	**3.41**						
Maximum		**188.4**	**9.75**	**130.2**	**5.10**						

Table AIII.4 (cont.): Algorithm performance with exponential weighting of 0.50 on the 80 B747-400 take-offs.

Run #	Filename	Weight /lbs	Run time /s	Rotation ground speed /kt	Rotation distance /m	Monitored time /s	Speed @ start of monitor /kt	Monitored distance /m	Time to ¼ dist. /s	Speed @ ¼ dist. /kt	Time to ½ dist. /s	Speed @ ½ dist. /kt
1	doce1	134080	29	163	1354	20	64	1176	7.0	102	12.0	127
2	doce2	124800	26	174	1367	21	57	1261	7.8	104	13.0	134
3	doce3	117440	24	132	967	16	62	796	5.3	87	9.3	105
4	doce4	122880	27	154	1205	21	49	1107	7.8	91	13.0	118
5	doce5	119680	21	129	794	18	32	758	7.0	74	11.5	98
6	doce6	127360	29	154	1312	26	31	1277	10.5	87	16.8	116
7	doce7	118400	28	153	1247	22	47	1153	8.3	91	13.5	117
8	doce8	130240	28	141	1138	24	32	1093	9.5	80	15.3	106
Minimum		**117440**	**21**	**129**	**794**	**16**	**31**	**758**	**5.3**	**74**	**9.3**	**98**
Average		**124360**	**27**	**150**	**1173**	**21**	**47**	**1078**	**7.9**	**90**	**13.0**	**115**
Maximum		**134080**	**29**	**174**	**1367**	**26**	**64**	**1277**	**10.5**	**104**	**16.8**	**134**

Table AIII.5: Run details of the 8 B737-400 take-offs.

Run #	Monitored distance /m	Algorithm prediction error Exponential weighting = 0.50 /m last ¾ dist.	/% last ¾ dist.	/m last ½ dist.	/% last ½ dist.
1	1176	40.5	2.99	7.9	0.58
2	1261	53.9	3.94	3.7	0.27
3	796	19.8	2.05	13.3	1.37
4	1107	21.6	1.79	6.3	0.52
5	758	28.5	3.59	5.3	0.67
6	1277	23.5	1.79	10.6	0.81
7	1153	6.6	0.53	6.2	0.50
8	1093	22.6	1.99	12.6	1.11
Minimum		**27.1**	**2.33**	**8.2**	**0.73**
Standard Deviation		**14.3**	**1.11**	**3.5**	**0.36**
99% confidence		**60.4**	**4.92**	**16.5**	**1.56**
Maximum		**53.9**	**3.9**	**13.3**	**1.4**

Table AIII.6: Algorithm performance with exponential weighting of 0.20 on the 8 B737-400 take-offs.

ANNEX

-

College of Aeronautics Reports

CoA-0010 and CoA-0013

COLLEGE OF AERONAUTICS

CRANFIELD UNIVERSITY

REPORT CoA-0010

\-

DESIGN CONCEPT AND PERFORMANCE STANDARD FOR A TAKE-OFF PERFORMANCE MONITOR DESIGN INTENDED FOR USE ON PART 25 CERTIFIED AIRCRAFT

David Zammit-Mangion
Martin Eshelby
16 May 2000

Cranfield College of Aeronautics

CONTENTS

APPENDIX

LIST OF FIGURES

ABBREVIATIONS

AEO	All engines operative
AFM	Airplane flight manual
AIAA	American Institute of Aeronautics and Astronautics
ASDA	Accelerate-stop distance available
ASDR	Accelerate-stop distance required
ASI	Airspeed indicator
NACA	National Advisory Committee for Aeronautics
NTSB	National Transportation Safety Board
OEI	One engine inoperative
PF	Pilot flying
PNF	Pilot not flying
RAE	Royal Aircraft Establishment
SAE	Society of Automotive Engineers
TODA	Take-off distance available
TODR	Take-off distance required
TORA	Take-off run available
TORR	Take-off run required

NOTATION

D_{crit}	Scheduled distance to V_1
D_1	Actual distance covered to V_1
S_{LO}	Scheduled distance to lift-off
S_{SCREEN}	Scheduled distance to screen height
S_{STOP}	Scheduled accelerate-stop distance
V_R	Rotation speed
V_{LO}	Lift-off speed
V_{SCREEN}	Speed at screen height
V_1	Decision speed
V_2	Climb safety speed

1. BACKGROUND

In order to take-off, an aircraft must accelerate down the runway and achieve an airspeed allowing it to become airborne and climb away over any obstacles. Further to this basic requirement, Part 25 (Group A) certified aircraft must be capable of also successfully completing the take-off manoeuvre[1] if an engine fails at any stage during the run. This effectively requires the run to be rejected if failure is experienced in the early stages at low speed, since the reduced thrust will not be sufficient to allow the aircraft to become airborne within the remaining length of the runway. If, instead, the failure is experienced towards the end of the run, the take-off is continued on the grounds that insufficient runway will be available to bring the aircraft safely to a halt. This implies that the aircraft must have the necessary excess thrust installed in order to ensure that it can still accelerate to the scheduled airspeed and achieve a minimum positive climb once the engine has failed.

The take-off run can therefore be seen to consist of two stages, namely an initial stage during which the run must be aborted if an anomaly is detected, and a final stage in which the run must always be continued (unless the aircraft is clearly not airworthy). The critical point dividing the two stages is identified as the decision speed V_1 (Figure 1).

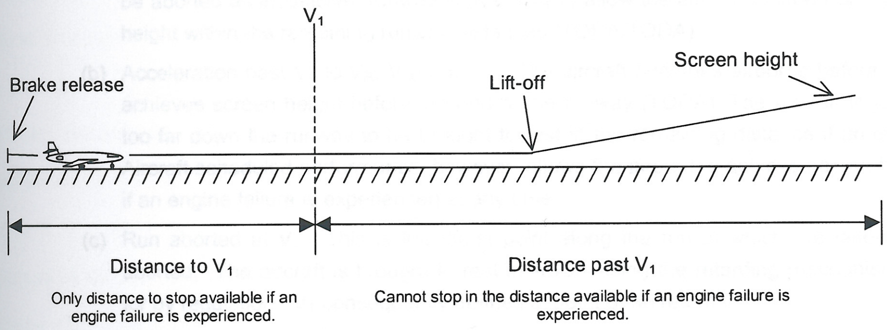

Figure 1: The decision speed V_1 as a point of no return during take-off.

Aircraft take-off performance is often measured in terms of key distances required to reach salient points during the manoeuvre. To this effect the regulations define three distances - the take-off run required (TORR), the take-off distance required (TODR) and the accelerate-stop distance required (ASDR). TORR is the distance from brake release required (or

---

[1] A take-off attempt is in this text defined as successful if the manoeuvre is completed without an accident, and unsuccessful otherwise.

allowed) for the aircraft to lift off the runway, TODR is the distance required to achieve screen height[2], whilst ASDR is the distance required from brake release to bring the aircraft to a halt if the run is aborted at V_1, the latest possible moment (Figure 2). Likewise, airfields are described by the three respective distances available, referred to as TORA, TODA and ASDA respectively. Safety is then assured during take-off by ensuring that the required distances fit within those available.

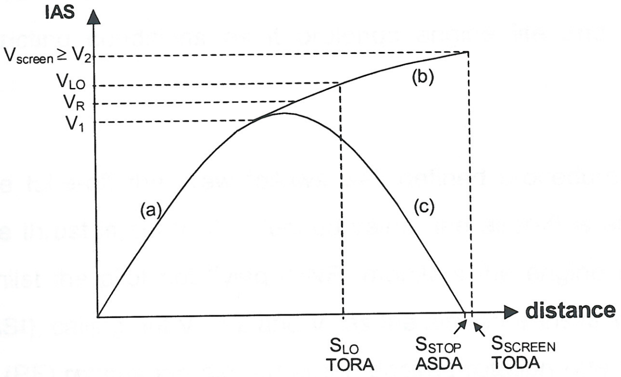

Figure 2: The take-off performance schedule.

(a) Acceleration to V_1, all engines operative (AEO). Sufficient runway is available to bring the aircraft safely to a halt if the run is aborted. In the event of an engine failure the run must be aborted as insufficient runway is available to allow the aircraft to lift-off or reach screen height within the remaining runway distances (TORA/TODA).

(b) Acceleration past V_1 to V_R, V_{LO} and V_2. The aircraft becomes airborne before TORA and achieves screen height before the end of the runway (TODA). The aircraft is too fast and too far down the runway to be brought to rest in the remaining distance if an engine fails. Aircraft scheduled performance, however, allows the aircraft to achieve screen height even if an engine failure is experienced at any time.

(c) Run aborted at V_1. This is the latest point along the run at which the take-off may be aborted. The aircraft is brought to rest in ASDA using the retarding mechanisms allowed for by regulation. V_1 consequently defines a 'point of no return'.

The regulatory bodies require aircraft manufacturers to demonstrate the field performance of an aircraft type by declaring TORR, TODR and ASDR for all operating conditions. The claimed performance must be 'representative of the average new production aeroplane' and has various leeways added to allow for adverse variations in individual aircraft performance, unforeseen changes in operational conditions and even pilot abuse. Furthermore, the general approach is that the aircraft is assumed to be flown by a crew not requiring

---

[2] The screen height is the clearance height above any obstacles, currently 35ft for take-offs from dry runways and 15ft for wet conditions.

'exceptional piloting skill or alertness'[3]. These requirements are detailed in JAR and ACJ 25.101-113 [1].

Aircraft operators are provided with the manufacturer's performance data so that they can ensure that the aircraft is only dispatched if the calculated TODR, TORR and ASDR fit within the field lengths available on the runway from which the take-off is to be made. If excess runway is available, operators can execute the take-off at reduced thrust, thereby effectively increasing the required distances to match those available[4]. This is a common procedure adopted in non-restricting conditions as it prolongs engine life and also favours noise abatement policies.

When attempting the take-off the crew follows well defined procedures that are standard worldwide. Once the thrust is set to the desired value, the aircraft is allowed to accelerate down the runway whilst the pilot not flying (PNF) monitors the engine instruments and the airspeed indicator (ASI), calling out V_1, V_R and V_2 as the aircraft transits the salient airspeeds. At V_R the pilot flying (PF) rotates the aircraft at the desired rotation rate to the target attitude and, as the aircraft unsticks, it climbs out at the predetermined airspeed. This is usually achieved by flying on instruments such as the ASI and Flight Director to control attitude and airspeed. A crucial aspect of the take-off procedure (herein referred to as the V-speed technique) is that whilst monitoring the progress of the run, the crew observe the aircraft's airspeed but have no instrument providing information of the aircraft's position on the runway. As a result, they cannot objectively judge whether the aircraft's performance is within the scheduled threshold - that is, whether the aircraft will lift-off and achieve screen height within the scheduled values of TORR and TODR respectively, or, in the case of a rejected run, whether it is capable of coming to a stop within the calculated ASDA. They only have their intuition and experience to go by and considering the fact that they operate different aircraft in continuously changing operating conditions, detecting subtle under-performance would at best be described as difficult. In any case, such judgement is invariably subjective which, in the authors' opinion, is not satisfactory in critical conditions.

The whole operation involving take-off is effectively an open-loop action, where, once the dispatch conditions are calculated, the aircraft is assumed to perform within particular performance limits and really left at that. It is very possible, therefore, that the aircraft may be under-performing without the crew being aware that they might not be meeting one or more of the runway distance constraints. Due to the significant amount of leeway - particularly that

---

[3] JAR25.105(b).

[4] Provided this is approved by the airplane flight manual (AFM).

of allowing for an engine failure at V_1 when no engine failure is experienced – an aircraft which is under-performing will most likely take-off successfully and this masks the seriousness of the issue. Poor take-off performance may be the result of a variety of shortcomings, including variations in piloting technique, inaccurate weight calculations, mis-set thrust and variations between actual and scheduled ambient temperature, pressure and wind.

Although it is unlikely that poor performance alone will result in an unsuccessful take-off, if an incident is experienced, the attempt is then more likely to result in an accident. Several runway excursions and failed take-offs in which poor performance has been a major contributory factor have in fact occurred, the most well known of which probably being Air Florida's fatal Flight 90 on 13 January 1982. The aircraft took off and, for a number of reasons, stalled and crashed less than a mile from the runway. The NTSB accident report [2] states that the although the aircraft achieved V_1 and the target lift-off speed, it used 5400ft of runway instead of the 3500ft expected of a normal aircraft of the type at the dispatch weight and existing environmental conditions. It also states that the performance was below normal from the beginning of the take-off roll. In these circumstances, it appears that the accident could well have been averted if the crew were informed that the aircraft was under-performing. Such accidents highlight the shortcoming of the V-speed technique and, notwithstanding the fact that concern was noted as early as 1954 [3], no significant changes or improvements have yet been introduced to alleviate the problem.

In the light of this discussion the role of the performance monitor would be to provide objective and timely indication of aircraft performance and whether the take-off attempt is progressing in a satisfactory manner or otherwise, allowing the crew to abort the run early if necessary. The need for such an instrument is becoming all the more relevant as new targets in reducing the accident rate in aviation are being set. The FAA is currently committed towards reducing the US accident rate by 80% from 1996 levels by 2007 [4], clearly in view of the fact that air transport is expected to double in 15 years and the number of accidents occurring per year needs to be kept at an acceptable level. It is generally believed that the industry has largely exhausted current technologies and practices in safety and new approaches need to be implemented. This is an ideal time, therefore, to consider developing a take-off performance monitoring system so that the accident rate at take-off, a statistic that is largely dependent on the outcome of procedures dating from the early post-war years, can be reduced.

2. DESIGN CONCEPT

2.1 Basic principles

The authors acknowledge that the major hurdle that has to be overcome from a system point of view is acceptance by the aviation community, particularly pilots and the regulatory bodies. It is only then that a design will have the potential to be introduced into the flight deck. The two key attributes that are considered crucial in these circumstances are system reliability and value in terms of presenting only that information which is required by the crew in a manner that is convenient and conducive to operational safety.

The V-speed technique is a well-established procedure, the merits of which are virtually unquestioned today. Consequently, the authors believe that introduction of the performance monitor into the flight deck should not introduce new procedures that could conflict with those already in place. Specifically, since the performance monitor's role is to *aid* the crew in controlling the aircraft, procedures to operate the monitor should integrate as well as possible with those currently in place. Considering the previous designs' failure to enter operational service and the resulting general lack of confidence in the concept of performance monitoring, compliance with current procedures is considered a key concept necessary to foster acceptance, particularly within the pilot community. Only when such acceptance is achieved with reliable operation in service should bolder designs, which perhaps require different procedures to be adopted to take advantage of particular improvements, be developed.

It is clear that in these circumstances the services of the take-off performance monitor are required only up to V_1, beyond which the system should be deactivated. Since the fundamental question during take-off is whether sufficient runway is still available for the intended manoeuvre (either continued or aborted run), the authors believe that the best way to consider viability is to forward predict the performance of the aircraft by estimating the *actual* TORR, TODR and ASDR. These estimates would indicate the actual (unfactored) positions on the runway where the aircraft is expected to lift-off, achieve the screen height and come to a halt if the run is aborted at the latest allowable moment (V_1) respectively. The key issues in this approach are the forward prediction and decision to calculate the expected distances required to quantify performance. The merits of the former are discussed in Section 2.2 of this text. The latter is relevant because some previous designs have relied on simple acceleration monitoring to determine the viability of the run. These monitors essentially compared achieved acceleration with a minimum threshold (usually described as a function of airspeed). The main drawback of such an approach is that the leeway indicated does not directly and unequivocally translate to a measure of safety associated with the run. This drawback is highlighted in the critical situation when the acceleration crosses or fluctuates across the threshold performance: it is not directly evident whether the distance criteria will be met (Figure 3). In such circumstances the crew may possibly attempt to decide on the viability of the run by performing a mental integration of the leeway indicated by the indicator. Besides being subjective, such mental processing is undesirable, as during take-off the crew workload is already high. This processing can easily be assigned to a computer instead, allowing the objective determination of the leeway in question. The instrument would then effectively be transformed into a system that measures the leeway in *distance*, further substantiating the authors' view on distance measurement. This does not, nevertheless, mean that acceleration monitoring is not considered useful. In fact, other parities have already declared that acceleration monitoring may be useful as a secondary (cross-check) means of monitoring [5]. The authors further believe that acceleration monitoring can also provide an immediate response to a sudden drop in performance and is therefore certainly of value.

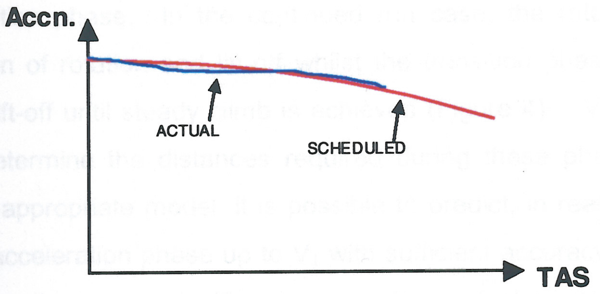

Figure 3: Comparison between actual and scheduled acceleration profiles in a typical marginal case.

It is difficult to translate information presented in this manner into a prediction of whether the aircraft will meet the scheduled distance requirements.

2.2 The scope of forward prediction

Forward prediction of performance, that is, forward predicting the actual distances required, is considered to be a necessary attribute because such a faculty supports the *early* detection and indication of an anomaly. In contrast with non-predictive monitoring, which could take the form, for example, of a comparison of the actual distance covered with that scheduled for the particular airspeed at that instant, predictive monitoring is capable of indicating an anomaly *before* the performance becomes unacceptable. Such early indication is critical in the take-off environment because the leeways and the associated safety margins available rapidly diminish as the run progresses. As the ground speed increases, not only does the rate of distance covered increase, but so does the braking distance required to bring the aircraft to a halt if the run is aborted. It follows, therefore, that quick reaction is of paramount importance. A standard operating procedure of at least one major airline operating wide-bodied aircraft stipulates that a run is to be aborted for any system failure up to 80kts and only for engine failure (or other incident of similar or greater seriousness) at higher speeds. This procedure suggests that aborting a run below 80kts is not considered to be either unduly hazardous or even disruptive to normal operations, highlighting the relevance of providing early warning if poor performance is detected.

2.3 Estimating performance

The take-off is usually segmented into a number of phases for the purposes of performance prediction. The period between brake release and V_R (V_1 in the case of an aborted run) is herein termed the acceleration phase and the braking period in an aborted run is referred to as the deceleration phase. In the continued run case, the rotation phase is the period between initiation of rotation and lift-off whilst the transition phase describes the aircraft's trajectory from lift-off until steady climb is achieved (Figure 4). Various models have been developed to determine the distances required during these phases of flight [6,7,8]. By selection of the appropriate model, it is possible to predict, in real-time, the actual distance required in the acceleration phase up to V_1 with sufficient accuracy. This is largely because during this time, the more significant parameters affecting performance either remain constant or have a known characteristic. This, however, cannot be said of the post-V_1 segments of the run, as the performance in these phases depends on a number of factors that cannot be accurately determined in advance[5]. The distance past V_1 to V_R, for example, is greatly dependent on how close to the target speed the PF initiates the rotation. The point (IAS) at which rotation is initiated can vary significantly between crews. Suffice it to say that at rotation a typical large jet transport aircraft would be travelling at about 150kt and accelerating at about 3kt/s. Consequently, if rotation is initiated 3kt off the scheduled V_R, a distance error of the order of 80m is introduced. The rotation rate and technique play a significant role in the distance covered between V_R and lift-off, as does piloting technique on

---

[5] The literature normally estimates scheduled performance, where allowing for excess leeway is the norm and the use of scheduled values does not conflict with the fact that the relevant parameters cannot be determined with accuracy. This, however, is not the case with the requirements of real-time performance prediction, where accurate distance estimates need to be calculated.

the distance from lift-off to the screen height. Early studies carried out by the Aeronautical Research Council [9] report that a significant scatter in the actual rotation and lift-off speeds and airborne distance to 35ft. was recorded in repeated runs performed by different crews.

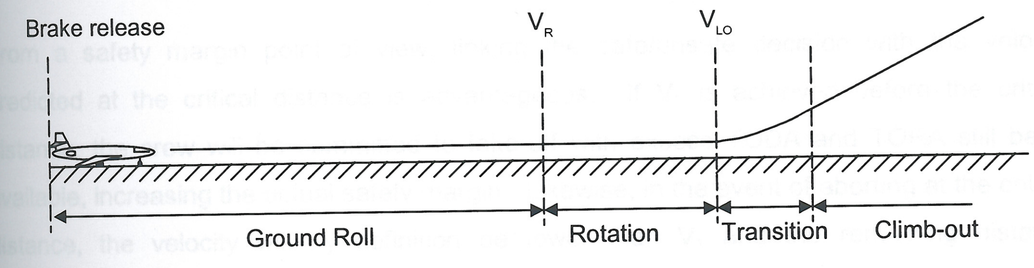

Figure 4: The four phases of take-off for the AEO continued-run case.

Difficulty is also encountered when attempting to calculate the braking distance required in the case of a rejected run. Not only does this greatly depend on crew reaction time to implement maximum braking (which is particularly relevant close to V_1, as the aircraft will be travelling at the highest speed at this moment), but the braking capacity of the aircraft cannot be accurately predicted. There are numerous factors affecting braking, including the temperature and wear condition of the brakes and tyres and, most important, the surface conditions of the runway ahead at the particular time. In fact, it is currently not possible with the technologies available to calculate a braking distance estimate that is meaningful for the purposes of reliable take-off performance monitoring.

In these circumstances, when predicting the TORR, TODR and ASDR, it is best to allow for the scheduled distances provided by the manufacturer for all post-V_1 distance estimates. These estimates have a degree of leeway built into them, inherently increasing the safety margin of the take-off run. Besides, they are the regulated distances legally considered as necessary and sufficient to ensure safety, and use of these distances should not raise objections from operators or the regulatory bodies. Finally, using expected values for parameters that cannot be accurately predicted to estimate performance for the actual run in effect relegates calculations to a simple re-evaluation of scheduled performance, even if no leeways are introduced. These arguments justify reducing the task of the performance monitor to estimating the distance-to-V_1 and then comparing it to its scheduled counterpart, as the predicted and scheduled distances post-V_1 are now by definition equal. Defining the scheduled distance-to-V_1 as the *critical distance*, $D_{crit.}$, the primary role of the monitor would be to predict whether or not V_1 will be achieved within the critical distance and whether there is any indication of the post-V_1 performance falling below its scheduled counterpart. The concept of critical distance effectively defines a point on the runway, and not an indicated airspeed, as the point of no return[6], but this can be kept transparent to the crew, allowing them to still refer to V_1 as the decision point.

From a safety margin point of view, linking the safe/unsafe decision with the velocity predicted at the critical distance is advantageous. If V_1 is achieved before the critical distance, the crew will be committed to take-off with excess TODA and TORA still being available, increasing the actual safety margin. Likewise, in the event of aborting at the critical distance, the velocity will by definition be lower than V_1 and the remaining distance (scheduled as the braking distance from V_1) will not be as critical in allowing the aircraft to be brought to a standstill. Consequently, not only does the concept of using the critical distance, rather than V_1 as the 'decision point' not disrupt the current practice during take-off but it also improves the safety margin.

---

[6] This concept is not original and has been suggested in several previous publications.

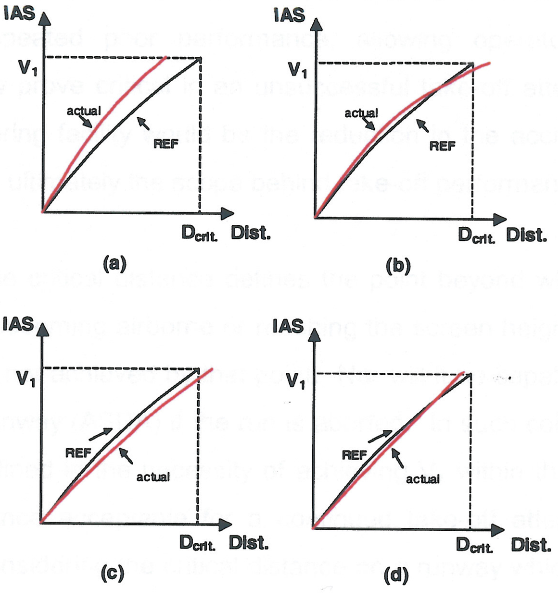

Figure 5: The concept of predicting performance to V_1 - The four possible performance characteristics compared to scheduled performance and associated manoeuvre viability.

(a) Normal situation where performance is superior to regulated (reference line). V_1 is achieved before D_{crit}, adding to the leeway in distance still available. The probability of a successful take-off is therefore higher than that assumed during the pre-dispatch calculations.

(b) Performance superior to regulated in initial stages but poor acceleration in the latter part of the run will not allow V_1 to be reached before D_{crit}. Poor acceleration coupled with a reduction in the distances available post-V_1 seriously jeopardises the probability of a successful take-off. Early prediction is required if the run is to be aborted at low speed.

(c) Performance inferior to regulated throughout run. Result similar to (b).

(d) Initial performance below scheduled but acceleration allows V_1 to be achieved before D_{crit} (eg. rolling take-off). Satisfactory performance increases the probability of successful take-off , similar to (a).

2.4 Aircraft performance limit criterion

It is perhaps easy to perceive the need for a take-off monitor in cases that are constrained by field length. Performance monitoring, however, can also be very useful in runs which are not field limited. In these latter cases it would still be advantageous to provide a warning when something may be amiss, a feature which surely would have been welcome on Air Florida's Flight 90. The identification of poor performance in unrestricting fields will provide the crew with the option to perform a lower risk[7] rejected run instead of taking the problem to the air if so decided. The performance monitor may also prove useful in revealing particular adverse situations such as repeated poor performance, allowing operators to pick up such deficiencies before they prove critical in an unsuccessful take-off attempt. The compound effect of such a monitoring facility would be the reduction in the accident rate experienced during take-off, which is ultimately the scope behind take-off performance monitoring.

In field limited cases the critical distance defines the point beyond which the aircraft is not considered capable of becoming airborne or reaching the screen height within the remaining TORA or TODA if V_1 is not achieved by that point. Nor will it be capable of coming to a halt before the end of the runway (ASDA) if the run is aborted. In such conditions, therefore, the performance limit is defined in the necessity of achieving V_1 within the critical distance and the *minimum performance acceptable* for a continued take-off attempt is the scheduled performance. When considering the critical distance on a runway which is very long and not restricting the operation of the aircraft (i.e. runway lengths are in excess of the minimum required by regulation), however, the question arises of how the critical distance should be defined. Conceptually, it can be defined as the distance to the latest point that will allow a go/abort decision to result in the safe completion of the manoeuvre. In this case, it would be the point calculated backwards from the far end of the runway when considering the distances required to achieve either screen height or bring the aircraft to a halt from V_1 (Figure 6). This definition, however, has a drawback. It would result in the critical distance (D_{crit}) being longer than the scheduled distance-to-V_1 calculated to be sufficient for an aircraft with satisfactory performance. Consequently, it would be possible, in a situation where the aircraft barely meets this extended critical distance requirement whilst performing outside the scheduled limit, for the monitor to suggest that it is safe to continue the run. In such conditions, the leeway allowed from V_1 to the screen height may then be insufficient and clearly this constitutes an unsafe situation.

If, on the other hand the critical point is defined as the distance-to-V_1 as calculated by the scheduled performance from the near end of the runway, the monitor will advise the crew of an unsafe situation if the performance is outside the scheduled limit, even though the excess runway will probably be sufficient to allow the aircraft to become airborne. It is the authors' opinion that although this approach may marginally increase the rejection rate during take-off, it is the correct philosophy to follow, since from a performance point of view the aircraft will not be operating to minimum requirements and taking to the air in such a condition should be

---

[7] Since excess field lengths are available, the prospect of aborting the run constitutes a lower risk when compared to field-limited runs.

considered unsafe. The predictive nature of the instrument, providing early warning of such a situation at relatively low speeds well before V_1, combined with the excess runway available beyond the critical point, warrants a safer option in the rejection of the run.

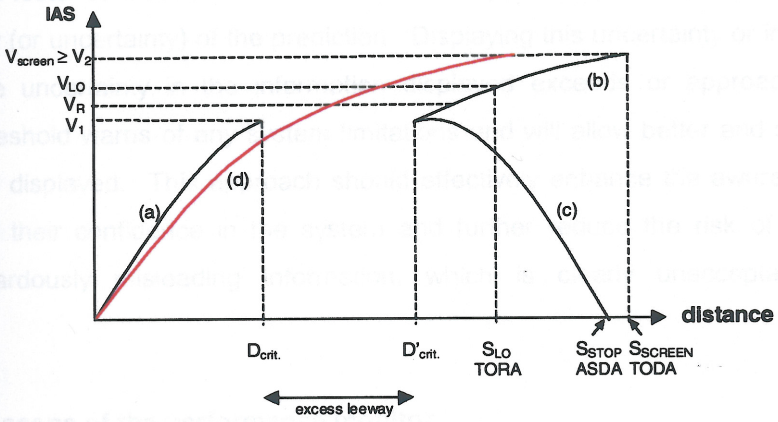

Figure 6: Aircraft performance limit criterion for unrestricting field lengths.

(a) Scheduled performance to V_1, all engines operative (AEO), defines the *critical distance* $D_{crit.}$, as measured from the near end of the runway. Meeting this performance requirement increases the probability of a successful take-off due to the excess leeway available.

(b),(c) Scheduled (minimum performance) distance-to-V_1, $D'_{crit.}$, measured backward from the far end of the runway, taking into account the scheduled post-V_1 distances required. Provided the post-V_1 performance can be met, achieving V_1 at $D_{crit.}$ satisfies current safety criteria.

(d) Defining the critical distance as $D'_{crit.}$ will allow an aircraft with a performance poorer than that acceptable in a field-limited case to take to the air. Since such poor performance may compromise the aircraft's airworthiness, a safe indication is undesirable.

2.5 Algorithm optimisation

In the current V-speed technique, the crew are well trained to identify any discrete anomaly, obvious problem or unsatisfactory engine performance and to then take positive action as appropriate. In this environment the authors believe that the take-off performance monitor would be most useful if it were designed to be sensitive to, and optimised for, the detection of subtle under-performance which is otherwise difficult to detect. In this way, the system would be compensating for the one major shortcoming of the V-speed technique and would also complement the mechanisms that already provide indication of any anomaly on the flight deck.

2.6 Prediction confidence estimate

A degree of uncertainty is associated with any measurement or prediction. Consequently, if the system is to foster confidence in the information it supplies, it should provide an estimate of the accuracy (or uncertainty) of the prediction. Displaying this uncertainty or informing the crew when the uncertainty in the information displayed exceeds or approaches a pre-determined threshold warns of any system limitations and will allow better and safer use of the information displayed. This approach should effectively enhance the awareness of the crew, increase their confidence in the system and further reduce the risk of the system providing hazardously misleading information, which is clearly unacceptable in this application.

2.7 Extended scope of the performance monitor

The ultimate goal of a take-off performance monitor is to ensure safety during the manoeuvre. Besides this obvious advantage, the performance monitor may also offer commercial advantages to operators. By indicating the performance during take-off, less leeway in the scheduled distances may be sufficient to ensure a satisfactory safety record so it would be possible to permit aircraft to take-off at higher dispatch weights whilst maintaining the desired safety targets. In order to provide such benefits, however, the performance monitor will have to have demonstrated sufficient reliability so that no false or misleading information is generated as to result in the unnecessary rejection of take-off runs or, more seriously, lead to the development of a dangerous situation or an accident.

2.8 A closer look at scheduled performance

The TODR and TORR for the all engines operative (AEO) case are calculated by determining the average distances required (referred to as gross performance) and then factoring these values by 15%. The factored performance is then referred to as net performance. Since different aircraft operating under the same conditions are expected to exhibit a normal distribution in performance with a standard deviation in field length of 3% [10], a 15% increase constitutes 5 standard deviations and caters for all but about 1 in 10^7 runs. The one engine inoperative (OEI) continued and aborted run cases are designed to provide the same level of safety despite the fact only the gross performance is allowed for[8]. Although gross performance by definition allows a 50% probability of failure to meet the distance requirements if an engine fails close to V_1, considering the probability of such an event occurring at a critical moment when operating in a field limited runway results in an overall probability of failure of the same order as the AEO case [10]. In this way the risk of accident during take-off is kept to an acceptable level.

When considering the take-off manoeuvre on a run-by-run basis as a performance monitor does, however, the usage of gross and net performance renders the assignment of the critical distance difficult. For the AEO case, the critical distance is the net distance, whilst for the OEI case the gross distance should be considered, resulting in a conflict in the definition of a single critical distance. If the gross value of the critical distance were to be selected, 50% of the AEO cases would theoretically be wrongly indicated as unsafe by the monitor. If the net critical distance were to be selected instead, the OEI case would not be correctly allowed for. In fact, in cases where the aircraft performs worse than the gross scheduled performance but within net performance[9], the monitor would indicate that sufficient leeway is available to either continue or abort the run before V_1. This is incorrect from an OEI performance point of view, because if an engine then fails close to V_1, the probability of the run resulting in an accident becomes significantly higher than 50%.

This dilemma is not specific to the monitor design presented in this report, but is rather related to the V-speed technique and scheduled performance calculations. Consequently, all performance monitors that relate in any way to scheduled performance are faced with this problem. This inconsistency results in a section along the runway, defined between the gross and net critical distances in which neither the continued run, nor the rejection option is viable if an engine fails in this region close to V_1. Although the probability of such an occurrence is low when seen globally, this shortcoming needs to be addressed by the regulatory bodies if the rate of accidents during take-off is to be reduced. Until then the performance monitor will have to consider the AEO (net) performance only and accept the inherent risk related with an engine failure around V_1.

---

[8] Regulations require the scheduled TODR and TORR to be the longer of the AEO (net) and OEI (gross) performances.

[9] By definition, this should occur on nearly 50% of all runs.

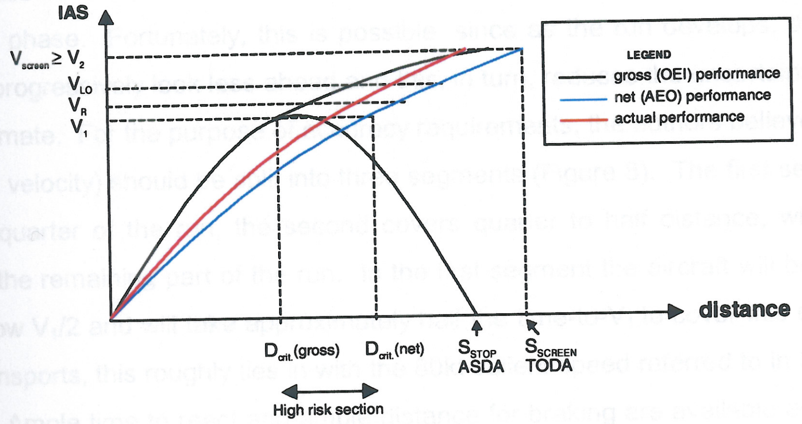

Figure 7: The critical distance in gross and net performance.

The actual performance presented satisfies the AEO case but if an engine failure is experienced near V_1, the probability of either achieving the screen height in TODA or coming to a stop in ASDA is significantly reduced. Under such circumstances, the high-risk section identified in the figure is a zone in which the continued and aborted run options are both not viable if an engine failure is experienced.

3. PERFORMANCE STANDARD

From an operational point of view the reliability of a performance monitor can be considered as a measure of how often the instrument will give false warnings or fail to warn of an unsafe situation when one exists. The effect of such failures ranges from a nuisance in the case of unnecessarily aborting early in the run to catastrophic when the system fails to alert the crew of an unsafe situation and the aircraft fails to become airborne. The occurrence of such failures clearly has to be kept to a very low probability. Since the accuracy of the prediction is considered to be critical in generating correct advisory warnings in marginal conditions, prediction accuracy is directly linked to system reliability. The minimum performance standard for take-off performance monitors, SAE AS-8044 [11], recommends that 'the probability that TOPM system tolerances will, of themselves, cause an error greater than ±5 percent in the apparent all-engine operating take-off distance to rotation speed shall be 0.01 or less'.

The authors, however, are of the opinion that this recommendation does not adequately address the issue of accuracy, nor does it consider the nature of the prediction required. As the aircraft approaches V_1, it will be travelling faster and less time is available for the crew to decide whether to abort the run. Consequently, the crew need greater reassurance that the advice or indication provided by the system is correct as the critical moment approaches. This translates to the prediction accuracy needing to be greater towards the end of the acceleration phase. Fortunately, this is possible, since as the run develops, the monitor is required to progressively look less ahead and this, in turn, reduces the uncertainty associated with the estimate. For the purpose of accuracy requirements, the authors believe that the run to V_1 (target velocity) should be split into three segments (Figure 8). The first segment refers to the first quarter of the run, the second covers quarter to half distance, whilst the third constitutes the remaining part of the run. In the first segment the aircraft will be travelling at speeds below $V_1/2$ and will take approximately half the time-to-V_1 to cover this distance. For large jet transports, this roughly ties in with the 80kt salient speed referred to in Section 2.2 of this report. Ample time to react and ample distance for braking are available and as a result the accuracy of the monitor in this segment is not considered critical, with a basic indication of progress deemed sufficient. In the second segment, the aircraft will achieve approximately $^2/_3V_1$ and by the end of it only a third of the time-to-V_1 will be still available for the initiation of an aborted run. Aircraft speeds are higher, but still well below V_1. As a result, if the crew elect to abort the take-off in this segment, less braking distance than that scheduled at V_1 will be necessary to bring the aircraft to rest. This leeway, together with the addition of more than half the distance-to-V_1 that will also be available for braking, renders the event of aborting a run of relatively minor consequence. In the case of borderline performance, a slightly inaccurate prediction would not jeopardise safety should the crew elect not to abort at this stage. During this segment of the run, therefore, it is considered sufficient to have a monitor prediction accuracy of 6% on 99% of the runs.

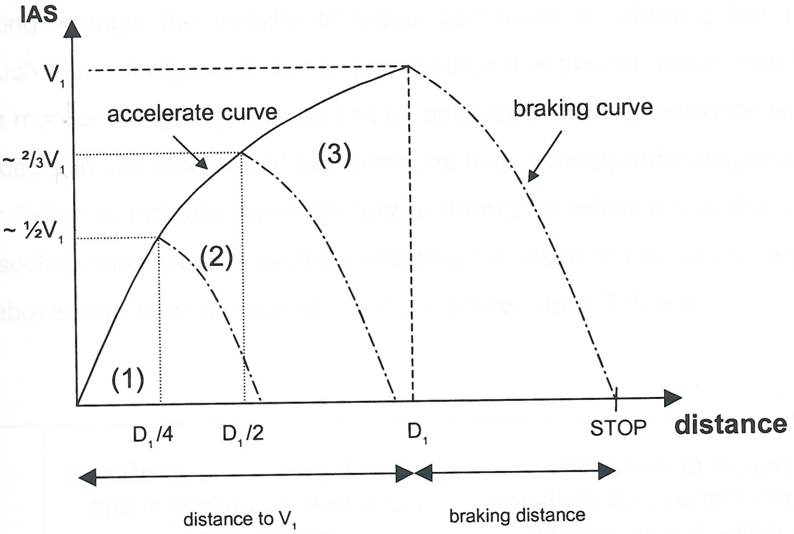

Figure 8: Segmentation of the run-to-V_1 for the purpose of hazard identification.

(1) Run to ¼D_1. Low IAS with ample distance to bring the aircraft to a halt safely. Aborting in this early stage of the run will not result in any significant increase in risk and is very unlikely to disrupt operations.

(2) Run from ¼D_1 to ½D_1. During this stage the aircraft is accelerating to higher speeds but sufficient leeway is still available to render the option of aborting the run a relatively low-risk manoeuvre.

(3) Run from ½D_1 to D_1. The aircraft is fast approaching V_1, rendering the decision to abort critical. Due to the high speed involved, the aircraft will cover this segment of the run in only 1/3 of the time from brake-release to V_1.

The third segment covers the remaining half of the critical distance. During this time, the aircraft will be approaching V_1 and a relatively large distance is covered in just a third of the time-to-V_1. It is at this stage that decisions are most critical and the urgency associated with the decision aggravates the situation further. Besides the fact that the full scheduled braking distance will be required to bring the aircraft to rest in the event of a rejected run, any excess leeway previously available in the unused distance-to-V_1 is quickly being covered. As a result, the decision to abort a run is considered to be relatively hazardous and high precision in performance prediction is mandatory to ensure the crew is not led to hesitate or abort unnecessarily. Furthermore, as the aircraft will be approaching the point of no return, in the case of the continued take-off, the crew must be confident in the monitor's prediction and that the take-off is indeed viable. The authors consequently believe that the accuracy in this phase should be within 3% on 99% of the runs.

The issue of primary concern in this context is the possibility of the monitor misleading the crew by indicating wrongly the viability of either continuing or aborting the run. The occurrence of such a possibility needs to be quantified so that the risk associated with using the performance monitor in flight operations can be assessed. Wrong indication with respect to the go/no-go decision can take one of two forms, namely, wrongly indicating unsatisfactory performance, or failing to indicate unsatisfactory performance when this is the case. The probabilities of such occurrences on systems meeting the prediction accuracy requirements recommended above have been calculated[10] and are presented in Table 1:

Run section	Probability of correctly detecting and indicating unsatisfactory performance (correct alarm)	Probability of indicating unsatisfactory performance when performance is satisfactory (false alarm)
¼ dist. – ½ dist.	57%	2 in 10,000
½ dist. – end	63%	4 in 1 million

Table 1: Performance of monitors meeting the recommended prediction accuracy.

As a higher prediction accuracy than that recommended herein may be difficult to achieve in practice, the success rate of detecting unsatisfactory performance may only be increased at the expense of increasing the probability of false alarm (Appendix I). This would be achieved by reducing the critical distance, which in effect re-defines the threshold of performance in the monitor to correspond to a performance level more stringent than scheduled performance. The performance resulting from such a modification, with the critical distance chosen to correspond with 112% of the gross performance instead of the regulated 115%, is presented in Table 2[11].

---

[10] Refer to the attached appendix for the formal derivation and calculation of the results.

[11] It is relevant to note that the figures in Tables 1 and 2 assume that the probability density functions of both the prediction error and aircraft take-off performance are normal (Gaussian) in nature and independent of each other. The density function of take-off performance may not necessarily be so, particularly in regions pertinent to unsatisfactory performance warranting the rejection of a run. Furthermore, the analysis considers only the 'alarm' function of the monitor, which translates to the indication or otherwise of 'go' and 'abort' signals. Most of the incorrect indications would be expected to be associated with runs having marginal performance, but the analysis takes no account of the effect of displaying marginal performance in analogue format, which would allow the crew to be aware of the case. Such factors would probably result in better monitor performance in the field than predicted in Tables 1 and 2.

Run section	Probability of correctly detecting and indicating unsatisfactory performance (correct alarm)	Probability of indicating unsatisfactory performance when performance is satisfactory (false alarm)
¼ dist. – ½ dist.	88%	2 in 1,000
½ dist. – end	99%	2 in 10,000

Table 2: Monitor performance with a critical distance corresponding to 112% of gross performance.

AS-8044 states that a performance monitor is intended to only provide advisory information to the crew and may not automatically initiate action to abort a take-off. This is in agreement with the design philosophy presented in this text, where the role of the instrument is considered advisory in nature. Three types of performance monitor are also defined, namely Types I, II and III. Type I monitors are those which compare the achieved aircraft performance to its scheduled counterpart. Such monitors do not have any predictive capacity. Type II monitors are defined as those which, apart from providing the comparison and indication of Type I systems, also predict the continued take-off situation (parameters such as location where take-off will be complete, the effect of a critical engine failure, etc.). Type II monitors do not, however, predict stopping distance. Systems with such a predictive capacity are classified as Type III. They perform this prediction on the basis of the current speed and position of the aircraft on the runway, using reported or estimated runway conditions [11]. Using this classification of monitor design, the approach presented in this text can be effectively classified as a Type III because although only the distance-to-V_1 is actually predicted, the TODR, TORR and ASDR are implicitly compared with TODA,TORA and ASDA respectively.

4. DISPLAY REQUIREMENTS

Display considerations are of significant relevance to system design if a performance monitor is to provide useful information and avoid misleading to the crew. It is considered inadequate of a monitor display to provide only a safe/unsafe indication, as this method of indication would fail to give the crew quantitative knowledge of the progress of the run. It would also lack the capacity of providing a warning of any deterioration in performance prior to an unsafe indication being announced. This shortcoming has long been recognised [12] and is endorsed by AS-8044.

The significance of the provision of quantitative information with respect to the progress of the run suggests that the display should have an analogue format. Further information of relevance may also need to be displayed to ensure the crew are provided with the best possible situational awareness. The authors appreciate, however, that providing a complicated display with an extensive suite of parameters is not conducive to safe flight due to the possibility of excessively increasing the pilot workload, particularly in situations of marginal performance. It is consequently believed that only the minimum information pertinent to the progress of the run should be displayed, and the display format should be unambiguous and as simple and easy to read as possible. Only thus would the instrument be capable of *reducing*, rather than increasing, pilot workload in critical situations. Although the amount of information available in the cockpit is continuously increasing, there is a tendency to limit this to a minimum during take-off to ensure avoiding crew overload. In fact, some operators already consider one indication and one confirmation of a relevant fault sufficient to justify a decision to abort the run.

An interesting issue is whether information directly relevant to safety, such as that pertaining to the condition of brakes, tyres, engines and flaps, should be displayed. Apart from the fact that monitoring certain parameters reliably and quantifying their effect on the outcome of the take-off still constitute a major hurdle today, the presentation of such information may prove to be distracting to the crew and consequently counter-productive. It is acknowledged that this subject is debatable and merits further study, but at an introductory level, the authors consider such monitoring and information presentation as counter-productive.

5. SUMMARY

In conclusion, therefore, the salient points of this report can be listed as follows:

1. The scope of the performance monitor is to enhance safety during take-off. Commercial advantages may also be possible by allowing increased take-off weights in operations with take-off performance monitoring.
2. The function of the monitor is to be advisory in nature. Procedures for its use need to integrate seamlessly with the V-speed technique.
3. In view of Point 2 above, the monitor is required to indicate performance only up to V_1, beyond which the crew are committed to the manoeuvre.
4. The system should be optimised to detect subtle under-performance, which is otherwise difficult to detect with current procedures.
5. The system needs to forward predict performance to provide early indication and warning of an impending danger.
6. The preferred way of quantifying performance and viability of take-off is to compare the distance requirements with scheduled performance. Acceleration monitoring may provide a useful secondary (cross-check) source of information.
7. Due to the inaccuracies involved with the prediction of post-V_1 distances, only the distance-to-V_1 need be explicitly determined. Scheduled performance is then allowed for the post-V_1 distances. This reduces the monitoring problem to a comparison between the expected and scheduled distances to V_1. The latter is termed the *critical distance*.
8. High system reliability is necessary to ensure confidence in the indication. For this purpose, the distance to V_1 is divided into three segments, with a recommended maximum prediction error in the latter two of 6% and 3% respectively on 99% of the runs.
9. A measure of the uncertainty associated with the prediction should be calculated by the system.
10. In operations that are not field-limited, the critical distance should correspond to the scheduled (net) performance.
11. A conflict in the definition of critical distance exists when considering the AEO and OEI cases. This needs to be further addressed.

12. The monitor display should be simple and easy to read unambiguously. The go/no-go display as a sole means of indication is considered unsatisfactory and therefore an analogue display of performance would be necessary.

ACKNOWLEDGEMENT:

The authors would like to thank Professor Anton Buhagiar, of the Department of Statistics and Operations Research, University of Malta, for his assistance with the statistical analysis presented herein.

REFERENCES:

[1] Joint Aviation Authorities. *Joint Aviation Requirements JAR 25 - Large Aeroplanes.* Civil Aviation Authority, UK, 1994.

[2] Anonymous. *Aircraft Accident Report. Air Florida Inc. Boeing 737-222, N62AF. Collision with 14th Street Bridge near Washington International Airport, Washington, D.C., January 13, 1982.* NTSB report no. NTSB-AAR-82-8, 1982.

[3] Morris G J and Lina L J. *Description and preliminary flight investigation of an instrument for detecting subnormal acceleration during take-off.* NACA Technical Note TN-3252, 1954.

[4] http://www.faa.gov/safetyinfo2.htm as on 15/5/00.

[5] Small J T. *Feasibility of using longitudinal acceleration (N_x) for monitoring takeoff and stopping performance from the cockpit.* Proc. 27th Symposium of the society of Experimental Test Pilots, CA, 1983, pp. 143-155.

[6] Anonymous. *Jet Transport Performance Methods.* Boeing Flight Operations Engineering, 1989.

[7] Ojha S K. *Flight performance of aircraft.* AIAA Education Series, AIAA, 1995. ISBN 1-56347-113-2.

[8] Mair W A and Birdsall D L. *Aircraft performance.* Cambridge University Press, 1992. ISBN 0-521-56836-6.

[9] O'leary C O, Cannell J N and Maltby R L. *Take-off tests on a transport aircraft including the use of a 'SCAT' take-off director.* Aeronautical Research Council R&M 3508, 1968.

[10] Stinton D. *Flying qualities and flight testing of the aeroplane.* Blackwell Science Ltd. 1996. ISBN 0-632-02121-7.

[11] Anonymous. *Takeoff performance monitor (TOPM) system, airplane, minimum performance standard for.* SAE, Aerospace Standard AS-8044, 1987.

[12] Hoekstra H D. *Take-off safety indicator.* US Patent no. 2,922,892. 1960.

APPENDIX

-

DERIVATION AND CALCULATION OF THE PROBABILIES OF THE GENERATION OF A FALSE ALARM AND THE FAILURE TO GENERATE AN ALARM

The performance of an aircraft for known operating conditions is usually modelled by a normal distribution with an average defined by the gross performance and a standard deviation of 3%. Let this distribution be defined as $F_p(x) = N(\mu_p, \sigma_p)$.

A measurement or prediction can also be assumed to have a normal distribution of error. Assuming no bias, the density function of the error would be $N(0, \sigma_m)$.

In the field of take-off performance monitoring, the performance prediction of any particular run with performance x_i would therefore have a probability density function that is normally distributed, herein defined as $F_m(x) = N(x_i, \sigma_m)$. Refer to Figure A1.

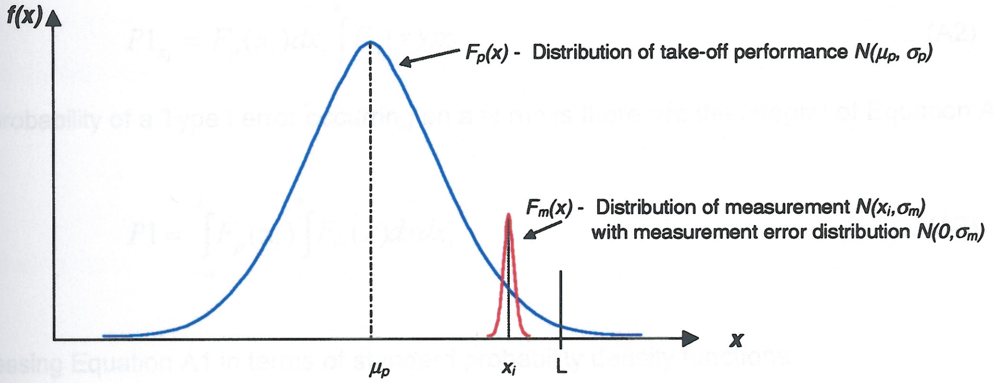

Figure A1: The probability density function of the prediction error superimposed on that of take-off performance.

$F_p(x)$ is the normal distribution of performance in terms of the target distance x.
$F_m(x)$ is the normal distribution of the monitor prediction on a run with actual performance x_i.
x_i is the actual target distance of the run being monitored.
L is the limit of allowable performance (scheduled performance).

The issue of interest in this context is the determination of the probability of the system generating a false alarm and the probability it of failing to generate an alarm with respect to the go/no-go decision. Although the display as proposed in this report would have an analogue format, these probabilities are of significant interest and need to be quantified.

The generation of a false alarm is often referred to as a Type I error, whilst the failure to generate an alarm is referred to as a Type II error.

Generation of a false alarm - Type I Error

The probability of a Type I error is the probability that the performance is satisfactory with the instrument indicating otherwise. Consequently, this is the probability that x_i is less than L (Figure A1) and, simultaneously, the monitor prediction $(x_i+\delta_i)$ is greater than L, where δ_i is the prediction error.

Mathematically, this probability, herein defined as *P1*, is given by:

$$P1 = P\{(x_i < L)|(x_i + \delta_i > L)\} = P\{(x_i < L) and (\delta_i > L - x_i)\} \quad \text{... (A1)}$$

The probability that a run will have a particular performance x_i and, simultaneously, experience a Type I error is given by:

$$P1_{x_i} = F_p(x_i)dx_i \int_L^{\infty} F_m(x)dx \quad \text{... (A2)}$$

The probability of a Type I error occurring on any run is therefore the integral of Equation A2:

$$P1 = \int_{-\infty}^{L} F_p(x_i) \int_L^{\infty} F_m(x)dxdx_i \quad \text{... (A3)}$$

Expressing Equation A1 in terms of standard probability density functions:

$$P1 = P\left\{\left(\frac{x_i - \mu_p}{\sigma_p} < \frac{L - \mu_p}{\sigma_p}\right) and \left(\frac{\delta_i - \mu_m}{\sigma_m} > \frac{L - x_i - \mu_m}{\sigma_m}\right)\right\} \quad \text{... (A4)}$$

where μ_m, the average measurement error, is, by definition, zero. The standard units are defined by Equations A5:

$z_1=(x_i-\mu_p)/\sigma_p$ ... (A5a)

and $z_2=(\delta_i)/\sigma_m,$ ... (A5b)

Then: $$P1 = P\{(z_1 < K1) and (z_2 > K2.(K1 - z_1))\} \quad \text{... (A6)}$$

where $K1 = (L-\mu_p)/\sigma_p$ ... (A7a)

$K2 = \sigma_p/\sigma_m$ ... (A7b)

$$\Rightarrow \quad P1 = \int_{-\infty}^{K1} f(z_1) \int_{K2.(K1-z_1)}^{\infty} f(z_2) dz_2 dz_1 \qquad \ldots \text{(A8)}$$

$K2$ also defines the ratio (σ_1/σ_2), the ratio of the standard deviations of z_1 and z_2.

CASE I - Probability of a Type I error in the last ¾ of the run

The performance standard developed in this work recommends that the maximum prediction error during the last ¾ distance to target velocity be 6% of the target distance on 99% of the runs. This error implicitly refers to $2.3\sigma_m$. The take-off runs most likely to result in a Type I error are those in which the actual target distance covered is close to that corresponding to threshold (net) performance L. Consequently, the performance requirement can be adequately expressed by Equation A9:

$$2.3\sigma_m \approx 0.06xL = 0.06x1.15\mu_p \qquad \ldots \text{(A9)}$$

Considering that σ_p=$0.03\mu_p$,

$$\frac{\sigma_p}{\sigma_m} \approx 1 \qquad \ldots \text{(A10)}$$

and $K1 = 5$ … (A11a)

$K2 = 1$ … (A11b)

Referring to Equations A6 and A8, $P1$ can thus be expressed as:

$$P1 = P\{(z_1 < 5) and (z_2 > 5 - z_1)\} = \int_{-\infty}^{5} f(z_1) \int_{(5-z_1)}^{\infty} f(z_2) dz_2 dz_1 \qquad \ldots \text{(A12)}$$

Using BMDP statistical software, the value of $P1$ is calculated to be:

$$P1 = 2.03 \times 10^{-4}$$

This implies that only about 2 in 10,000 of all runs will be incorrectly identified as unsatisfactory in the last ¾ of the run.

CASE II - Probability of a Type I error in the last ½ of the run

The performance standard developed in this work recommends that the maximum prediction error during the last ½ distance to target velocity be 3% of the target distance on 99% of the runs. Following the arguments in Case I, this performance requirement can be expressed by Equation A13:

$$2.3\sigma_m \approx 0.03xL = 0.03x1.15\mu_p \qquad \text{... (A13)}$$

$$\Rightarrow \qquad \frac{\sigma_p}{\sigma_m} \approx 2 \qquad \text{... (A14)}$$

with $K1 = 5$ ... (A15a)

$K2 = 2$ ... (A15b)

P1 is then expressed as:

$$P1 = P\{(z_1 < 5) and (z_2 > 10 - 2z_1)\} = \int_{-\infty}^{5} f(z_1) \int_{2.(5-z_1)}^{\infty} f(z_2) dz_2 dz_1 \qquad \text{... (A16)}$$

Using BMDP statistical software, the value of *P1* is calculated at:

$$P1 = 3.69x10^{-6} \qquad \text{(A17)}$$

This implies that less than 4 in 1 million runs are expected to be incorrectly identified as unsatisfactory in the second half of the run.

Missed alarm - Type II Error

The probability of a Type II error is the probability that the performance is unsatisfactory with the instrument indicating otherwise. Consequently, this is the probability that x_i is greater than L and, simultaneously, the prediction $(x_i+\delta_i)$ is less than L:

$$P2 = \{(x_i > L) and (\delta_i < L - x_i)\} \qquad \text{... (A18)}$$

The probability of a Type II error occurring is therefore also given by:

$$P2 = \int_{L}^{\infty} F_p(x_i) \int_{-\infty}^{L} F_m(x) dx dx_i \qquad \text{... (A19)}$$

Expressing Equation A18 in the standard form:

$$P2 = P\{(z_1 > K1) and (z_2 < K2.(K1 - z_1))\} \qquad \text{... (A20)}$$

$$\Rightarrow \qquad P2 = \int_{K1}^{\infty} f(z_1) \int_{-\infty}^{K2.(K1-z_1)} f(z_2) dz_2 dz_1 \qquad \text{... (A21)}$$

CASE I - Probability of a Type II error in the last ¾ of the run

As in the case for Type I errors, the take-off runs most likely to result in a Type II error are those in which the actual distance requirement is close to the threshold (net) performance L. As a result, *K1* and *K2* assume the same values:

K1 = 5 ... (A22a)
K2 = 1 ... (A22b)

P2 can then be expressed as:

$$P2 = P\{(z_1 > 5) and (z_2 < 5 - z_1)\} = \int_{5}^{\infty} f(z_1) \int_{-\infty}^{(5-z_1)} f(z_2) dz_2 dz_1 \qquad \text{... (A23)}$$

With BMDP statistical software, the value of *P2* is found to be:

$$P2 = 1.23\text{x}10^{-7}$$

Since the probability of a run having unsatisfactory performance is expected to be 2.87x10^{-7} ($P\{x_i > 5\sigma_p\}$), about 57% of all runs with unsatisfactory performance will be correctly identified as such within ¼ distane gone[A1].

CASE II - Probability of a Type II error in the last ½ of the run

P2 is, in this case, expressed as:

$$P2 = P\{(z_1 > 5) and (z_2 < 10 - 2z_1)\} = \int_{L}^{\infty} f(z_1) \int_{-\infty}^{2.(5-z_1)} f(z_2) dz_2 dz_1 \qquad \text{... (A24)}$$

Therefore, $P2 = 1.05\text{x}10^{-7}$

This implies that more than 63% of all runs with unsatisfactory performance should be correctly identified as such within ½ distane gone.

[A1] Most of the remaining 43% that will be wrongly identified as satisfactory will have marginally unsatisfactory performance.

Trading missed poor performance for false alarms

It is immediately evident that in an environment where a monitoring system is susceptible to error, the probability of occurrence of one type of error can be reduced at the expense of the increased occurrence for the other[12].

In effect, this is achieved by adjusting the threshold of acceptable performance on the monitor. This implies that if, for example, it is considered necessary to improve the detection rate of unsatisfactory performance, the monitor will have to be modified generate an alarm when the performance *approaches* the threshold limit. This creates a greater confidence that an unfavourable situation will not go unnoticed, but clearly it also increases the false alarm rate.

Defining the new threshold of performance as L_2 (differing from the limit of scheduled performance L) results in a modification of the equations describing the probability of occurrence of Type I and Type II errors. The probability of a Type I error is now the probability that x_i is less than L and, simultaneously, the prediction $(x_i+\delta_i)$ is greater than L_2:

$$P1' = \{(x_i < L) and (\delta_i > L_2 - x_i)\} \qquad \text{… (A25)}$$

In terms of the standard form of the functions:

$$P1' = P\{(z_1 < K1) and (z_2 > K2.(K3 - z_1))\} = \int_{-\infty}^{K1} f(z_1) \int_{K2.(K3-Z_1)}^{\infty} f(z_2) dz_2 dz_1$$

… (A26)

where: $K3 = (L_2-\mu_p)/\sigma_p$ … (A27)

Likewise,

$$P2' = \{(x_i > L) and (\delta_i < L_2 - x_i)\} \qquad \text{… (A28)}$$

$$\Rightarrow \quad P2' = P\{(z_1 > K1) and (z_2 < K2.(K3 - z_1))\} = \int_{K1}^{\infty} f(z_1) \int_{-\infty}^{K2.(K3-Z_1)} f(z_2) dz_2 dz_1$$

… (A29)

---

[12] This trade-off is described by the Operating Characteristic that is unique for the application.

PREDICTION ERROR WITH PERFORMANCE THRESHOLD AT 1.12μ_P (μ_p+4σ_p)

The probability of erroneous indication with a monitor performance threshold set at 1.12μ_p is given below:

Type I error, ¼ distance gone:

$$P1'_{0.25D_1} = P\{(z_1 < 5)and(z_2 > (4-z_1))\} = \int_{-\infty}^{5} f(z_1) \int_{(4-z_1)}^{\infty} f(z_2) dz_2 dz_1$$

... (A30)

Type I error, ½ distance gone:

$$P1'_{0.5D_1} = P\{(z_1 < 5)and(z_2 > 2.(4-z_1))\} = \int_{-\infty}^{5} f(z_1) \int_{2.(4-z_1)}^{\infty} f(z_2) dz_2 dz_1$$

... (A31)

Type II error, ¼ distance gone:

$$P2'_{0.25D_1} = P\{(z_1 > 5)and(z_2 < (4-z_1))\} = \int_{5}^{\infty} f(z_1) \int_{-\infty}^{(4-z_1)} f(z_2) dz_2 dz_1$$

... (A32)

Type II error, ½ distance gone:

$$P2'_{0.25D_1} = P\{(z_1 > 5)and(z_2 < 2.(4-z_1))\} = \int_{5}^{\infty} f(z_1) \int_{-\infty}^{2.(4-z_1)} f(z_2) dz_2 dz_1$$

... (A33)

The values of the above probabilities are presented in Table A1:

Dist. gone	$L_2 = L = 5\sigma_p$ (115% gross perf.)		$L_2 = 4\sigma_p$ (112% gross perf.)	
	Type I error	Type II error	Type I error	Type II error
¼ dist. gone	2.03×10^{-4}	0.428	2.34×10^{-3}	0.121
½ dist. gone	3.69×10^{-6}	0.367	1.73×10^{-4}	0.0116

Table A1: Expected probabilities of Type I and Type II errors with performance threshold set at 115% and 112% of gross performance.

COLLEGE OF AERONAUTICS

CRANFIELD UNIVERSITY

REPORT CoA-0013

-

AN INVESTIGATION OF THE SUITABILITY OF USING CURVE-FITTING TECHNIQUES TO PREDICT TAKE-OFF DISTANCE

David Zammit-Mangion
27 July 2000

Cranfield College of
Aeronautics

CONTENTS

LIST OF FIGURES

LIST OF TABLES

ABBREVIATIONS

AEO	All engines operative
AIAA	American Institute of Aeronautics and Astronautics
ASDA	Accelerate-stop distance available
ASDR	Accelerate-stop distance required
ASI	Airspeed indicator
GPS	Global positioning system
IAS	Indicated airspeed
OEI	One engine inoperative
IRS	Inertial referencing system
NASA	National Aeronautics and Space Administration
NFLC	National Flying Laboratory Centre (College of Aeronautics, Cranfield University)
PNF	Pilot not flying
SAE	Society of Automotive Engineers
TAS	True airspeed
TODA	Take-off distance available
TODR	Take-off distance required
TORA	Take-off run available
TORR	Take-off run required

LIST OF SYMBOLS

a	Longitudinal acceleration
A, B, C	Coefficient constants
C_D	Coefficient of drag
C_L	Coefficient of lift
D	Drag
D_1	Distance-to-V_1
D_{LO}	Distance to lift-off
D_{SCREEN}	Distance to screen height
D_{STOP}	Accelerate-stop distance
G	*Constant*
J, K, L	Coefficient constants
k_1, k_2	Constants
m	Mass
M, N	2nd order polynomial roots
S	Wing reference area
T	Thrust, time
T_1	Time to V_1
v_w	Wind speed
V	True airspeed, velocity
V_g	Ground speed
V_{LO}	Lift-off speed
V_R	Rotation speed
V_{SCREEN}	Speed at screen height
V_1	Decision speed
V_2	Take-off safety speed
W	Weight
μ	Coefficient of rolling friction
θ	Runway slope
ρ	Air density

1. INTRODUCTION

The ultimate scope of the take-off manoeuvre is to achieve the target airspeed within the available runway length, thereby allowing the aircraft to become airborne and fly out of the airfield above any obstacles. Consequently, aircraft take-off performance is usually expressed in terms of the velocity achieved as a function of distance run along the runway (Figure 1). Prior to dispatching the aircraft, the operators ensure that the performance will be adequate for the runway in use with the scheduled operating and environmental conditions. This is done by limiting, if necessary, the maximum weight at which the aircraft is dispatched. It follows that the performance must then be monitored by the crew during the take-off run to confirm that the progress is as expected and that the aircraft will, in fact, become airborne within the runway constraints. Current procedures, however, do not help the crew develop an objective picture of the situation. Although the PNF monitors the airspeed, the crew have no objective notion of how far down the runway they are, how far they should have been, or, indeed, where the aircraft will become airborne and achieve the screen height. Such knowledge is clearly essential in the assessment of performance and in determining whether the actual aircraft's TODR and TORR fit the runway's TODA and TORA[1]. In the absence of any instrumentation providing this information, the crew can only judge the aircraft's progress visually by monitoring the acceleration perceptually or by checking the engine gauges to ensure that the scheduled thrust is actually available. This renders any resulting judgement subjective, particularly since crews usually fly different aircraft in different operating conditions.

The difficulty in assessing the progress of the take-off run is a serious shortcoming from the point of view of the crew's role of monitoring the aircraft. Once the aircraft is dispatched with the assumption that it will perform sufficiently well to meet the runway constraints, the crew's role is largely reduced to simply executing a well-rehearsed manoeuvre, monitoring mainly engine health and aircraft systems. In effect, this reduces the take-off manoeuvre to an open loop system from a performance point of view. Although V_1 is used to identify the point beyond which the run should not be aborted if an engine failure occurs, the decision-speed criterion is only valid if this salient airspeed is not achieved too far down the runway. The whole take-off procedure consequently relies on the assumption of good performance up to that point and conceptually this needs to be confirmed by the crew during the take-off run.

---

[1] Before V_1 the crew also need to know where the aircraft will come to rest if the run is aborted and thus need to compare the actual ASDR with ASDA.

The role of the take-off performance monitor is to cover the current shortcomings by providing objective information regarding the progress of the take-off run to the crew.

A consideration of paramount importance during the design phase is system reliability. As is the case for most aircraft monitoring systems, the instrument will only be expected to warn of an impending danger on rare occasions during operations[2]. On such occasions it must avoid failing to warn of the existence of an impending danger or anomalous situation. The system must also avoid wrongly generating a false warning when no danger exists. In order to achieve this, the instrument usually needs to be at least an order of magnitude more reliable than the system being monitored. This can only be achieved with accurate measurement of the parameters being monitored and the correct selection and design of algorithm so that actual aircraft performance can be estimated with the required precision.

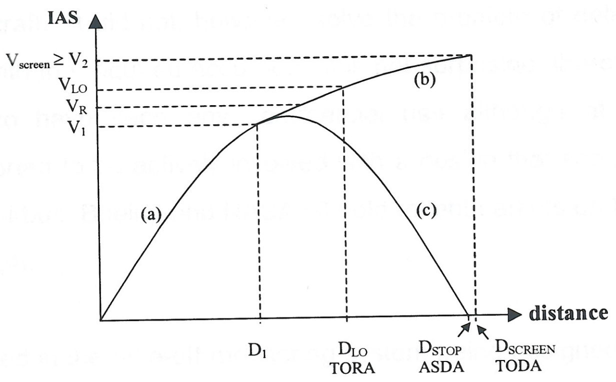

Figure 1: Minimum take-off performance schedule.

(a) Acceleration to V_1, all engines operative (AEO). Sufficient runway is available to bring the aircraft safely to a halt if the run is aborted. In the event of an engine failure the run must be aborted as insufficient runway is available to allow the aircraft to lift off or reach screen height within the remaining runway distances (TORA/TODA).

(b) Acceleration past V_1 to V_R, V_{LO} and V_2. The aircraft becomes airborne before TORA and achieves screen height before the end of the runway (TODA). The aircraft is too fast and too far down the runway to be brought to rest in the remaining distance if an engine fails. Aircraft scheduled performance, however, allows the aircraft to achieve screen height even if an engine failure is experienced at any time.

(c) Run aborted at V_1. This is the latest point along the run at which the take-off may be aborted. The aircraft is brought to rest in ASDA using the retarding mechanisms allowed for by regulation. V_1 consequently defines a 'point of no return'.

---

[2] The good safety record in aviation translates to a low probability of malfunction and as a result it can be expected that a monitoring system would be called upon to warn of any danger only on rare occasions.

The accurate determination of the *actual* [3] TODR, TORR and ASDR during the run has always been a difficult task. This is not only because of the difficulty in measuring the relevant parameters with the required accuracy, but also because of the number of variables which cannot, with the current technology available, be determined in advance. This includes variables such as the time that will be *actually* required by the crew to react to an engine failure, the strength of a wind gust that will be encountered further along the runway and the *actual* braking capacity[4] in the event of a rejected take-off. Faced with this difficulty, various design methodologies have emerged in an attempt to develop a successful instrument. Most of the earlier designs tended to monitor acceleration as a measure of performance and did not explicitly calculate the distances required during take-off. The introduction of powerful digital computers, however, has rendered feasible the modelling of the aircraft as a point mass and the development of algorithms solving the equations of motion to determine (predict) the distances required. The use of such detailed modelling has probably greatly increased the accuracy of the predictions due to the capability of accurately determining the behaviour of the aircraft. It did not, however, solve the problem of determining the several critical parameters with the required accuracy. It is not surprising, therefore, that no monitor to date is known to have seen any commercial use although at least one airframe manufacturer is reported to be actively involved with a design that should be flight tested in the near future [1]. Airbus, Boeing and NASA all hold recent patents on take-off performance monitor designs [2,3,4].

The approach adopted in the take-off monitoring system being designed by the author at the College of Aeronautics focuses on the prediction of the distance required to V_1. The reasons for this approach are presented in a prior technical report [5]. During this phase, the pitch of the aircraft relative to its direction of motion remains largely invariant and the more significant parameters affecting performance either remain constant or have a known characteristic. This greatly facilitates the accurate prediction of the distance to the target velocity. When calculating the distance to V_1 or V_R, most of the previous designs have relied on the instantaneous measurement of the relevant parameters of interest and standard or assumed (scheduled) values for those variables that cannot be determined at the time of calculation. The accuracy of any calculation is consequently restricted by the uncertainty associated with the values used. The author believes that greater accuracy can be achieved if the required information is instead extracted from a section or complete history of the actual run. In this

---

[3] TORR, TODR and ASDR are correctly defined as scheduled distances required and have several leeways built into the estimates. The *actual* TORR, TODR and ASDR are in this text defined as the *actual* distances, from brake release, required to lift-off, achieve the screen height, or come to a halt if the run is aborted from V_1. No leeways are included.

[4] The actual braking capacity depends not only on the efficiency of the brakes, but also on the status of the aircraft tyres and the runway surface in the section on which wheel brakes will be applied.

way, parameter values are less likely to be affected by instantaneous spurious errors and therefore the prediction can be calculated with better accuracy. Furthermore, the past history of the run is a shadow of what is to be expected provided that the situation is invariant [6]. This is precisely the case when monitoring the performance to V_1, provided no discrete incident such as an engine failure or severe gust is encountered further down the runway. The author's approach should consequently be well suited for the early detection of subtle under-performance that could be otherwise difficult to detect by the crew. This is a major objective of the system being designed, as the crew are already well supported to identify a discrete and significant anomaly such as an engine failure. A performance monitor with the described features would consequently be able to complement the present knowledge and awareness of the crew [7].

In the light that it is good engineering practice to keep algorithms as simple as possible whilst providing the required accuracy, a novel approach has been adopted in the design of the take-off performance monitoring algorithm. Rather than reverse-model the past history of the current run to extract the various parameters for use in the same equations of motion, a study has been carried out to investigate whether curve-fitting techniques would be appropriate to predict aircraft performance. The curve would be fitted to the run history and then extrapolated to the target velocity (V_1). Provided a good fit is obtained, the fitted curve should implicitly contain all the information of the various parameters controlling the take-off run, rendering their explicit calculation unnecessary. If, then, the various parameters remain unchanged or at least their differentials do not have any discontinuities, the extrapolated curve should provide a good prediction of the performance of the aircraft. The obvious approach for curve-fitting techniques in these circumstances is the method of least squares, where instrumentation errors are averaged out to zero. Ideally, the function in question would be derived from theory and then fitted on the data collected during the take-off run. This would ensure that the error due to inadequate modelling is very small. This report presents the findings of an investigation of the suitability of such an approach.

2. THE EQUATIONS OF MOTION

For the purpose of calculating the distance to V_1, the aircraft is usually modelled as a point mass exposed to linear forces (Figure 2).

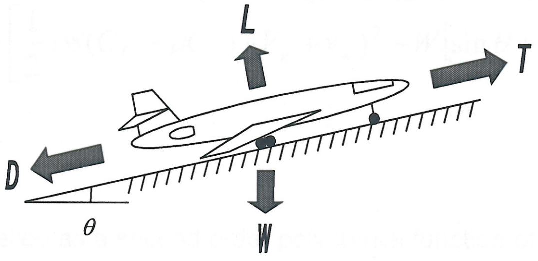

Figure 2: The forces acting on the point mass model of the aircraft during take-off.

Resolving along the runway:

$$T - D - W\sin\theta = ma \qquad \text{... (1)}$$

The total drag *D* comprises the aerodynamic drag and rolling friction:

$$D = \frac{1}{2}\rho V^2 S C_D + \mu(W\cos\theta - \frac{1}{2}\rho V^2 S C_L) \qquad \text{... (2)}$$

The true air speed (TAS) *V* differs from the ground speed V_g by the longitudinal component of the wind velocity v_w:

$$V = V_g + v_w \qquad \text{... (3)}$$

The acceleration is therefore expressed, in terms of ground speed, as:

$$a(V_g) = \frac{T - \left[\frac{1}{2}\rho S(C_D - \mu C_L)\right](V_g + v_w)^2 - W[\sin\theta + \mu\cos\theta]}{m} \qquad \text{... (4)}$$

This equation is integrated to obtain the distance to V_1:

$$D_1 = \int_0^{V_1-V_W} \frac{mV_g}{T - \left[\frac{1}{2}\rho S(C_D - \mu C_L)\right](V_g + v_w)^2 - W[\sin\theta + \mu\cos\theta]} dV_g \qquad \ldots (5)$$

The thrust can be modelled as a second order polynomial function of airspeed:

$$T = A(V_g + v_w)^2 + B(V_g + v_w) + C \qquad \ldots (6)$$

For the purpose of calculation, v_w has to be assumed constant because it cannot be presented as a function of the take-off run progress. Following mathematical manipulation, Equation 5 can then be presented as a function of V_g:

$$D_1 = \int_0^{V_1-V_W} \frac{mV_g}{J(V_g)^2 + K(V_g) + L} dV_g \qquad \ldots (7)$$

where:

$J = A - \frac{1}{2}\rho S(C_D - \mu C_L)$ ... (8)

$K = 2Av_w + B - v_w\rho S(C_D - \mu C_L)$ ... (9)

$L = Av_w^2 + Bv_w + C - \frac{1}{2}v_w\rho S(C_D - \mu C_L) - W(\sin\theta + \mu\cos\theta)$ ... (10)

J, *K* and *L* are constants provided the thrust characteristic does not change (no change in thrust setting, ambient temperature and pressure during the run) and the aircraft attitude remains the same. The weight, rolling friction coefficient and runway slope are also assumed to be constant.

The denominator of Equation 5 is the square polynomial which describes the acceleration profile as a function of the ground speed. Since the acceleration of large transport aircraft (Part 25 certified or equivalent) is known to drop as the aircraft accelerates down the runway (Figure 3), the square polynomial must have real roots, one being positive and one negative. Also, the second order coefficient must be negative.

The roots of the denominator in Equation 7 are likewise expected to be real, with one root being positive, the other negative, and the second order coefficient negative. This is ensured because when transforming the expression *a(V)* to *a(V_g)* the wind speeds will be very small compared to the roots of the polynomial, ensuring that the general attirbutes of the characteristic remain unchanged.

Equation 7 can thus be expressed as:

$$D_1 = \int_{0}^{V_1 - V_W} \frac{V_g}{G(V_g - M)(V_g - N)} dV_g \qquad \dots (11)$$

where M is the positive root, N the negative root and G=J/m.

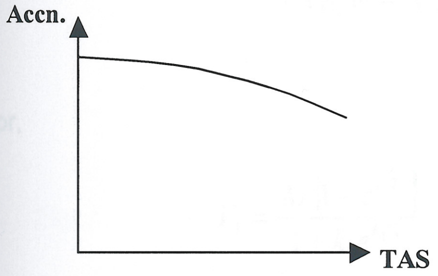

Figure 3: The acceleration profile during the take-off run to V_1.

Curve-fitting to a second order polynomial would result in a function with real roots and a negative second order coefficient.

The definite integral is then given by:

$$D_1 = \frac{1}{G(M-N)} \left[\left\{ M \ln(M - V_g) - N \ln(V_g - N) \right\} \right]_{V_g = 0}^{V_g = V_1 - v_w} \qquad \dots (12)$$

This results in the solution:

$$D_1 = \frac{1}{G(M-N)} \left\{ M \ln\left[\frac{M - (V_1 - v_w)}{M} \right] - N \ln\left[\frac{(V_1 - v_w) - N}{-N} \right] \right\} \qquad \dots (13)$$

If the thrust is modelled as a third order polynomial function, then the denominator of Equation 7 would be a third order function, resulting in a solution for D_1 which is similar in format to Equation 13, but with a third logarithmic expression. The only assumption required to ensure this formulation would be that the third order polynomial would have three real roots.

If the solution of $V_g(t)$ is desired, this can be obtained by integrating Equation 4 with respect to time:

$$Time-to-V_1 = \int_0^{V_1-V_W} \frac{m}{T-\left[\frac{1}{2}\rho S(C_D-\mu C_L)\right](V_g+v_w)^2-W\left[\sin\theta+\mu\cos\theta\right]}\,dV_g$$

... (14)

Using the same concept to solve the integral as that used in the calculation of D_1, the Time-to-V_1 is expressed as:

$$Time-to-V_1 = \frac{1}{G(M-N)}\left\{\ln\left[\frac{M-(V_1-v_w)}{M}\right]-\ln\left[\frac{(V_1-v_w)-N}{-N}\right]\right\}$$

... (15)

or,

$$V_1 = \frac{M\left\{1-e^{k_1T_1}\right\}}{1+k_2e^{k_1T_1}}$$

... (16)

where: T_1 is the time-to-V_1

$k_1 = G(M-N)$

$k_2 = -M/N$

3. BASIC REQUIREMENTS FOR CURVE-FITTING

Attempting to curve-fit Equation 13, 15 or 16 on relevant data during the run is not a straightforward issue due to the relative complexity in the algebra involved. In these circumstances it may be more advantageous to attempt to rely on curvi-linear regression instead, provided a good fit is obtained on the performance profile of choice. Since the profiles of interest are not linear, second or higher order polynomial fitting would be necessary[5]. Curve-fitting polynomials of orders higher than 2, however, can pose problems when extrapolating, as these may quickly depart from the actual performance profile and thus fail to adequately model the aircraft over the complete range of interest. This effect is caused by the high order roots which would be optimised for best-fit in the range over which the data is sampled and strictly no consideration is given to future data. In these circumstances, use of a second

---

[5] The theoretical functions in question describing the motion of the aircraft during the ground run are monotonic in nature. It can therefore be expected that a Taylor series may adequately describe the function of interest, the order of which would depend on the actual profile and the accuracy required.

order fit is probably the most appropriate because the resulting polynomial would have a relatively controlled curviture within the window of interest (Figure 4).

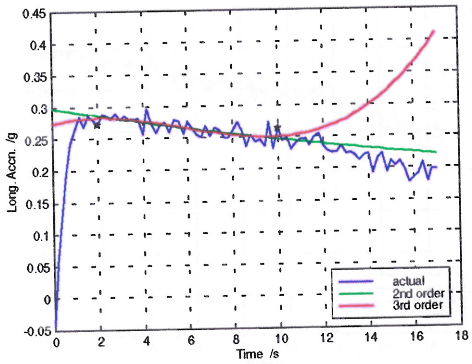

Figure 4: Acceleration profile of the Jetstream-100.

5Hz sampling rate with 2nd order and 3rd order polynomials fit in the 2s-10s window and extrapolated to target time. The 3rd order fit is inappropriate for prediction purposes as the fitted curve departs the actual characteristic when extrapolated.

A good model inherently requires a good fit. The quality of fit can be conveniently measured through regression analysis, but the modelling qualities (the capability of the fitted polynomial to match the developing characteristic) cannot be measured by such techniques. Fortunately, under normal, steady take-off conditions the expected take-off distances should not change along the run. This implies that successive fits should not result in different polynomial coefficients in a good model. This attribute conveniently provides a means of appraisal of the modelling qualities of the polynomial.

Several issues and considerations affect the quality of fit. Effects such as signal noise and discontinuities in the developing characteristic can cause significant changes in the coefficients between fits. These are clearly detrimental to the prediction accuracy, as exemplified in Figure 5. Correct selection of sampling rate is also of relevance. Whilst a larger data sample population ensures that random measurement errors are efficiently cancelled out, there seems to be a limit in the extent that the population size affects fit accuracy, with too high a sampling rate providing no evident advantage. Care must also be taken if the data is to be filtered. Whilst it is advantageous to filter out random error (noise), care must be taken to ensure that any change in the signal due to an anomaly in the actual characteristic is not inadvertently also filtered out. This would lead to signal degradation and would compromise the ability of the algorithm to detect and respond to the anomaly.

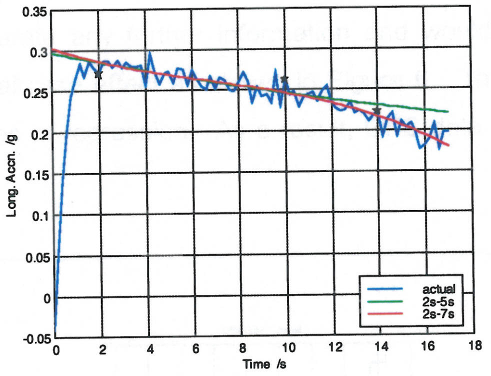

Figure 5: 2nd order fit on an acceleration profile of the Jetstream-100, 5Hz sampling rate. As the run progresses, the fit predicts a different acceleration, rendering it unsuitable for performance prediction purposes.

All the above considerations necessitate the careful selection of the performance profile on which regression is to be carried out. Consequently, this study has been directed towards determining which characteristic, if any, would adequately approximate a quadratic equation within the expected operational envelope, so that extrapolation would result in the early and correct prediction of the takeoff distance required.

4. DATA SET SELECTION

In the analysis of aircraft performance during take-off, the parameters of relevance are acceleration, velocity, position and time. One of the major requirements originally set out in the rationale of this study was to only make use of data from systems or sources that are widely used on today's existing aircraft fleets. This effectively restricted the range of data considered to that supplied by the air data computer, IRS and GPS.

4.1 GPS data

GPS data is generally updated every second, and this is clearly too slow for use in the dynamic environment of the take-off run as not enough data points would be collected to ensure a good fit. Attempting to sample the data at a higher frequency than 1Hz is futile since this would not generate any further information and would only result in the over-sampling, generating a staircase effect as shown in Figure 6. This feature is certainly not favourable for the purposes of regression. As a result, GPS data has not been considered for selection.

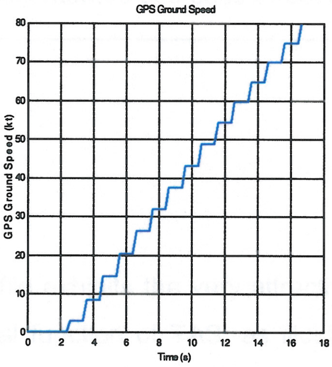

Figure 6: Graph of GPS ground speed data, showing how over-sampling results in the staircase effect that is detrimental to curve-fitting.

4.2 IRS data

4.2.1 IRS positional data

IRS longitude and latitude on the LTN-90 have an update rate of 8Hz and a resolution of 0.000172° when transmitted in binary format [8]. With 1° of latitude constituting 60nm (111.12km), this resolution translates to approximately 19m in the North-South direction. This is inadequate, not only because of the large quantisation error involved, but also because it reduces the number of samples possible in the early stages of the run if the staircase effect is to be avoided. This latter restriction limits the accuracy of fit (or alternatively delays the achievement of the desired accuracy) at a time when the curve-fitting process is attempting to provide the first estimates of the take-off run required. Such an effect is clearly undesirable and therefore IRS positional data was not considered any further.

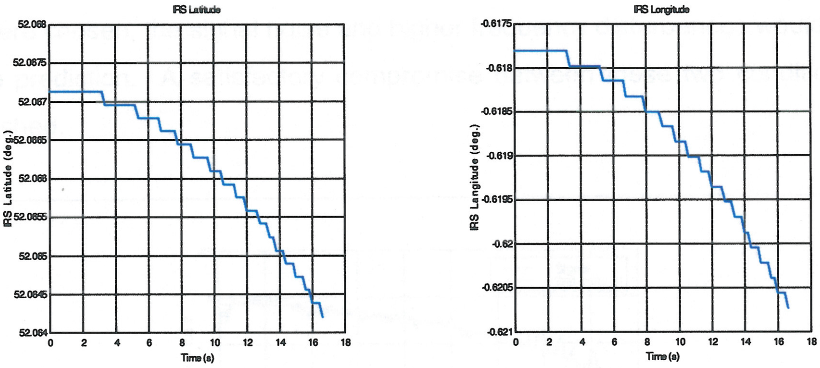

(a) (b)

Figure 7: Graph showing IRS longitude and latitude signals during a ground run, highlighting the accentuated staircase effect at the beginning of the run.

4.2.2 IRS acceleration profile

The longitudinal acceleration profile exhibits the very attractive feature that it is theoretically defined as a 2nd order polynomial function of TAS, as illustrated by Equation 4. Figure 8 confirms the theoretical model, with a very good 2nd order fit obtained for the whole run. On further observation, however, it is evident that any attempt to fit segments of the run and extrapolating to the target velocity would result in different polynomials, a difficulty discussed in Section 3 of this text and illustrated in Figure 5. This is caused by the fact that the acceleration profile is very sensitive to performance change, with slight disturbances producing large rates of change of acceleration. Whilst such a characteristic favours the quick detection of an anomaly, it is susceptible to erroneous predictions on the extrapolation of a least-squares fit.

Another disadvantage is that longitudinal acceleration is relatively noisy. Although the regression technique adopted averages out noise disturbances, the addition of a new data point to the regression can significantly affect the fit which, when extrapolated, would effectively result in the amplification of the noise signal. A way round this problem could be the filtering[6] of either the acceleration signal or the result derived from the curve fit, but this does not seem to offer any improvements to the fit quality or prediction accuracy. Choosing a cut-off frequency as low as 0.05Hz does smooth the characteristic nicely, but any significant aircraft disturbances with a low frequency component would then also be filtered

---

[6] The LTN-90 manual suggests the use of a second order Butterworth filter or equivalent.

out or partially degraded. If, on the other hand, a higher cut-off frequency such as 0.2Hz (Figure 9) were chosen, the signal noise and higher frequency disturbances would be allowed to affect the prediction. A satisfactory compromise between these two conditions has not been established.

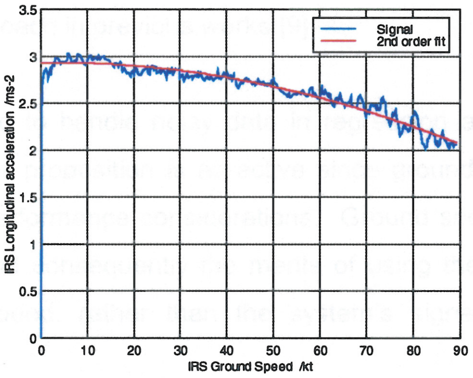

Figure 8: Graph showing IRS longitudinal acceleration vs. IRS Ground Speed and second order polynomial curve fit.

The acceleration value has been adjusted to compensate for the gravitational vector due to the platform's inclination (gsinθ) and the curve is fitted between 7kt and 90kt.

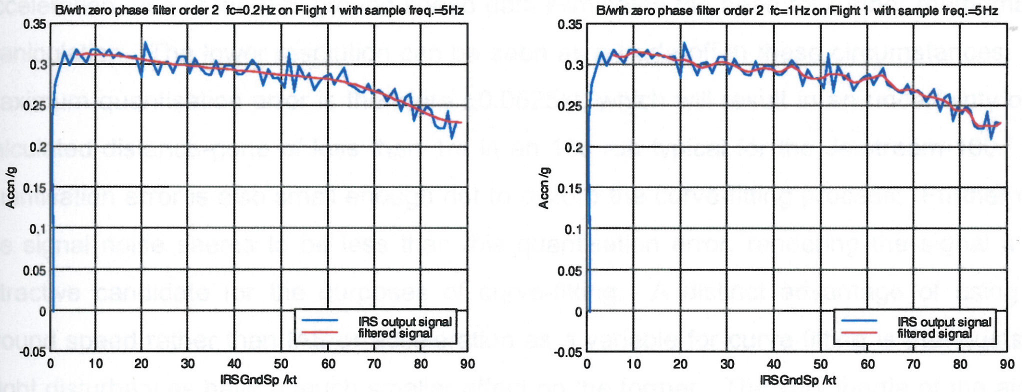

(a)

(b)

Figure 9: 0.2Hz and 1Hz filtering of acceleration data.

These arguments by no means imply that acceleration data may not prove to be useful in take-off performance monitoring. The quick response of the signal to performance change, the very characteristic which is detrimental to curve-fitting, in fact renders the concept of non-predictive monitoring of acceleration very attractive as a secondary facility to provide immediate indication of any anomaly. When compared to acceleration monitoring, curve-fitting techniques would be slow to respond to a discrete anomaly and consequently the former may provide convenient complementary means with which to monitor performance. The use of acceleration monitoring as a *secondary* monitoring means has been already suggested as a viable approach in previous works [9].

A standard technique used to handle noisy data in regression analysis is to curve fit the *integral* of the signal. This proposition is attractive since ground speed is a parameter of great interest in take-off performance considerations. Ground speed is in any case directly available from the IRS, and consequently the merits of using the acceleration signal as a source for the ground speed, rather than the system's signal output, have not been investigated.

4.2.3 IRS Ground Speed

With IRS and GPS positional information considered inadequate for the purposes of take-off performance monitoring, IRS Ground Speed offers a convenient alternative to determine the distance travelled and the distance-to-go. The LTN-90 ground speed signal has a sensitivity of 0.125kt, and although higher resolution may be achieved by integrating the longitudinal acceleration, use of the IRS ground speed data eliminates the need for further mathematical manipulation. The lower resolution can be seen as a trade-off in these circumstances. The maximum quantisation error is therefore ±0.0625kt, which will result in an uncertainty of the calculated distance-gone of less than 1m in an 18s run typical for the Jetstream-100. This quantisation error is also small enough not to disturb the curve-fitting process. Furthermore, the signal noise seems to be less than this quantisation error, rendering the signal a very attractive candidate for the purposes of curve-fitting. A distinct advantage of using IRS ground speed rather than IAS or acceleration as a variable for curve-fitting is that gusts and slight disturbances have a much smaller effect on the former. The very inertia of the aircraft actually smoothes out disturbances in ground speed and facilitates the curve-fitting technique.

4.3 IAS

As V_1 and V_R are indicated airspeeds, it would perhaps seem obvious to select IAS as one of the monitored parameters. In practice, however, the use of IAS presents two major difficulties, namely:

- The pitot-static system, which constitutes the package sensing IAS, is not sensitive at low airspeeds. The air data system on the Jetstream indicates 0kt IAS for low speeds and becomes accurate at about 45kt. The Jetstream will achieve 45kt after about 8s in a typical takeoff run, and clearly this is too late to start collecting data for real-time prediction purposes (Figure 10).

- Gusty wind conditions show up as fluctuations on the ASI. Although such fluctuations will average out to zero in the long term when using curve-fitting techniques, they can cause misleading variations in the real-time prediction of the take-off distance required.

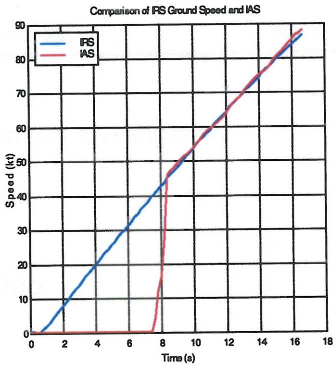

Figure 10: Traces of the IRS ground speed and IAS during a typical ground run.

5. CHARACTERISTIC SELECTION

Following the arguments of Section 4, IRS ground speed was used as the fundamental source of data from which the relevant performance profile would then be constructed. Timing was available from the on-board computers, allowing the integration of the signal to obtain the distance-gone. The three parameters (time, ground speed and distance gone) can be paired up in a number of combinations for the purposes of performance monitoring. The remainder of this work was consequently concentrated on the investigation of which characteristic might be best suited for the scope of curve-fitting and performance prediction.

Experimental data for use on this investigation was collected on four different runs on the NFLC's Jetstream-100 G-NFLC. All runs were continued AEO take-offs, conducted on Cranfield's runway 22 and initiated with brake release following application of full power. Conditions on all runs were good, with low surface winds. Sample rates varied from 5Hz to 20Hz. Data was acquired and processed using the NFLC's in-house developed software and then transferred to MATLAB® format prior to analysis on the software package.

Run	Date	Sample rate	Run to target speed
1	04/02/1998	5Hz	391.0m / 17.0s
2	10/02/1998	20Hz	371.5m / 16.2s
3	09/11/1998	10Hz	386.1m / 17.2s
4	12/11/1998	20Hz	448.0m / 17.5s

Table 1: The data runs used in this investigation.

5.1 Velocity-distance relationship

5.1.1 S vs. V characteristic

The velocity-distance profile is often approximated to a square function[7] in performance calculations [10,11]. This suggests that a second order polynomial might adequately fit the data and therefore could be used to predict the distance to V_1. The results obtained are presented in Table 2 and in graphical form in Appendix I.

---

[7] The distance is proportional to the square of the velocity if the acceleration is assumed constant.

Run	Error in estimate /m (% tot. dist.) (+ve = over-estimate)		Error in estimate /m (% tot. dist.) (+ve = over-estimate)		
	¼ dist. gone	½ dist. gone	8s to go	6s to go	4s to go
1	-29.7 (-7.6%)	-22.6 (-5.8%)	-29.7 (-7.6%)	-25.6 (-6.6%)	-19.0 (-4.9%)
2	-30.3 (-8.2%)	-23.0 (-6.2%)	-30.3 (-8.2%)	-27.9 (-7.5%)	-20.1 (-5.4%)
3	-34.1 (-8.8%)	-22.9 (-5.9%)	-34.1 (-8.8%)	-27.9 (-7.2%)	-19.4 (-5.0%)
4	-41.0 (-9.2%)	-26.6 (-5.9%)	-37.2 (-8.3%)	-29.4 (-6.6%)	-21.8 (-4.9%)

Table 2: Performance of 2nd order polynomial fit to S vs. V characteristic.

The graphs in Appendix I indicate that the fitted curve tends to 'lag' behind the developing actual profile and that it is not capable of producing sufficient curvature. As a result, the algorithm underestimates the distance required, and this is exhibited in Figures A.I(c)-(d). Indeed, this might be expected since a square fit assumes constant acceleration throughout the run, whilst this drops as the run develops. This effectively results in the actual characteristic having a steeper curve than would be described by the fitted polynomial.

5.1.2 S vs. V^2 characteristic

Since 3rd and higher order polynomials were being avoided in this work, a 2nd order polynomial was fitted to the S vs. V^2 characteristic in an attempt to eliminate the problem of the lack of curvature expressed in Section 5.1.1. The S vs. V^2 characteristic should be approximately linear. Any non-linearity due to the drop in acceleration could perhaps be described adequately by the second order coefficient of the polynomial fit. The results obtained are presented in Table 3 and Appendix II.

Run	Error in estimate /m (% tot. dist.) (+ve = over-estimate)		Error in estimate /m (% tot. dist.) (+ve = over-estimate)		
	¼ dist. gone	½ dist. gone	8s to go	6s to go	4s to go
1	-12.8 (-3.3%)	-10.6 (-2.7%)	-12.8 (-3.2%)	-11.8 (-3.0%)	-8.5 (-2.2%)
2	-17.4 (-4.7%)	-12.1 (-3.3%)	-17.4 (-4.7%)	-17.2 (-4.6%)	-9.9 (-2.7%)
3	-15.0 (-3.9%)	-8.2 (-2.1%)	-15.0 (-3.9%)	-10.9 (-2.8%)	-6.6 (-1.7%)
4	-19.6 (-4.4%)	-10.7 (-2.4%)	-16.7 (-3.7%)	-11.2 (-2.5%)	-10.7 (-2.4%)

Table 3: Performance of 2^{nd} order polynomial fit to the S vs. V^2 characteristic.

These results fail to indicate any significant improvement over those of Section 5.1.1 (Table 2 and Appendix I). This could have been due to the fact that a polynomial of the form Ax^2+Bx+C describing the function $s(v^2)$ would only involve the coefficients of the first three *even* orders of the function $s(v)$. In order to also express the *odd* orders, the polynomial describing $s(v^2)$ would have to be of the form: $Ax^2+Bx^{3/2}+Cx+Dx^{1/2}+E$. The normal equations describing the least square fit of this polynomial are presented in matrix form in Equation 17:

$$\begin{bmatrix} E \\ D \\ C \\ B \\ A \end{bmatrix} = \begin{bmatrix} n & \sum x^{1/2} & \sum x & \sum x^{3/2} & \sum x^2 \\ \sum x^{1/2} & \sum x & \sum x^{3/2} & \sum x^2 & \sum x^{5/2} \\ \sum x & \sum x^{3/2} & \sum x^2 & \sum x^{5/2} & \sum x^3 \\ \sum x^{3/2} & \sum x^2 & \sum x^{5/2} & \sum x^3 & \sum x^{7/2} \\ \sum x^2 & \sum x^{5/2} & \sum x^3 & \sum x^{7/2} & \sum x^4 \end{bmatrix}^{-1} \begin{bmatrix} \sum y \\ \sum x^{1/2} y \\ \sum x\, y \\ \sum x^{3/2} y \\ \sum x^2 y \end{bmatrix} \qquad \ldots (17)$$

The performance of the fit described above is presented in Table 4 and Appendix III. These results indicate that the inclusion of the added coefficients did not improve prediction accuracy.

Run	Error in estimate /m (% tot. dist.) (+ve = over-estimate)		Error in estimate /m (% tot. dist.) (+ve = over-estimate)		
	¼ dist. gone	½ dist. gone	8s to go	6s to go	4s to go
1	-22.7 (-5.8%)	-17.1 (-4.4%)	-22.7 (-5.8%)	-19.4 (-5.0%)	-14.2 (-3.6%)
2	-22.2 (-6.0%)	-17.7 (-4.8%)	-22.2 (-6.0%)	-21.8 (-5.9%)	-15.4 (-4.2%)
3	-27.9 (-7.2%)	-16.7 (-4.3%)	-27.9 (-7.2%)	-21.4 (-5.5%)	-13.9 (-3.6%)
4	-25.6 (-5.7%)	-18.5 (-4.1%)	-24.7 (-5.5%)	-20.3 (-4.53%)	-15.9 (-3.5%)

Table 4: Performance of $(Av^2+Bv^{3/2}+Cv+Dv^{1/2}+E)$ fitted to the S vs. V^2 characteristic.

5.1.3 V^2 vs. S characteristic

Curve-fitting was also attempted on the inverse function of S vs. V^2. The results obtained are presented in Table 5 and Appendix IV.

Run	Error in estimate /m (% tot. dist.) (+ve = over-estimate)		Error in estimate /m (% tot. dist.) (+ve = over-estimate)		
	¼ dist. gone	½ dist. gone	8s to go	6s to go	4s to go
1	-8.8 (-2.3%)	-7.5 (-1.9%)	-8.8 (-2.3%)	-8.2 (-2.1%)	-5.5 (-1.4%)
2	-14.9 (-4.0%)	-9.1 (-2.5%)	-14.9 (-4.0%)	-14.9 (-4.0%)	-6.9 (-1.8%)
3	-9.6 (-2.5%)	-3.4 (-0.9%)	-9.6 (-2.5%)	-5.3 (-1.4%)	-3.4 (-0.9%)
4	-13.1 (-2.1%)	-7.0 (-1.6%)	-9.9 (-2.2%)	-7.0 (-1.6%)	-7.0 (-1.6%)

Table 5: Performance of 2nd order polynomial fit to the V^2 vs. S characteristic.

5.1.4 V vs. S characteristic

The V vs. S characteristic did not fit a 2^{nd} order polynomial over the complete run (Figure 11) and was therefore not considered any further.

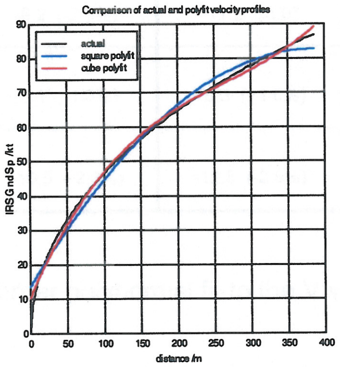

Figure 11: Failure of fit on V vs. S characteristic.

5.1.5 V vs. log(S) characteristic

An alternative way of reducing the curvature of the V vs. S graph can be reduced by plotting V vs. log(S). On this occasion, a third order polynomial was found to produce the best fits and, perhaps surprisingly, remained well behaved throughout the run.

Run	Error in estimate /m (% tot. dist.) (+ve = over-estimate)		Error in estimate /m (% tot. dist.) (+ve = over-estimate)		
	¼ dist. gone	½ dist. gone	8s to go	6s to go	4s to go
1	+13.0 (+3.3%)	-5.8 (-1.5%)	+12.0 (+3.1%)	-5.8 (-1.5%)	-5.8 (-1.5%)
2	-11.2 (-3.0%)	-9.2 (-2.5%)	-11.2 (-3.0)	-11.2 (-3.0)	-8.6 (-2.3%)
3	+10.3 (-2.7%)	-5.1 (-1.3%)	+6.3 (+1.6%)	-5.1 (-1.3%)	-5.1 (-1.3%)
4	-14.5 (-3.2%)	-10.5 (-2.3%)	-12.5 (-2.8%)	-10.5 (-2.3%)	-10.5 (-2.3%)

Table 6: Performance of 3rd order polynomial fit to the V vs. log(S) characteristic.

5.2 Velocity-Time relationship

5.2.1 V vs. T characteristic

Equation 16, which describes the velocity-time profile, is theoretically non-linear. However, this characteristic is, in practice, fairly linear over the period of interest (up to V_1). This suggests that the profile could possibly be successfully described by a 2nd order polynomial. Curvi-linear regression did, in fact, result in a good fit, but, as was the case in other good fits, it failed to adequately express the drop in acceleration as the run progresses. The results are presented in Table 7 and Appendix VI.

Run	Error in estimate /m (% tot. dist.) (+ve = over-estimate)		Error in estimate /m (% tot. dist.) (+ve = over-estimate)		
	¼ dist. gone	½ dist. gone	8s to go	6s to go	4s to go
1	-15.0 (-3.9%)	-13.9 (-3.6%)	-15.0 (-3.8%)	-14.8 (-3.8%)	-11.9 (-3.0%)
2	-19.3 (-5.2%)	-15.9 (-4.3%)	-19.3 (-5.2%)	-19.3 (-5.2%)	-13.8 (-3.7%)
3	-20.4 (-5.3%)	-13.5 (-3.5%)	-20.4 (-5.3%)	-17.1 (-4.4%)	-11.2 (-2.9%)
4	-25.6 (-5.7%)	-15.8 (-3.5%)	-23.6 (-5.3%)	-17.8 (-4.0%)	-13.7 (-3.1%)

Table 7: Performance of 2nd order polynomial fit to the V vs. T characteristic.

5.2.2 T vs. V characteristic

The results obtained by using the T vs. V characteristic for the 2nd order polynomial fit are presented in Table 8 and Appendix VII. The performance is very similar to that of the V vs. T fit, with the algorithm being incapable of compensating for the drop in acceleration in the latter parts of the run.

Run	Error in estimate /m (% tot. dist.) (+ve = over-estimate)		Error in estimate /m (% tot. dist.) (+ve = over-estimate)		
	¼ dist. gone	½ dist. gone	8s to go	6s to go	4s to go
1	-17.7 (-4.5%)	-15.9 (-4.1%)	-17.7 (-4.5%)	-17.1 (-4.4%)	-13.7 (-3.5%)
2	-20.8 (-5.6%)	-17.4 (-4.7%)	-20.8 (-5.6%)	-20.8 (-5.6%)	-15.4 (-4.1%)
3	-23.0 (-6.0%)	-16.0 (-4.1%)	-23.0 (-6.0%)	-19.6 (-5.1%)	-13.7 (-3.5%)
4	-28.5 (-6.4%)	-18.9 (-4.2%)	-26.5 (-5.9%)	-20.9 (-4.7%)	-16.0 (-3.6%)

Table 8: Performance of 2nd order polynomial fit to the T vs. V characteristic.

6. DISCUSSION

All the characteristics studied, except for V vs. S, exhibited mainly similar performance characteristics. Good fits have been achieved on the complete run, indicating that the profiles can be adequately described by the polynomials employed. The curves obtained from fitting on only a segment of the run (which simulate a 'fit-to-current' during real-time operation of the algorithm), however, did not model the extended performance profile accurately enough. A tendency to lag behind the latter when extrapolated can be noticed, with the curves 'pulling in' towards the actual function as the run progressed. This is clearly illustrated in Figures (a) and (b) in the seven appendices. The cause of this effect seems to be the inability of all the fitted curves to adequately take into account the drop in acceleration as the run progresses.

In Equations 4 and 6 that describe the take-off run, all parameters except for wind velocity v_w, coefficient of rolling friction μ and runway slope θ, can be assumed to be constant, provided no anomaly occurs during the run. A change in wind velocity will affect the thrust and drag functions and result in a slight change in the acceleration and ground speed profiles. The greatest influence on the distance covered, however, is caused by the effect of a gust at V_1, as this can significantly alter the ground speed at which the salient point is reached. The resulting distance-to-V_1 prediction error is approximately given by[8]:

$$\xi_{D_1} \approx \frac{2V_{1g}.\Delta v_{w1} - (\Delta v_{w1})^2}{2a_1} \qquad \ldots (18)$$

where: V_{1g} is the ground speed at V_1

Δv_{w1} is the change in longitudinal wind component at V_1

a_1 is the aircraft's acceleration at V_1

This error cannot be predicted or compensated for with technology currently. In order to facilitate performance comparison between the different runs without this random error effecting results, the target ground speed has been assumed constant in this work. The predictions, therefore, are strictly those of the distance to a particular ground speed and not to V_1, but are nevertheless more indicative of the accuracy of the model and the adequacy of the fitting technique adopted.

The coefficient of rolling friction can be assumed to be constant in most conditions but difficulties arise when patches of severe contamination such as standing water are present on the runway. Not only is prior detection in real-time currently not feasible but their presence may also result in additional drag incurred in the displacement of the contaminant. Since no contamination was experienced on the four test runs carried out, the extent of its effect could not be assessed in this study.

A change in runway slope along the run will result in a change of acceleration of $g\sin\theta$, or approximately $0.17 ms^{-2}$ per degree of slope change. The extent of the effect on the distance-to-V_1 depends on where the change in slope is experienced during the run. Fortunately, although an early change in slope results in a large change in the distance-to-V_1 (up to 7% per degree of slope change for the Jetstream-100 run), its effect is taken well into account by the fitted curve once the change in slope is experienced. The algorithm, however, cannot forward predict the effect of a change in slope further down the runway, but then this would result in a relatively small error. Nevertheless, since runway slope changes are predictable, it would be possible to compensate for them and take their effect into account if such measures are considered necessary. The segment of Cranfield's runway 22 relevant to the Jetstream's ground run to V_1 has a change in slope towards its further end

---

[8] Equation 18 assumes constant acceleration for the period $V_{1g} \pm \Delta v_{w1}$.

(Figure 12). This contributes to a distance prediction error of the order of 2 to 3m, which was not considered sufficiently significant to warrant compensation.

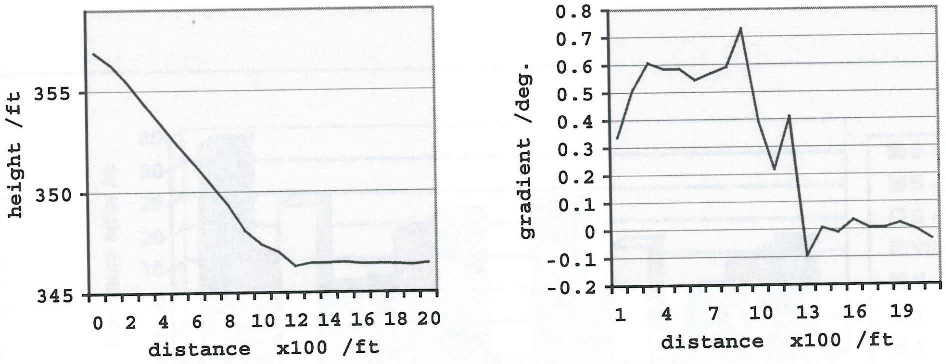

Figure 12: Runway 22 elevation and gradient profile for the first 2000ft.

The performance and adequacy of the different fits can be compared by considering their respective prediction error and repeatability. Figures 13 and 14 indicate that the characteristics resulting in the least prediction error are V^2 vs. S and V vs. log(S). Both exhibit greatest accuracy not only at ½ distance gone (approximately equivalent to 2/3 time-to-V_1) but also at ¼ distance gone (approximately ½ time-to-V_1).

In order to ensure a good fit a large data population is required. This implies the need for a high data-sampling rate, but from an engineering point of view a compromise needs to be established to limit the complexity or length of the calculations within the algorithm. The sampling rates of 5Hz, 10Hz and 20Hz were used for comparison in this study. The smaller population size associated with the 5Hz sampling rate is found to tend to allow the last data point to carrying a high weighting in the selection of the optimal coefficients. This results in relatively large fluctuations between successive fits (expressed as a noise component in the time domain). This is evident on all the figures (c) when compared to (d), (e) and (f) in the appendices. Although filtering could be used to eliminate this noise component, the relatively low sampling rate results in the noise signal having a low frequency that is in the same frequency range as any disturbance likely to be encountered. Consequently filtering may conflict with system performance requirements. The 10Hz and 20Hz sampling rates result in noise components not only exhibiting lower amplitudes but also having higher frequency components. If this were to be filtered out, it would place less stringent requirements on filter design and therefore would be less likely to adversely affect system performance. A visual comparison of the 10Hz and 20Hz sampling rates suggests that 10Hz is adequate for the scope of monitoring take-off performance.

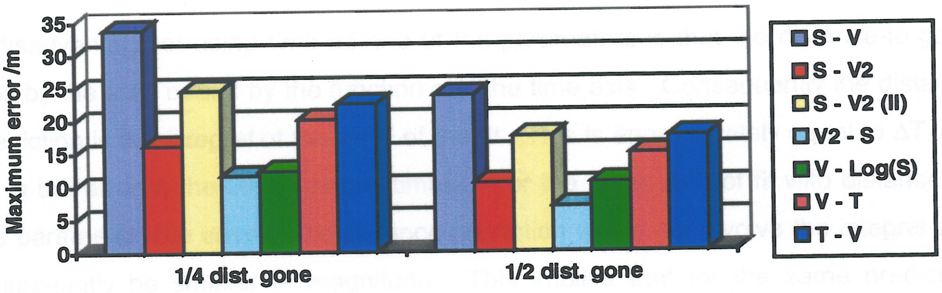

Figure 13: Graph of absolute maximum error experienced after ¼ distance and ½ distance gone.

Values plotted are the average for the four runs.

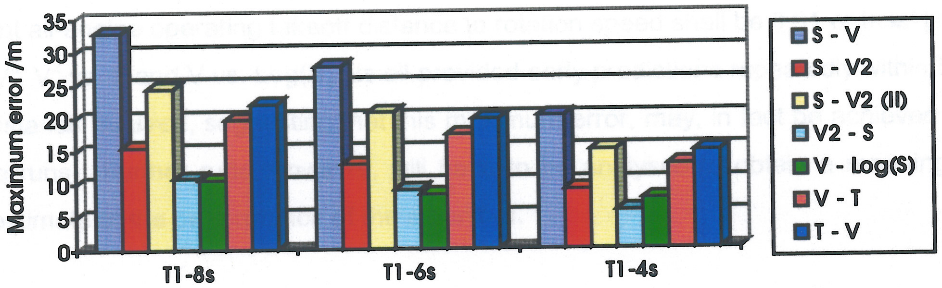

Figure 14: Graph of absolute maximum error experienced at 8s, 6s and 4s before V_1.

Values plotted are the average for the four runs.

All algorithms used in the different fits employed the same curve-fitting procedures, except for the case where fraction powers were taken into account when fitting the S vs. V^2 characteristic. The only other differences introduced were in the manipulation required to determine the distance-to-go-to-V_1. In profiles where the ground speed was selected as the independent variable[9], the calculation involved a straight-forward evaluation of $y=f(V_1)$. Where the ground speed was the dependent variable, however, the second parameter's value[10] at V_1 had to be determined by solving the equation $y = f(x) - V_1$. Although efficient standard algorithms, such as the secant method, exist, they are more complex when compared to the solution of the equation $y=f(V_1)$ and therefore impose a penalty in the execution time of the algorithm.

A distinct disadvantage of using time as one of the parameters is that the distance-to-go is represented by the area bound by the function and the time axis. Consequently the distance error in prediction is the *integral* of the error of the fit. This is approximately equal to $\Delta T_1.V_1$, where ΔT_1 is the error in the target-time estimate. For the same lack of fit with distance as the second parameter, the error in the distance prediction would not involve the integral and would consequently be smaller in magnitude. This implies that for the same prediction accuracy, the fits on the V vs. T and T vs. V characteristics need to model the relevant profile more closely. The same applies to the fit on the V vs. log(S) characteristic, because the distance error is proportional to the exponent of the model error. It is perhaps quite surprising, therefore, that the 3rd order polynomial fit provided such accurate predictions.

The Aerospace standard for take-off performance monitors recommends that 'the probability that TOPM system tolerances will, of themselves, cause an error greater than ±5 percent in the apparent all-engine operating takeoff distance to rotation speed shall be 0.01 or less' [12]. The S vs. V^2, V^2 vs. S and V vs. Log(S) fits all provided early predictions repeatedly within 5% of actual distance required, suggesting that this maximum error, may, in fact be achieved on 99% of the runs. Further runs, however, will have to be analysed to obtain a meaningful statistical estimate of the performance of the algorithm.

A more accurate model and greater prediction accuracy would result if the fitted curve could be made to pull in further towards the actual characteristic. Techniques that could potentially provide an increase in curvature are:

- Curve-fitting only a sliding window of given length (i.e. considering only the latest few seconds of the recent run history). This technique supports a quicker response to a change in acceleration and may result in a reduction in the amount of 'lag' the fit suffers. The window size would need to be established empirically.

---

[9] Ground speed is one of the parameters in all the characteristics considered, presented either as the independent or dependent variable.

[10] Either distance gone, log of distance gone, or time.

- Applying weighted least square techniques. This approach considers the complete run history but puts more focus on recent data. Whilst enjoying the same advantages as sliding window techniques, this method also exhibits the advantage of providing a gradual fading out less recent data.
- Introducing a controlled bias in the second order coefficient, or a controlled, carefully selected third order coefficient. This approach would increase the curvature of the fitted polynomial by an appropriate amount, thereby attempting to compensate for the fitted 2nd order polynomial's lack of curvature early in the run.

For such compensation models to be successful, the prediction error in the original fit needs to be predictable and repeatable. In these circumstances, this attribute is more important than absolute accuracy, as it is the former that determines the amount of error that cannot be eliminated by compensation. The performance variation between the four runs for the various fits is presented in Figures 15 and 16. All fits except that on the V vs. Log(S) profile exhibit good repeatability with the S vs. V^2 fit and with fractional powers having a slightly better repeatability throughout.

One of the fundamental assumptions in curvi-linear regression is that the data actually represents a fixed characteristic with invariant coefficients. This will be the case for the correctly modelled normal take-off run provided no discrete anomaly is encountered at any stage. Regression techniques, therefore, are well suited for the requirement of detecting subtle under-performance. It would be advantageous, however, to have an algorithm that could also correctly respond to discrete changes, as this would allow the monitor to confirm the crew's identification of a discrete anomaly. The behaviour of the curve-fitting algorithms in the presence of discrete anomalies therefore warrants further investigation to assess their performance in this respect. A change in conditions would effectively result in a different polynomial (different coefficients), and this may upset the fit. If this is found to be the case, other tools such as non-predictive acceleration monitoring may need to be considered to support the curve-fitting technique.

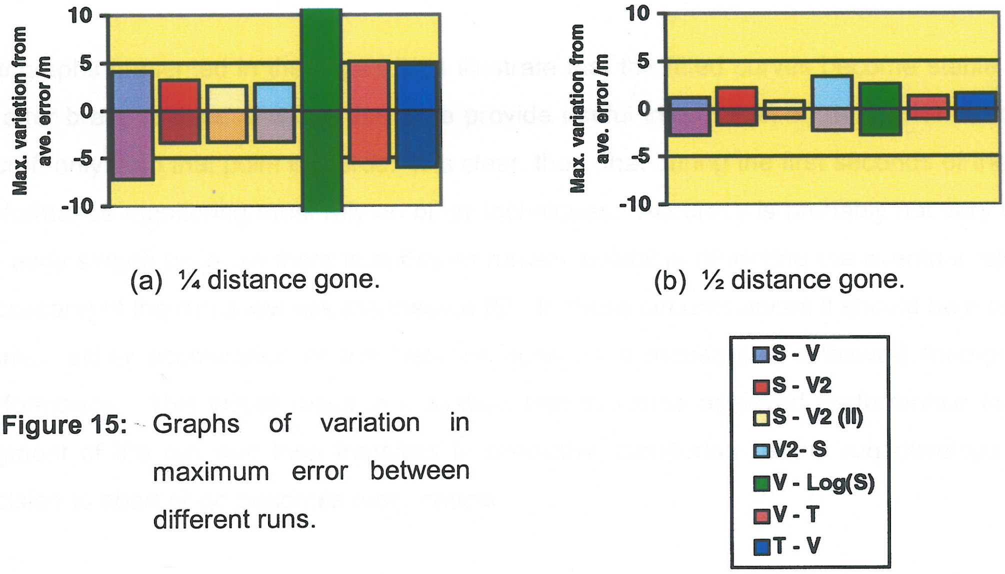

(a) ¼ distance gone.

(b) ½ distance gone.

Figure 15: Graphs of variation in maximum error between different runs.

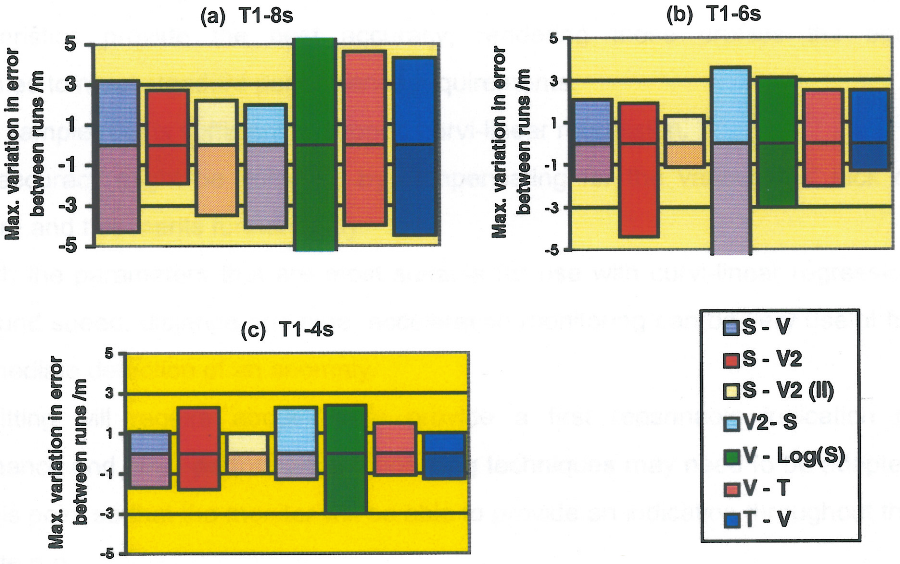

Figure 16: Graphs of variation in maximum error between different runs.

7. CONCLUSION

The graphs presented in the appendices illustrate that the fitted curves become stable at about 7s after brake release and can therefore provide useful information on the performance of the aircraft only from that point onwards. It is clear, then, that during the first seconds of the run any performance monitoring must rely on other techniques. Accuracy is probably not very critical in the early stages because there is sufficient runway available rendering the eventual rejection (if necessary) of the run a low risk manoeuvre [5]. In these circumstances it should be adequate to monitor either acceleration or the distance gone as a measure of achieved (non-predictive) performance. This would result in a system that indicates achieved performance in the first segment of the run and then transfers to predictive monitoring as the run develops and the decision to abort or go becomes more critical.

In conclusion, therefore, the following findings have resulted from this study:

- Curve-fitting techniques have a potential in predicting aircraft performance to V_1. Normal curvi-linear regression applied to the S vs. V^2, V^2 vs. S and V vs. Log(S) characteristics provide the best accuracy, rendering these profiles the best candidates to meet standard performance requirements.
- A 10Hz sample rate is sufficient to support curvi-linear regression.
- Better accuracy might be achieved by compensating for the various fits' lack of curvature and this merits further study.
- Although the parameters that are most suitable for use with curvi-linear regression are ground speed, distance and time, acceleration monitoring can be very useful for the immediate detection of an anomaly.
- Curve-fitting will require about 7s to provide a first reasonable indication of performance and other performance monitoring techniques may need to be adopted up to this point so that the monitor will be able to provide an indication throughout the complete run.
- Further study is required to determine the performance of curve-fitting in the presence of anomalies during the run.

REFERENCES:

[1] Jensen D. *Airbus' answer to safety with avionics.* Avionics Magazine, June 1999, pp. 22-27.

[2] Coquin L et al. *System for deriving an anomaly signal during the take-off of an aircraft.* US Patent no. 5,668,541. 1997.

[3] Cleary P J, Kelman L S and Horn R L. *Aircraft performance margin indicator.* US Patent no. 4,638,437. 1987.

[4] Middleton D B, Srivatsan R and Person L H. *Airplane takeoff and landing performance monitoring system.* US Patent no. 5,449,025. 1996.

[5] Zammit-Mangion D and Eshelby M. *Design concept and performance standard for a take-off performance monitor design intended for use on Part 25 certified aircraft.* Technical Report CoA-0010, College of Aeronautics, Cranfield University, Bedfordshire, UK, 2000.

[6] Hines W W and Montgomery D. *Probability and statistics in engineering and management science.* Wiley, 1980. ISBN 0-474-14759-7.

[7] Zammit-Mangion D and Eshelby M. *Design and validation using flight data of a method for predicting the ground run required for take-off.* Proc. ICAS 2000, Harrogate, August 2000. Awaiting publication.

[8] Anonymous. *LTN-90-100 Component Maintenance Manual.* Litton Aero Products, Part no. 464600.

[9] Small J T. *Feasibility of using longitudinal acceleration (N_x) for monitoring takeoff and stopping performance from the cockpit.* Proc. 27th Symposium of the Society of Experimental Test Pilots, CA, 1983, pp. 143-155.

[10] Anonymous. *Jet transport performance methods.* Boeing Flight Operations Engineering, 7th Edition, May 1989.

[11] Ojha S K. *Flight performance of aircraft.* AIAA Education Series, AIAA, 1995. ISBN 1-56347-113-2.

[12] Anonymous. *Takeoff performance monitor (TOPM) system, airplane, minimum performance standard for.* SAE, Aerospace Standard AS-8044, 1987.

APPENDICES

APPENDIX I

2^{ND} ORDER FIT TO S vs V CHARACTERISTIC

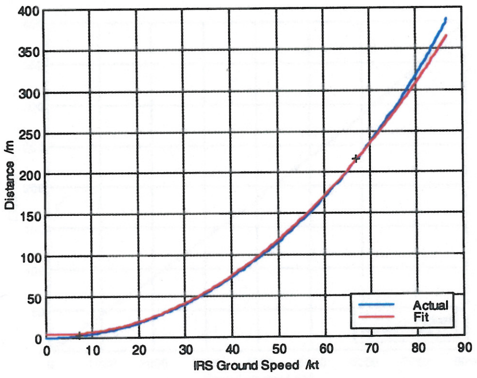

Figure A.I(a): Run 1.

Fit from 2s to ¾ run time (12.9s).

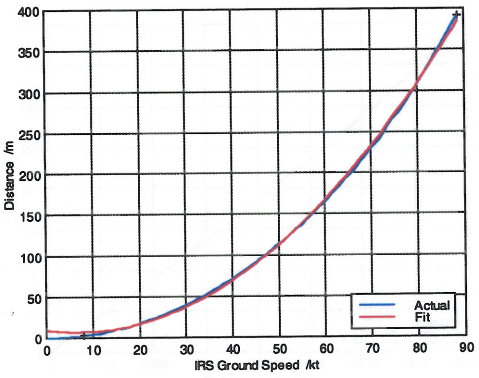

Figure A.I(b): Run 1.

Fit from 2s to the end of run.

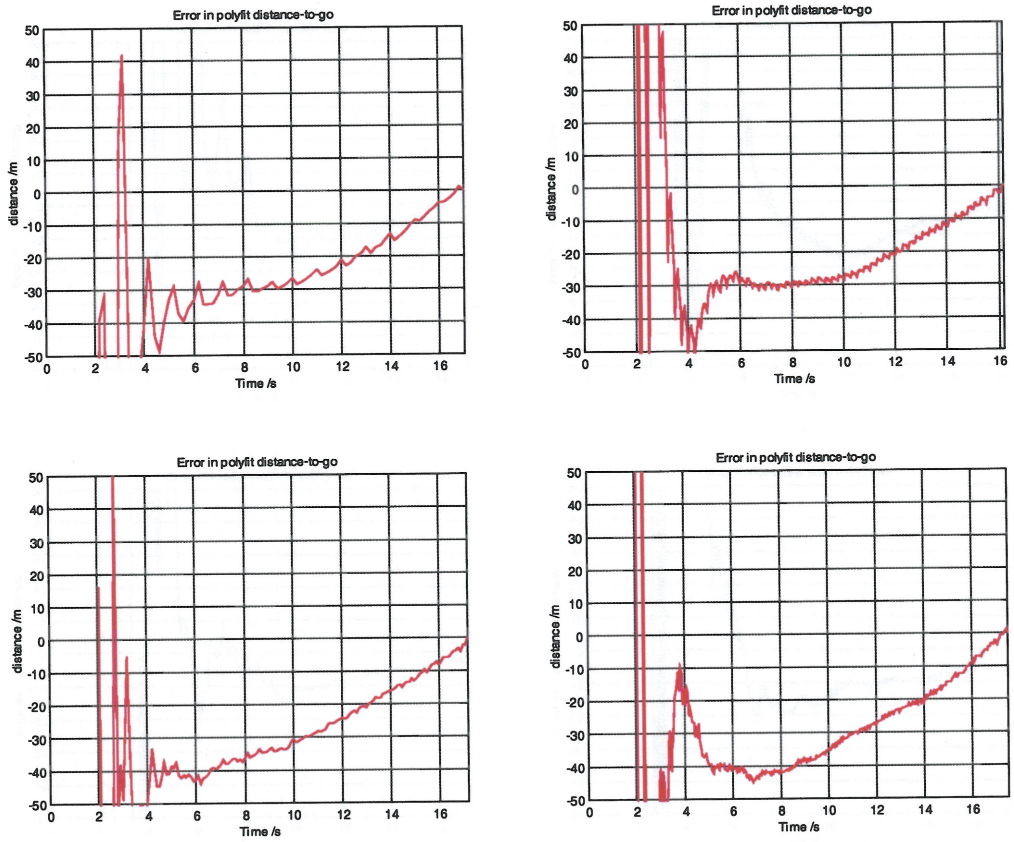

Figures A.I (c) Run 1, (d) Run 2, (e) Run 3, (f) Run 4:

Error in the distance-to-go estimate of the polynomial fit.

The error is calculated as the difference between the fit estimate and actual distance covered.

APPENDIX II

2^{ND} ORDER FIT TO S vs V^2 CHARACTERISTIC

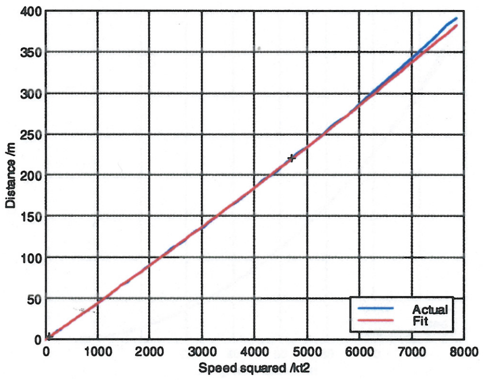

Figure A.II(a): Run 1.
Fit from 2s to ¾ run time (12.8s).

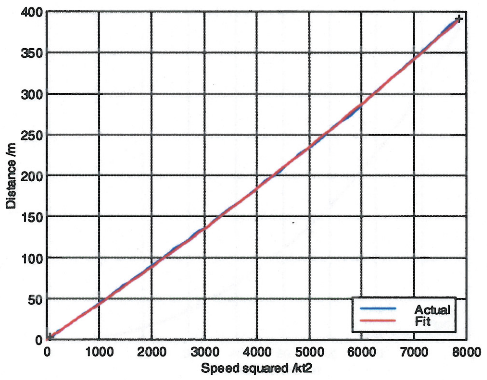

Figure A.II(b): Run 1.
Fit from 2s to the end of run.

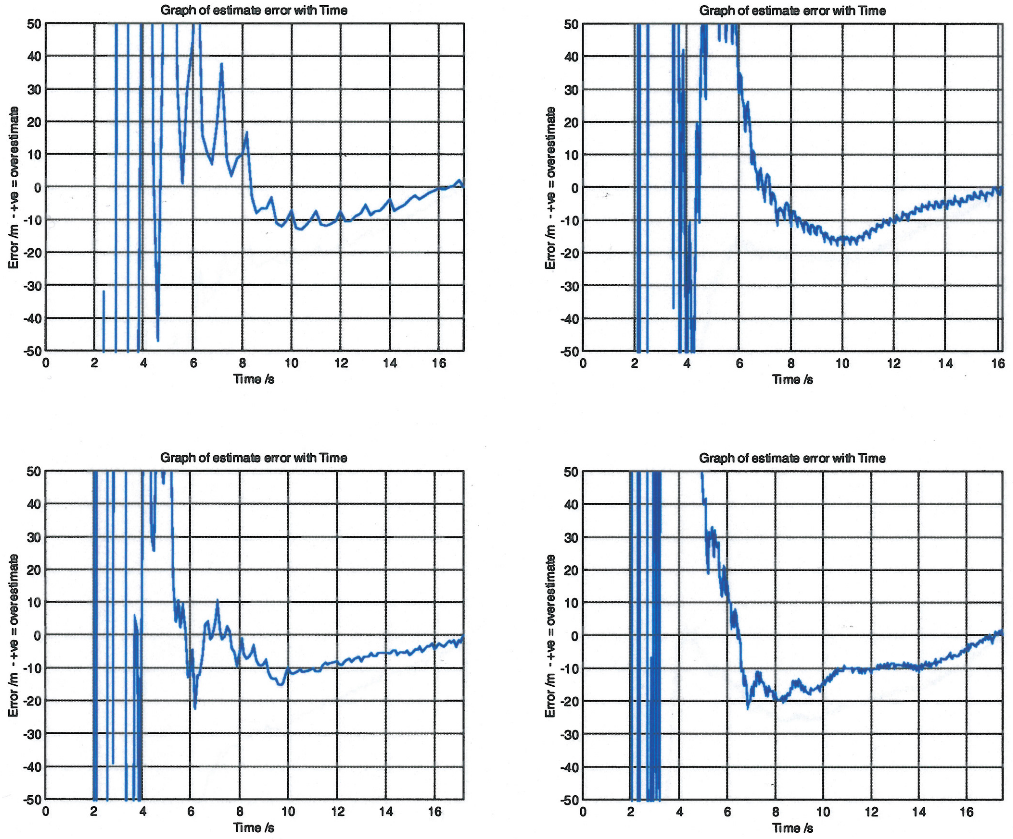

Figures A.II (c) Run 1, (d) Run 2,
(e) Run 3, (f) Run 4:

Error in the distance-to-go estimate of the polynomial fit.

The error is calculated as the difference between the fit estimate and actual distance covered.

APPENDIX III

$(Ax^2+Bx^{3/2}+Cx+Dx^{1/2}+E)$ FIT TO S vs V^2 CHARACTERISTIC

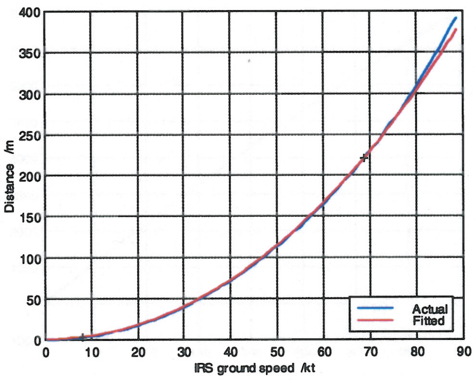

Figure A.III(a): Run 1.
Fit from 2s to ¾ run time (12.8s).

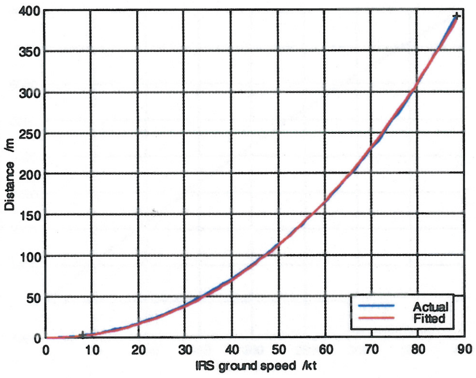

Figure A.III(b): Run 1.
Fit from 2s to the end of run.

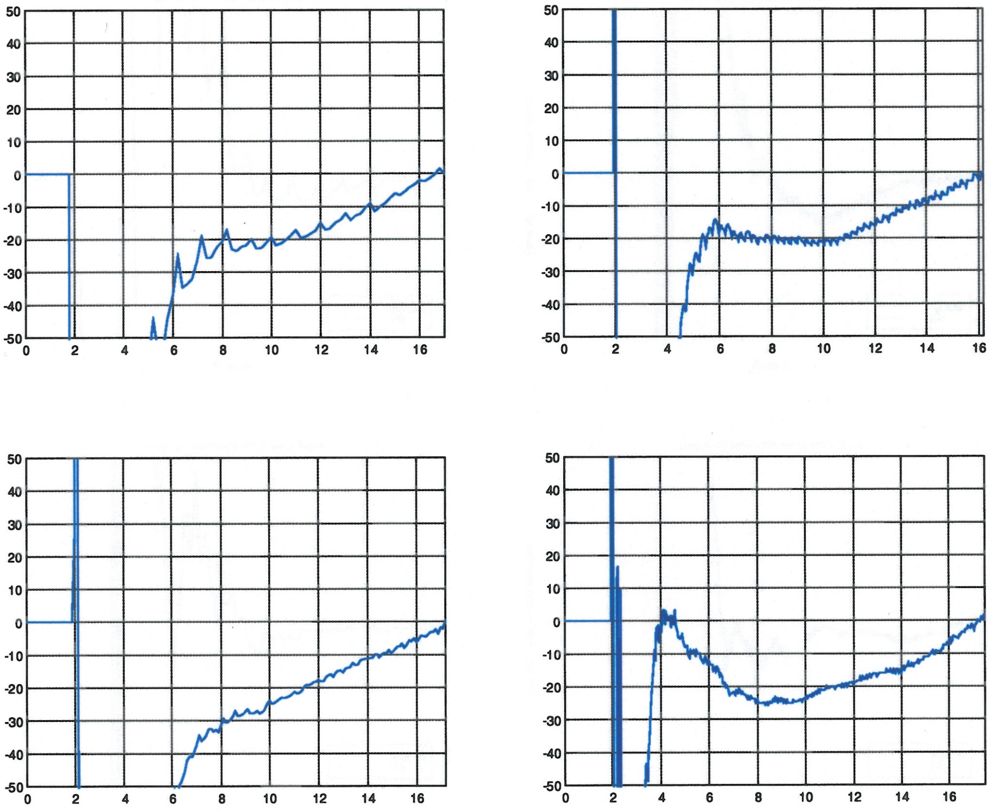

Figures A.III **(c)** Run 1, **(d)** Run 2,
(e) Run 3, **(f)** Run 4:

Error in the distance-to-go estimate of the polynomial fit.

The error is calculated as the difference between the fit estimate and actual distance covered.

APPENDIX IV

2^{ND} ORDER FIT TO V^2 vs S CHARACTERISTIC

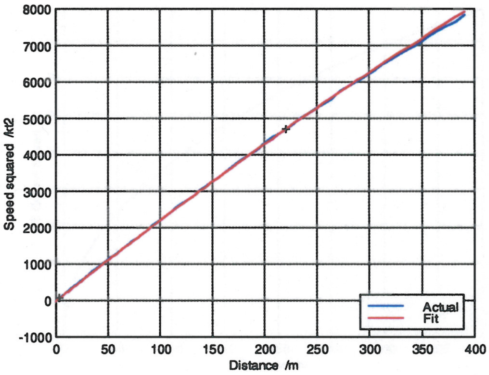

Figure A.IV(a): Run 1.

Fit from 2s to ¾ run time (12.8s).

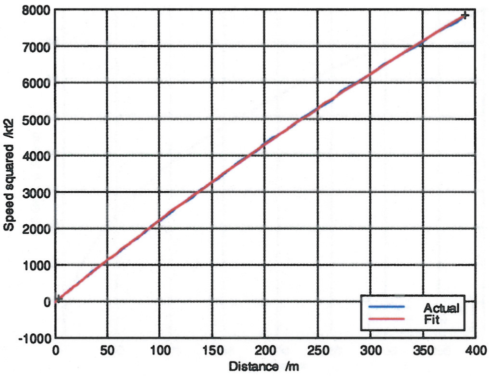

Figure A.IV(b): Run 1.

Fit from 2s to the end of run.

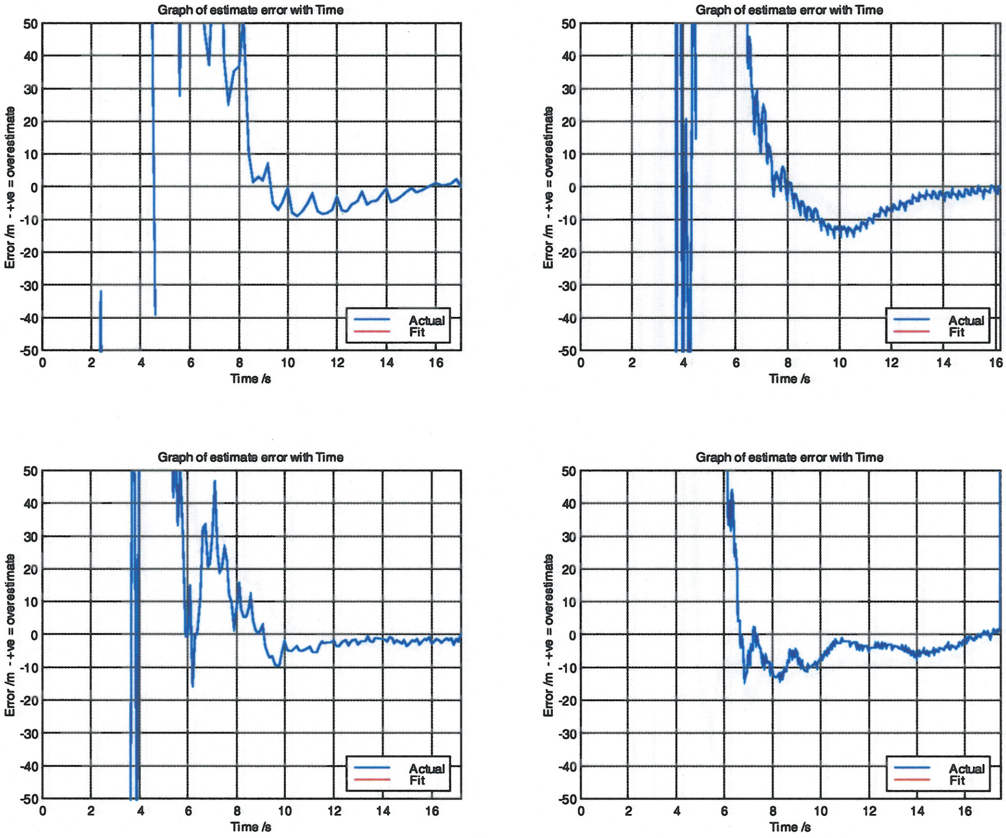

Figures A.IV (**c**) Run 1, (**d**) Run 2,

(**e**) Run 3, (**f**) Run 4:

Error in the distance-to-go estimate of the polynomial fit.

The error is calculated as the difference between the fit estimate and actual distance covered.

APPENDIX V

3rd ORDER FIT TO V vs log(S) CHARACTERISTIC

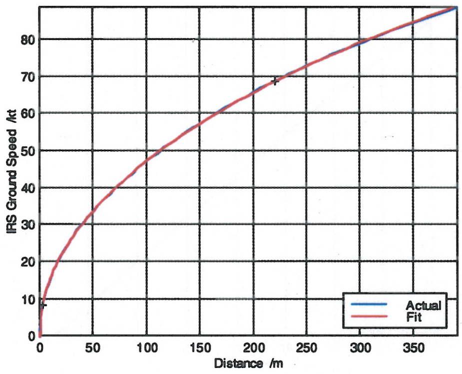

Figure A.V(a): Run 1.
Fit from 2s to ¾ run time (12.8s).

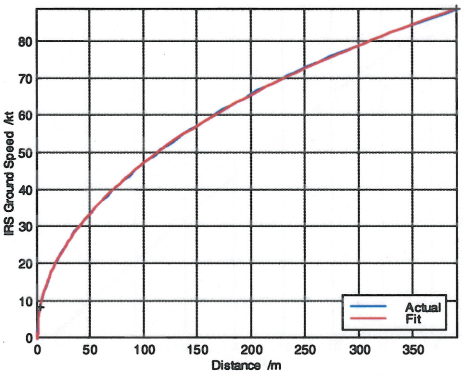

Figure A.V(b): Run 1.
Fit from 2s to the end of run.

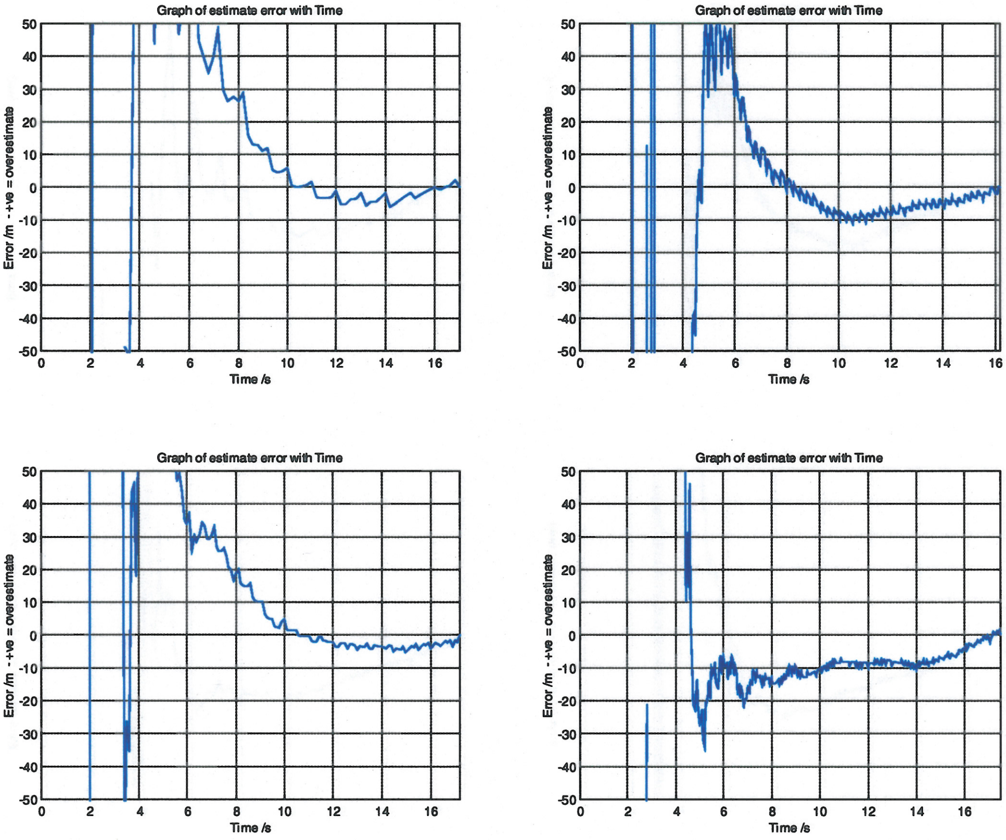

Figures A.V (c) Run 1, (d) Run 2,
(e) Run 3, (f) Run 4:
Error in the distance-to-go estimate of the polynomial fit.

The error is calculated as the difference between the fit estimate and actual distance covered.

APPENDIX VI

2nd ORDER FIT TO V vs T CHARACTERISTIC

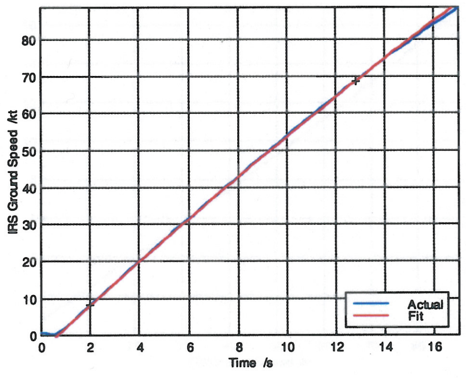

Figure A.VI(a): Run 1.

Fit from 2s to ¾ run time (12.8s).

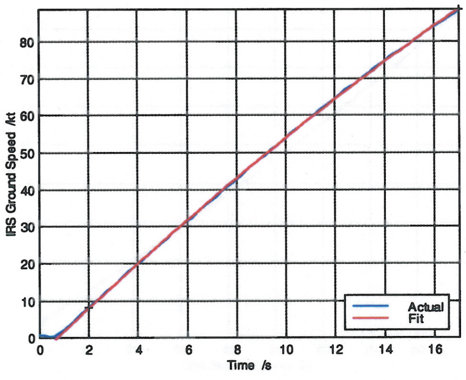

Figure A.VI(b): Run 1.

Fit from 2s to the end of run.

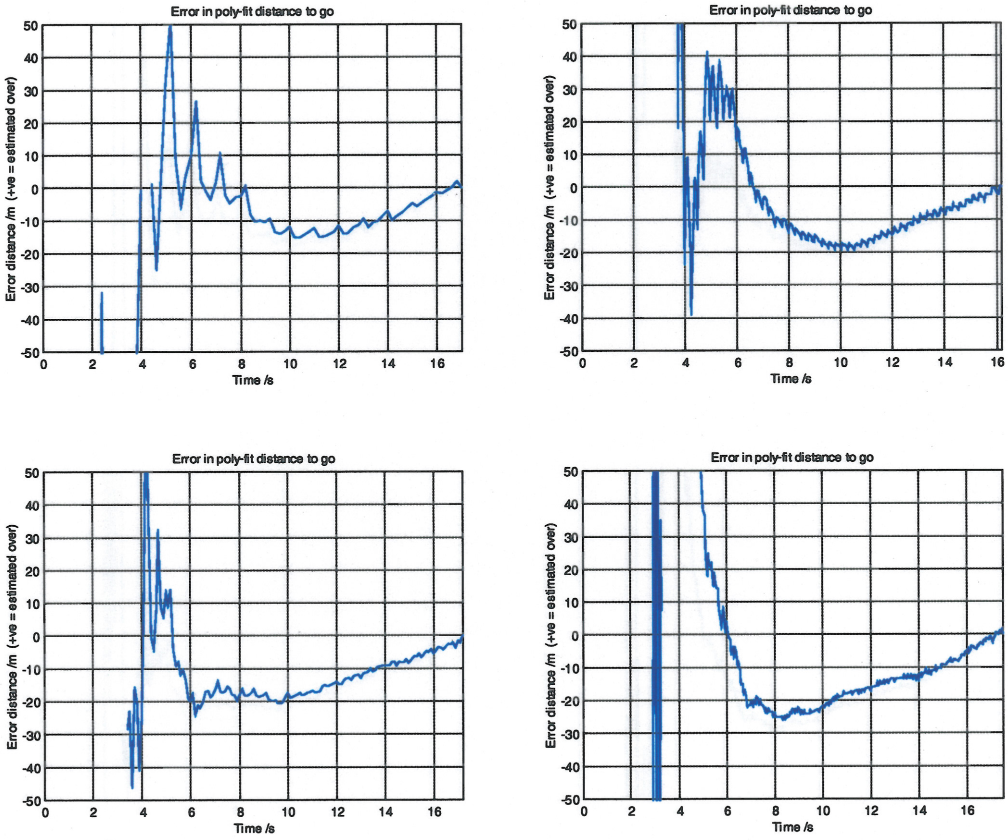

Figures A.VI **(c)** Run 1, **(d)** Run 2,

(e) Run 3, **(f)** Run 4:

Error in the distance-to-go estimate of the polynomial fit.

The error is calculated as the difference between the fit estimate and actual distance covered.

APPENDIX VII

2nd ORDER FIT TO T vs V CHARACTERISTIC

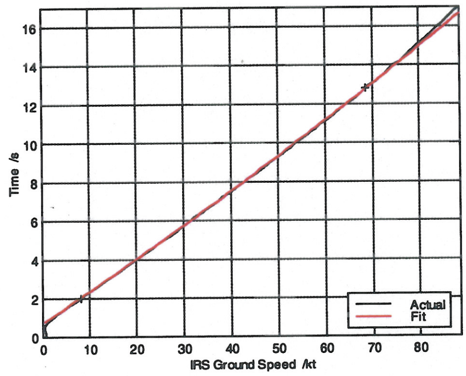

Figure A.VII(a): Run 1.
Fit from 2s to ¾ run time (12.8s).

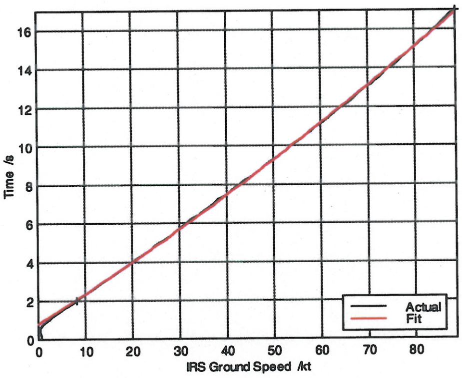

Figure A.VII(b): Run 1.
Fit from 2s to the end of run.

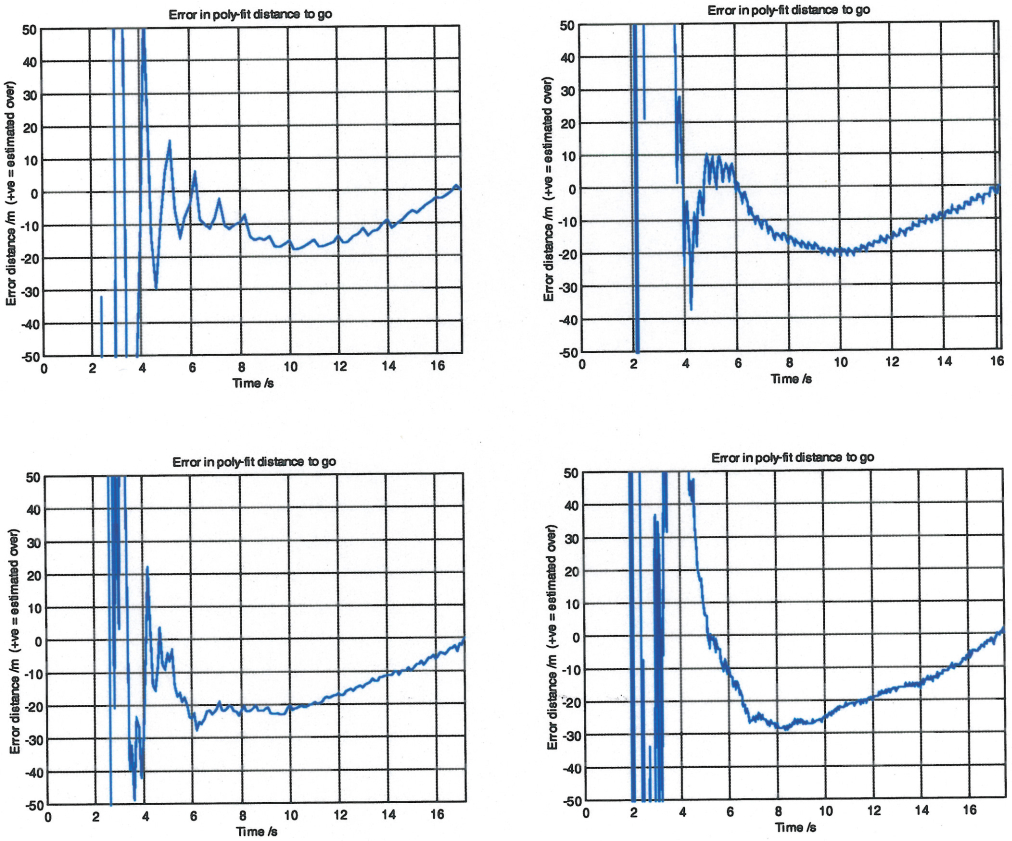

Figures A.VII **(c)** Run 1, **(d)** Run 2,
(e) Run 3, **(f)** Run 4:

Error in the distance-to-go estimate of the polynomial fit.

The error is calculated as the difference between the fit estimate and actual distance covered.